John Whitmer

MEng Mechanical Engineering

Cornell Cup

5/15/14

Personal Contributions

Cornel Cup was an exciting and rewarding project to work on this past year. We took on a challenging problem and produced a working solution. The multidisciplinary aspect of the Cornell Cup project team was a new experience for me and very informative.

I personally did a lot of work on the robotic arms for C3PO. This included the mechanical design of the arms, developing the kinematic equations for the arms, and also testing the arms. I also had a large role in selecting parts and materials to order and in assembling the arm. I also did a lot of my work on the head for R2-D2. On R2-D2, I developed the attachment method for attaching the head turn motor bearing to the rest of the body. I also developed the attachment method for the head turn motor, including both attaching the motor to the frame and attaching the turning wheel to the motor shaft. In addition to the main design work that I did on C3PO and R2-D2 I also helped design the test stand for C3PO. I also spent a lot of time in the lab area assisting with the assembly of all part of both robots and worked with the ECE's in attaching the electrical circuits to the robots.

The mechanical design of C3PO's arms required extensive use of SolidWorks in designing the individual parts as well as creating the overall assembly. I also created most of the part drawing that were used for machining C3PO's arms.

In developing the kinematic equations for C3PO's arm I used a method known as the Denavit – Hartenburg method. The Denavit – Hartenburg method is a systematic method for assigning coordinate frames so that a standard form transformation matrix may be use to transition from one frame to another. The Denavit-Hartenburg method works for developing the forward kinematic equations. These are important but not really useful as they are deterministic not goal oriented. Inverse kinematic equations are more useful but incredibly more difficult to find. I spent a large time working on the inverse kinematics equations this year. Inverse kinematics do not generally have a close form solution. Because C3PO's arm did not include a working elbow, its motion was constrained to a surface of a constant sphere centered at his shoulder. This meant that there were infinite solutions for the position of his hand in space. Because of this I

had to included the orientation of the hand in the calculations as well to solve the kinematics.

Working on the Cornell Cup was a rewarding experience this past year. I greatly enjoyed working on the challenging problems that can arise when designing robots.

Controlling a Robotic Arm

Building the structure of a robotic arm is an interesting design project but it is not very useful unless the arm can be controlled. This section will detail the steps necessary to control the position of a robotic arm. For a more detailed discussion see Introduction to Robotics Analysis, Systems, Applications by Saeed Niku.

Workspace

The first step in controlling a robotic arm is to understand the arm's workspace. A workspace is the area in space that the arm can reach. It describes the physical limits of the arm. A workspace also takes into account the surrounding environment. For example a robotic arm that is mounted on a table cannot reach below the table and so its workspace stops at the surface (see Figure 1). A robotic arm also cannot pass through itself. Determining a robotic arm's workspace is important when planning trajectories.

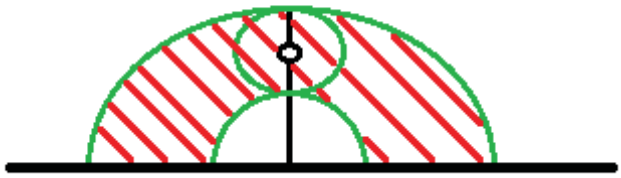

Figure 1: Sample Workspace for a Robotic Arm with 2 Revolute Joints in a Plane

In the case of the C3PO robotic arm, the work space is defined by the various ranges of motion of each joint which can be limited by a number of factors such as servo limits, cable wrapping, body interaction and linkage constraints. For example, joints which are servo actuated have a maximum rotation angle of 180 degrees. These constraints should be well defined in the free body diagram to construct the work space.

Forward Kinematics

Forward kinematic equations are equations that relate the joint inputs to the final position of the end effector. Forward kinematics are a deterministic approach that assumes the input angles are known and will then find the final position.

Coordinate Transformations and Rotation Matrices

To fully define the position and orientation of a point in space six pieces of information are needed: the X, Y, Z coordinates, and the rotations about the X Y and Z axes. A common method for describing this is to use matrices. The standard form of a transformation matrix is as follows:

$$T = \begin{bmatrix} n_x & o_x & a_x & P_x \\ n_y & o_y & a_y & P_y \\ n_z & o_z & a_z & P_z \\ 0 & 0 & 0 & 1 \end{bmatrix}$$

Equation 1: Transformation Matrix

This matrix can be separated into four column vectors: n, o, a, and P where the P vector describes the position and the other three describe the orientation. Vectors n, o, and a are unit vectors that relate the end effector's local coordinate frame to the global coordinate frame. When controlling a robotic arm it is important to know how a joint location will affect the end position. There are three types of joint motions: pure translation, pure rotation about an axis, and a combination of translations and rotations. Each motion has a transformation matrix associated with it shown below.

$$Trans(d_x, d_y, d_z) = \begin{bmatrix} 1 & 0 & 0 & d_x \\ 0 & 1 & 0 & d_y \\ 0 & 0 & 1 & d_z \\ 0 & 0 & 0 & 1 \end{bmatrix}$$

Equation 2: Pure Translation

$$Rot(x, \theta) = \begin{bmatrix} 1 & 0 & 0 & 0 \\ 0 & \cos(\theta) & -\sin(\theta) & 0 \\ 0 & \sin(\theta) & \cos(\theta) & 0 \\ 0 & 0 & 0 & 1 \end{bmatrix}$$

Equation 3: Pure Rotation about the X-axis

$$Rot(y, \theta) = \begin{bmatrix} \cos(\theta) & 0 & \sin(\theta) & 0 \\ 0 & 1 & 0 & 0 \\ -\sin(\theta) & 0 & \cos(\theta) & 0 \\ 0 & 0 & 0 & 1 \end{bmatrix}$$

Equation 4: Pure Rotation about Y-axis

$$Rot(z, \theta) = \begin{bmatrix} \cos(\theta) & -\sin(\theta) & 0 & 0 \\ \sin(\theta) & \cos(\theta) & 0 & 0 \\ 0 & 0 & 1 & 0 \\ 0 & 0 & 0 & 1 \end{bmatrix}$$

Equation 5: Pure Rotation about Z-axis

If a robotic arm at a given position and orientation (has a specific T matrix), undergoes a rotation about the Z-axis its T matrix will change. A change relative to the global coordinate frame is pre-multiplied with the previous T matrix while a change relative to the local coordinate frame is post-multiplied with the previous T matrix.

$$T_{new} = Rot(z, \theta) * T_{old}$$

Equation 6: Rotation about the Global Z-axis

$$T_{new} = T_{old} * Rot(z, \theta)$$

Equation 7: Rotation about the Local Z-axis

Denavit – Hartenberg Method for assigning coordinate frames

The Denavit – Hartenberg (D-H) method is a systematic approach for assigning coordinate frames to a robotic arm with multiple joints. The first step in the D-H method is to assign the z-axis for every joint. In the D-H method the z-axis is the rotation axis for a revolute joint. The next step is to place the x-axis for each joint. A joint's x-axis needs to be collinear with the common normal between its z-axis and the priors joint's z-axis. Figure 2 shows the coordinate frames for the three joints that make up the shoulder of the arm.

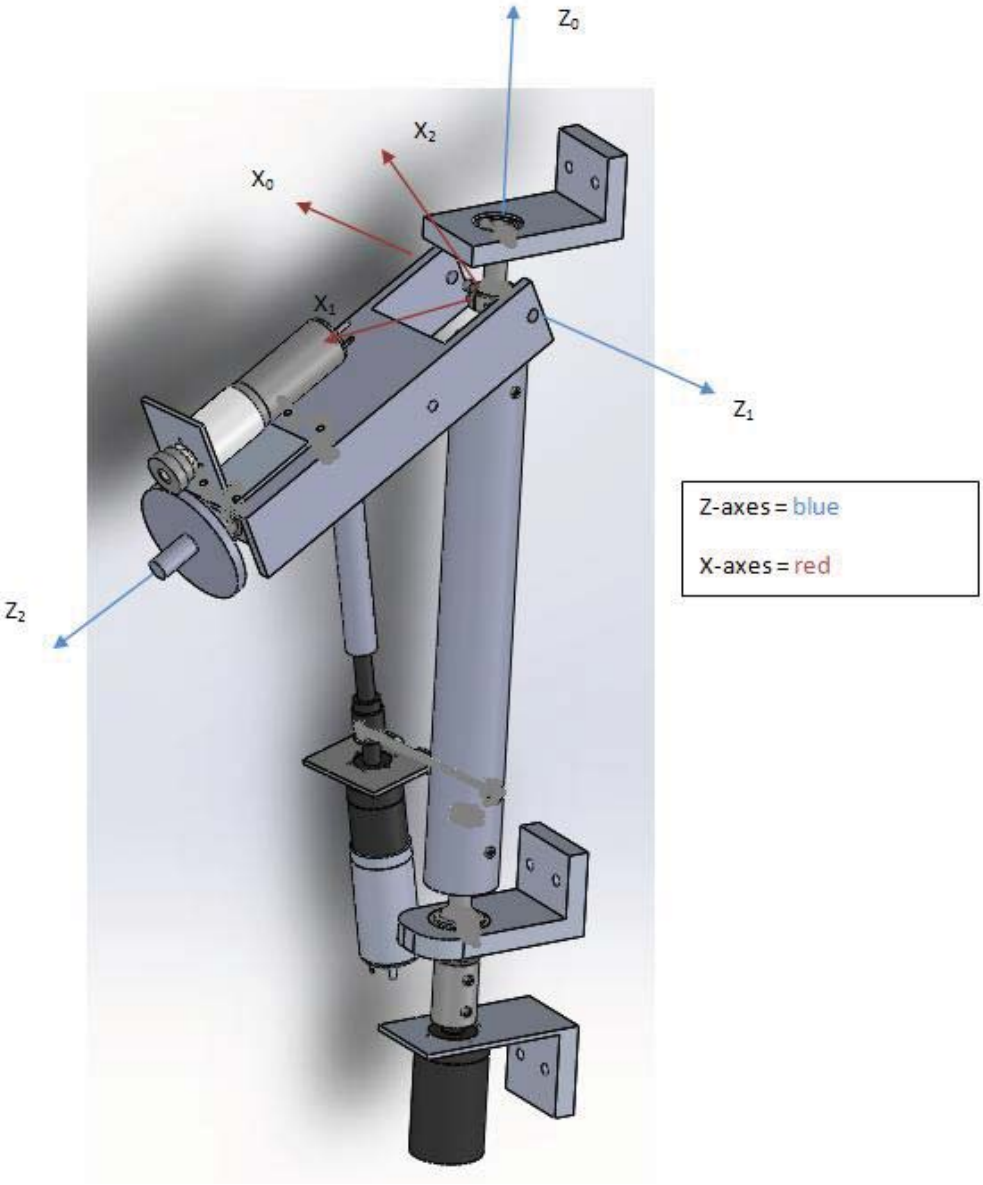

Figure 2: Coordinate Frames for the Shoulder

After the coordinate frames have all been assigned fill out the D-H parameters table shown in Table 1.

Table 1: D-H Parameters Table

Joint	θ	d	a	α
1	-90	0	0	90

"Θ" is the angle about which a frame must be rotated on its z-axis in order to make its x-axis parallel with the next frame's x-axis. This is an unknown for a revolute joint and represents the actual joint angle. The parameter "d" is the distance that the frame must be translated along its z-axis in order to make its x-axis and the next frame's x-axis collinear. The parameter "a" represents the distance the frame must translate along its x-axis to make the origin coincident with the next frame's origin. The angle "α" is the angle that the frame must be rotated about the x-axis to line up the two z-axes. A frame undergoing these four transformations (2 rotations and 2 translations) will be at the same location and orientation as the next frame in the arm. Once the parameter table has been filled out for every joint, the next step in the D-H method is to create the transformation matrices. Equation 8 shows the standard form for a transformation matrix between two joints in a robotic arm using the D-H method.

Equation 8: Transformation Between Two Joints

$$A_n = \begin{bmatrix} cos\,(\theta_n) & -sin(\theta_n)\,cos\,(\alpha_n) & sin(\theta_n)\,sin\,(\alpha_n) & a_n cos\,(\theta_n) \\ sin\,(\theta_n) & cos(\theta_n)\,cos\,(\alpha_n) & -cos(\theta_n)\,sin\,(\alpha_n) & a_n sin\,(\theta_n) \\ 0 & sin\,(\alpha_n) & cos(\alpha_n) & d_n \\ 0 & 0 & 0 & 1 \end{bmatrix}$$

The robotic arm designed for C3P0 requires a total of seven A matrices. The complete transformation from the shoulder to the end of the arm would be given by Equation 9.

$$T_{total} = A_1 A_2 A_3 A_4 A_5 A_6 A_7$$ **Equation 9: Total Transformation in A matrices**

These are the basics of using the D-H method to determine a robots forward kinematics. The D-H method is not the only method but its systematic approach makes it an often used method in industry.

Inverse Kinematics

Inverse kinematics is the opposite of forward kinematics. While forward kinematics used inputted joint angles to determine a final position and orientation, inverse kinematics uses a desired location and orientation to determine the necessary joint angles. Inverse kinematics is goal oriented. There are multiple methods of finding inverse kinematics but they all rely on having previously solved for the forward kinematics. The reasons for using inverse kinematics in a robot should be relatively obvious. The designer would like to think in terms of the goal to achieve rather than the movement of each joint. For example, C3PO should be able to wave to a crowd or sign its name. This is a series of movements in which the end effector, the hand, describes a precise path through space. To describe this path through the multiple degrees of freedom of the shoulder, elbow and wrist joints through a series of servo angles would be extremely complex. Thus, the designer is motivated to use inverse kinematics. There are two broad categories and methods, analytical and numerical.

Analytical Methods

Solving for a systems inverse kinematics analytically is a difficult challenge. Sometimes it is impossible to find a complete closed form solution as a robotic arm may have multiple configurations that have the same end point position and orientation. These scenarios arise when there is an over-defined system.

An object's position and orientation, as mentioned previously, are described by six pieces of information. A robotic arm with more than six joints is an over-defined system and will have multiple solutions. A system with fewer than six joints is an under-defined system and will not be able to reach any desired position and orientation. A robotic arm with three joints, for instance, can control its final position, or its final orientation, but not both. Analytically solving for a systems inverse kinematics is complex and there is no set method for doing it.

If operating in a simple case, such as a 2-D two-joint arm, an analytically derived inverse kinematics solution is readily available. The objective is to express the joint angles in with the final end effector position as the input variables. In the following example, a two-joint arm operating in the X-Y Cartesian plane is used to demonstrate the basic algebra and trigonometry involved.

Figure 3: 2 Dimensional Arm Example

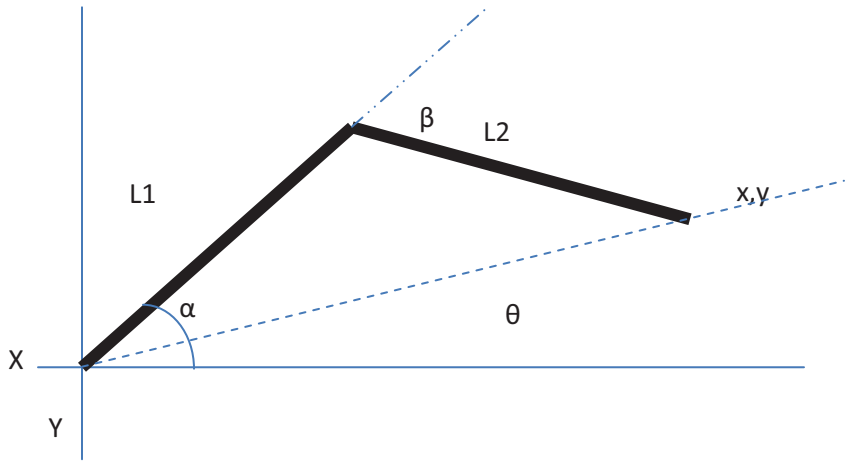

In the above Figure 3, an arm with length L1 is rotated about an angle α and is attached to a second arm with length L2. The angle formed by the intersection of L1 and L2 is β. The manipulation of α and β defines the position x, y of the arm. The forward kinematics of the system is easy to derive and is shown below:

Equation 10: System describing 2-D, 2-Arm forward kinematics

$$x = \cos(\alpha + \beta)\, L2 + \cos(\alpha) * L1$$
$$y = \sin(\alpha + \beta)\, L2 + \sin(\alpha) * L1$$

The following equation set derives the inverse kinematics of the system. An additional term θ is added which is simply the angle between the end of the arm and the X-axis of the coordinate plane.

Equation 11: System describing 2-D, 2-Arm inverse kinematics

$$\cos(\theta) = \frac{x}{\sqrt{x^2 + y^2}}$$
$$\theta = \arccos\left(\frac{x}{\sqrt{x^2 + y^2}}\right)$$
$$\cos(\propto - \theta) = \frac{L1^2 + x^2 + y^2 - L2^2}{2L1\sqrt{x^2 + y^2}}$$
$$\alpha = \theta - \arccos\left(\frac{L1^2 + x^2 + y^2 - L2^2}{2L1\sqrt{x^2 + y^2}}\right)$$
$$\cos(\pi - \beta) = \frac{L1^2 + L2^2 - x^2 - y^2}{2L1L2}$$
$$\beta = \pi - \arccos\left(\frac{L1^2 + L2^2 - x^2 - y^2}{2L1L2}\right)$$

While not the most intuitive of equations, the above system derives the angles of the actuator joints in terms of the desired target positions. Thus, the position of the end effector can be requested and the system will respond with angles β and $\propto$. However, as the system grows in complexity, this method quickly becomes unusable. Even in the very simple case described above, there are some readily apparent issues. First, there can be multiple angles that are valid solutions which are known as redundancies. Second, in an actual mechanical system there are limits to the angles that the actuators can achieve which are not expressed in these equations. Lastly, and most readily apparent, the derivation of the system is quite complex and might not be available if the number of joints or dimensions are increased from this simple 2-D and two-joint system. This leads to the use of iterative numerical techniques to accomplish the inverse kinematics problem.

Numerical Methods

While for complex systems it may be impossible to find an actual analytic solution to inverse kinematics, it is possible to solve numerically. These numerical methods involve making very small changes. The benefit of these methods is that not only may the joint motions for the final location be solved for, a path to travel along may also be defined. Multiple numerical methods will be outlined below.

Jacobian Pseudo-Inverse Method

A Jacobian (denoted by J) simply stated is a matrix of derivatives. This method operates under the assumption that for very small changes, the effects of each joint are independent. The Jacobian of a robotic arm would relate a small change in joint angles to a corresponding small change in position and orientation. To illustrate this example, an additional link may be added to the previously analyzed robotic arm. The objective will be to move from the current location x,y to the objective x1, y1. Let the vector between the current position and the objective be defined as **E**. This method will utilize small

changes in x,y denoted as δx, δy towards the goal of reducing **e** zero by incrementally changing the angles by δα, δβ, and δμ.

Figure 4: 2-Dimensional, 3-Arm Example

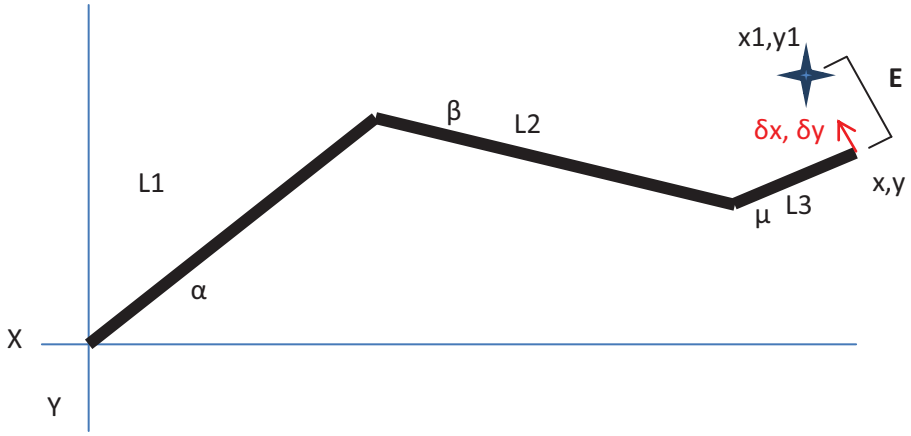

Equation 12: System describing 2-D, 3-Arm forward kinematics

$$\begin{bmatrix} x \\ y \end{bmatrix} = \begin{bmatrix} \cos(\propto +\beta+\mu)\,L3 + \cos(\alpha+\beta)L2 + \cos(\alpha)\,L1 \\ \sin(\propto +\beta+\mu)\,L3 + \sin(\alpha+\beta)L2 + \sin(\alpha)\,L1 \end{bmatrix}$$

Equation 13: System deriving 2-D, 3-Arm Jacobian

$$\begin{bmatrix} \dot{x} \\ \dot{y} \end{bmatrix} = J \begin{bmatrix} \dot{\propto} \\ \dot{\beta} \\ \dot{\mu} \end{bmatrix}$$

$$\begin{bmatrix} \dot{x} \\ \dot{y} \end{bmatrix} = \begin{bmatrix} \frac{\partial F_x}{\partial \propto} & \frac{\partial F_x}{\partial \beta} & \frac{\partial F_x}{\partial \mu} \\ \frac{\partial F_y}{\partial \propto} & \frac{\partial F_y}{\partial \beta} & \frac{\partial F_y}{\partial \mu} \end{bmatrix} \begin{bmatrix} \dot{\propto} \\ \dot{\beta} \\ \dot{\mu} \end{bmatrix}$$

$$J = \begin{bmatrix} -\mathrm{L3} * \sin(\propto +\beta+\mu) - \mathrm{L2} * \sin(\alpha+\beta) - L1 * \sin(\alpha) & -\mathrm{L3} * \sin(\propto +\beta+\mu) - \mathrm{L2} * \sin(\alpha+\beta) & -\mathrm{L3} * \sin(\propto +\beta+\mu) \\ \mathrm{L3} * \cos(\propto +\beta+\mu) + \mathrm{L2} * \cos(\alpha+\beta) + L1 * \cos(\alpha) & \mathrm{L3} * \cos(\propto +\beta+\mu) + \mathrm{L2} * \cos(\alpha+\beta) & \mathrm{L3} * \cos(\propto +\beta+\mu) \end{bmatrix}$$

Returning to the previous logic of the analytical solution, it is helpful to express the angles of the actuators in terms of the target position. In general for finding inverse kinematics both sides of the equation are multiplied by J^{-1}. Using this method requires that very small steps in angles, t, from one point to another be taken. Like all numerical methods this is subject to error, the smaller the step size used the more accurate the result.

Equation 13: System describing 2-D, 3-Arm angular movement with respect to positional changes

$$\begin{bmatrix}\alpha\\ \beta\\ \mu\end{bmatrix}_{t+1} = \begin{bmatrix}\alpha\\ \beta\\ \mu\end{bmatrix}_{t} + \Delta t \begin{bmatrix}\dot{\alpha}\\ \dot{\beta}\\ \dot{\mu}\end{bmatrix}_{t}$$
$$\begin{bmatrix}\alpha\\ \beta\\ \mu\end{bmatrix}_{t+1} = \begin{bmatrix}\alpha\\ \beta\\ \mu\end{bmatrix}_{t} + \Delta t J^{-1} \begin{bmatrix}\dot{x}\\ \dot{y}\end{bmatrix}_{t}$$

Thus, at each new step, t, the angles of the joints are defined by the current angles, the inverse of the Jacobian and the change in position towards the goal position. To solve for the update angles at t+1, the inverse of the Jacobian is required. The form of this matrix will depend on the rank of the Jacobian. There are three cases for an m x n matrix: m>n, m=n, m<n. In each of these three cases the pseudo inverse, A^+ of the Jacobian is as follows:

Equation 14: Pseudo Inverse Matrices for m x n Jacobians

$$A^+ = \begin{cases} A^T[AA^T]^{-1} \text{ for m} < n \\ A^{-1} \; for \; m = n \\ [A^T A]^{-1} A^T \text{ for m} > n \end{cases}$$

Thus, in the case described above, the Jacobian is a 2x3 matrix and the pseudo inverse would be defined as: $[J^T J]^{-1} J^T$. Therefore, the solution of angular movement for the three joints α, β and μ to reach the target location x1,y1 is defined as:

Equation 14: Angular change required to update 2-D, 3 Arm angles with respect to position

$$\begin{bmatrix}\Delta\alpha\\ \Delta\beta\\ \Delta\mu\end{bmatrix} = J^+ e$$
$$\begin{bmatrix}\Delta\alpha\\ \Delta\beta\\ \Delta\mu\end{bmatrix} = [J^T J]^{-1} J^T \begin{bmatrix}\Delta x\\ \Delta y\end{bmatrix}$$

Other Numerical Methods

The pseudo inverse method can lead to some instability in converging on the target location when operating near singularities in the robotic arm's workspace. In the case described above, the system approaches singularities when the arm is straightened and the angles β and μ approach zero. Another method can be utilized known as the damped least squares method to find the angular changes needed to approach the target location. This method utilizes a dampening constant λ in order to mitigate instability near singularities and to optimize convergence to the new target location. The Jacobian is still required to find the solution using this method. The fundamental equation for damped least squares is shown below:

Equation 14: Damped Least Squares Method

$$\begin{bmatrix}\Delta\alpha\\ \Delta\beta\\ \Delta\mu\end{bmatrix} = J^T[JJ^T + \lambda^2 I]^{-1}\begin{bmatrix}\Delta x\\ \Delta y\end{bmatrix}$$

The damping constant λ should be selected such that it is large enough to ensure that the system exhibits stable behavior near singularities but should not be so small that it converges on the target location too slowly.

Solving Numerical Methods

Once the system of equations has been developed using either the Pseudo Inverse Jacobian or the Damped Least Squares method, any ODE solving algorithm can be utilized to solve for the change in angles. One commonly used method would be to utilize the **ode23** or **ode45** functions in MATLAB. These utilize 2nd and 3rd order and 4th and 5th order Runge-Kutta methods respectively. These methods can be used to solve the differential equation systems.

Other numerical methods are available to the designer in order solve the systems of equations defined by the various methods described above. Methods such as gradient descent and cyclic coordinate descent are other numerical methods to minimize the error between the end effector and the target position. The basic logic of these methods is to minimize the error function found in Equation 15.

Equation 15: Optimization methods

$$E(\theta) = (P - X(\theta))^2$$

The E(θ) is the error vector from the target position, P, and the current position X. Gradient based optimization is a common method for iteratively minimizing the error function. This generally requires increased computational cost at each step, but yields a quick convergence to the optimum solution. Cyclic coordinate descent is another method which manipulates one joint angle to minimize the error function and then iterates those passes over multiple steps to find the global error minimum for the total joint system. This reduces the computational complexity required.

Summary

The control of the robot is one of the critical items to reach target performance goals. Designers can use forward or inverse kinematics methods to precisely position joint angles to reach desired end effector positions. Inverse kinematics are commonly used to position joint angles as a function of the target end position. If the systems are simple, an analytical method can be used to derive joint angles as a function of end effector position. However, in most real world applications, the use of iterative numerical methods must be used because of the inability to derive closed form analytical solutions.

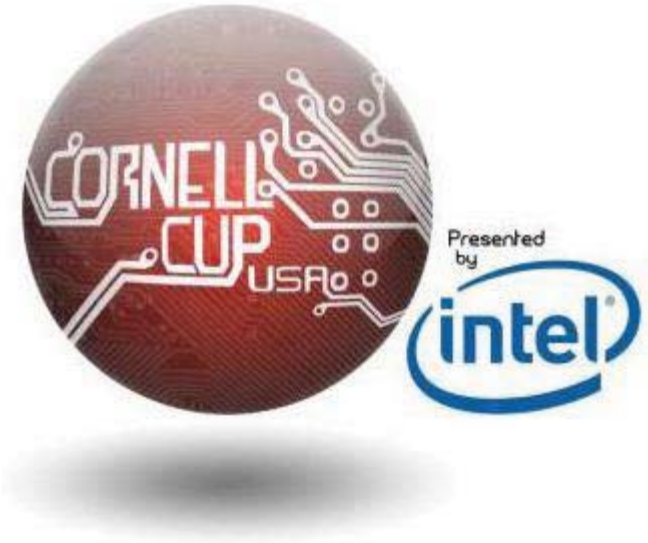

I-3PO

Made for students,
by students

Table of Contents

1 Neck

1.1 Problem Description for neck

Cornell Cup USA project team built a C-3P0 themed humanoid robot for the competition on May 3-4, 2014. Instead of having a normal, fixed neck, the team decided they wanted to implement a telepresence solution using the Oculus Rift (In this paper, also called the Rift). In order to do that, a neck must be created on the robot that would allow for 3 degrees of rotation of the head, in which there are embedded two cameras for use with the Rift. The system must be responsive and accurate enough such that the wearers of the headset do not get motion sick, something that is very common when using the Rift.

1.2 Oculus Rift and telepresence

The Oculus Rift is a virtual reality headset primarily used for video game purposes. It consists of a plastic casing that entirely covers the user's field of view. Inside the casing there are two small screens pointed at the user's eyes that show the same image from slightly different angles to allow for the parallax effect. The Oculus Rift also contains accelerometers that measure the roll, pitch, and yaw of the headset.

For the telepresence solution, the three accelerometers are mapped directly to three servos that control the neck, and two cameras in the head stream their feed directly to the screens of the Rift. This allows for the illusion that the user is viewing the world the I-3P0's eyes and is controlling the movement of the robot's head.

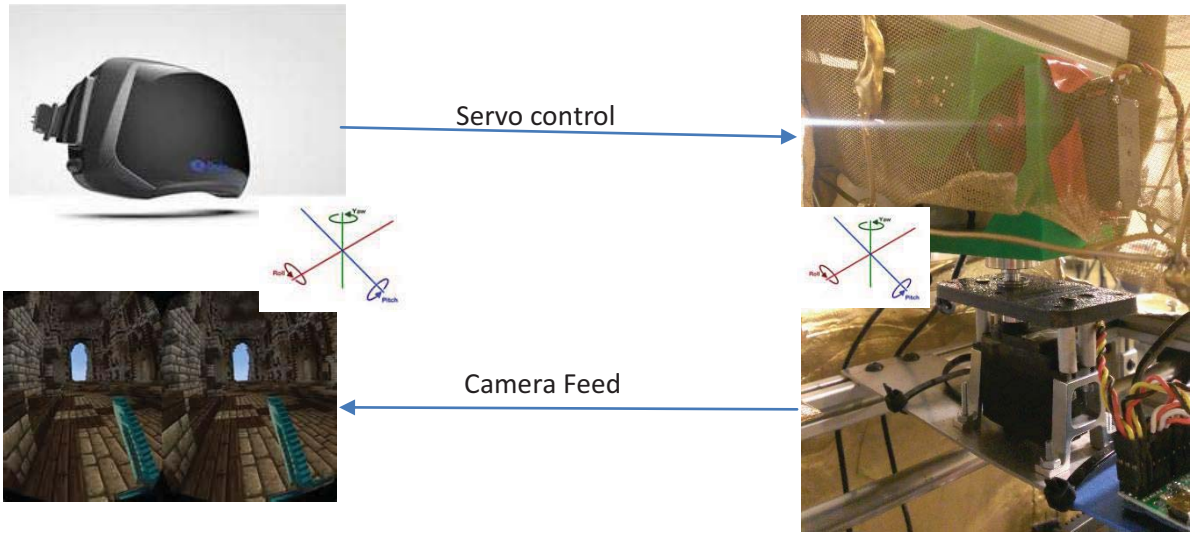

Figure 1: Flow of communication in the setup

1.3 Timeline

A timeline for this design is shown here. Each task is paired with a deliverable that is displayed in this paper.

Deadline	*Task*	*Subtask*
9-Feb	Research existing pan/tilt systems	
11-Feb		Compile sketches of designs
13-Feb		Develop pros/cons of each design
14-Feb	Determine necessary features	
16-Feb	sketch final design	
23-Feb	CAD design	
24-Feb	determine materials	
26-Feb		create stress analysis
28-Feb	order parts	
27-Feb		research vendors
1-Mar	machine part	
1-Mar		create drawings
7-Mar	assemble pieces	
15-Mar	Test system	
1-Apr		iterate on design

1.4 Research

Pan/tilt systems are very common in camera architecture. Consistently, the pan (left/right)

2:Left: http://cinecity.co.nz/ Right: http://thingiverse.com

motion is on the load bearing (first) joint. Existing systems have each joint in succession, so each joint has to bear the load of the successive joints. The pan motion is chosen for the first joint because it does not have to lift against gravity. Being the first joint, having to move around two joints later, this would require the least amount of force.

Each of the two above systems have the tilt system supported on both sides of the camera, this is definitely something useful to look for in a design. When servos are holding position with a large load, they are known to exhibit quite a bit of noise, something that is undesirable in our setup. Having this load bearing on one of the intermediate axis may quell that effect a little.

A Pan/tilt system designed for servos is readily available for purchase from servocity.com. There is one of this model in the lab, so that was used for even closer investigation.

Figure 3: existing servo pan tilt system

The two degree system shown here consisted of many small plastic plates held together by screws. While the design worked well kinematically, in practice, the joints were flimsy and deformed a lot under the load of a head. However it is a good model to base the methods of how to orient the servos on. Also, the servos are connected to the brackets via small servo arms. The screws that connect the pieces often strip the plastic and come loose under large loads, which is something I want to reduce.

Servo supply companies like servo city have in stock a large variety of servo mounts and accessories including plates with bearings, 90° mounts and others. The one pictured below would be good to base the yaw motion servo off of because the bearing through the plate would constrain any translational motion. As discussed before, the yaw motion is moving the most weight, so it is the most important to be reinforced.

Figure 4: potential example of a good pan system

1.5 Determine necessary features

A list of functional requirements for the system is shown here:

- Provide 3 degrees of control. Roll, Yaw, Pitch
- Provide 180° for Yaw
- Provide 90° for Roll and Pitch
- Have noise levels low enough such that users do not get motion sick
- Support a 2 lb head on the end effector

1.6 Sketch final design

Next I drew some sketches about what I wanted the shapes of the brackets to be in to allow for 3 degrees of movement. The yaw is very similar to the servo city model shown above, with normal servo mounting brackets extending down to mount the system. Extending up from the servo, an extender arm passes through a bearing in a horizontal plate so that the yaw axis is fairly well constrained.

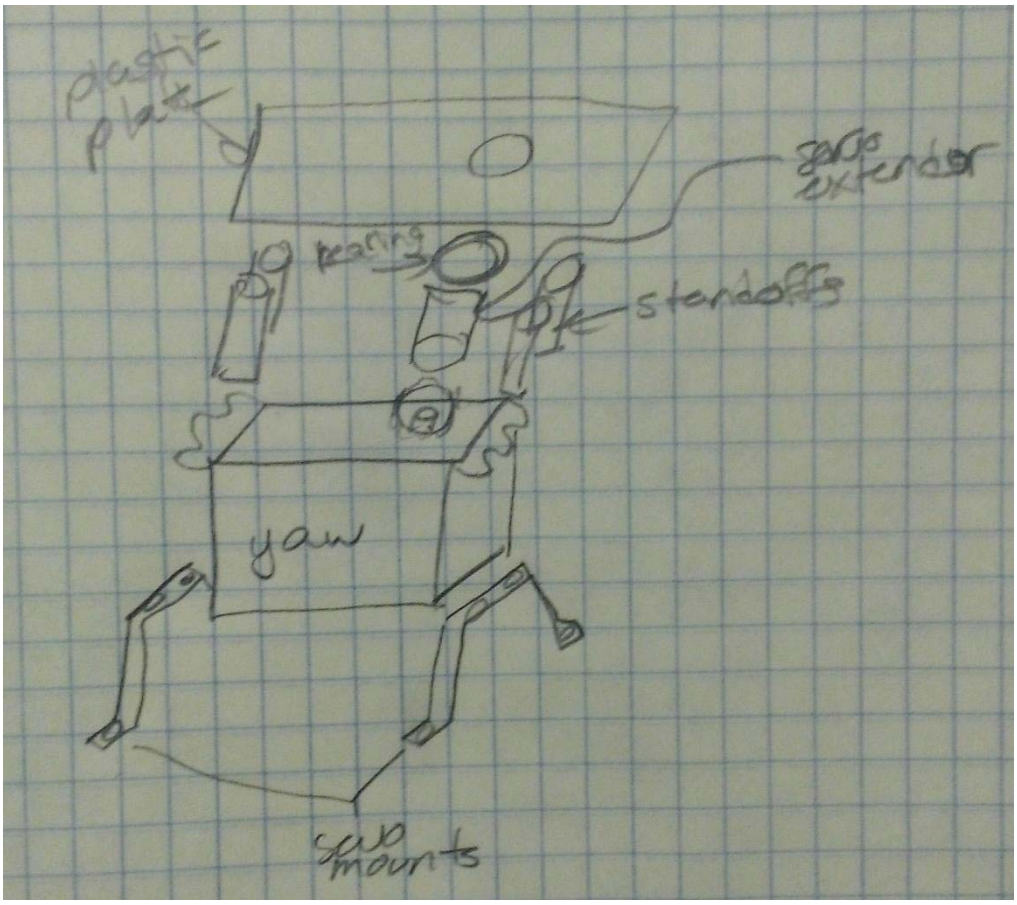

The next bracket is a 90 degree connector so that the next servo can be mounted vertically. This is different than any of the research pieces because I decided to put a strut in the bend of the bracket to increase the rigidity, and also there is a servo shaped hole so that the servo can be mounted directly into the bracket and not connected to some servo-arm interface that becomes loose.

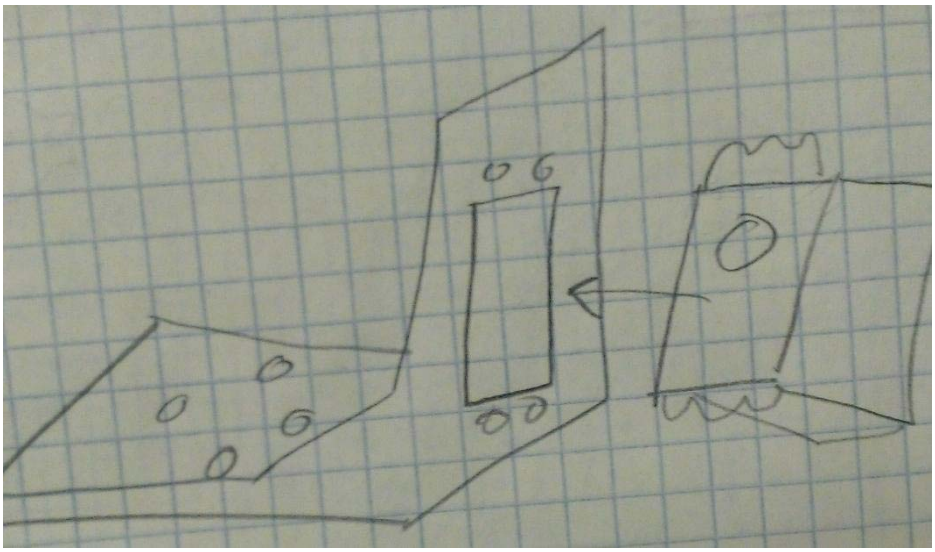

The next bracket consists of a flat plate that the servo rests on, with two arms extending out from either end to secure the servo into.

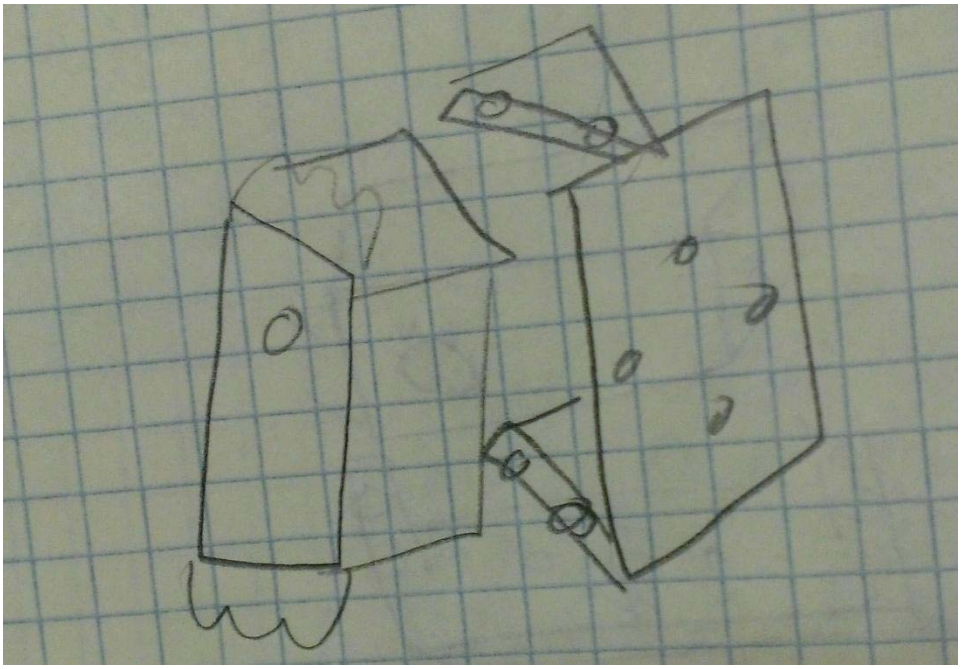

The final bracket is similar to the first 90° bracket, except without a servo shaped hole in it, because this will be used to mount the head to. It is the end effector.

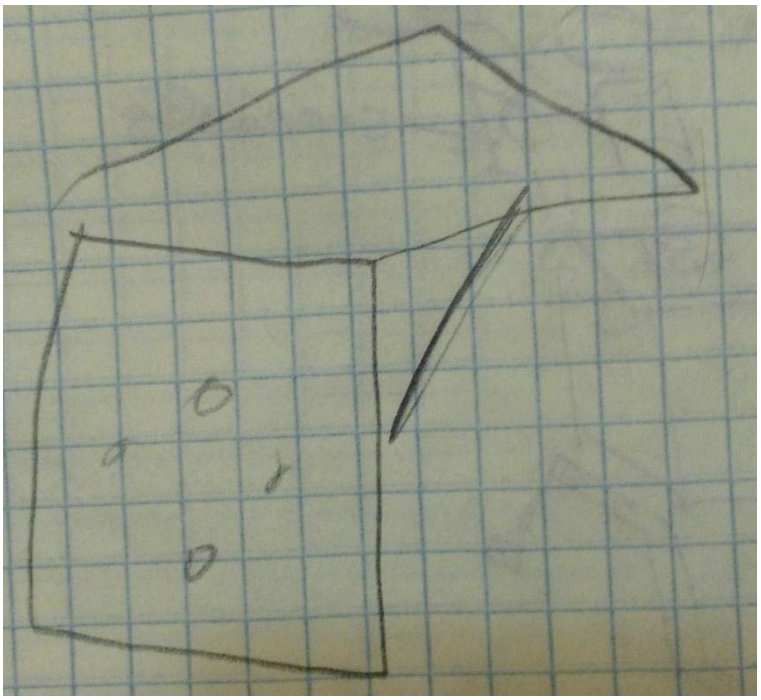

1.7 CAD design

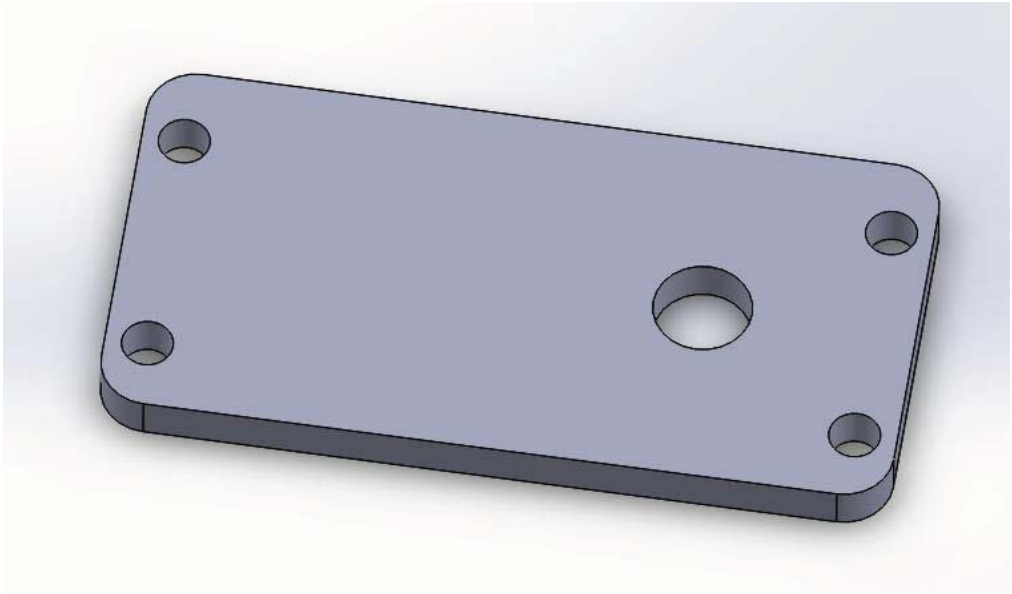

Figure 5: Yaw axis support

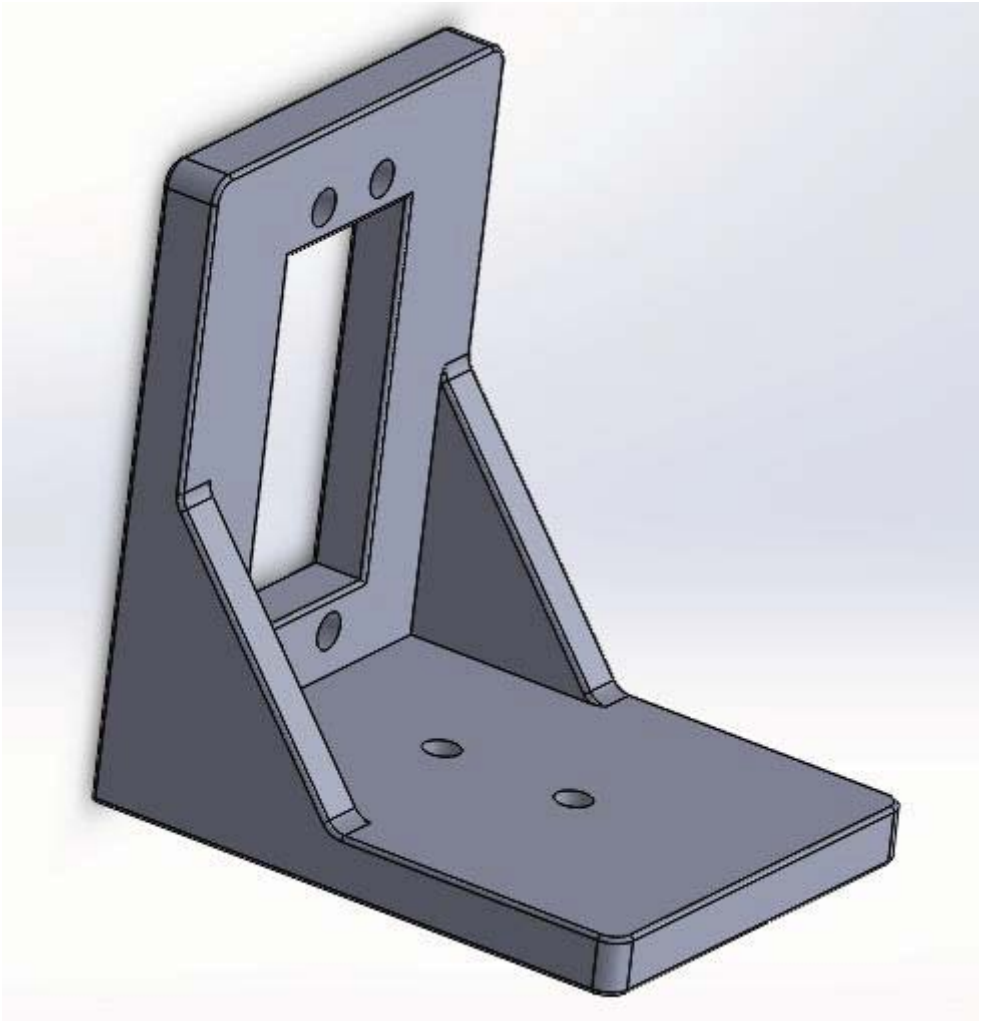

Figure 6: Yaw axis bracket

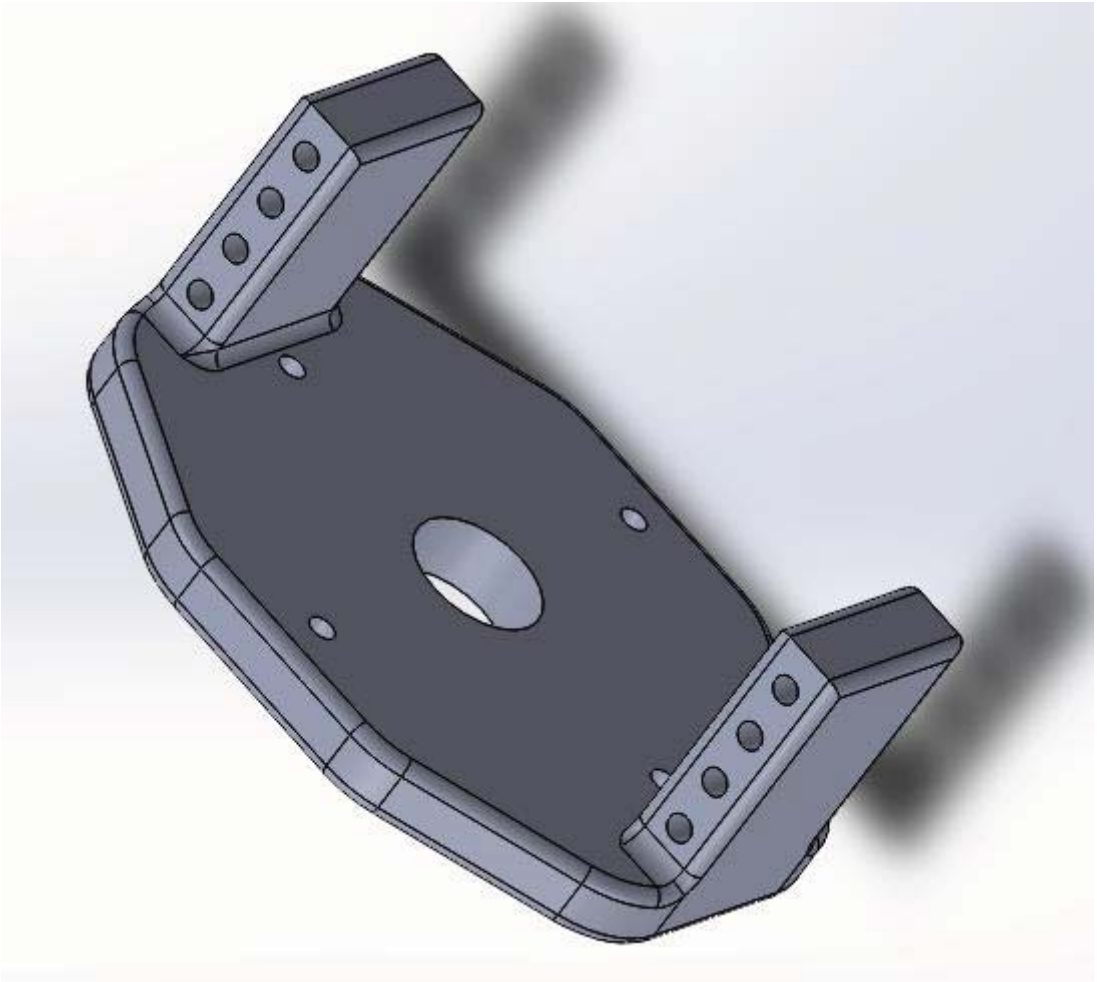

Figure 7: Roll axis

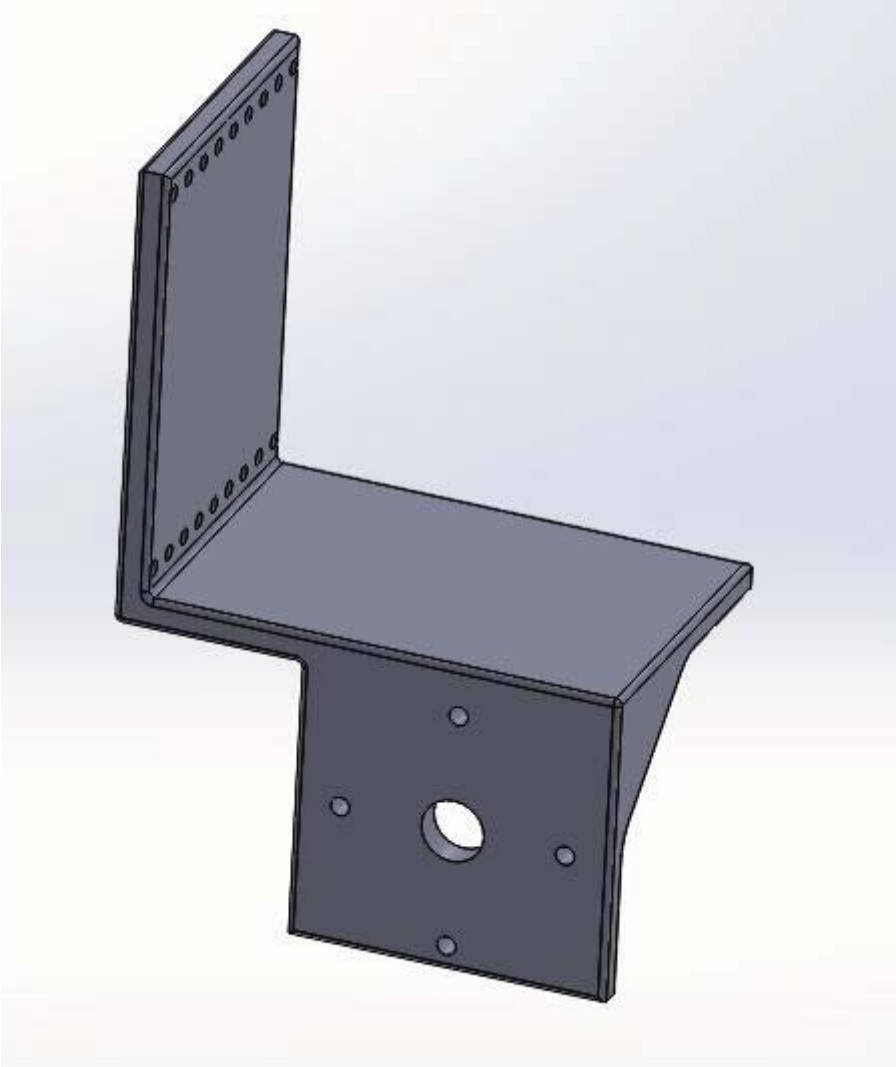

Figure 8: Tilt axis/ end effector

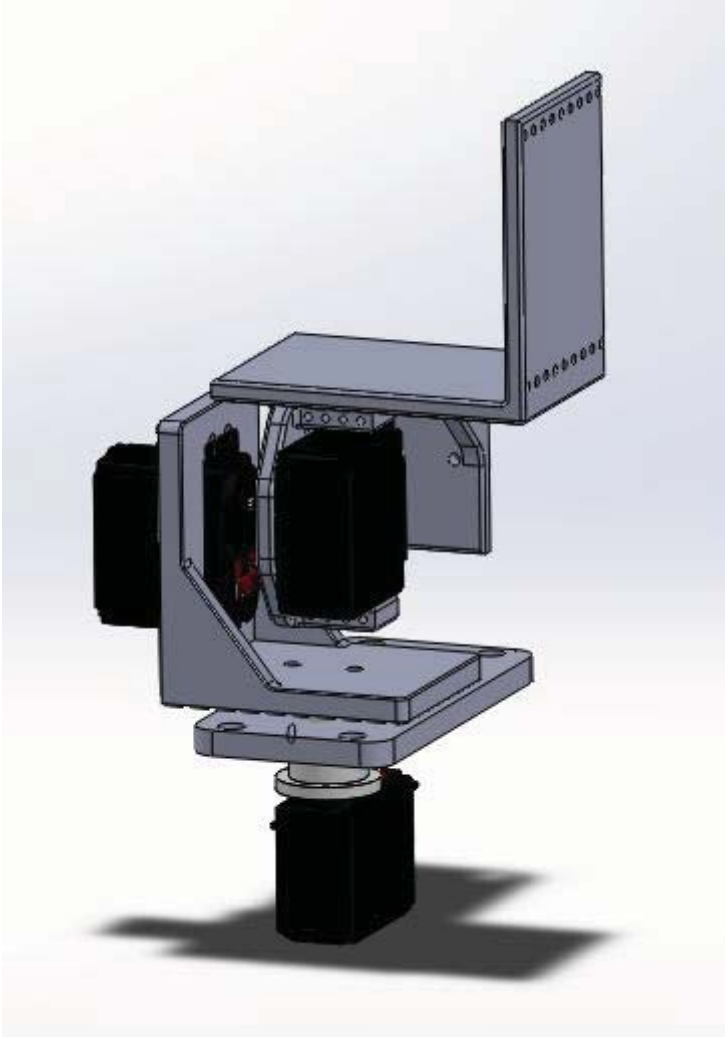

Figure 9: Complete neck assembly

1.8 Determine materials

To guarantee rigidity, the obvious material to make this out of would be metal plates. However the shaping and cutting of such small metal material is non-trivial, and it also weighs more than other solutions, so I decided against that route.

Researched options were generally made out of plastic, however to obtain the strainge shapes of the brackets, each one consisted of multiple pieces of plastic held together by screws. Also, plastic is so malleable, that under load, the screws holding plastic joints can become loose cause the system to wobble, or even fall apart.

However, with the onset and availability of 3D printing, I now have the ability to make complex shapes out of plastic with a single piece. This allows me to reinforce the shapes with struts, make custom shaped holes to eliminate the need for the servo arms. It also allows me to rapidly iterate on the design/ make duplicates.

1.9 Order parts

Once the CADs were complete, I passed them off to Cornell's rapid prototyping lab, and would often get them back the next day.

Screws, standoffs, and bearings were bought from mcmaster.com

Part	Purpose	Part Number	price
M2.5 Screws	Screw in face of servos, attach hubs	92290A055	3.81
8-32 screws	Servo mounting	91735A199	5.40
Standoffs	Mount for yaw plate	91125A220	2.58 ea.
Bearing	Yaw motion constraint	57155K387	5.21

Servo arms, servos, and servo mounts were purchased from servocity.com

Part	Purpose	Part Number	Price
Hub horn	Connect servos to brackets	525130	4.99 ea
Hitec 625MG	Servo	32625S	31.49 ea
Servo mount	Mount yaw servo	SVM275-115	6.99

1.10 Machine parts

Because 3D printing was utilized, no machining was necessary

1.11 Assemble pieces

Assembly of the pieces is a delicate process. The steps are outlined here

1. Press fit bearing into horizontal plate
2. Attach plate to servo via standoffs
3. Manually center the servo position, and place the servo extender and hub onto the yaw servo in the position it will be in when facing forward
4. Screw in the first bracket to the yaw servo hub.
5. Screw servo into the proper hole, with the gear on the upper side
6. Manually center the servo position, and place the next servo hub onto the roll servo in the position it will be in when facing forward
7. Screw the next bracket onto the hub and place the final servo in its place with the gear on the upper side
8. Manually center the servo position and attach hub on servo in the orientation it would be in when facing forward.
9. Attach final bracket to the servo hub.

1.12 Test System

A video of the system in action can be found at the link
https://drive.google.com/file/d/0B1Mhh4L-xJ28QzlQZmJWT05lemc/edit?usp=sharing

The only issues with the initial run were:

- there was no good way to attach the cameras to the end effector, so the design changed from that of the sketch to the final CAD, adding a mounting plate for the cameras.
- After diassembling and reassembling the system multiple times, the threading in the plastic became loose which caused issues with fastening.

The only iterations on the design we the addition of the camera mounting plate, and the removal of a corner on one of the pieces to fix a collision.

1.13 Future work

The first thing to do would be to reprint the whole assembly to fix the problems of the loose screws. Because of minor mistakes in assembly and transportation, the screws have become loose. 3D printed holes act like lock-nuts, the first time you screw something in, it cuts little threads into the plastic, that are very hard to remove, but if you do end up taking the screw out, the fit is never quite as tight. Since the 3D printed holes act in this manner, a fresh set of holes would offer the best fit.

Also, on the first $90°$ connector, it would be good to add in a bearing support on the opposite side of the servo head, like in many of the researched examples. The stress incurred during operation can cause stripping of the plastic gear that is attached to the servo head.

2 I-3P0 Arms

2.1 Initial Definition of Tasks

When we first took on the task of designing I-3P0's arm, the first task we completed was getting an initial idea of what tasks we wanted I-3P0 to accomplish. At this point, we did not worry about what was feasible to design in the given period of time. Instead, we concentrated on coming up with any possible objective that we could potentially want I-3P0 to be able to do with his arms. This allowed us to gain an initial idea of what to look for when researching, so that we could pay special attention to see how these problems or other similar problems might have been solved in the past.

2.2 Initial Research

When we began researching, we wanted to get a good idea of the different types of arms that had already been created and begin looking for potential solutions to some of the initial tasks that we had defined. We were told to keep in mind that there were many different ways to build a solution for how to get I-3P0 to accomplish a task. For example, one of the jobs we wanted I-3P0 to be capable of doing was to sign his name. We were told that in addition to physically signing his name with a pen and forming each of the letters individually, to also consider more creative ways such as stamping his name or printing his name with a printer.

When we started looking for ideas, we came across many different types of arms. Many of the arms we found were arms that were meant for assembly lines. We also came across prosthetic arms and arms designed to help people with disabilities. Additionally, we discovered some arms that had been designed specifically for droids. As we came across designs that we liked, we were instructed to write down anything that might be helpful in order to prevent us from having to do the same research multiple times. While these documents had links to the sources, they also contained enough figures and descriptions so that it was unnecessary for anyone looking at the document to need to go back to the source to gather the pertinent information.

2.3 Performance Definition

The next step in the research process was creating a performance definition. One purpose of the performance definition was to come up with a consensus of what we want I-3P0's arms to be able to do on a technical basis. We decided that we wanted three degrees of freedom in the shoulder (twist, bird, and punch motions), two degrees of freedom in the wrist (left/right and up/down motions), as well as being able to power down and hold the position that the arm was in. Additionally, we came up with metrics on what we wanted the range of motion to be and the speed and acceleration with which we wanted I-3P0 to be able to perform the motion at. Since all motions were rotational, the range was given in degrees, the speed was given in degrees/second, and the acceleration was given in degrees/second^2. In order to determine the range of motion and the speed at which we wanted the arm to move, we used our own arms to model what different ranges and speeds would look like for different motions. In order to come up with the acceleration, we doubled the number that we had

come up with for the velocity. This was because if the value for the acceleration of an object is at least twice the value of the speed of the object, an object is generally perceived as moving faster.

2.4 Actuator Research

The next step in creating I-3P0's arm was to begin researching in depth different solutions that would be able to meet our performance definition. We originally considered four different ways in which we might be able to actuate the arm. The options that were considered were servos, linear actuators, motors, and pneumatics.

2.4.1 Servos

We found that one of the major benefits of servos is that they are relatively small and light-weight. Additionally, they have a large range of motion and are relatively inexpensive. They are also easy to use and assemble. On the flip side, they do not accelerate particularly quickly. Furthermore, they are not as precise or as strong as other actuators.

2.4.2 Linear Actuators

In researching linear actuators, we noticed that while they were good at handling large torques and are easy to work with, they had many drawbacks. The primary drawback was that they are really slow. Additionally they are fairly bulky and do not have a large range of motion.

2.4.3 Motors

For motors, we discovered that the major pros were that they have a large torque capacity, a large range of motion, and can accelerate quickly. While they are bigger than servos and, they are generally decently sized; however, the bigger drawback is that they can be heavier. While motors can be more expensive than other actuators, they are definitely within the budget.

2.4.4 Pneumatics

Pneumatics uses pressurized gases to create mechanical motion. It allows for a high torque capacity and will allow for the arm to move and accelerate quickly. However, it is also really expensive, bulky, and does not have a large range of motion. Additionally, it would be really hard to assemble and repair, and working with gases would introduce another set of difficulties.

2.5 Decision Matrix

After researching different methods to actuate the arm, we created a decision matrix to help us objectively weigh the pros and cons of each different method. The first step in creating the decision matrix was listing the attributes that were important to us. We categorized the attributes into four different categories: general attributes, attributes dealing with the range of motion, attributes dealing with angular acceleration, and qualitative attributes. The general attributes were size, cost, power usage, speed, and torque capacity. Range of motion considered the range of motion for the wrist left/right motion, the bird motion, the punch motion, the twist motion, and the wrist lift motion.

Angular acceleration attributes took into account the angular acceleration for those same five motions. The qualitative attributes were the ease of assembly, reparability, durability, ease of use, and manufacturability. After listing all of the attributes, we came up with metrics for each of the attributes so that we could quantitatively rate each one. Additionally, we also listed what our minimum requirement for the part was. This way, we would be able to easily eliminate any actuators that did not meet the minimum criteria, and therefore would be unsuitable to use. Next, we created a normalizing scale. We decided that for each attribute, we would give each type of actuator a one, a three, or a five, depending on how well it exceled in that area. A five was the best rating an actuator could receive and one was the worst. A one generally meant that the actuator either did not meet or just barely met the minimum criterion. If an actuator was extremely unsuitable for doing a particular task, it was given a zero for that criterion. When coming up with the normalizing scale, for every attribute, we had to define what a one looked like, what a three looked like, and what a five looked like. Furthermore, we had to make sure that all cases were covered in the scale. After coming up with a normalizing scale for each attribute, we weighted each attribute, so that attributes that were more important received a higher weight. Finally we gave each type of actuator a one, three, or five for each criterion based on the normalizing scale and then multiplied the rating by the weight to get the weighted rating. The weighted ratings for each attribute were summed for each type of actuator in order to see which actuators appeared to perform best under these conditions. After all of the calculations were completed, based on the decision matrix, the servo had the most points. The servo was closely followed by the motor. The linear actuator and the pneumatics both received similar ratings that were much less than the servos and the motors.

2.5.1 Motion Specific Decision Matrices

After creating a large decision matrix encompassing all five different motions, we decided to come up with decision matrices that were specific to each different type of motion. This decision was made as a result of the fact that it was unnecessary to build the entire arm out of the same actuator and different types of actuators could potentially be better for different types of motion. While the servo still came out the forerunner for each different type of motion, it did slightly distance itself from the motors. Additionally, the linear actuator fared much better, as it received scores that were comparable to the scores for the motors. However, pneumatics still scored way below the rest of the actuators.

2.6 Original Design

Based on the scores of the decision matrices and how each of the different actuators was rated for different attributes, we originally decided to use motors in the shoulders and servos in the wrists. Even though the servos scored higher in the decision matrices for all of the motions in the shoulder, we wanted to make sure that there would be sufficient torque. For the wrist, on the other hand, we wanted to make sure that the actuators were as light as possible, as extra weight in the wrist greatly increases the torque in the shoulder. While linear actuators scored decently for each of the individual motions, and even scored better than motors for all of the shoulder movements, we thought that they were too slow to give us the desired results in the shoulder and too bulky and heavy to be in the wrists.

2.6.1 Finding Specific Actuators

After deciding on the type of actuators we wanted to use, we needed to search for the specific models that we wanted to use. In order to decide on the motors that we wanted, we used the process outlined in the motor selection guide. To figure out which servos would be best to use, we looked up specs for the servos on Servo City's website. We first found which servos would be capable of handling the required amount of torque. From there, we considered other factors including size, cost, and angle of rotation.

2.7 Current Arm Design

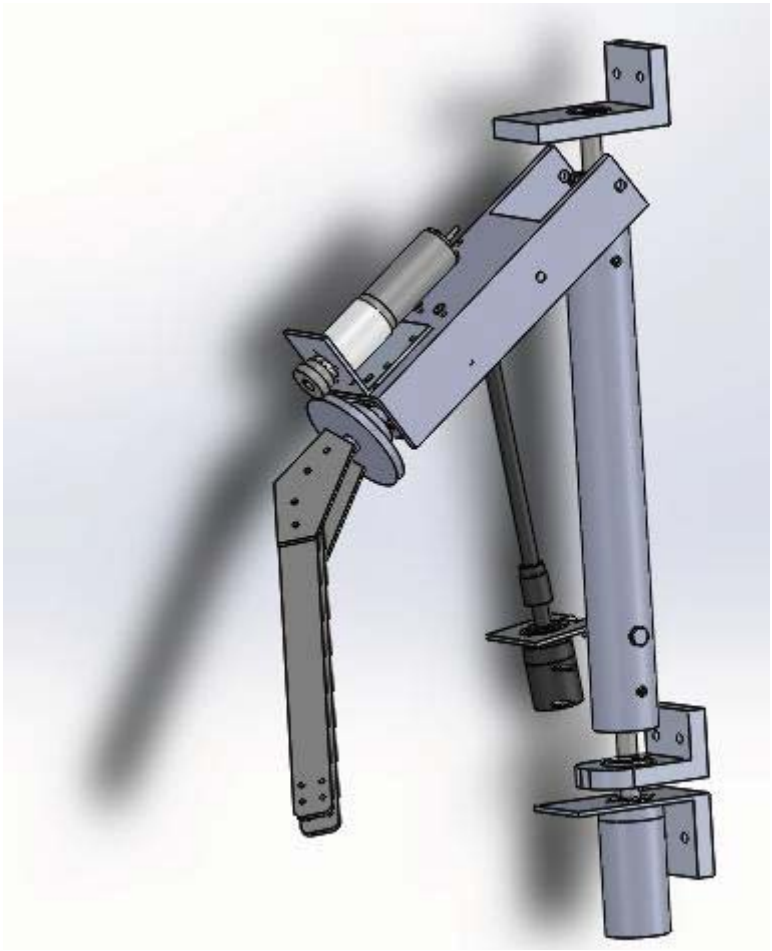

Figure 10:The Current I-3P0 Arm

The current arm design features a total of 5 revolute joints, 3 joints that make up the shoulder, and two joints that make up the wrist. A human's arm has a total of seven revolute joints, three in the shoulder, an elbow, and three in the wrist. It was determined that a seven jointed arm would be more complex than necessary. As many joints as possible were removed while still maintaining the required functionality. This resulted in the removal of the elbow joint and a wrist that is unable to rotate.

The Original design featured a set of successive joints with the motors located in the shoulder. This design had many flaws. One flaw was that it needed large high power motors because two of the motors needed to work against gravity. Another flaw was that because the motors were located in the shoulder the center of mass was fairly high. This would also require each motor to have an external gear system. Finally this design needed a lot of unique complicated structures that would have to be custom machined. These flaws prompted a change to the current design picture above.

The Current arm design moves two of the shoulder motors down towards the waist area. This causes the center of mass the shift down which will help with the overall stability of the robot. The design change also makes it so that only one motor has to work against gravity. This allows for smaller less expensive motors to be used. The two motors moved down to the waist no longer require external gearing and the new system as a whole is comprised of mostly stock parts. The main downside to this design is that the lift motor uses a spindle drive which is very expensive.

2.8 Lower Arm Concept

I3P0 lower arm was not previously designed in the last semester. The lower arm design was required to attach the hand to the motion of the upper arm.

2.8.1 Lower Arm Requirements

Due to the time frame, the lower arm, including the elbow was to be created via a fixed elbow design. The elbow design would be attempted again later in this document. The arm is required to support 1.5 kg of mass held in the hand and enable I3P0 to write his name. These requirements focused on strength and precision.

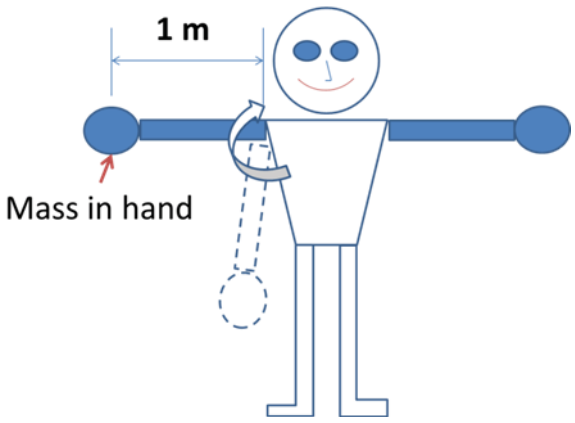

Figure 11: Front View - arm fully extended with mass in hand

2.8.2 Transforming requirements into measured values

The arm must support 1.5 kg at a distance of 1 m from the shoulder joint, as shown in Figure 11. The attachment for the lower arm is roughly half of that distance.

The torque is assumed to be related to gravity and the mass in the hand. The torque moment placed on the attachment point of the shoulder is located at 0.5m

Torque due to Gravity ($M_{gravity}$) = $mgL = m_{hand}gL = (1.5kg)\left(9.81\frac{m}{s^2}\right)(0.5m) = 7.36\ Nm$

The mass of the arm itself will need to be added into the equation, once and architecture is selected. Different designs will place different moments at the joint that interfaces the upper and lower arm.

2.9 Concept Generation

There are many ways to attach the upper arm to the shoulder and many concepts were generated. The designs needed to be rigid and lightweight. After narrowing down the possible options to designs that were remotely feasible, there were two concepts that required further review.

2.9.1 Carbon Fiber arm

The carbon fiber tubes from DragonPlate.com that is located in Elbridge, NY, roughly 45 minutes from Cornell's campus provided very light weight tubing that could be a major benefit to the overall.

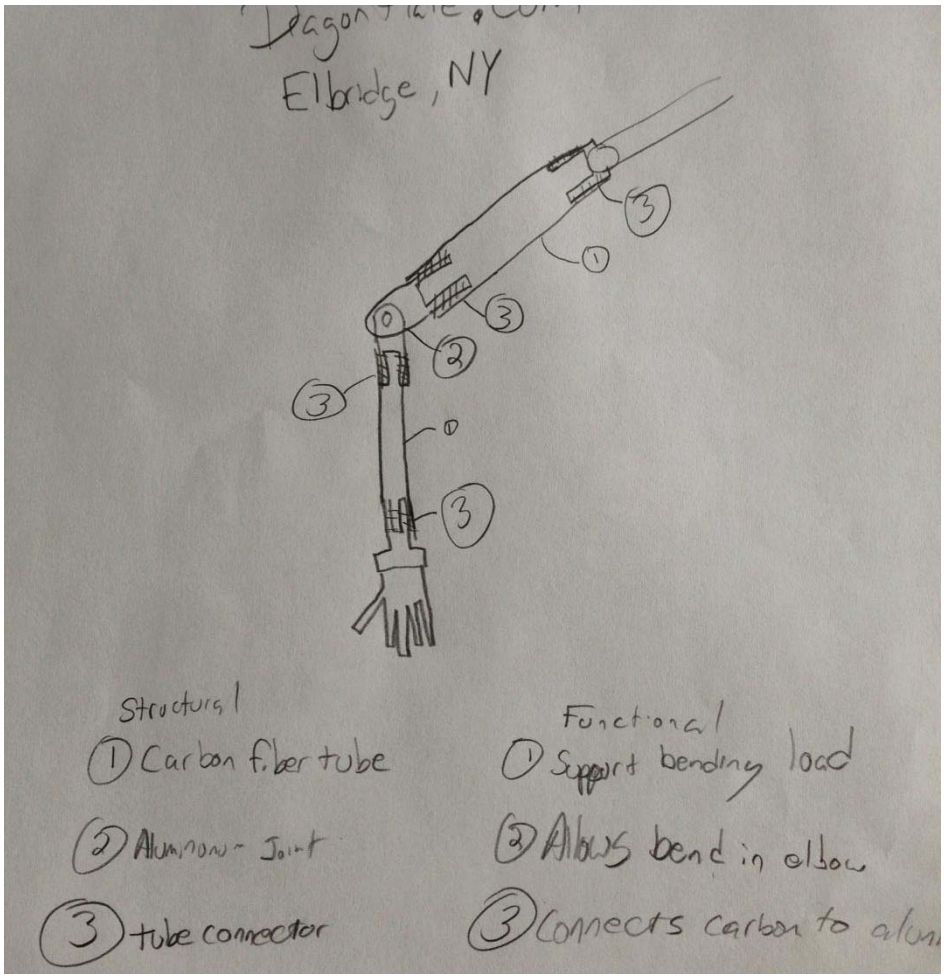

Figure 12: Initial Carbon Fiber concept sketch

Figure 13: Carbon fiber tubing example

Figure 14: Carbon fiber tube end - Female

Figure 15: Carbon Fiber tube end - Male

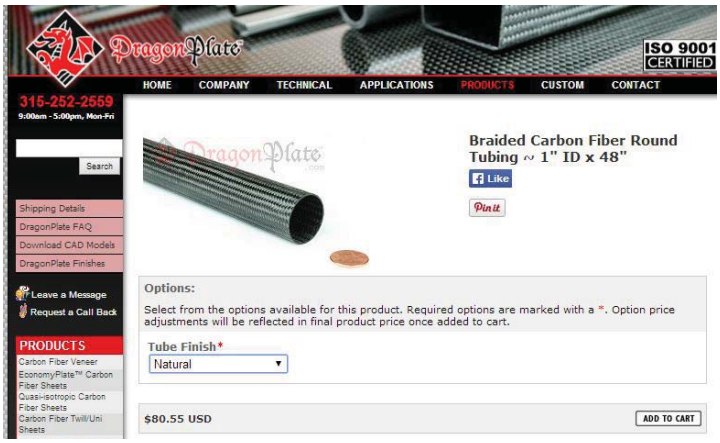

Figure 16: Carbon fiber tubing price

2.9.2 Two Plate Concept

The two plate concept was created in response to concerns for our ability to acquire materials quickly and manufacturing capability at the Cornell shop. This concept is more simplistic but easy to manufacture.

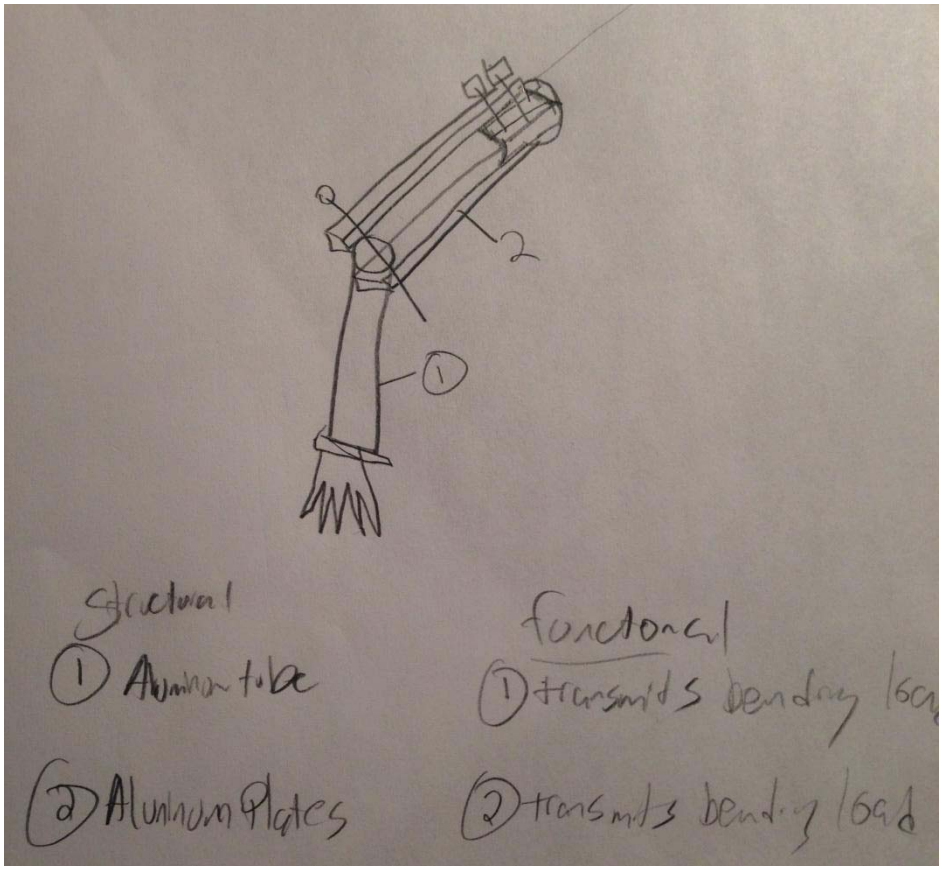

Figure 17: Initial two plate concept sketch

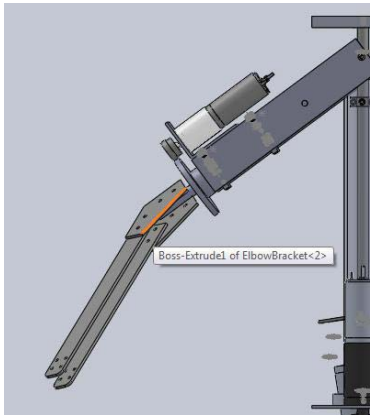

Figure 18: Two Plate design as shown in Solidworks

2.10 **Concept Selection**

The two chosen concepts were both excellent ideas; however, time and our ability to make the parts became a significantly limiting factor. You can see by the weighting factors in the decision matrix in Figure 19. If there was more time available, the carbon fiber arm had significant technical advantages due to stiffness and weight.

Attribute	Metric	Carbon Concept	Two Plate Concept	Weight	Carbon Concept	Two Plate Concept
Weight	kg	5	3	1	5	3
Stiffness	mm/kg	5	3	2	10	6
Ease of assembly	# steps	3	3	5	15	15
Time to aquire	Days	3	5	5	15	25
Time to fabricate	Days	3	5	5	15	25
				Total	**60**	**74**

Figure 19: Decision Matrix for lower arm

The two piece arm was selected due to its ease of manufacture, time to acquire parts, and time to fabricate. Additionally, any re-work can be handled at the Cornell lab.

2.11 **Right Wrist Design**

The first change that was made to the wrist design was to use less powerful servos. This change was brought about for two different reasons. First, it was cheaper and more convenient to use less powerful servos because we already had them in the lab. Second, when we had originally specked I-3P0, we wanted him to be able to hold a five pound mass; however, as our plans became more concrete, we realized that metric was a gross overestimate of the amount of weight that he would need to hold. The right hand was designed to be able to wave (which would not require him to hold any additional weight) and shake hands (where the weight of the person's hand he would be shaking would be supported by that person and not the droid). Therefore, the only weight that the servos would need to support was the weight of the hand, allowing us to use servos that were already available to us.

The second change that was made was to reorient the servos. Originally the servos were configured in the same way as the servos on the left wrist, which would have allowed I-3P0 to move his hand to the left and right as well as up and down (directions of movement refer to when the palm is facing the ground). The problem with this orientation was that even with the bird, twist, and turn motions in his arm, there was no way to change the orientation of his hand so that his fingers would be parallel to the ground when shaking hands with someone and perpendicular to the ground when waving. Additionally, there was no motion that we wanted I-3P0 to do that would require him to move his wrist up and down. Therefore, in order to allow him to orient his hand to the correct positions for waving and shaking hands, we reconfigured the orientation of the servos is his wrist. This gave him the ability to rotate his hand along the axis of the arm as well as move his hand right and left (see Figure 20).

Figure 20: New orientation of servos. The photo is oriented so that the palm of his hand is visible. The bottom servo allows for the twisting motion and the top allows for the right and left motion.

The third change that was made to the design of the wrist was changing the way the servos in the wrist were connected. When the hand was built, we realized it was a lot heavier than anticipated. We feared that the plastic mounts used in the original design would be too weak to support the hand and any moments applied to the hand from people shaking it, so the whole connection was redesigned so that it could be made out of aluminum. We used a Hitec ServoBlocks kit (a servo plate, a ball bearing plate, a servo spline shaft hub, and two hub plates) similar to the connector shown in . To connect the second servo we used a mount that had been made for a previous robot (see **Error! Reference source not ound.**).

Figure 21: Right wrist servo connector

Figure 22: New way to connect servos in right wrist.

Finally, we came up with a way to attach the wrist to the forearm. To do this, we used two more hub plates which connected the servo plate to the forearm. Locknuts were used to keep the screws in place. When the mount was attached to the forearm, the screws connecting the servo plate to the hub plates

were not aligning properly, as the servo plate was slightly too wide. In order to make everything fit nicely, we sanded down the sides of the servo plate a little bit.

2.12 **Right Hand**

As mentioned previously, the right hand was tasked with two objectives: wave and shake hands. While waving did not require the fingers to move at all, we wanted the hand to be able to grip another person's hand when shaking. When researching ideas, the first thing that we looked at was toy hands. The way that toy hands work is that when you push the button, it pulls the connecting rods towards the handle of the toy. The rods are connected to the tips of the finger, causing the fingers to bend.

When researching toy hands, we came across a hand that someone had made based off of the same concept. It used plastic tubing and string and allowed each of the fingers to be animated separately. The hand was designed to be operated manually, so that when a person pulled on a string, the corresponding finger would bend.

We decided to take this idea and modify it slightly so that we could hook the fingers up to a servo in order to automate it. We used tubing that had a 0.75" outer diameter and 0.125" thickness. After making the hand, we determined that it would have been better to use tubing that was thinner and more flexible, as it took a lot of force to move the fingers. For the string, we first tried using wire, as it was available in the lab. However the wire stretched too much, requiring even more force, and if pulled too much it could break. Therefore we ended up using 0.058" nylon twine that had a breaking strength of 150 pounds, which was a lot more force than we would need to apply to it.

In order to construct the hand, we traced a hand on a piece of paper and marked all of the places on the paper hand where the fingers bent. We then cut the tubing so that it was about an inch longer than the distance from the tip of the finger to the bottom of the hand. Once all of the tubes were cut to length, we marked where all of the joints were on the tube and cut out holes in the tubing where the joints were. The holes were made big enough that the tubing can bend there easily. Since the tubing was not completely straight, we cut the holes on the inside arc of the tubing. This made the fingers look more natural. After we finished cutting out the joints, we took the string and threaded it through the tubing. We tied the string around the top most section of the tubing, and left more than a foot of string at the other end for each finger. In order to make it easier to move the fingers in the future, we pulled the string as tight as possible and taped it to the end of the fingers so that all of the joints were bent and let it sit overnight.

After the fingers had a chance to sit for a while, we attached all of the fingers except the thumb together. To do this, we untapped the string and straightened the fingers out. Then we lined up all of the fingers and taped a piece of sheet metal that was about the width of the hand and about .375 inches tall across the back of the hand when the knuckles would be using electrical tape. The next thing we did was get two more pieces of sheet metal that were about the width of the hand wide and about an inch

long. In both of these pieces of metal, we drilled two holes so that one hole was centered in the space between the pinky finger and the ring finger and the other hole was centered in the space between the middle finger and the pointer finger. We drilled the holes so that they were large enough that the screws would fit through them. In one of the two pieces, we drilled four additional holes so that it could be attached to the metal servo hub. After all of the holes are drilled, attach hub to the servo, the metal to the hub and then squeeze the hand between the two pieces of metal and secure with the screws and lock nuts. Finally, we attached the thumb with electrical tape. After it was completely assembled, we added golden tape around it to make it look more aesthetically pleasing.

The last thing we did was mobilize the fingers by attaching them to the servo. Because the plastic was not as flexible as desired, it required a servo that was able to provide more torque. When attaching the hand to the servo, it was determined that it worked better when the strings were pulled straight than it did when the strings were pulled at an angle. In order to pull them all straight, holes were drilled in a piece of sheet metal about the width of the hand and half an inch long was. We drilled four holes on the one side of the piece of metal so that there was the same amount of space between them as there was between the strings. On the other side, we drilled one hole in the center. We then tied the four strings attached to the fingers to the piece of metal. We then tied a different piece of string to the single hole on the metal and tied the other end to the servo arm. When attaching the string to the servo arm, it was important to put the right amount of slack in the string so that the servo would be able to move the fingers, but the fingers would not move when other motors or servos in the arm or wrist were moved. In order to prevent unwanted movement, we chose a servo arm that was fairly large (about 3 inches long) and added enough slack in the string so that when the servo had rotated 90 degrees the string was finally pulled taut, and then as the servo rotated from 90 degrees to 180 degrees, the fingers would clench. One problem that we encountered was that the fingers were not all moving the same amount when they were being pulled. In order to resolve this problem, we taped the fingers together at the tips so that they would move together. The servo that was attached to the fingers was attached to the inside of the forearm with a servo plate and a hub plate. To see the final product and how it was attached to the forearm, see **Error! Reference source not found.**, **Error! Reference source not found.**, d **Error! Reference source not found.**.

Figure 23: View of palm of right hand.

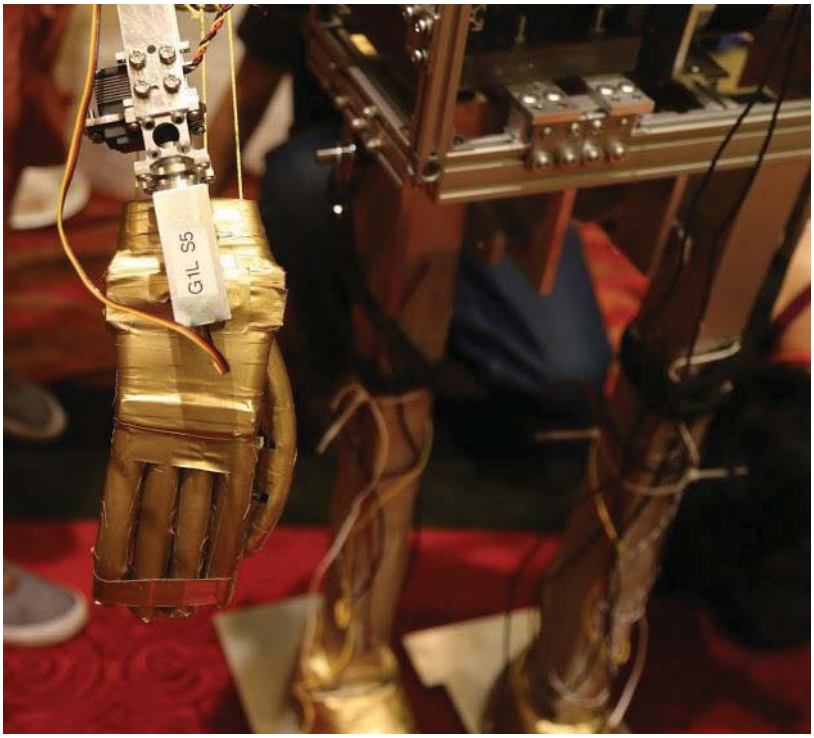

Figure 24: View of back of right hand.

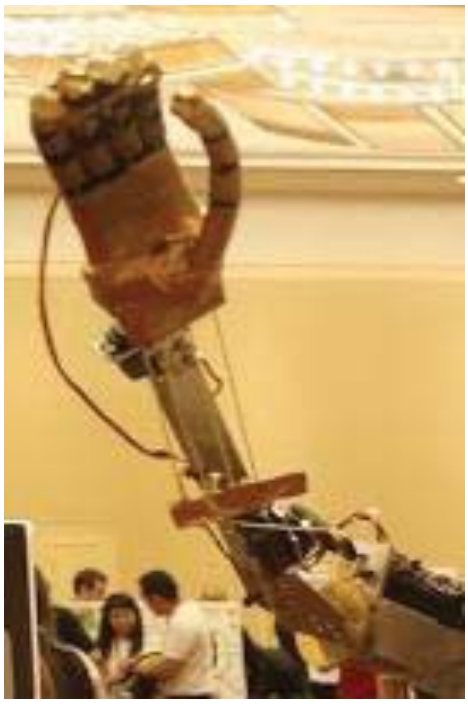

Figure 25: View of hand attached to forearm.

2.13 Lower Arm and Writing Hand Documentation

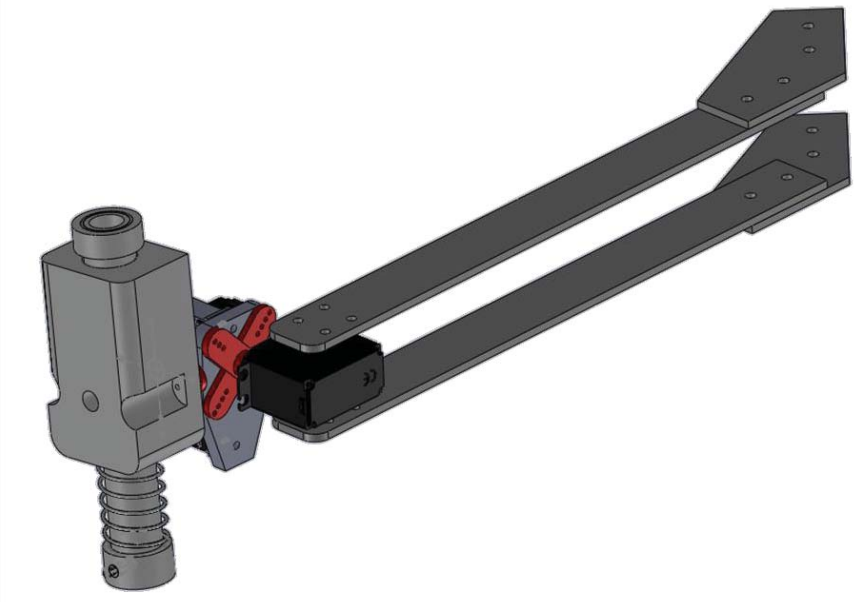

2.13.1 Overview

One of the main initial objectives for I-3P0 was to be able to write his own signature. This task was achieved, and I-3P0 was able to write not only his signature, but also any pen stroke that the user chose to input. The end product allowed users would be able to draw a series of letters in a MATLAB GUI, and have the motion from the pen strokes be translated into servo commands. The entire lower forearm and end effector were both designed and manufactured in the spring 2014 semester, and this document will detail design considerations and experimental challenges in the process. The writing hand end effector was under-actuated, with only two of three degrees of freedom being controlled by servos. The last degree of freedom was passively controlled by spring pressure on the writing surface.

2.13.2 Lower Forearm Considerations

The lower forearm was designed primarily to be lightweight, sturdy, and able to hold the wrist/hand. Secondary design requirements included potential vibration damping and (originally) the ability to experience the load of a 5-lb weight being lifted by the hand. Two $1/8" \times 1" \times 11"$ strips of aluminum, cut out of sheet metal, were used to create the forearm. The final product was sufficient for our needs, and did not exhibit any adverse behavior.

The elbow required more thought, as the writing arm of I-3P0 was not given a “bird motor.” Therefore, it is unable to lift its shoulder up (as if to reach a high-shelf). This was a problem for writing, because the pen must lose contact with the surface somehow in order to write separate letters. If the pen is on the surface, the two degrees of freedom that the servos possess are insufficient, as simply turning the servo would cause the pen to drag along the surface, which was unacceptable. Therefore, the elbows were bent at ~10 to allow the turn motors, mounted on the shoulder to allow roll motion. Rolling the elbow around to pick the pen off the surface was the solution that was then used.

2.13.3 Writing Hand

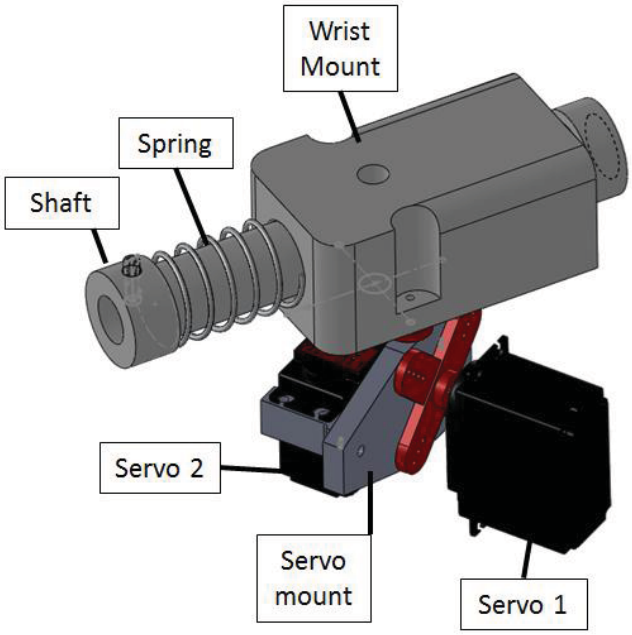

Figure 26: Wrist assembly of writing hand

The objective of the writing hand was to be able to accommodate a range of writing utensils and use them to draw letters. The pen tip would protrude approximately half an inch from the end of the shaft, pictured in Figure 26. The most important aspect of the design is the length of the wrist mount and writing shaft, as an insufficient length would be geometrically prone to “locking”, which is a prevalent and well documented issue in linear motion systems. The design was successful as it allowed for a wide range of motion for the servos without any of the components colliding. The compression spring’s purpose is to ensure that the pen is always in contact with the surface as a letter is being written. It has a k-value of approximately 2 lb/in, which is weak enough to allow for fluid servo control.

A material breakdown of the writing hand’s major components is shown below:

Major Component	**Material/Equipment**
Servo1 & 2	Hitec HS-7965 high-torque, digital, metal-geared servos
Servo Mounts	Servo city plate mounts, universal mounts, aluminum servo mounts
Compression Spring	Steel Wire (1080 Carbon), 0.029" Diameter
Wrist Mount	Delrin Block
Shaft	Delrin Rod, 0.75” Diameter

The servos were selected based on sufficient output torque, and presence of a metal gear. The hand was expected to be put under mechanical stress, and plastic gears would most likely strip. The material selection for the writing hand were filtered first by weight constraints (no metal, as it was too heavy), and then mechanical properties like high-strength and dimensional stability/hardness, and cost. Delrin was chosen since it was readily Machinable, cheap, and capable of high loading while still retaining tight tolerances.

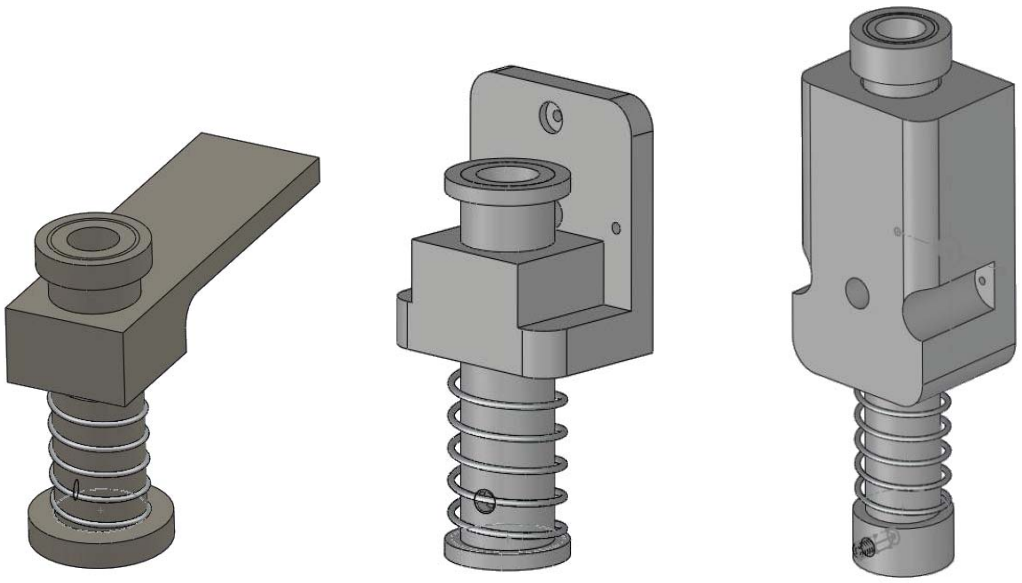

Figure 27: From left to right: 1st, 2nd, and 3rd iteration of the writing hand design

Three iterations of the original design were created, as seen in Figure 27: From left to right: 1st, 2nd, and 3rd iteration of the writing hand design. The second iteration was manufactured, but exhibited prohibitive frictional and locking issues during linear translation that necessitated a third design iteration. The third design was significantly more reliable than the second, although still occasionally experienced locking problems, which will be discussed below. MATLAB servo-control code supports the user-interaction with the hand. An analysis into the configuration space of the hand using inverse kinematics was initially considered, but was not fully implemented.

2.13.4 Locking Issues

Shaft locking was mistakenly not considered during the design process of the first two iterations. When the guide for a shaft is too short compared to the diameter and length of the shaft itself, the shaft is very prone to mechanical locking, as illustrated in Figure 28. Therefore, as the servo tried to turn the writing hand such that the shaft would slide into the mount and compress the spring, The shaft would get jammed, and put tremendous pressure on the pen tip, and the servo. To solve the problem, the shaft was modeled as a cantilevered beam, and a few calculations were performed to fully evaluate my peers. The solution to this issue was purely geometric, and was independent of the force applied to the end of the shaft. It was a function of the ratio between the extended shaft and the length of the bearing/mount. Theoretically, a very small force applied at a certain angle will still trigger the locking event.

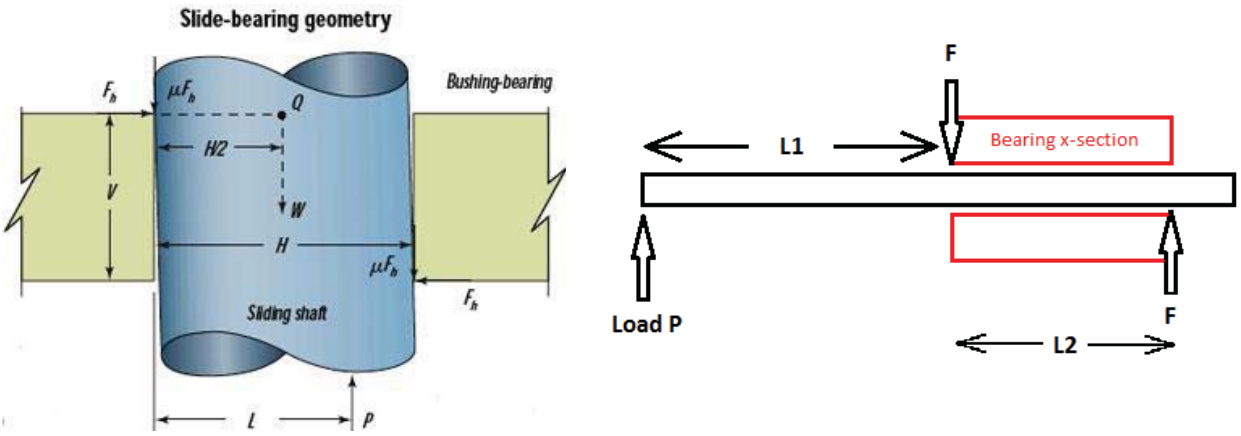

Figure 28: Left, Geometry of shaft-locking forces and torques; Right, Geometry based off of our design

A quick calculation was done to determine the appropriate lengths for the wrist components. The most important parameter is the ratio of the lengths L_1 and L_2.

2.13.5 Analysis

P = force being applied

L = distance out from shaft that P is being applied

s = center to center spacing of bearings

f = resultant force on bearings by shaft

F = friction force on each bearing

μ = coefficient of friction (about 0.25 when not moving)

Moment Balance $$f \times s = L \times P$$
$$L / s = f / P$$

Friction Force: $$F = f \cdot \mu$$

Total friction force pushing up is $2 \times F$. To lock up the slide, the total friction force must be equal to (or greater than) P.

P = 2 * F = 2 * f * μ

Substitute for P:

$$L/s = f / (2 \times f \times \mu) = 1 / (2 \times \mu) \Rightarrow L/s = 1 / (2 \times \mu)$$

Note that all forces cancel out.

Assume static coefficient of friction is 0.25 (μ = 0.25) then L / s = 2. The dynamic coefficient off friction for Delrin is 0.30, and the ratio becomes 1.67:1. The end product was made with a safety factor of **2.5 ratio between L_1 and L_2** to allow for tolerance forgiveness.

2.13.6 Linear motion manufacturing guidelines and considerations

Various design cookbooks and professional websites, always have “rules-of-thumb” when considering such a system. Some notable guidelines are shared. Bores that accommodate the sliding shaft should be

always be greater than 1.5 times the diameter of the shaft itself, and for cantilevered beams, the cantilever length should never be greater than 2 times the guide bore length. In addition, aluminum has been a material noted to seize easily, and to avoid this aluminum and wood. Brass and stainless steel, which are much harder materials, are better suited for linear bearing applications. Lastly, sliding members should be smooth, cylindrical shafts (obviously) to reduce friction and achieve high tolerances.

2.13.7 Initial testing and modeling

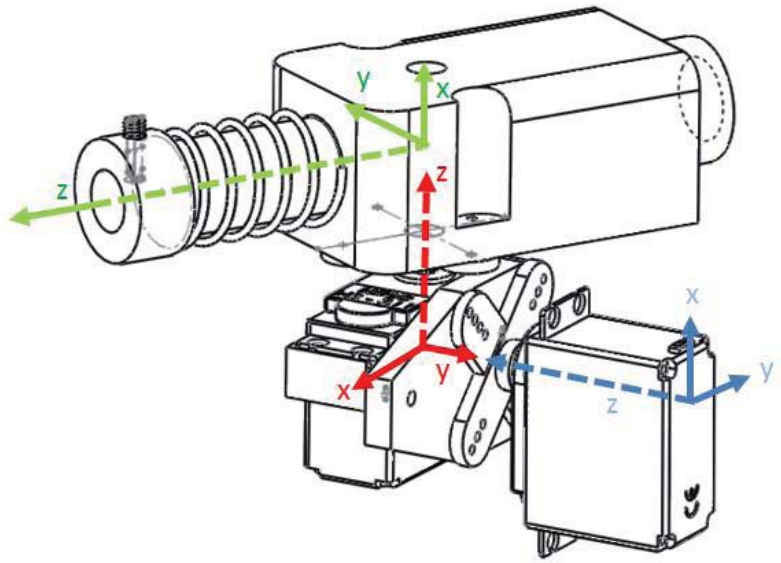

Figure 29: Breakdown of coordinate frames. Different colors are used for reference frames. Dotted lines represent the z-axis in every case.

MATLAB was used in conjunction with a Pololu Maestro 18-channel servo controller to operate. Testing initially intended to perform inverse kinematics calculations. The three reference frames used the Denavit-Hartenburg Method to attempt to solve an inverse kinematics problem. Eventually, this solution was not pursued, and substituted for much easier solutions (lookup tables.

2.14 Changes in the Design

After going through the motor selection guide, we realized that the motors for the bird motion would have to be really bulky, and even the largest, most powerful motors that Maxon had were not capable of providing the necessary torque. As a result, we had to look for other solutions to the problem. We found a spindle that could support the necessary torque. While more powerful, the spindle was also more expensive than the motors, especially combined with the brake, which when added to the spindle

would allow us to power down I-3P0 while keeping his arm in the same position. As a result, we began searching for even more alternatives.

2.14.1 Other Arms

One suggestion was to search for robotic arms that had already been made. With this option, we could design one arm ourselves and purchase the other arm and have a robot with one utilitarian arm and one arm that was more true to the movie. However, when we began searching for arms, we found that most robotic arms were not the size that we wanted and were built for assembly lines, not to function on droids. Additionally, the other arms were much more expensive than our design. As a result, we decided against using an arm that had already been designed.

2.14.2 Connection Point

The connection point for the lift motor was moved approximately 1.5 inches further down the upper arm as shown in Figure 30. This reduced the load on the lifting motor.

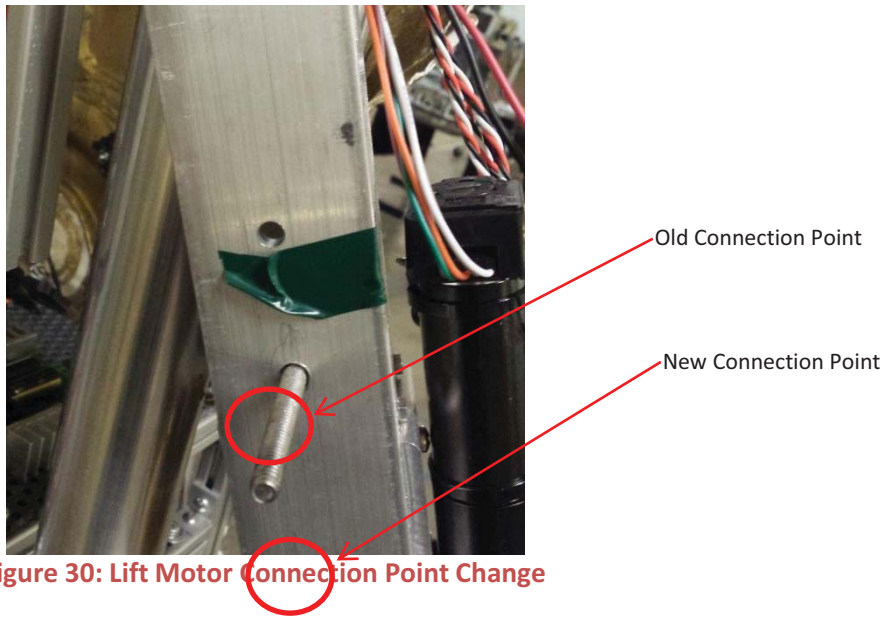

Figure 30: Lift Motor Connection Point Change

2.14.3 Turn Motor

The turn motor for each arm was replaced with a servo system shown in Figure 31. This was mainly the result of one of the turn motors having a bad encoder that prevented it from being tuned properly. The servos were smaller lighter and easier to control but were a little worse on performance.

Figure 31: Servo Assembly

2.14.4 Twist motor bracket

Another change made to the arm design involved the twist motor bracket. Originally a mistake was made in calculating the center to center distance between the two gears that caused them to not mesh correctly. This was corrected by milling down the bottom of the twist bracket 1.3 mm so that the gears meshed properly. A third attachment point was also added to the twist motor bracket in order to reduce the play in the part.

2.15 Arm Motor Selection

The general process for selecting the actuation method for the I-3P0 arm is:

1. Determine the requirements "What does it need to do?"
2. Transforming the requirements into forces, power, torque, etc…
3. Generating ideas that can achieve the requirements
4. Selecting a design direction knowing not all requirements can be met
5. Create final spec for the actuation components

2.15.1 Requirements, "What does it need to do?"

The team determined what the arm needs to do based on best estimates from reviewing Star Wars movies and basic measurements of the team members own arms. These estimates were translated into performance metrics for the various joints on the arm. The length of the arm

was determined to be 1 meter in length and it should carry a 1.5 kg mass in the hand. The speed of the shoulder joint should be 90 degrees per second and have acceleration rate that is numerically twice its speed (180 degrees/s^2). Additionally, the twist motion of the upper arm should have the same angular velocity and acceleration as the shoulder joint. The 3 degrees of freedom in the upper arm joint are lift, turn, and twist. These motions are illustrated in the figures below (Note: The motor to bend the elbow is not included in this document, however, its functionality is assumed).

Next we looked into how it would be used (use cases), this highlighted the need for the arm to be able to support its own weight when the power is turned off. This will be important in the selection of the lift motor.

Finally, one of the top level system requirements is that I-3P0 should be able to sign his own name. This must be considered closely in the actuator selection because they must enable enough precision and repeatability to allow him to write.

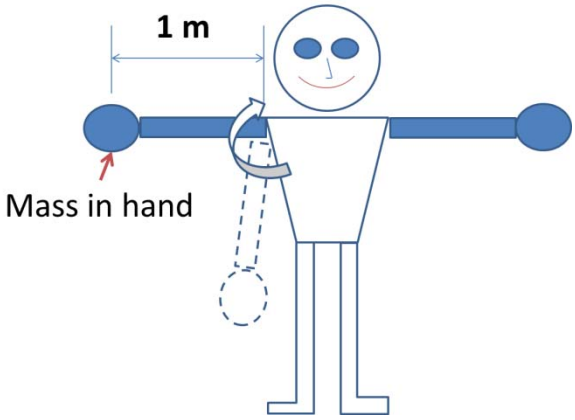

Figure 32: Front View, Lift motion

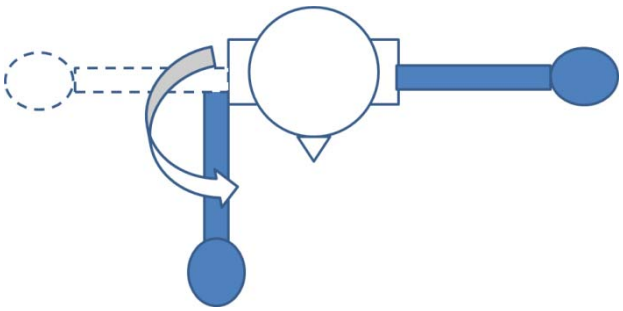

Figure 33: Top View, Turn motion

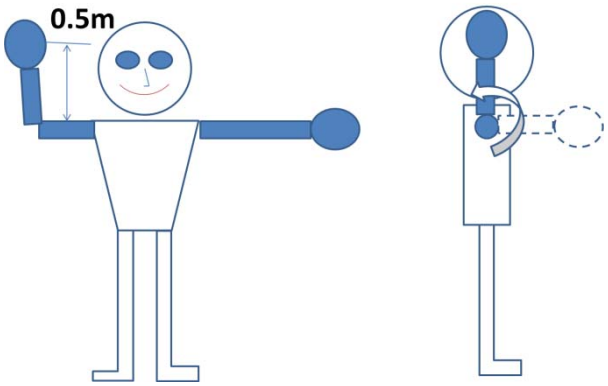

Figure 34: Front view and side view, Twist motion

2.15.2 Transforming requirements into Forces, Power, Torque, etc…

Now that the requirements are known, it's time to translate them into numbers that mean something for the actuators. The calculations will focus on the "worst case" condition that highlights the maximum values of forces, speeds, torque, power, etc... The actuation method must enable operation in the worst case conditions and if it is not possible, the team must review what "is" achievable and how that may impact the overall system goals.

2.15.2.1 Lift Motion

The lift motion is in its worst case condition with the arm fully extended and parallel to the ground. The effects of gravity and inertia are at the peak values.

Requirements

- 90 deg/s
- 180 deg/s^2
- 1m arm length (L)
- 1.5kg mass in hand (m_{hand})
- Precise enough to enable writing name

Assumptions

- Arm mass = 5kg evenly distributed (m_{arm})
- Mass in hand is a point load @ 1m (L)

Calculations

Calculation process, Inertia→Velocity & Accel→Torque→Power→Operating point

Arm Inertia (I_{arm})= $\frac{1}{3}m_{arm}L^2 = \frac{1}{3}(5kg)(1m)^2 = 1.67\ kg \cdot m^2$

Mass Inertia (I_{mass}) = $m_{hand}L^2 = (1.5kg)(1m)^2 = 1.5\ kg \cdot m^2$

Angular velocity (n) = $90\frac{deg}{s} = 15\ rpm$

Acceleration (α) = $180\frac{deg}{s^2} = 3.14159\frac{rad}{s^2}$

Torque due to Inertia ($M_{inertia}$) = $I\alpha = (I_{arm} + I_{hand})(\alpha) = (1.67\ kg \cdot m^2 + 1.5\ kg \cdot m^2)\left(3.14159\frac{rad}{s^2}\right) = 9.95\ Nm$

Torque due to Gravity ($M_{gravity}$) = $mgL = m_{hand}gL + m_{arm}g\frac{L}{2} = (1.5kg)\left(9.81\frac{m}{s^2}\right)(1m) + (5kg)\left(9.81\frac{m}{s^2}\right)\left(\frac{1m}{2}\right) = 14.7\ Nm + 25.4\ Nm = 39.2\ Nm$

Torque (M) = $M_{inertia}$+$M_{gravity}$= 9.95 Nm + 39.2 Nm = 49.2 Nm

Power (P_{lift}) = $P\left(Watts\ \ or\ \ \frac{Joule}{sec}\right) = \frac{M(Nm)*n(RPM)}{\frac{60\ sec}{1\ min}*\frac{1\ rotation}{2\pi\ radians}} = \frac{49.2\ Nm*15\ rpm}{\frac{60\ sec}{1\ min}*\frac{1\ rotation}{2\pi\ radians}} = 77.3\ Watts$

Component	Mass (kg)	length/distance from axis (m)	Inertia (kg*m^2)					
Arm	5	1	**1.67**					
Mass in Hand	1.5	1	**1.50**					
	Deg/s	Deg/s^2	rad/s	rad/s^2	rps	rps^2	rpm	rpm^2
Speed (n)	90		1.57079633		0.25		**15**	
Accel (α)		180		**3.14159**		0.5		30
Torque (M)	Due to Gravity (Nm)	Due to Inertia (Nm)	Sub-total (Nm)	Total (Nm)				
Arm	24.5	5.24	29.76	**49.19**				
Weight	14.7	4.71	19.43					
Power (W)	**77.3**							
	Power (W)	Torque (Nm)	Speed (rpm)					
Operating Point	77.3	49.2	15					

Figure 35: Excel spreadsheet calculation

Now that the torque, velocity, and power based on the shoulder joint axis is known, the values need to be translated into a linear force for use with a linear actuator. The force and velocity tradeoffs will assist in the design and selection process.

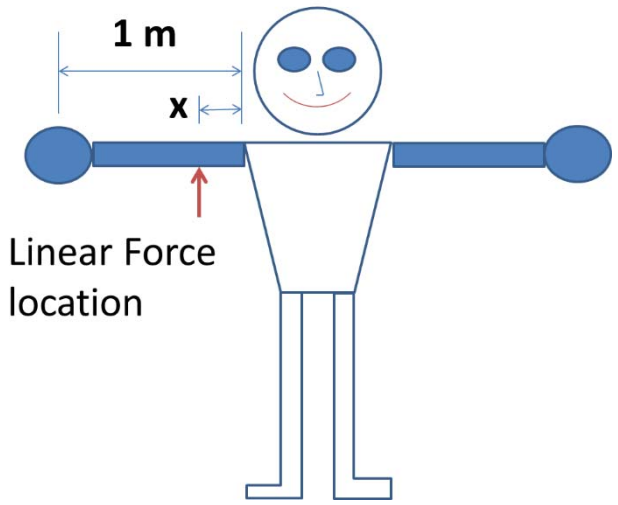

Figure 36: Location for linear actuator attachment

The chart below shows the relationship of the linear force location to the linear force required to achieve the torque value (M) that was calculated above at 49.2 Nm. Additionally, it is good to understand the sensitivity of how variations in your spec point will influence the force. The chart also plots a 40 Nm torque value as well as a 60 Nm torque value giving roughly a +/- 10 Nm tolerance band around the calculated spec point. The tolerance band is only placed on the chart for visual reference.

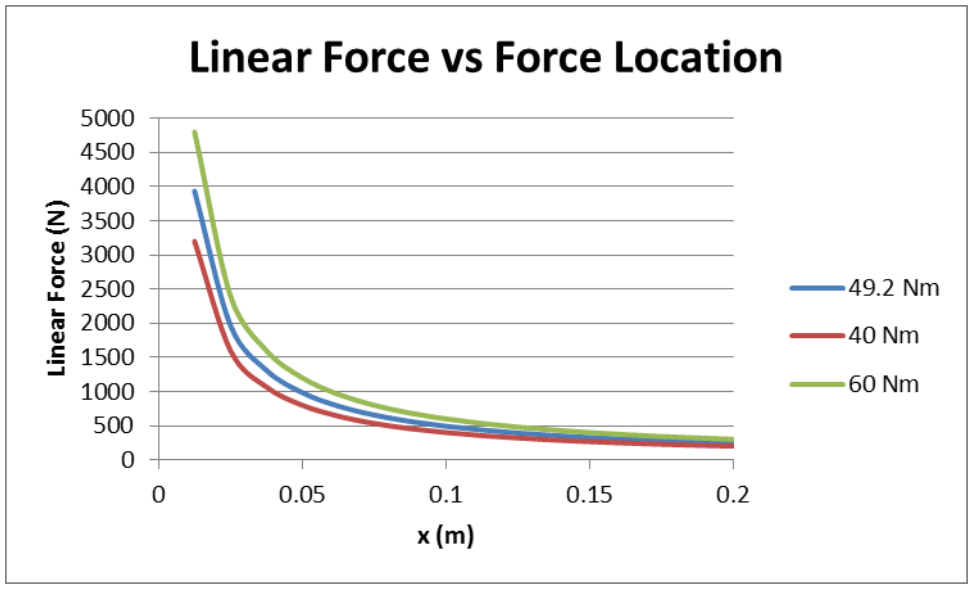

Figure 37: Calculation of linear force vs. distance from pivot point

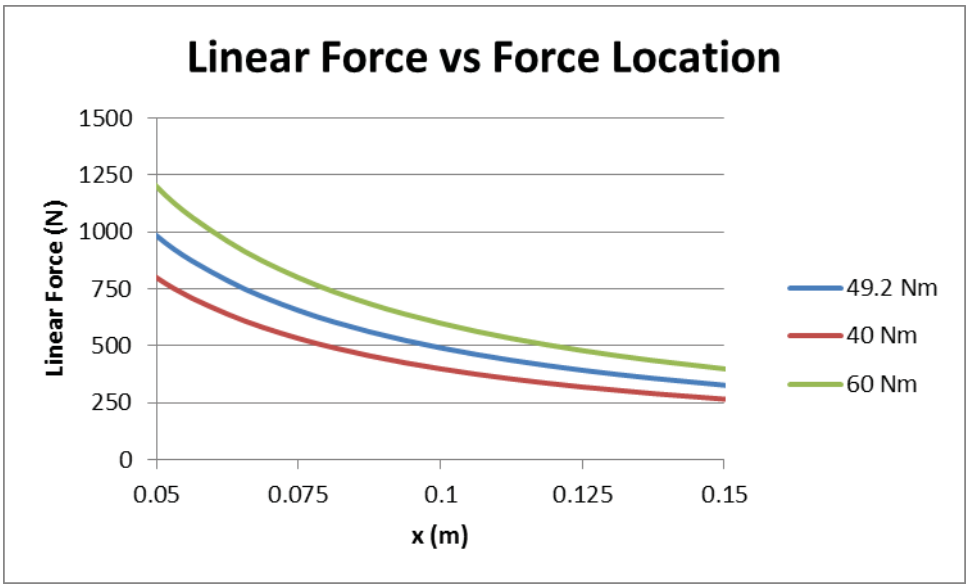

Figure 38: Linear force vs. distance (zoomed in to relevant range of "x")

The linear velocity is also a key metric that must be known. The tradeoffs are shown based on the target rotational velocity as well as +/- 10 rpm. The values are inversely proportional to the force as the "x" distance changes.

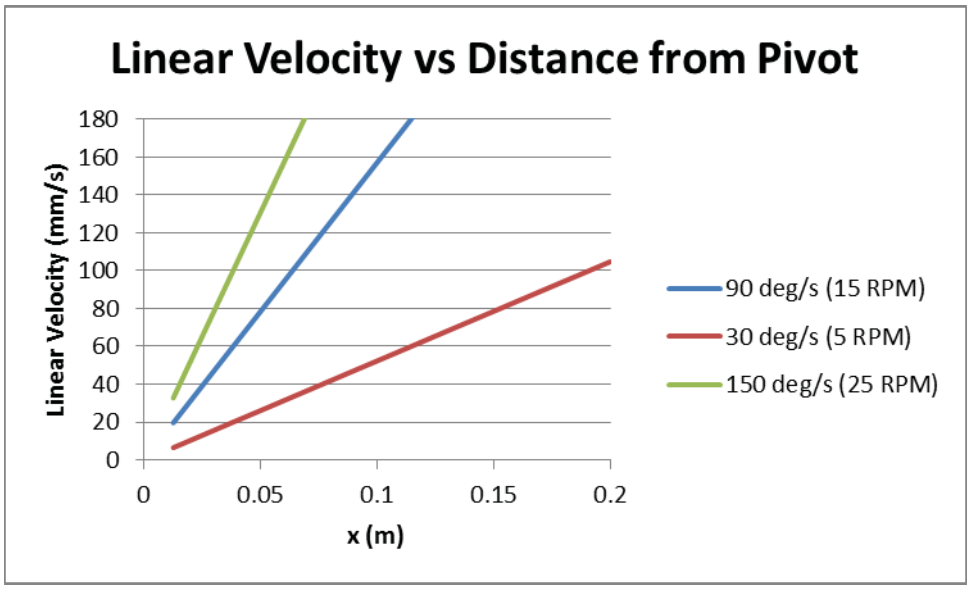

Figure 39: Linear velocity vs distance from pivot "x" (limited at 180 mm/s due to max available spindle speed from Maxon Motors)

At this point, very clear tradeoffs will need to be made and it may force changes to the initial requirements based on what is most important to the arm design team.

The spec point at x=75mm, n=90 deg/s, and M=49.2 Nm for a linear actuator is:

- **656 N**
- **117.8 mm/s**

2.15.2.2 Turn Motion

Based on the design of the axis of motion for the shoulder, the axis for the twist motion is perpendicular to the ground. Thus, gravitational forces will not impact the actuator force, torque, or power. The assumption is that the robot will always have the torso in a vertical orientation. The "worst case" determined for this actuator is due to the inertia of the arm when fully extended with the mass in the hand. By utilizing the same calculations as the lift motion and zeroing out the gravitational forces, the excel spreadsheet values are shown in the figure below.

Component	Mass (kg)	length/distance from axis (m)	Inertia (kg*m^2)					
Arm	5	1	**1.67**					
Mass in Hand	1.5	1	**1.50**					
	Deg/s	Deg/s^2	rad/s	rad/s^2	rps	rps^2	rpm	rpm^2
Speed (n)	90		1.57079633		0.3		**15**	
Accel (α)		180		**3.14159**		0.5		30
Torque (M)	Due to Gravity (Nm)	Due to Inertia (Nm)	Sub-total (Nm)	Total (Nm)				
Arm	0.0	5.24	5.24	**9.9**				
Weight	0.0	4.71	4.71					
Power (W)	**15.6**							
	Power (W)	Torque (Nm)	Speed (rpm)					
Operating Point	15.6	9.9	15					

Figure 40: Operating point calculation for turn motion

The design requires the motor output shaft to directly turn the arm. The operating point for the turn motion is:

- 9.9 Nm
- 15 RPM

2.15.2.3 Twist Motion

The twist motion allows the upper arm to rotate about the axis of the upper arm. The "worst case" for this actuator is determined when the arm is horizontal to the ground with the elbow bent at 90 degrees.

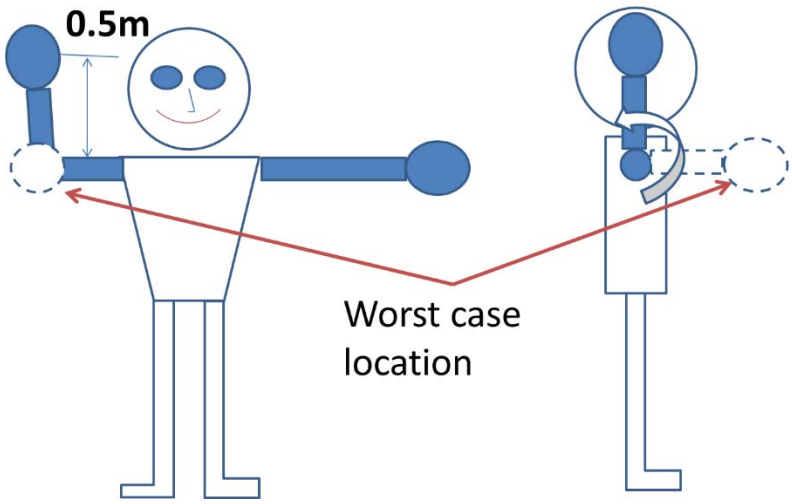

Figure 41: Worst case position for twist motion

Using the same calculations as the lift motion and changing the arm length to 0.5m and the arm mass to 2.5 kg, the calculation values are shown below

Component	Mass (kg)	length/distance from axis (m)	Inertia (kg*m^2)					
Arm	2.5	0.5	**0.21**					
Mass in Hand	1.5	0.5	**0.38**					
	Deg/s	Deg/s^2	rad/s	rad/s^2	rps	rps^2	rpm	rpm^2
Speed (n)	90		1.57079633		0.25		**15**	
Accel (α)		180		**3.14159**		0.5		30
Torque (M)	Due to Gravity (Nm)	Due to Inertia (Nm)	Sub-total (Nm)	Total (Nm)				
Arm	6.1	0.65	6.79	**15.3**				
Weight	7.4	1.18	8.54					
Power (W)	**24.1**							
	Power (W)	Torque (Nm)	Speed (rpm)					
Operating Point	24.1	15.3	15					

Figure 42: Operating point calculation for Twist motion

The operating point for the twist motion is

- 15.3 Nm
- 15 Rpm

2.15.3 Generating Ideas to Meet Requirements

2.15.3.1 Lift Motion

Many concepts were thought of for the lift concept

- Electric motor + Cable linear actuation
    - Pro: high power, high ratio, motor mounted lower in chassis
    - Con: precision, complex system to make it apply force in both directions
- Hydraulic linear actuation with electric motor pump
    - Pro: Extremely high force possible
    - Con: Low Efficiency, Messy when it leaks, high mass of system
- Electric motor + planetary gear drive + external spur gear 3:1
    - Pro: precision, power is possible
    - Con: Backlash of external spurt gears will reduce precision, mass located high on torso, packaging difficult
- Electric motor + Spindle drive linear actuator
    - Pro: Very good precision, packaging with mass located low on torso
    - Con: Limited speed/power choices available from Maxon

2.15.3.2 Turn Motion

The ideas for turn mainly surrounded electric motors; there may be additional methods possible.

- Electric motor + planetary gear drive+ external 3:1 spur gear
    - Pro: smaller diameter motor possible, lower cost motor
    - Con: Precision due to backlash of gears, packaging of external gears
- Electric motor + planetary gear drive
    - Pro: direct drive of arm, high precision possible, packaging is easier
    - Con: large diameter gear drive to handle torque value

2.15.3.3 Twist Motion

Ideas for twist were again mainly surrounding the electric motors available from Maxon Motors

- Electric motor + Planetary gear drive + external 3:1 spur gear
    - Pro: smaller diameter motor, lower motor mass located high on torso
    - Con: reduced precision with external spur gear set
- Electric motor + planetary gear drive
    - Pro: Precision, less components
    - Con: Diameter of gear drive to handle torque, very limited options

2.15.4 Selecting a Direction Knowing that All Requirements May Not be met

Through the process of selecting the actuation method for each of the 3 degrees of freedom it was important to judge each of the ideas on the same scale. The actuation methods were then

placed into a decision matrix, also known as a Pugh Matrix. An example of this matrix is shown below.

Atrribute	Metric	Requirements	Normalizing Scale	weight
size	volume and Length, Width, Height (linear m)	no individual component is larger than 1.5x the human counterpart	1=1.5x, 3=same size, 5= smaller	3
cost	price of parts	average of $100 per part	1=$1000+, 3=100-1000 5=less than 100	4
power usage	look up specs/run time on XX V battery?	TBD	5=meets Req 3=2x Req 1=3x Req	4
speed	Actuator max speed (deg/s)	meets performance definition at max load	1=meets Req 3=2x Req 5=3x Req	4
Torque capacity	at full arm extention the force at the hand (N m)	min 5lbs at hand	5= exceed spec, 3 = meet spec, 1 = below spec	5
RANGE OF MOTION (deg)				
range of wrist left/right motion	measurement of possible motion	meets performance definition	1=90-110 3=110-170 5=exceeds 170	0
range of bird motion	measurement of possible motion	meets performance definition	1=90-110 3=110-170 5=exceeds 170	0
range of punch motion	measurement of possible motion	meets performance definition	1=90-110 3=110-170 5=exceeds 170	0
range of twist motion	measurement of possible motion	meets performance definition	1=90-110 3=110-170 5=exceeds 170	2

Figure 43: Example portion of the Decision Matrix for Actuators

Through the selection process there are a few key details and tradeoffs that needed to happen for each of the motions. The original requirements needed to be reviewed and compromises made.

The arm design and motor layout is shown in the figure below:

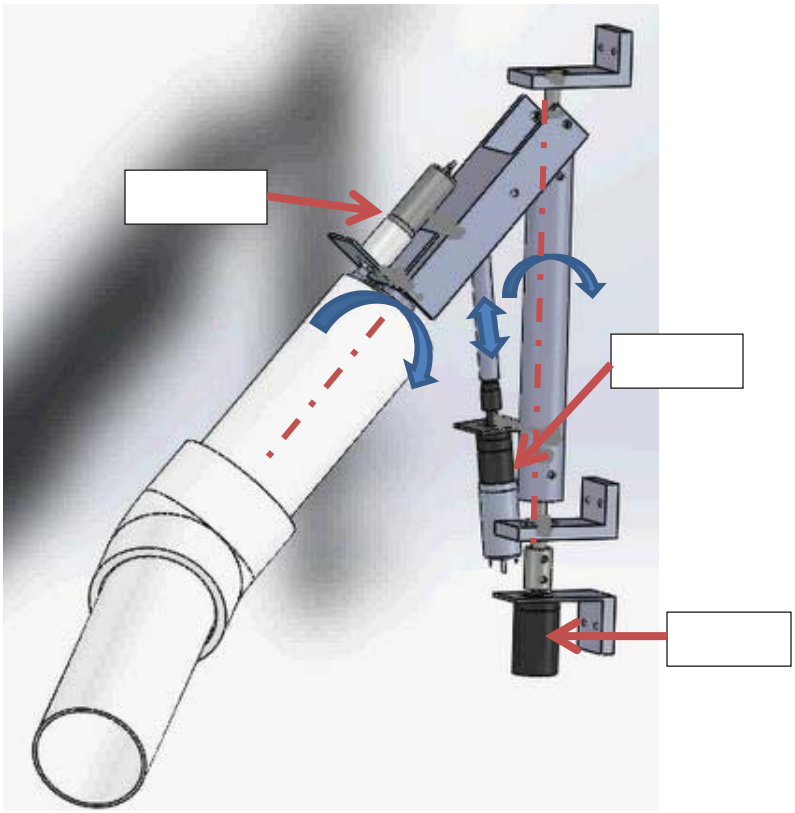

Figure 44: I-3P0 Arm Actuator layout concept

2.15.4.1 Lift Motion

The lift motion required the most tradeoff of meeting the entire set of requirements. The precision of the actuation method combined with its easy packaging and low center of gravity location directed us to choose the linear actuation method with the electric motor + spindle drive from Maxon Motors. This spindle drive also allowed the installation of a brake that actuates when the power is off and a precision position sensor.

Figure 45: Maxon Spindle Drive example

The biggest challenge was finding an actuator that met the criteria of 656 N and 117.8 mm/s per the spec point requirement calculated above. After reviewing Maxon Motor catalog there were 3 spindle types that provided the linear actuation

Ball Screw

- High efficiency
- Not self-locking (requires additional brake)
- High load capacity

Metric Spindle

- Self-locking
- Low cost

Trapezoidal Spindle

- Self-locking
- Low cost
- Higher load capacity than metric spindle

After reviewing the specs of all of the available spindles it became apparent that ***none*** of them are capable of meeting the spec point for both force and speed. The charts below show how one or the other parameter can be met, but not both. The charts show the Spindle Drive GP 32 S options that are in the relevant range for both speed and load. The actuator attachment is at 75mm from the pivot point of the arm.

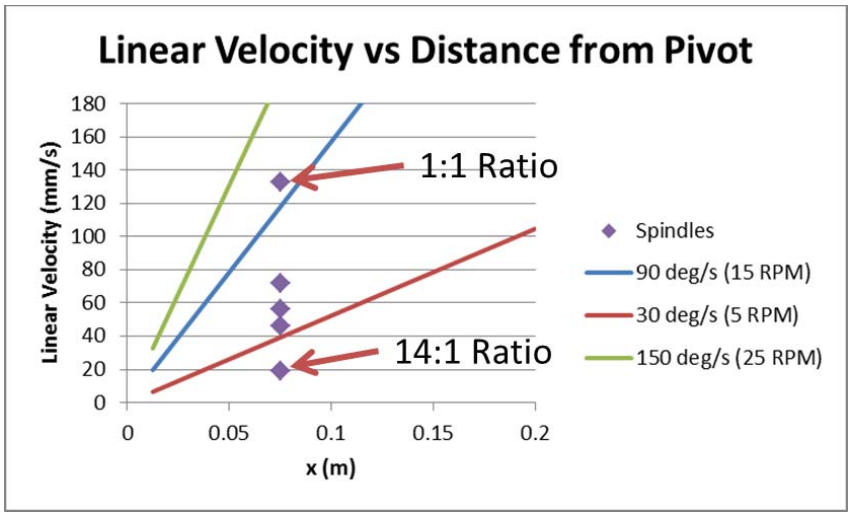

Figure 46: Maxon GP 32 S Ball Screw spindle drive options vs. the velocity specification

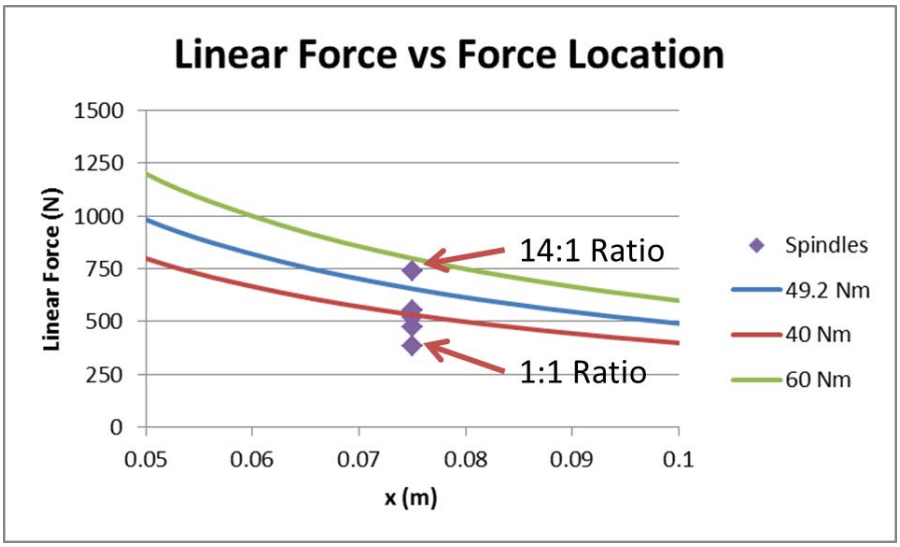

Figure 47: Maxon GP 32 S Ball Screw spindle drive options vs. the force specification

The takeaway from the figures above is that we can meet either the torque spec or the velocity spec but not both. After reviewing the important criteria with the team, the decision was made to reduce the max velocity and max force spec for the best possible balance between the two metrics. Ideally, the team would like to find a higher power linear actuator without reducing the precision. The axial positioning precision for the GP 32 S Ball Screw is listed at 0.037mm.

If the arm ends up with less mass than 5kg or has a different mass distribution, the possibility exists to change the selection of spindle drive. As the arm gets lighter or has lower inertia than the specification, the force required is decreased. If the arm gets light enough and the required linear force is 386 N or less, the 1:1 ratio spindle could be selected and achieve the velocity specification at an "x" position of 75mm.

2.15.4.2 Turn Motion

The challenge with the turn motion was the high torque value. The location of the motor is in a good location that is lower on the robot chassis and enables a lower center of mass.

- 9.95 Nm
- 15RPM

When the spec point was placed into Maxon Motors selection program, there were a few options

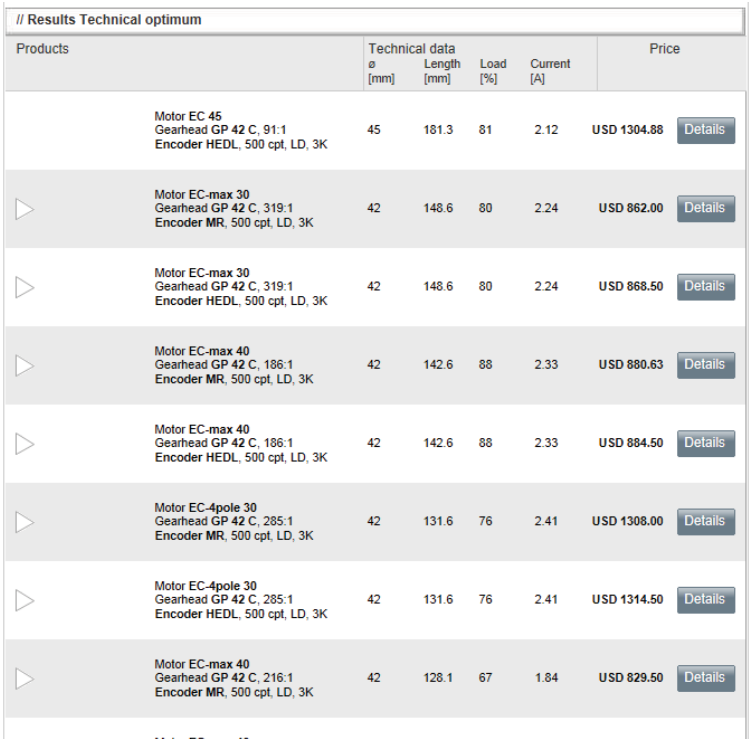

// Results Technical optimum

Products	Technical data ø [mm]	Length [mm]	Load [%]	Current [A]	Price	
Motor EC 45 Gearhead GP 42 C, 91:1 Encoder HEDL, 500 cpt, LD, 3K	45	181.3	81	2.12	USD 1304.88	Details
Motor EC-max 30 Gearhead GP 42 C, 319:1 Encoder MR, 500 cpt, LD, 3K	42	148.6	80	2.24	USD 862.00	Details
Motor EC-max 30 Gearhead GP 42 C, 319:1 Encoder HEDL, 500 cpt, LD, 3K	42	148.6	80	2.24	USD 868.50	Details
Motor EC-max 40 Gearhead GP 42 C, 186:1 Encoder MR, 500 cpt, LD, 3K	42	142.6	88	2.33	USD 880.63	Details
Motor EC-max 40 Gearhead GP 42 C, 186:1 Encoder HEDL, 500 cpt, LD, 3K	42	142.6	88	2.33	USD 884.50	Details
Motor EC-4pole 30 Gearhead GP 42 C, 285:1 Encoder MR, 500 cpt, LD, 3K	42	131.6	76	2.41	USD 1308.00	Details
Motor EC-4pole 30 Gearhead GP 42 C, 285:1 Encoder HEDL, 500 cpt, LD, 3K	42	131.6	76	2.41	USD 1314.50	Details
Motor EC-max 40 Gearhead GP 42 C, 216:1 Encoder MR, 500 cpt, LD, 3K	42	128.1	67	1.84	USD 829.50	Details

Figure 48: Maxon Motor suggestions to achieve the spec point for the Turn motion

2.15.4.3 Twist Motion

The twist motion spec point

- 15.3 Nm
- 15 rpm

After including the external 3:1 ratio, the new spec point is

- 5.1 Nm
- 45 RPM

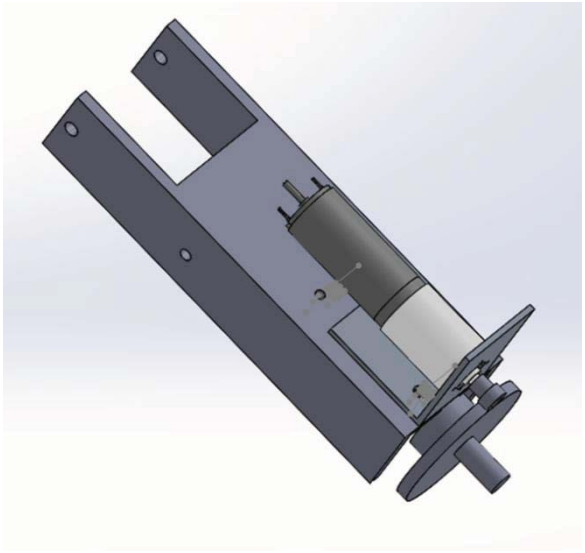

Figure 49: Twist motion, highlighting the 3:1 external gear ratio

The problem with 5 Nm is that the number of selections for motor and gear combinations was reduced drastically. Getting the max torque below 4.5 Nm was required and after discussion of a more accurate arm and hand mass the values were reduced to

- **4 Nm**
- **45 RPM**

// Results Technical optimum

Products	Technical data ø [mm]	Length [mm]	Load [%]	Current [A]	Price	
Motor EC-max 30 Gearhead KD 32, 152:1 Encoder MR, 500 cpt, LD, 3K	32	131.7	89	1.95	USD 832.63	Details
Motor EC-max 30 Gearhead KD 32, 152:1 Encoder HEDL, 500 cpt, LD, 3K	32	131.7	89	1.95	USD 839.13	Details
Motor EC-4pole 22 Gearhead GP 32 C, 111:1 Encoder HEDL, 500 cpt, LD, 3K	32	109.2	79	2.01	USD 1121.13	Details
Motor EC 32 Gearhead GP 32 C, 159:1 Encoder HEDS, 500 cpt, 3K	32	103.2	76	1.95	USD 778.13	Details
Motor EC-i 40 Gearhead GP 32 C, 86:1 Encoder HEDL, 500 cpt, LD, 3K	40	79.2	80	2.30	USD 746.00	Details
Motor EC-4pole 22 Gearhead GP 32 C, 132:1 Encoder HEDL, 500 cpt, LD, 3K	32	91.7	84	2.16	USD 1043.63	Details
Motor EC-max 30 Gearhead GP 32 HP, 111:1 Encoder MR, 500 cpt, LD, 3K	32	118.9	85	2.35	USD 746.50	Details
Motor EC-max 30 Gearhead GP 32 HP, 111:1 Encoder HEDL, 500 cpt, LD, 3K	32	118.9	85	2.35	USD 753.00	Details
Motor EC-4pole 30						

Figure 50: Maxon Motor suggestions for Twist motion spec

2.15.5 Final specification and selection

The final component part numbers are listed below; the detailed specs are shown in the appendix. CAD models are available on Maxon Motors website.

2.15.5.1 Lift Motion – Final Spec

Spindle Drive GP 32 S Ø32 mm, Ball Srew, Ø10 x 2
Part number 363973

RE 35 Ø35 mm, Graphite Brushes, 90 Watt
Part number 323890

Encoder HEDL 5540, 500 CPT, 3 Channels, with Line Driver RS 422
Part number 110512

Brake AB 28, 24 VDC, 0.4 Nm
Part number 228387

2.15.5.2 Turn Motion – Final Spec

Planetary Gearhead GP 42 C Ø42 mm, 3 - 15 Nm, Ceramic Version
Part number 203129

RE 40 Ø40 mm, Graphite Brushes, 150 Watt
Part number 218009

Encoder MR, Type L, 256 CPT, 3 Channels, with Line Driver
Part number 225783

2.15.5.3 Twist Motion – Final Spec

Planetary Gearhead GP 32 A Ø32 mm, 0.75 - 4.5 Nm, Metal Version
Part number 166167

RE 30 Ø30 mm, Graphite Brushes, 60 Watt
Part number 310008

Encoder HEDS 5540, 500 Counts per turn, 3 Channels
Part number 110511

2.16 Future work

2.16.1 Elbow Actuation

Introduction

Due to early design decisions, the I3P0 arm decided to move forward without elbow actuation. It was decided to choose this path due to the number of actuation motors used already. However, late in the project, we decided to attempt an elbow actuation design. This section covers the ideas that were generated but never implemented due to time constraints.

Requirements

The elbow actuation design was undertaken to allow I3P0 to wave. However, in review of the upper arm requirements, it must also be able to hold 1.5 kg and enable I3P0 to write his name. Adding the additional requirements made it a bit more challenging. The force, power, and range of motion required to wave were quite low compared to the overall system requirements. It was a good reminder to go back and look at the system level requirements otherwise we could have mismatched parts. If we have a capable upper arm to carry 1.5 kg, but the elbow can only handle 0.5 kg, then the upper arm would have been overdesigned.

Requirements

- 90 deg/s
- 180 deg/s^2
- 0.5 m forearm length (L)
- 1.5kg mass in hand (m_{hand})
- Precise enough to enable writing name
- Enable "Wave" motion of hand, ≈45° range of motion

Assumptions

- Forearm weighs 2 kg, mass evenly distributed

2.16.2 Transforming requirements into measurable parameters

Calculations

Calculation process, Inertia→Velocity & Accel→Torque→Power→Operating point

Arm Inertia ($I_{forearm}$)= $\frac{1}{3}m_{arm}L^2 = \frac{1}{3}(2kg)(0.5m)^2 = 0.33\ kg \cdot m^2$

Mass Inertia (I_{mass}) = $m_{hand}L^2 = (1.5kg)(0.5m)^2 = 0.375\ kg \cdot m^2$

Angular velocity (n) = $90\frac{deg}{s} = 15\ rpm$

Acceleration (α) = $180\frac{deg}{s^2} = 3.14159\frac{rad}{s^2}$

Torque due to Inertia ($M_{inertia}$) =

$$I\alpha = (I_{arm} + I_{hand})(\alpha) = (0.333\ kg \cdot m^2 + 0.375\ kg \cdot m^2)\left(3.14159\frac{rad}{s^2}\right) = 1.4\ Nm$$

Torque due to Gravity ($M_{gravity}$) = $mgL = m_{hand}gL + m_{arm}g\frac{L}{2} = (1.5kg)\left(9.81\frac{m}{s^2}\right)(0.5m) +$

$(2kg)\left(9.81\frac{m}{s^2}\right)\left(\frac{1m}{4}\right) = 7.4\ Nm + 4.9\ Nm = 12.3\ Nm$

Torque (M) = $M_{inertia}$+$M_{gravity}$= 1.4 Nm + 12.3 Nm = 13.7 Nm

Power (P_{elbow}) = $P\left(Watts\ \ or\ \ \frac{Joule}{sec}\right) = \frac{M(Nm)*n(RPM)}{\frac{60\ sec}{1\ min}*\frac{1\ rotation}{2\pi\ radians}} = \frac{13.7\ Nm*15\ rpm}{\frac{60\ sec}{1\ min}*\frac{1\ rotation}{2\pi\ radians}} = 21.5\ Watts$

2.16.3 Concept Generation

Due to package space available on the existing arm design, the installation was going to be a major limiting factor. There are many options that could meet the specification

Windshield Wiper Motor

Figure 51: Example windshield wiper motor

The principle behind the wiper motor is the output shaft of the motors is oscillating shaft motion. These motors have sufficient torque and power and the speed is also possible. The main challenges with this design are package space and positioning capability.

AM EQUIPMENT.COM

238 Series Motor

- 38 Nm (see conversion table on reference information page)
- SAE standard durability tested
- Compact size will retrofit into existing space
- Standard RFI suppression
- Water-resistant motor and plug connectors
- Dynamic park
- Available in 12V or 24V
- Available in low or high side switched
- A variety of pigtail adapter cords available

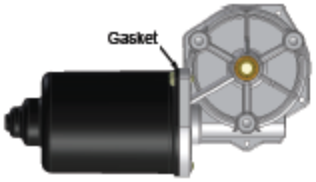

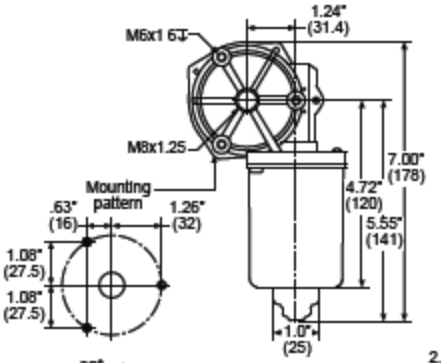

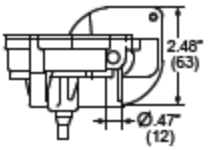

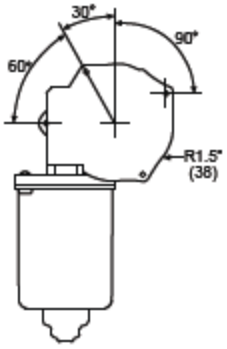

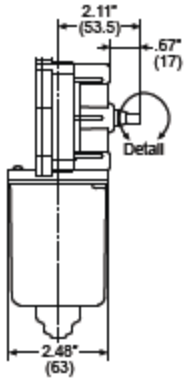

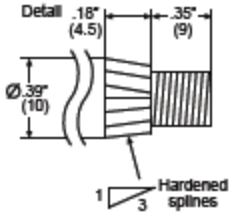

Part numbers:

238-1002	12V
238-1003	24V
238-1004	12V, low side switched
238-1005	24V, low side switched

PAGE 1 OF 2

Low Speed CCW Motor Shaft Rotation		
Data Point	Data Type	Value Range
No Load	Current (A)	1.1 - 0.9
	Speed (rpm)	44.6 - 36.5
Stall Load	Torque (Nm)	43.8 - 35.8
	Current (A)	23.8 - 19.4
Peak Power	Power (W)	45.4 - 37.2
	Torque (Nm)	22.3 - 18.2
Nominal (Peak Efficiency)	Power (W)	21.5 nominal
	Speed (rpm)	33.6 nominal
	Current (A)	3.9 nominal
	Torque (Nm)	6.2 nominal
Clockwise Motor Shaft Rotation		
Data Point	Data Type	Value Range
No Load	Current (A)	1.7 - 1.5
	Speed (rpm)	65.4 - 53.5
Stall Load	Torque (Nm)	37.2 - 30.4
	Current (A)	26.6 - 21.8
Peak Power	Power (W)	53.6 - 43.8
	Torque (Nm)	18.6 - 15.2
Nominal (Peak Efficiency)	Power (W)	31.5 nominal
	Speed (rpm)	46.8 nominal
	Current (A)	5.7 nominal
	Torque (Nm)	6.6 nominal

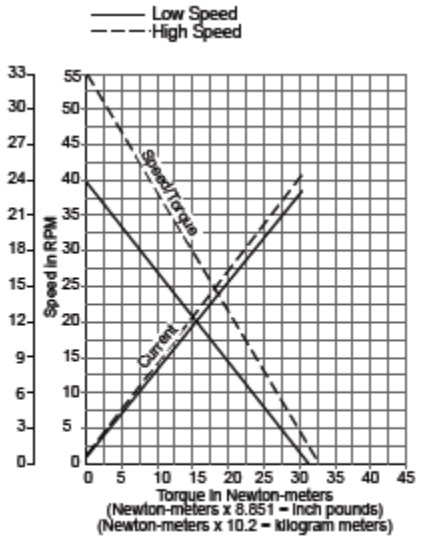

Push-Pull Cable Design

The wiper motor design proved difficult to package, so another design concept was created that would enable easier packaging of the actuation device. The design was a push pull cable that allowed a linear actuator to be mounted anywhere on the robot. This was intended to keep the mass on the arm low and not interfere with the other degrees of freedom on the arm itself.

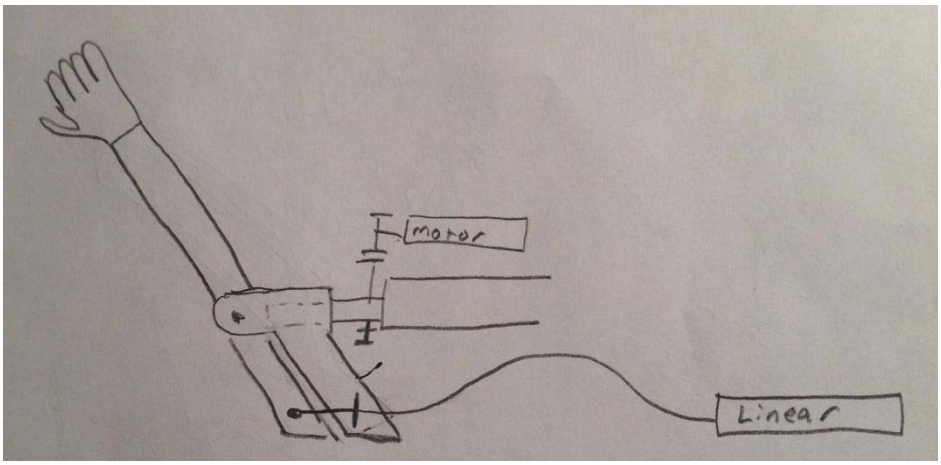

Figure 52: Push-Pull cable concept

WESCON'S PUSH-PULL CONTROL SYSTEMS

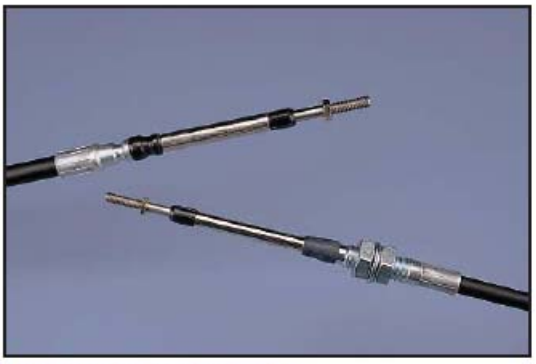

Push-Pull Cable Ends

Wescon Push-Pull Cable Assemblies are available in either groove or bulkhead end configurations. Also upon request Wescon offers a bulkhead/groove combination fitting in 40 and 60 series controls.

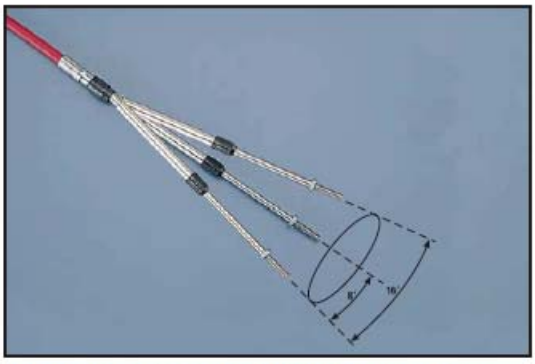

Wescon's Swivels Allow Deflection

Standard end fittings feature built-in swivels which allow an 8° deflection each side of center, or a total conical deflection of 16°, to accommodate the movement of the control arm.

Figure 53: Wescon push-pull cable examples

WESCON 40 Series Nylon Covered Core Push-Pull Control

Typical applications include throttle/shift (rear engine bus), activating electronic transmission or activating hydraulic valves.
6" minimum bend radius.

See page 9 for Part Number Codes.

Control Length (Inches)	"X"
Up to 60.00	± .31
60.01to 120.00	± .50
120.01 to 240.00	± .75
Above 240.00	± 1.00

Travel	Bulkhead Type Fitting		Grooved Type Fitting		Input Load Pounds (kg)
	"A"	"B"	"C"	"D"	
1"	4.62 (117.3)	3.19 (81.0)	4.00 (101.6)	2.56 (65.0)	120 (54.4)
2"	6.13 (155.7)	4.19 (106.4)	5.50 (139.7)	3.56 (90.4)	90 (40.8)
3"	7.62 (193.5)	5.19 (131.8)	7.00 (177.8)	4.56 (115.8)	75 (34.0)
4"	9.13 (231.9)	6.19 (157.2)	8.50 (215.9)	5.56 (141.2)	65 (29.5)
5"	10.62 (269.7)	7.19 (182.6)	10.00 (254.0)	6.56 (166.6)	60 (27.2)
6"	12.13 (308.1)	8.19 (208.0)	11.50 (292.1)	7.56 (192.0)	60 (27.2)

All Dimensions are Inches (mm)

NOTE:
1 Nuts fit over seals (typ)

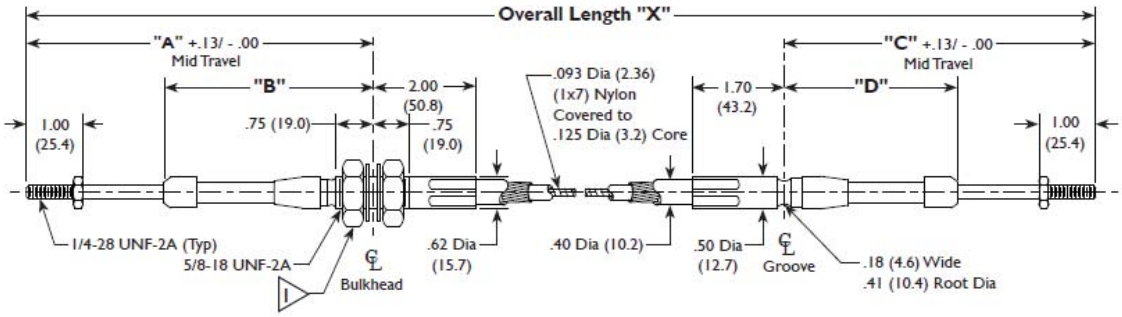

3 I-3P0 Balancing

3.1 Goals and Motivation

The fundamental control issue with humanoid bi-pedal robots is a mechanism for balancing. Balancing requires control of an unstable system and the ability to correct error quickly. The human balancing system uses feedback strategy to maintain a center of gravity through the repositioning of hips, knees, ankles, and core. While the majority of the control will stem directly from robust calculation and coding, we aim to emulate the human balancing system in a fluid, stable form.

The balancing mechanism will allow I-3P0 to stand still, “walk” forward, and come to a stop using a counterweight to shift the center of gravity with every step. We heavily evaluated two systems to mobilize and accurately place a mass to adjust the center of gravity: a track system in the x-y plane and a pendulum (inverted or upright). Each of the balancing components in the human body are often compared to inverted pendulums, which inspired some of our designs.

3.2 Performance Criteria

A list of performance criteria was created, and weights were assigned to each criterion by a group of four team members. Weights were verified with the rest of the team in a weekly meeting. The most

important aspects of the design were judged to be manufacturability and precise feedback. We needed a system that would be machinable in a short time frame, because we expected (and still expect) plenty of design iteration. In addition, given that balance is the key priority and precise balancing is needed, feedback is equally important. Other important criteria included the effectiveness of weight shifting—for example, the total center of gravity shift achieved by the system. These values are very important, but perhaps not as important as having precision in shifting (because a small center of gravity shift can be adjusted by external factors like changing the mass of the shifting weight). Cost and noise were judged to be the least significant criteria, with other criteria falling in between.

Performance Criteria	Weights
Manufacturability	5
Cost	1
Effectiveness at shifting weight	4
Response Time	4
Power Usage	3
Reparability	3
Durability	4
Ease of integration	3
Volume taken up	3
Ability to get feedback	5
Noise	1

Table 1: Performance Criteria Weights

3.3 Mechanism Requirements

The balance mechanism has a simple purpose-- to provide a counter weight that will evenly distribute total weight so as to make I-3P0 stable while upright. The mechanism to solve this goal has been proven in the last 10 years to be a difficult task. Since instability can cause lean in any direction, the counterweight should ideally be able to have the same degree of movement.

The success of the balancing mechanism is heavily dependent on the integration into other components of I-3P0, especially the walking mechanism. The current walking design implements a single motor to rotate two shafts at 180 degrees apart from each other. The shafts act as legs that shuffle I-3P0 forward. With every step, internal forces can shift the weight of the body side-to-side, or forward and backward. It is assumed that shifts in weight are not purely in one direction but with rapid feedback control, we believe it is possible to achieve a proper balancing mechanism using solely linear movement.

As mentioned previously, control of the system will come directly from robust programming.

- Accurately and quickly change the center of gravity to stabilize I-3P0
- Mechanism must be space efficient, it must leave room in the chassis for other components
- Mechanism must integrate into walking system
- Mechanism must be responsive to sensors and feedback systems

3.4 Primary Size and decision

Our preliminary design was based on the proportions of the human body, the ratio of weight distribution for every component, and weight requirement for the counter mass. Initial design provided the scheme of a rectangular shaped torso approximately 20x15x10 in., containing an inner shifting box of size 14 x10 x 5 in. The inner box would house a mass of 50 lbs (a preliminary estimate, using a total I-3P0 weight of 200 lbs), and shift left and right to maintain balance.

The two main designs we explored produced many variations of pendulum and track systems. We approached our design with the goal of actually completing the project by the showcase date so feasibility was the most important factor in determining design. Level of experience and budget were not heavily weighted factors.

3.5 Research

A large portion of the design process was based on the research collected throughout the initial idea phase of the project. We asked the team to browse any media on content related to walking robots, from videos to published literature to news articles. Many of the published papers were helpful at emphasizing the need for a robust controls system and how integral the control system/ balancing mechanism interface is. There are many commercial walking robots being developed over the last 20 years. The most notable is the Honda ASIMO, a personal assistant. We aimed to organize characteristics of these commercial robots and develop a way to see what qualities of design control allowed for the type of movement we desired. Listed here in a house of quality diagram, are 5 robots that can walk alone. They are not all a full scale human model but the controls systems can be translated into a larger scale.

3.6 Design Concepts

Some initial inspirations for weight shifting came from the Asimo, as shown in Figure 54.

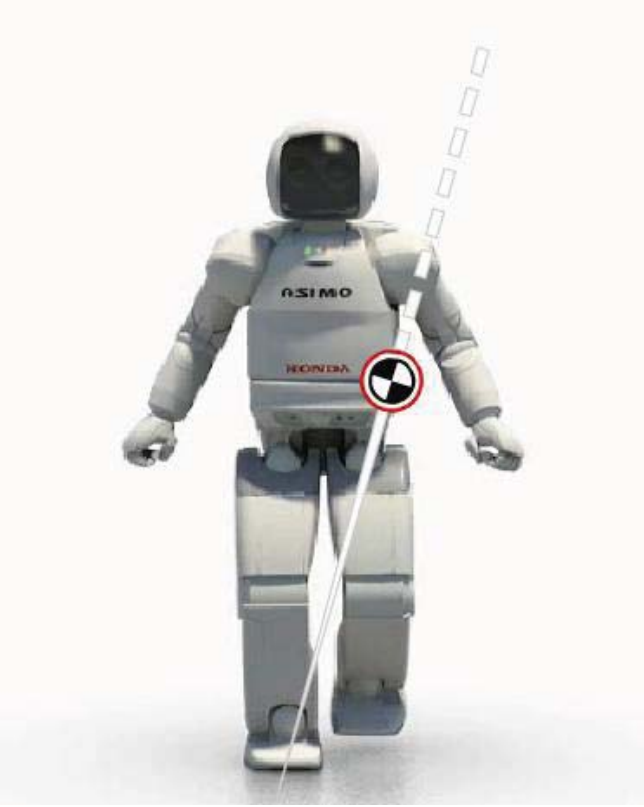

Figure 54: Center of Mass Weigh Shifting in the Asimo

3.6.1 Solutions

The basic issue with the balancing mechanism is the infinite ways a standing unbalanced structure can fall. Within the realm of our project duration, budget, and experience, it was decided that solutions involving only 2 degrees of movement would be the most feasible.

3.6.1.1 Track system

One of most plausible ideas to move a counterweight was a track system. A motor added to a mass would actuate transversely across the tracks. Based on the total weight of the system and the required weight of the counterweight, the tracks would be placed toward the lower half of the torso. Unlike the pendulum designs discussed later, there would be very little power used to keep the balancing system stationary. The system would provide a fair amount of stability, and seemed to be one of the most feasible solutions.

3.6.1.1.1 Two Track

One permutation of the track system that was discussed was the two track system which used two motors to move mass in both the x and y axis (forward/backward and left/right independently). Because weight shifts can

occur in any direction, the two track system would provide accuracy when moving the mass to balance the robot. This would be performed by having one track system attached directly to the torso structure, and then another track system mounted to the platform of the first to serve as a second degree of motion. Each system would have a motor would be responsible for movement in one direction, and the system as a whole could move a mass anywhere in a horizontal 2-D plane. This option would be robust and precise; however, controls and implementation might prove to be very difficult.

3.6.1.1.2 One Track and Bending

The Rockband robots, from past Cornell Cup teams, were able to bend a heavy torso forward and backward. If it were necessary for walking, we wanted to explore this type of motion as another form of balancing. Using a single track similar the one described above for sideways weight shifting, I-3P0 (with a bending joint) would be shifting his whole torso forwards and backwards to properly counteract imbalances forced upon by the walking mechanism. The bending motion would be carried out through a large linear actuation placed on a beam protruding from the back of I-3P0, attached to the upper torso area, as one can see in the rockband robot design. The linear actuator would be placed at angle and the torso on a pivot. As the linear actuator pushed, the torso would bend forward. This theory had many pitfalls however as the project it was based upon never produced a working bending mechanism. One of the main problems was the weight of the actuator which was approximately 20 pounds on its own. Balance of the actuation along with the rest of the torso would add additional source of error that could be avoided.

3.6.2 Pendulum

The ingenuity of using a counter weight at the end of the pendulum lies in its ability to add an additional degree of freedom of up/down, which can provide a more precise placement. As a team we discussed 3 possible mechanisms involving the pendulum

1. 2 motors- 2 degrees of freedom. Each motor would control a degree of freedom, left/ right or forward/ backward toward the top of the pendulum. The pendulum origin would have to be fixed meaning; the counterweight could only work within 2 possible “lines”. This greatly limits the ability of the mass to act in a specific location.

2. 2 motors- another configuration with two motors was to have an inverted motor attached to an actuator. The motor would provide rotational movement in the x-y plane and the actuator provide movement in the z axis. With the right tools, testing time, and experience this method

would have most precisely emulated human balancing. The mass at the end of the actuator would be able to move in all three planes.

3. 1 motor – The final configuration was simply the previous without the actuator. We were aware the difficulties in controlling an actuator on a motor and believed that movement in the x-y plane could be sufficient to fulfill our needs.

3.6.2.1 Inverted vs non inverted

The Pendulum design was discussed in two different configurations, inverted and non-inverted. In an inverted pendulum the center of mass is above the pivot point, while in a regular pendulum the center of mass is below.

The inverted pendulum was discussed first as it as the human body balance mechanism most closely resembles an inverted pendulum. The sway of the upper body correlated with each step allows the body to balance at any angle of step. The torso acts a counterweight to shift the center of gravity. The difficulty of implementing the mechanism is controlling a heavy weight to move to precise locations. The motors in play would likely always be powered, and the system would therefore have high energy costs.

A similar solution is the traditional pendulum. In this case, the connecting rod helps support the mass in the z-direction, reducing the amount of power needed to hold the mass in place. While this mechanism is a more reasonable to control than an inverted pendulum, the difficulty of accurately placing a mass in space still applies and the power usage is still significant.

3.6.3 Hip and Ankle Active Motors

This mechanism mimics another dynamic aspect of the human balancing system, the muscles of the hips and ankles to stabilize a system. The human body uses multiple joints in the leg as stabilizing points, including the knee, ankle, and hip. In this mechanism, actuators would be place on opposing sides of a joint to push/pull a “bone” or leg T-bar in the direction of a balanced system. This system would need to be implemented as part of the walking design; since the walking system chosen required balancing capabilities in the torso, this system was ruled out.

3.7 Preliminary Design

3.7.1 Choosing design

After much collaboration with the team responsible for the walking mechanism, it was decided counterbalancing in the left/ right direction would be our primary concern. The walking mechanism has the possibility of producing a lot of disruption in balance so we decided that the simplest solution would have to suffice in order to make the controls system as robust as possible. The following decision matrix provides a standardized evaluation of the proposed mechanism, producing two obvious solutions.

3.7.2 Decision Matrix

Criteria	Weigh t	2-Track System	Inverted Pendulum	Regular Pendulum	Hip and Ankle Motors in 2deg	1-Track and Bending	Gyroscopes	Springs (Hip and Ankles)
Feasibility	4	4	3	3	4	4	2	5
Manufacturability	4	4	3	3	4	4	1	5
Cost (low cost is high)	1	4	3	3	2	3	1	5
Speed	4	4	5	5	5	5	5	2
Power usage	1	5	2	2	1	2	3	5
Torque delivery/ Inertia	5	2	5	1	5	4	4	2
Sensor Compatibility	3	4	3	3	4	4	2	2
Feedback ability	3	4	4	4	4	5	2	2
Controllability	3	5	4	4	4	4	1	2
Size	1	3	2	2	5	3	3	4
Totals		109	109	89	121	119	74	90

Table 2: Decision Matrix for Balancing Mechanism

The decision matrix factored in the requirements and goals listed in the beginning of this this subsection. The delivery of the inertia was listed as the highest weighted criteria as it defined the success of the balancing mechanism. The top two options were revealed to be hip and ankle motors and a one track/ bending mechanism. Even though the hip and ankle motor option had the highest score, it was quickly ruled out after the walking mechanism was fully defined.

With one motor as the source of power in the legs, hip stabilization would not provide the necessary reflex to a system. A counter balance would have to be originating from a point close the torso/leg junction but tall enough to stabilize the torso and arms. In another instance of a

different walking mechanism, this method could have worked. For our purposes the one track system was developed more fully.

This idea led us through an evolution of configurations of a single track system. First with a bending motion involved and then as discussion continued, it was decided that the bending was not necessarily and in fact detrimental to the success of the system. Since weight shifts would be primarily in the coronal direction the need for balancing mechanisms in two directions could be less useful that predicted.

3.8 Material Selection

We decided to use T-slot bar in order to maximize the potential utility of the robot. The T-bar makes it very easy to swap out additional components for new ones later. If we wish to add addition components or even just swap out the electrical components we will need the extra versatility. Further, our only real issue we had with using T-Bar was the potential for I-3P0 to weight too much. However, after we determined that we would have to add a significant amount of dead weight anyway, the extra 5 lbs from the T-bar was almost negligible in terms of motor selection.

3.9 ECE Interfacing

Because I-3P0 will use tethered power, the power requirement for the motor is not a huge concern. However, the ECE team does need mounting slots for the atom board, motor controllers, and a few Arduinos—these requirements were the reason that the inner weight shifting box was made with T-bar. Using T-bar would allow for easy mounting and modularity in arrangement, both of which were deemed important for the ECE team.

In addition, the size of the atom board (around 10x7x1.5 in) determined the size of the inner box. To account for the 10 in dimension, the inner box was made almost as tall as the torso itself. Since the ECE components are the only things needed to be contained in the torso, we plan to put these components inside the moving box—reducing the amount of dead weight we would need to add to I-3P0.

3.10 Track Selection

3.10.1 System Type

There were a couple possibilities for creating linear motion on a track system. The three options we researched were a rack and pinion system, a screw drive, and a belt drive.

3.10.1.1 Rack and Pinion

A rack and pinion system is an easy way to create linear motion. In our case, we would need the rack to be stationary relative to the torso frame, with the pinion providing the

linear motion by twisting along the rack. This method is simple, space efficient, and provides good speed and acceleration.

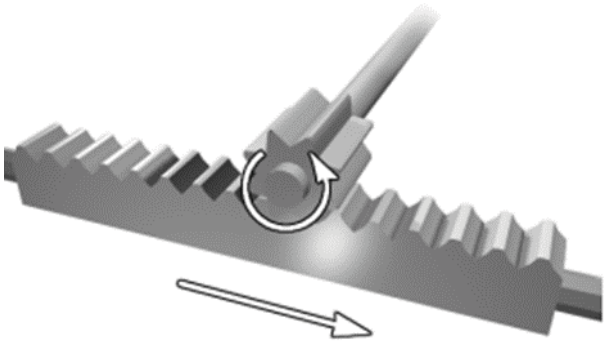

Figure 55: Rack and Pinon System
Source: (http://upload.wikimedia.org/wikipedia/commons/6/6b/Rack_and_pinion.png)

3.10.1.2 Screw Drive

A screw drive, such as a ball screw, is another mechanism to produce linear actuation:

Figure 56: Screw Drive System
Source: (http://www.velmex.com/in_stock_a40.asp)

The basic mechanism involves rotating a linearly stationary screw, which "screws" an attached cart along the axis of the screw. Mills commonly use a similar mechanism to shift the worktable side to side.

This method requires a high RPM to have a good travel speed, but is very precise and robust. However, most motors would have to be mounted to the side of the track, which in our case would reduce the distance of travel of the internal weight.

3.10.1.3 Belt Drive

Belt drive mechanisms are commonly used to produce linear motion, such as in the heavy duty belt drive actuator shown below:

Figure 57: Belt Drive System
Source: (http://www.designworldonline.com/explosion-proof-linear-actuators/)

Belt drives have a lot of the same pros as a rack and pinion system, but can also use up valuable side/side space like the screw mechanisms.

3.10.2 System Decision Matrix

A decision matrix was made to decide on the track system type to pursue. The rack and pinion system won, largely due to space optimization and speed.

Criteria	Weights	Rack and Pinion	Ball Screw	Belt Drive
Space optimization	4	5	2	3
Speed	2	4	2	4
Acceleration	3	4	2	4
Weight	1	2	2	3
Machinability	4	3	4	3
Likelihood to fail	5	3	4	2
Precision	3	3	5	3
Total		**78**	**71**	**66**

Table 3: Balancing System Decision Matrix

3.11 CAD Modeling

A preliminary CAD was designed for the chosen mechanism:

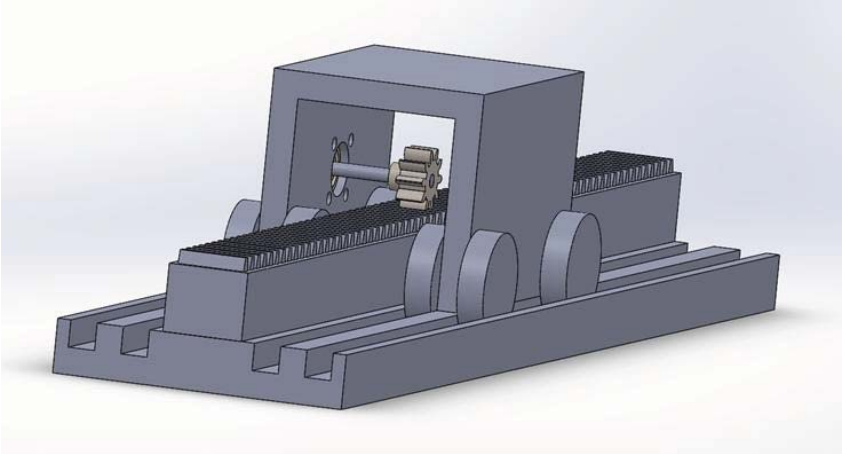

Figure 58: CAD for Preliminary Mechanism

In this design, a rolling cart (with platform on top) would roll along a simple track system. A pinion attached to the motor shaft would move the cart along the track.

Once a preliminary motor selection was completed, we added the chosen motor to the CAD. In the process, we changed some geometries of the system:

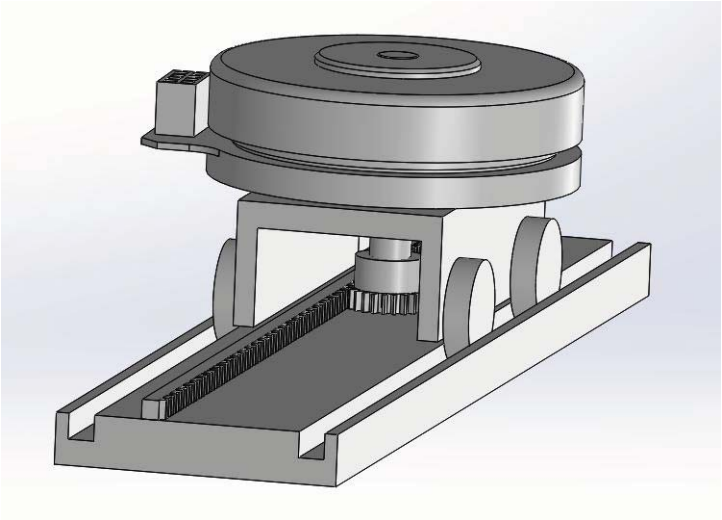

Figure 59: CAD for iterated mechanism with motor

The advantage of this design was its simplicity and machinability. However, we felt that it also had a significant problem--the lack of a mechanism to keep the cart on the tracks. I-3P0 will be walking around, and tilting as he walks. Any bump or forward/backward shift in weight could easily cause the cart to tilt off the track. Therefore, further design iteration was needed.

3.12 Motor Selection

Throughout the design process, it is important to simultaneously work on motor selection. Often, limits in motor specifications will force design changes to the entire system; therefore, it is valuable to keep up to date on both aspects.

The motor for the balancing mechanism was specced out with the following performance criteria:

1. Needs to move a 50 lb weight
2. Needs to move across a distance of 12” in less than 1 second

Because some Maxon motors have a shaft diameter of 10mm while others have a diameter of 12mm, we wanted to choose a pinion machinable to each bore size (including keyway, see R2D2 locomotion design). We ended up choosing a McMaster steel 14 1/2° rack and pinion combo with 24 pitch and 1.5 in. pinion diameter.

With this information, we can begin motor selection.

3.12.1 Torque/Speed Requirement

The most important criteria for choosing motors are the desired maximum speed and torque requirement. In the case of I-3P0, the acceleration requirement was the acceleration needed to make a 50lb weight traverse a distance of 12” from rest in one second. Converting to metric units, we have:

$$weight = 23\ kg$$

$$distance = .3048\ m$$

We can then calculate the required acceleration of the inner box:

$$d = .5at^2$$

$$.3048 = .5a$$

$$a = .6096\frac{m}{s^2}$$

Then, we can calculate the required force to provide that acceleration. It is important to take into account the friction caused by the carriages/bearing sleeves on their rails (see design section). In this case, we are using .2 as an upper estimate for the coefficient of friction between aluminum and HDPE.

$$F = ma + F_f$$

$$F = 23 * .6096 + .2 * 23 * 9.81 = 59\ N$$

Now, we can calculate the torque required to exert that force:

$$pinion\ diameter = .0381\ m$$

$$M = F * r = 59\ N * .01905\ m = 1.1\ Nm$$

We can approximate the top speed as 1 m/s. With the given pinion diameter, we can calculate the motor operating RPM:

$$RPM = \frac{1}{\pi D} * 60 = 501\ RPM$$

Therefore, our motor operating point is around 1.1 Nm, 500 RPM.

3.12.2 Motor Options

In this case, we were highly limited by the geometries of the balancing system. Although the operating point is very similar to that of R2D2's motors, the long feet motors for R2D2 would limit either the stroke length of the track system or the housing space for ECE components and our counterweight.

Therefore, the best solution was clearly the EC90 Flat. This motor is very short (even with a gearbox), would have minimal impact on housing space, and would have no impact on stroke length.

Figure 60: Maxon EC 90 Flat with MILE Encoder

To reach the proper ratio, a gearing system is required. We decided to use a planetary gearbox with ratio 4.3:1:

$$Torque = 4.3 * .91\ (efficiency) * .387\ Nm\ (nominal\ torque) = 1.51\ Nm$$

$$Speed = \frac{2650\ RPM}{4.3} = 616\ RPM$$

Although the motor may be a little overspecced based on the initial criteria, we can always run the motor at less power. In fact, it may be useful to have slightly overspecced motors, in case our requirements are increased after further iteration of the walking design. Therefore, the Maxon combination we decided on is:

Motor - EC 90 Flat Brushless, 90 Watt (323772)

Gear - Planetary Gearhead GP 52 C, Ceramic, 4.3:1 (223081)

Encoder - Encoder MILE 800CPT, 2 Channels, with Line Driver RS 422 (409996)

To confirm that the EC90 Flat would meet our requirements, we needed to make sure that factors such as the max radial load, electrical requirements, and thermal limits were all met.

3.12.3 Radial Load

The max radial load of the given gearhead is 500 N at 12 mm from the flange. At 18 mm, this corresponds to a max radial load of 333 N. Given that this is far greater than the transmitted force of 60 N, it is unlikely that we will approach this max radial load.

3.12.4 Thermal Limits

It is also important to make sure that the motor is operating below thermal limits. First, one must calculate the power losses in the motor using the equation:

$$P_J = P_{el} - P_{mech}$$

(where P_J = power loss, P_{el} = electrical power, P_{mech} = mechanical power)

The electrical power can be approximated using the efficiency losses in motor and gearbox. The maximum gearbox efficiency is 91%, while the motor efficiency is 83%.

Our requirement for torque after the gearbox is 1.1 Nm. Therefore, the required torque output of the motor (taking into account gearbox reduction) is:

$$M_{motor} = \frac{1.1}{4.3 * .91} = .281\ Nm = 281\ mNm$$

$$RPM_{motor} = 500\ RPM * 4.3 = 2150\ RPM$$

Using our operating point, we can calculate our mechanical power:

$$.281\ Nm * 2150\ rpm * \frac{2\pi}{60} = 63\ watts$$

Therefore, our electrical power is:

$$P_{el} = \frac{63\ watts}{motor\ efficiency} = \frac{63}{.83} = 76\ watts$$

Our power loss can then be calculated:

$$P_J = P_{el} - P_{mech} = 76 - 63\ watts = 13\ watts$$

In addition, we now have information on the current draw for our motors:

$$I = \frac{76\ watts}{24\ V} = 3.16\ A$$

With a power loss (heat dissipation) of 13 watts and values for the thermal resistances for the given motor, we can calculate the increase in motor temperature:

$$\Delta T_W = \left(1.89\ {}^{K}/_{W} + 2.99\ {}^{K}/_{W}\right) * 13\ W = 63.44\ K$$

This is a fairly large temperature increase. Using an ambient air temperature of 25°C, the motor will heat up to 88°C. While this is still below the thermal limit of 125°C, it is closer than we like. If a housing is used to cover the motor, overheating may be a problem. Therefore, it may be useful to explore cooling options to help accelerate motor heat dissipation.

3.13 Iterate Design

3.13.1 First generation - three tracks, three carriages

In revising the design, we came across linear slide mechanisms on McMaster. These prebuilt slide rails would allow us to focus solely on the rack and pinion layout, without having to design

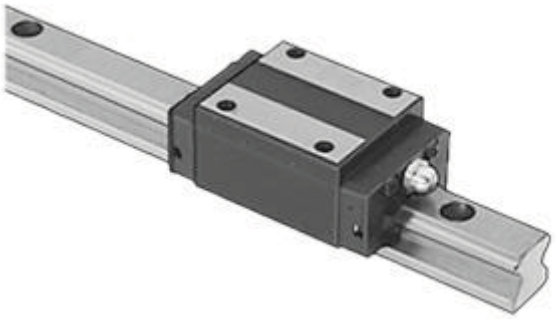

Figure 61: McMaster Threaded Hole Carriage w/ guide

a slide mechanism ourselves. The first option was a ball-bearing carriage and rail guide:

Although the system met all our criteria, it was clearly designed for a more intensive application. The max load allowed was almost 2000 lbs, while we were only looking for something to carry 50 lbs. This overcompensating for the specifications was reflected in the price of the system-- at the time of this writing, one carriage is sold for near $125, while the guide rail costs over $300 per meter.

Lots of similar carriages were sold for comparable prices. However, one option we came across was a polyethylene slide carriage--a high density polyethylene (HDPE) carriage that had a low enough coefficient of friction to slide smoothly across the provided rail:

Figure 62: McMaster Polyethylene Slide Carriage

In the process, we had to account for the increase in friction in the system in motor selection, which necessitated the addition of a gearbox to our previous motor. In addition, we added a basic torso frame CAD to show how the entire balancing mechanism might work. This preliminary CAD is shown below (without motor bracket):

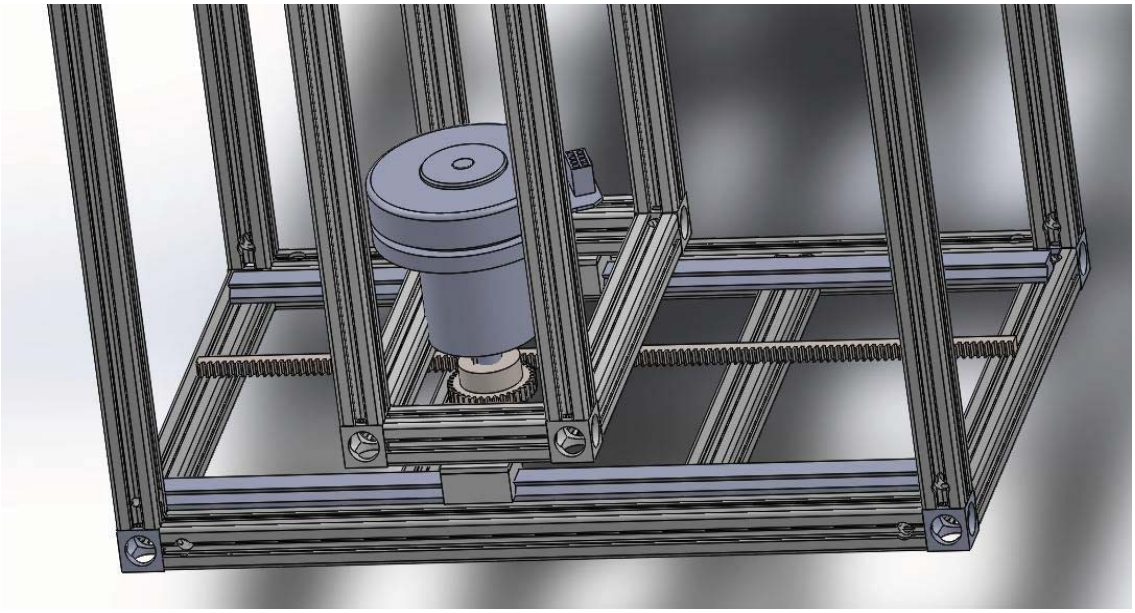

Figure 63: CAD with integrated Slide Carriage

The guide rails can be seen at the front and back of the outer chassis. In this design, only one carriage was used per rail; however, an additional rail on the side of the chassis was used to stabilize the moving box:

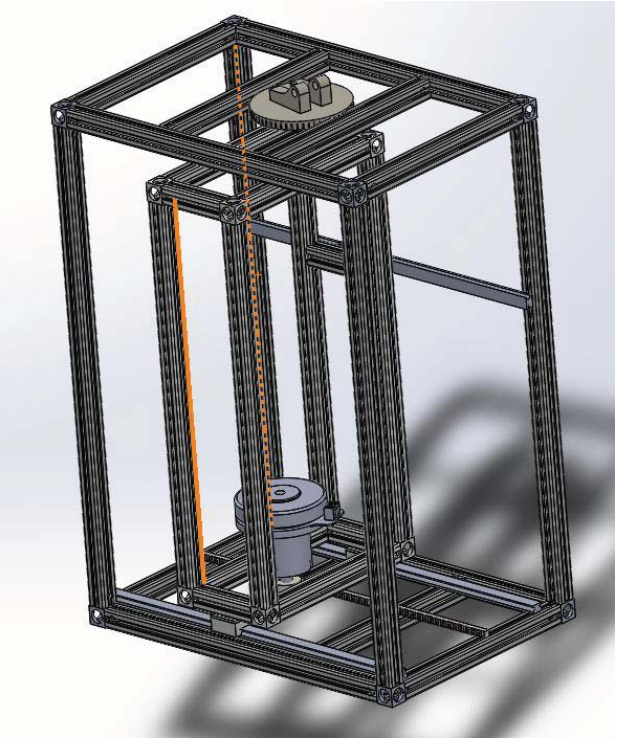

Figure 64: CAD with Integrated Slide Carriage

3.13.2 Second generation- two rails, four carriages

The biggest concern about the existing design was the stability of the system. We felt that four carriages at the bottom seemed more reasonable in supporting a system with a moving 50lb weight. However, the price of the balancing system would increase with extra support.

Therefore, we decided to make our linear slides even simpler. In addition to carriage systems, McMaster also has linear bearings built to slide on metal rods. Similar to the HDPE carriage, there are inexpensive HDPE sleeve bearings made to emulate more expensive linear bearings:

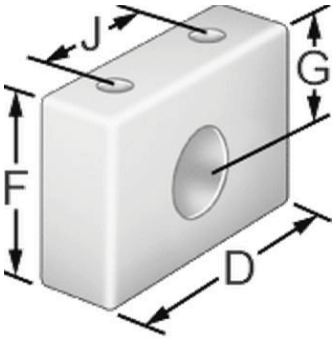

Figure 65: HDPE Sleeve Bearing

Instead of the slide rails we had used before, we could use metal rods with brackets on either end. In addition, we could use 4 of these bearing blocks (two on each shaft) to make the system more stable:

Figure 66: Torso CAD, shown with arm/leg mounting points, rack is hidden behind track rod

3.14 Revision of Requirements

We checked in with our walking team, and learned that they were planning on walking I3P0 at around 1.5 steps per second. At the same time, we made the decision to not statically balance I3P0 (he wouldn't be able to stand on one foot). Instead, we would allow him to walk without falling and have the electrical team make sure that he stopped and started in a balanced position with both feet on the ground. We also were able to get better estimates for the robot's overall weight (around 120 lbs), which allowed us to re-spec our motor requirements.

3.15 Balancing Mechanism

3.15.1 Matlab

A simple Matlab script was written to help us find operation points of our balancing system. We kept the mass of the moving weight (including motor) adjustable, and calculated the weight

shifting ability for a range of walking speeds. To quantify the ability to weight shift, we calculated the center of pressure for the robot, and labeled the distance between the center of pressure and the internal edge of the foot as “foot clearance”. For the robot to balance, the center of pressure had to be within the boundaries of the foot on the ground; therefore, foot clearance is a measure of the effectiveness of the weight transfer onto the grounded foot for balancing.

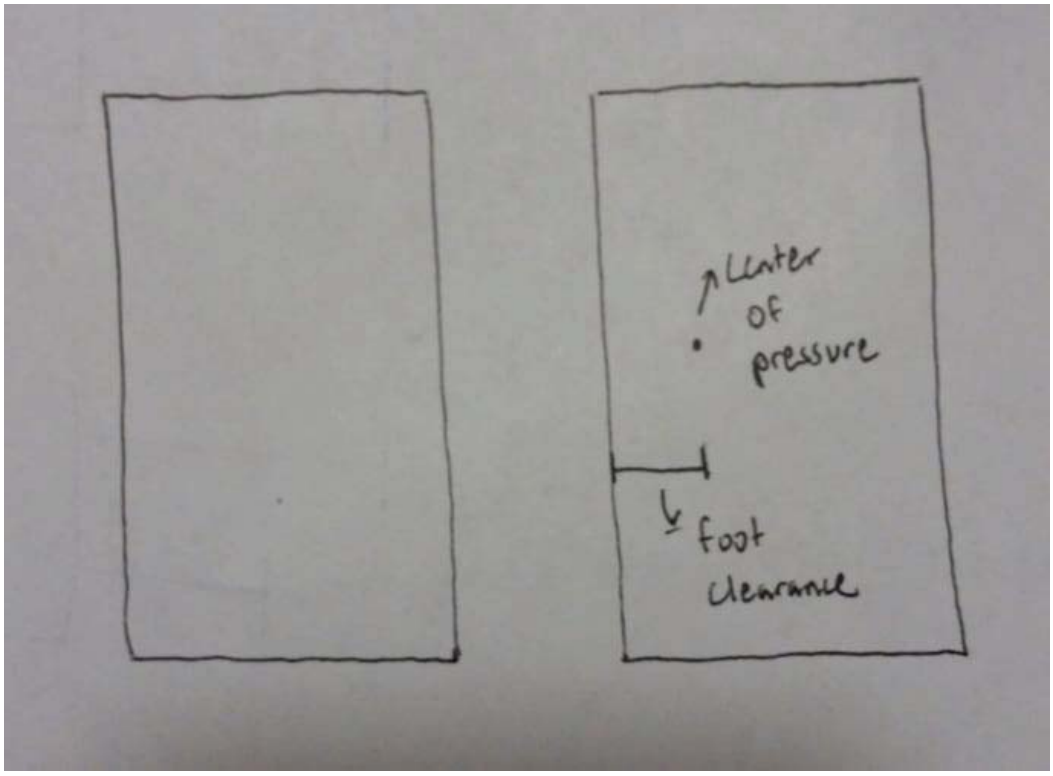

Figure 67

```
% Cornell Cup USA, Spring 2014
% Torso Balancing/ Weight-Shifting Mechanism

% MATLAB code to plot the foot clearance (from the center of mass of I3P0
% to the inner edge of the support polygon (foot)) of I3P0 against the
% revolutions/second of the walking motor. Multiple curves are plotted -
% these are different values of masses for the weight-shifting, and the
% line at 0.254m corresponds to a 1" foot clearance. Ideally, a mass and
% walking motor speed would be chosen at or above this clearance line. The
% weight-shifting motor follows a triangular velocity profile (constant
```

```
% acceleration/deceleration), the acceleration of which can be found using
% the formula: a = (4*path/T)^2/path. Also, note that the foot speed is
% twice that of the motor speed (2:1 gear ratio).


%% Clearing
close all
clear all
clc

%% Parameters
h = 1.524;              % height from internal weight to ground [m]
m_weight = 5;           % mass of internal weight [kg]
m_body = 52;            % mass of I3P0 (without internal weight) [kg]
path = .3048;           % track length [m]
g = 9.81;               % gravity [m/s^2]

n = 1;                  % index initialization

foot_clearance = zeros(10,15);  % distance from edge of foot
x = zeros(10,15);       % distance from absolute center
F = zeros(10,15);       % force
tau = zeros(10,15);     % torque
revps = zeros(10,15);

%% Calculations
% Set up right now to vary walking motor rps from .1 to 1.5 with given
% mass, and calculate foot clearance.

for rps =.1:.1:1.5 % rps = revs/sec --> corresponds to how many steps/sec

    for m_weight = 1:15     % mass weight: 1 kg -> 15 kg

        % Calculating acceleration for weight-shifting
        revps(m_weight,n) = rps;
        T = 1/rps;          % period of one cycle
        v_avg = 2*path/T;   % average velocity of travel
        v_top = 2*v_avg;    % top speed of travel
        a = (v_top)^2/path; % 2ad = vf^2

        x(m_weight,n) = h*a*m_weight/(g*(m_weight+m_body));
        foot_clearance(m_weight, n) = x(m_weight,n) - .006;

        % Calculating power required
        F(m_weight,n) = m_weight*a+m_weight*.2*g;
        tau(m_weight,n) = F(m_weight,n)*.01905;

    end

    n = n+1;
end

%% Plotting
figure(1)
```

```
hold on;

color_array = [[0 0 0]; [1 0 0]; [0 .5 0]; [.75 .75 0]; [.75 0 .75];...
    [0 1 1]; [1 .4 .6]; [.7 .7 .7]; [1 .5 .25]; [.6 .5 .4]; [0.75 0.3 0.1]];
axis([0 1.3 0 .1])

for m = 5:15
    plot(revps(m,1:(18-m)), foot_clearance(m,1:(18-m)), 'Color',
color_array(m-4,:))
end

xlabel('rps')
ylabel('foot clearance (m)')
line([0; 1.5],[0; 0])
line([0; 1.5],[.0254; .0254]) % 1 inch line
title('Weight-Shifting Mechanism Spec Determination')
legend('5kg','6kg', '7kg','8kg','9kg', '10kg', '11kg', '12kg', '13kg',
'14kg', '15kg')

hold off;

%% Final Decision
% Mass = 22 pounds (10 kg)
% Walking speed: 1.5 step/s
% Walking motor speed: 0.75 rev/s
% Acceleration of weight-shifting: 2.80 m/s^2
```

The output of the script is in Figure 68:

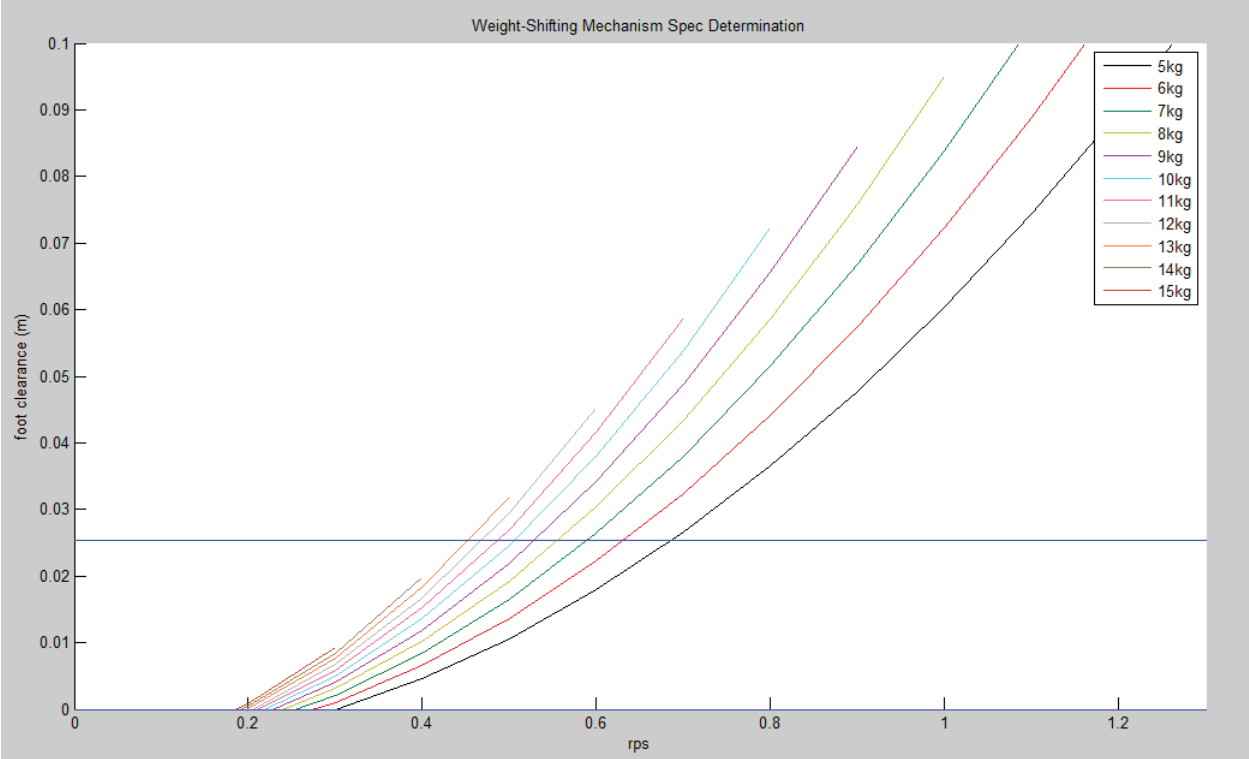

Figure 68

Each curve represents a certain weight shifting mass, going up in increments of 1kg. The top end of the curve cuts off where our motor is maxed out in terms of torque output. For the grey curve (12 kg weight), one can see that the maximum operating speed is around .6 revolutions per second—where .6 revolutions per second corresponds to .6 per second * 2 steps per revolution = 1.2 steps per second.

The horizontal blue line on the figure corresponds to a foot clearance of 1 in, which was the smallest possible safety factor we felt comfortable with. We aimed to operate at points above this limit. Given that our targeted speed was 1.5 steps per second (or .75 revolutions per second), we estimated that we would want around 10 kg of weight shifting.

It is important to note that this code was only intended to give us a rough estimate of the potential mass needed. We only considered the static balancing at the point when the robot was just lifting his foot, as that is the point when his center of mass is centered on his body and he is most unbalanced. Later in the step, the weight shifting element statically shifts the weight over the foot on the ground, which aids in balancing.

3.15.2 Balancing System

The concept for balancing system did not change throughout the design process, even while the design changed significantly. In each case, a rack and pinion system was used to accelerate a mass inside the chassis from side to side, counterbalancing the imbalance caused by stepping.

I3P0s legs are controlled by a 4 bar linkage, which results in a circular style of stepping. If he started out with both feet on the ground (one forward of the other), one foot would rise off the ground as the other pushed down into the ground and raised his body. This foot would remain off the ground until the driveshaft completed half a rotation, after which the other leg would raise in the same manner. When one leg is off the ground, the balancing system must shift the weight over to the leg that is still on the ground.

To shift this weight, a force can be applied horizontally on the torso. A simple moment balance around the foot still on the ground can show you why this is the case. This force must act throughout the entire stepping motion, from when the foot leaves the ground to when it returns to the ground. This force used to shift the weight on the torso comes from the equal and opposite force used to accelerate the weight element inside the torso (see Figure 69)

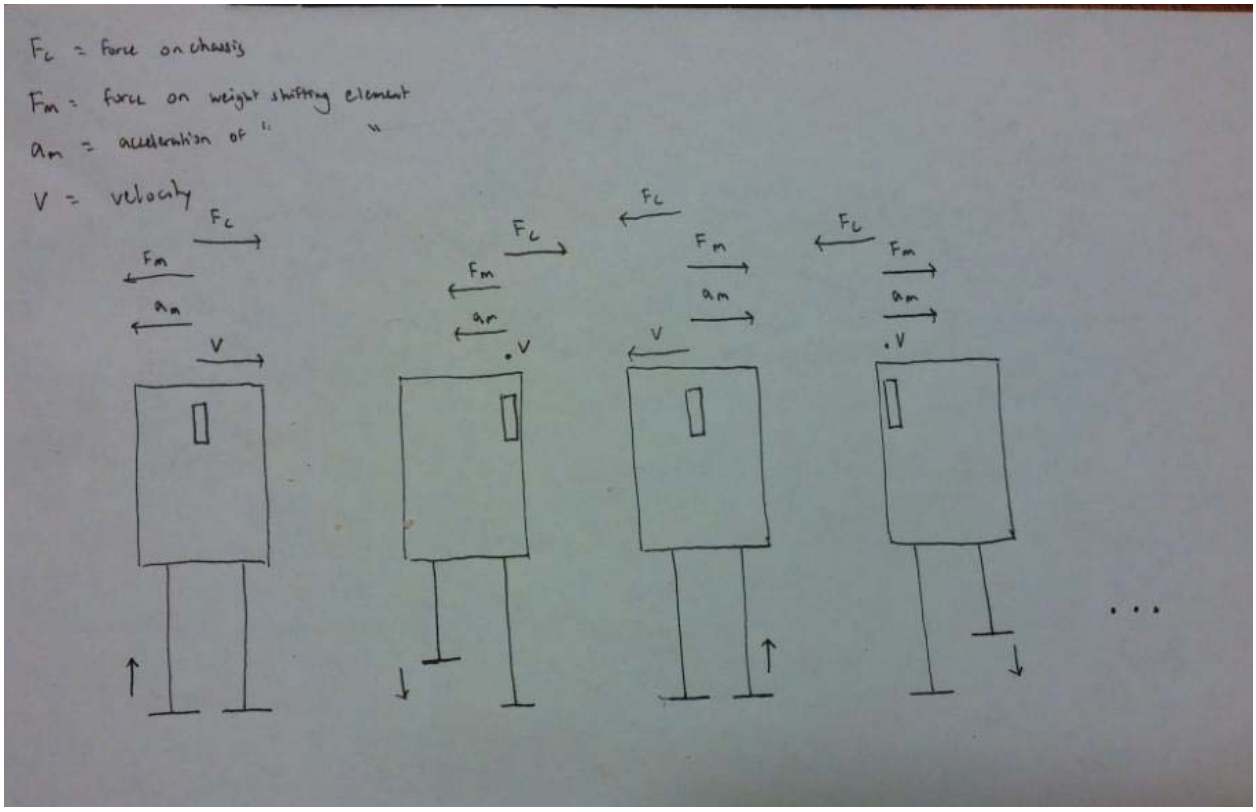

Figure 69

Therefore, we need the weight shifting element to be in the middle of the chassis at top speed at t = 0 with both feet on the ground, and slow down to zero (while reaching one side) and then back

to top speed at the middle in the course of one step. This matches a triangular velocity profile, with constant acceleration of the weight shifting element towards the side that is lifting off the ground. We gave this information, along with gear ratio, motor data, and track length to the ECE team, who implemented our triangular velocity profile and matched it with the walking motion.

3.16 Motor Change

3.16.1 Problems with current motor

Our selected motor, the EC90 flat from Maxon Motors, was backordered and had not come in by the time we were ready for testing. The ECE team was working on motor control throughout the semester, but were using a brushed motor in the prototype system we had constructed for them. The EC90 flat is a brushless motor, which would have required the use of a new, expensive controller—at this point in the process, we wanted to stick with the familiar brushed motor so the ECEs could be more comfortable implementing the specific control we needed.

At the same time, the ECE team informed us that they preferred that the boards not be mounted in a moving compartment. The wiring would become far more complicated, and they worried about tangling issues as the robot moved. This allowed us to ditch the inner t-bar frame box and simplify the balancing system considerably. In addition, this removed the size constraint for our motor; with the additional free space in the chassis we had plenty of space for a longer/larger motor.

3.16.2 New Motor

We used our updated requirements to spec a new motor. Maxon Motors did not appear to have a brushed motor that both suited our needs and was in stock, so we chose a DC gearmotor from Midwest Motion Products. **See Appendix for Datasheet** This motor was specced in a way similar to the way described above.

3.17 More Iteration

3.17.1 Dimensions

Removing the internal t-bar box allowed us to simplify our design considerably. The motor bracket was extended to provide the base for adding weight, and attached directly to the plastic sliders (see Figure 71). This greatly reduced the number of parts that needed to be machined.

The new motor was longer than the old one, but skinnier as well. The new dimensions allowed us to narrow the size of the shifting element to 3 in. wide, extending the total track distance from 10 inches to 12 inches.

3.17.2 Rack/Tube Mounting

At this point, the mounting mechanisms for tubes and the rack needed to be determined. Vibration damping pipe clamps were used to mount the ½ inch tube, and were screwed directly

into slide in fasteners in the t-bar. Rack mounting was more challenging--there was a significant axial force on the rack, the rack was too narrow to drill through (to bolt it to the t-bar), and the irregular rack surface made it hard to find an appropriate mounting solution.

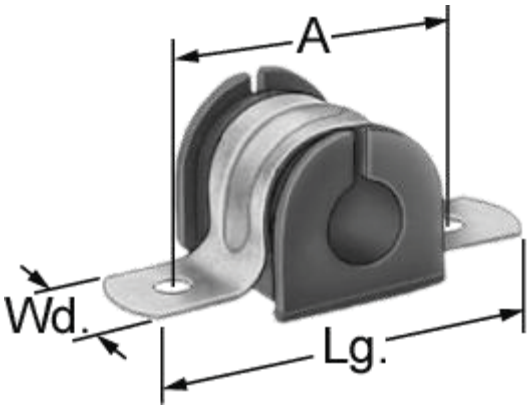

Figure 70

Moldable plastic was suggested as a way to make a mount that molded to the teeth of the rack. We used Instamorph moldable plastic plastics, which becomes moldable at 140°F. Instamorph suggests boiling water and waiting until it cools until near 140 degrees, and then adding the pellets to the water. When they become translucent/transparent, they can be molded into any shape before cooling to room temperature.

Our rack was made of carbon steel, and molding wet instamorph plastic onto the rack resulting in rusting. Therefore, we began using a heat gun to melt the plastic, which was faster and more effective. After heating the plastic, we molded it onto the rack and shaped it into a ½ tube shape with flanges. This allowed us to use the same pipe clamps we had used for the tubing to mount the rack in place. Since the rack and tubes were mounted onto the t-bar via clamps attached to fasteners, each tube/rack was independently adjustable along the t-bar. This allowed us to align the rack and pinion correctly after mounting.

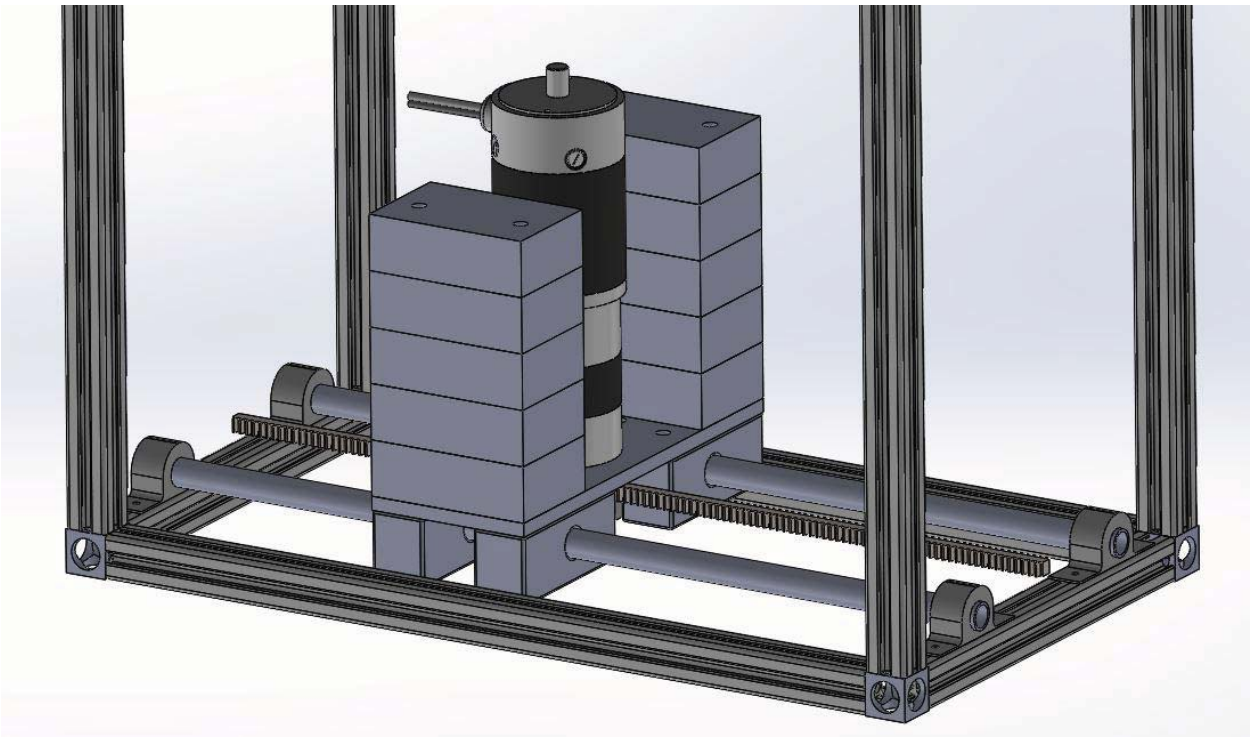

Figure 71

3.17.3 Weight

Using the Matlab code, we estimated that we'd need around 10kg (or 22 lbs) of weight for the weight shifting element. The motor + bracket weighed around 5 lbs, leaving 17 lbs of dead weight needed.

It was decided to use metal stock as weight, split into blocks to allow for adjustability (in case more or less mass was found to be needed during testing). Possible inexpensive materials were steel, cast iron, and lead, with relative densities of 7.82, 7.20, and 11.35 respectively. Lead was disqualified because of its toxicity. The pieces would likely need to be machined to attach to the weight shifting mechanism, so machinable steel seemed like the best choice.

Steel has a density of around .28 lbs/in^3, and we needed 17 lbs of dead weight. Therefore, the volume of the needed steel was around 60 cubic inches. The width of our motor bracket limited one dimension to 3 inches, and the screws from the motor bracket limited another dimension to 2 inches on each side. Therefore, we'd need 10 inches of depth total, or 5 inches of depth on each side (see diagram). We decided to split each side into 5 pieces, with dimensions 3"x2"x1". A couple extra pieces of steel were machined as well, in case additional weight was needed.

¼-20 bolts were used to mount the motor bracket to the sliding blocks, we decided to extend these bolts to attach the weight blocks to the motor bracket. Instead of bolts, we used ¼-20 threaded rod to hold the weights, motor bracket, and sliding blocks together-- with locknuts on either end.

3.17.4 Rack Bending

The rack was an extruded .25”x.25” square, and fairly flexible. When testing the system, we observed the pinion skipping on the rack when at top speed, likely due to bending of the rack. Therefore, we needed a way to clamp the pinion/rack firmly together. The clamping mechanism needed to be attached to the weight shifting element, or it would get in the way of the element itself. Our design is shown in Figure 72.

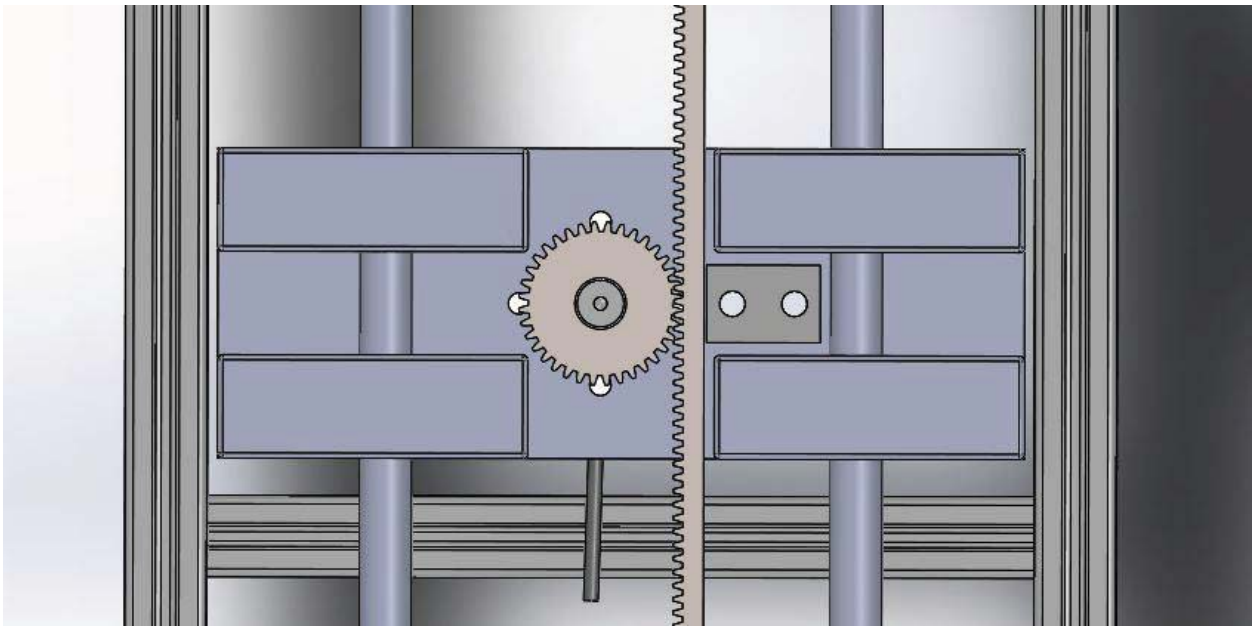

Figure 72

We use a simple aluminum block mounted to the motor bracket, mounted a set distance away from the rack. We added the soft side of a Velcro strip to the edge of the aluminum block, keeping pressure on the rack but allowing the shifting element to slide freely along the rack. The block was mounted to the bracket with two ¼-20 bolts.

3.17.5 Shift to the top

The mechanism of weight transfer goes through the rack itself, so the moment arm of the transfer depends on the height of the rack’s attachment to the chassis. Therefore, it was clearly the better design to suspend the weight shifting mechanism from the top of the torso instead of support it from the bottom. In addition, this allowed for more space in walking motor mounting, counterbalance mounting, and motherboard/motor controller mounting. The final design iteration is shown in Figure 73.

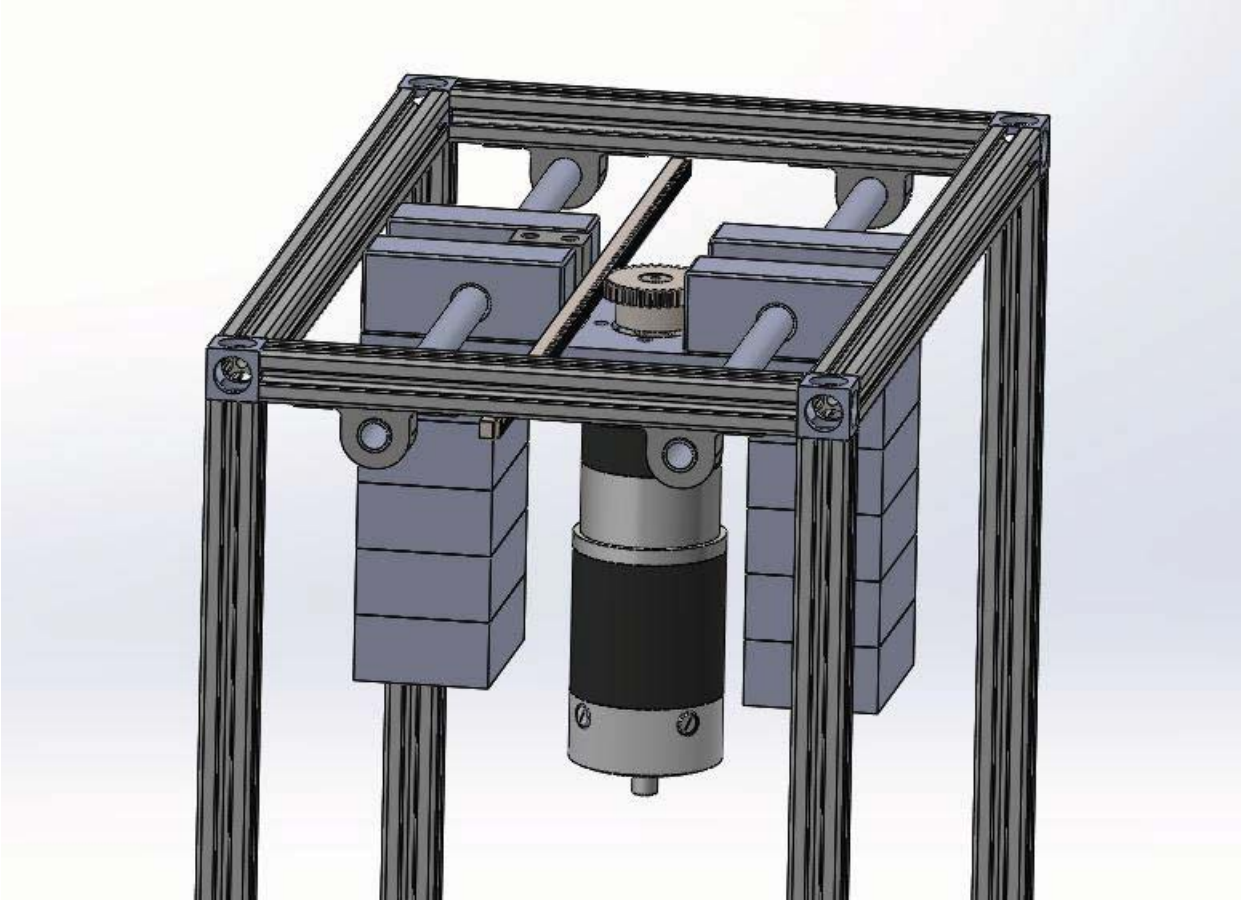

Figure 73

3.18 ECE Integration

In controlling the weight shifting motor, the ECE team wanted a way of calibrating the motor position between walks. The solution to this problem was a limit switch mounted to the edge of the t-bar on the side of the torso; when the weight shifting assembly shifted to one side of the torso, it would hit the limit switch and signal a known position. Epoxy was used to mount the limit switch to the chassis, because it was sturdy, rigid, and bound to the slick surface of the switch.

The ECE team also needed a way to mount their motherboard, motor controllers and servo controllers. We used perforated board to mount the boards, and extended the perf. Board to the t-bar framing on the sides of the torso, some of which was being used to mount I3P0s arms.

3.19 Torso Counterbalance

3.19.1 Problem overview

The asymmetric mounting of the walking motor created a large imbalance in the side-side direction of the robot. The 15 pound motor was almost entirely on the left half of the torso

causing, the left half to be much heavier than the right. Another imbalance came from the "bird" motor on the right side of the torso, since there is only a "bird" motor on the right side.

3.19.2 Transmission Shaft

The most elegant solution brainstormed was to use center the walking motor completely, so the center of gravity of the motor aligned with the center of the torso. However, this leads to many alignment issues. The walking system is designed such that the gear transmitting motion directly to the four bar linkages is immovable. If the motor was moved laterally from its initial position, a transmission shaft would be required to get the motors power to the legs. We deemed that we did not have the necessary space in the torso to align these mechanisms correctly, and thus abandoned this as a possible solution. Future iterations may allow us to pursue this as a more elegant and robust solution to the imbalance.

3.19.3 Counterweight

A somewhat less elegant, but much simpler solution was to simply add additional mass to the right side of the torso in order to counterbalance the weight of the motor. We estimated the imbalance by weighing each of the asymmetric parts; specifically, the walking motor and the "bird" motor system. Subtracting the weight of the "bird" motor (about 3 lbs.) from the walking motor (about 15 lbs.), we determined the necessary mass to be approximately 12 lbs. located on the right side of the torso at approximately the same height as the walking motor. It should be located near the walking motor to reduce possible moments that increase imbalance during walking.

We had a limited volume of space to work with on the right side of the walking motor so a relatively dense material was necessary to satisfy the weight requirement. Possible materials investigated were aluminum, steel, and lead. Aluminum (2712 kg/m^3) is not dense enough, and thus the required volume would not fit in the space available. Lead (11340 kg/m^3), has quite a high density however it was avoided due to its toxic nature. Steel (7850kg/m^3), while not as dense as lead, was decided to be the material of choice for this application. It is machinable, allowing for simple mounting to the torso. With a density of 7850kg/m^3 or 0.284 lb/in^3, a piece of machinable steel 42 in^3 was required for a 12 lb. counterweight. We purchased a 1"x6"x7" piece of stock as this fit the available space and did not require additional sizing.

3.19.4 Mounting

Since the size and location of the counterweight was an estimate, it was mounted in such a way which would allow lateral adjustment of the weight to help balance the torso more accurately. The mount involved ¾" x ¾" x 4" aluminum blocks on both the front and back sides of the torso, sitting on top of the bottom layer of the T-bar frame (see Figure 74). Two ¼" x 1.5" x 9.5" aluminum plates sat across the two aluminum blocks and were fastened with ¼"-20 screws. The steel plate sat on top of the two long aluminum plates and was fastened with (4) ¼"-20 nuts and bolts into each plate. The two ¾" x ¾" blocks were then fastened into the side of the T-bar

frame using the standard four-hole aluminum M5 plates as seen in Figure 74. It was necessary to raise the counter weight above the top surface of the T-bar frame to avoid contact between the weight and the top of the leg while walking.

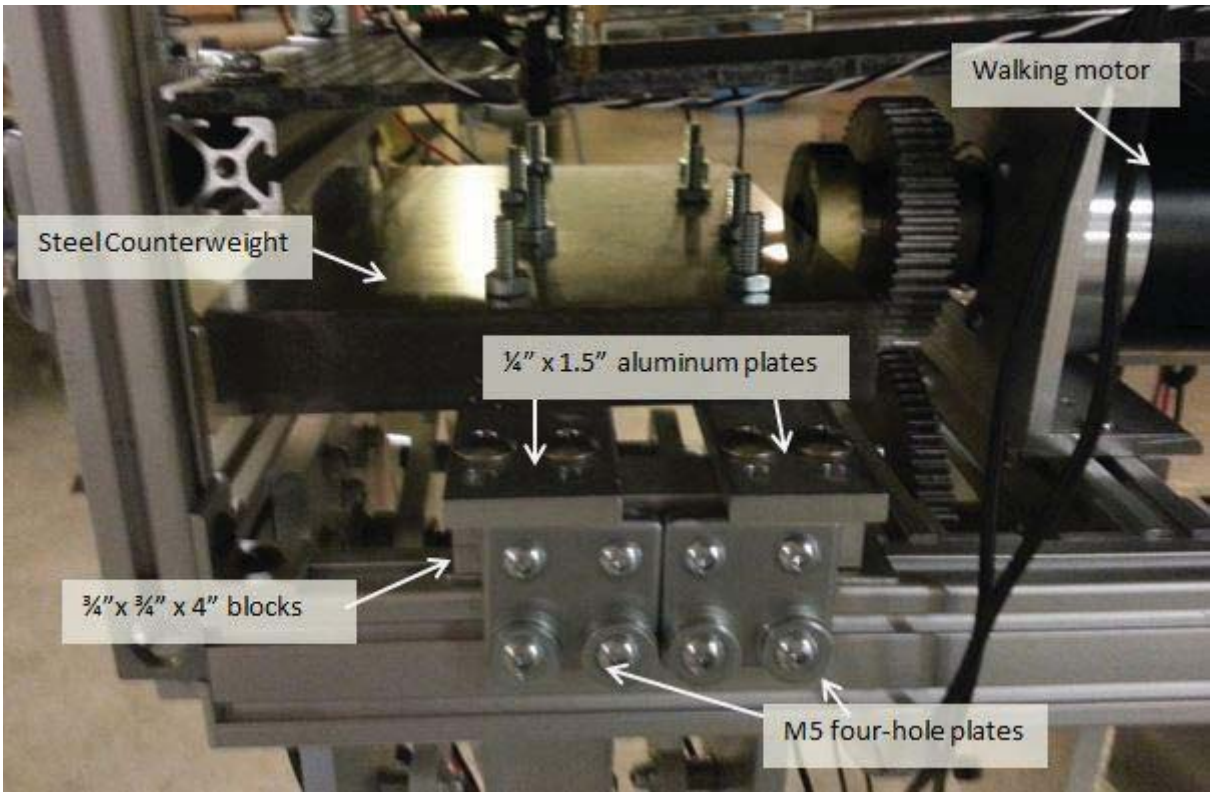

Figure 74: Counterweight system

4 I-3P0 Walking

4.1 Walking Mechanism Design Process

4.1.1 Introduction

The walking mechanism is one of three distinct sub-groups created to design I-3P0. The other two are the arm, including shoulder and elbow motion, and torso design, including balancing mechanisms. This section of the documentation covers the walking mechanism design process, the initial step of which was creating a comprehensive timeline with tasks and subtasks, deliverables and major deadlines. Each sub-group was designated as a milestone and the following is a list of tasks within the walking mechanism milestone.

1. Define Use Cases
2. Define Performance Criteria
3. Research Walking Mechanisms
4. Estimate Scale

5. Design
6. Material Selection
7. Integrate with ECE components
8. Integrate with rest of body
9. Prepare for Assembly
10. Assemble
11. Test Walking Mechanism
12. Iterate

All of these tasks were then broken down into sub-tasks and each task and sub-task was assigned a deliverable. Iteration steps were also included to allow time for unforeseen changes in the design.

4.1.2 Use Case Needs Determination

The main use case for the walking mechanism is that the system needs to translate forward, preferably with a bipedal human walking motion. However, this use case quickly breaks down into many sub-problems which include making I-3P0 stand, balance, and stop. In addition, beyond the system functioning, the system must be able to be disassembled and reassembled quickly and efficiently for the competition.

Possible misuses were also considered. Events such as control of the system is lost, the motors shutting down mid-step, and the system stepping on an unexpected object were all considered. Later in the design process, solutions of a kill switch and a mechanism such as a kill switch must be incorporated into the design. Similarly, if the system ceases to work mid-step, the walking mechanism must incorporate a method for the system to safely stop and remain balanced. At the very least, it must be able to balance itself until a team member is able to attend to the problem. Another consideration is mechanical specifications. For example, the specifications of the motors need to be over compensated for in order to allow for misuses, such as the system accidentally being pushed, or too much weight being put onto the system.

Following is a list of use cases determined:

- User commands I-3P0 to walk forward
- User commands I-3P0 to walk backward
- User commands I-3P0 to turn
- User commands I-3P0 to walk up/down stairs
- User commands I-3P0 to walk up/down ramp
- User sets I-3P0 upright
- User replaces damaged components
- User commands I-3P0 to stop walking
- User disassembles I-3P0 for packaging
- User reassembles I-3P0

Following is a list of potential misuses determined:

- User trips I-3P0
- User pushes I-3P0
- User drives I-3P0 into an obstacle
- User drives I-3P0 off stage

The “unnecessary” use cases remained on the list for possible pursuit if time allowed. However, they were given less weight in the design. The use case determination process goes hand in hand with that of the timeline creation. An iteration step exists in the timeline allowing for members to return to the timeline after defining use cases and re-format the timeline as is necessary. For example, an additional use case of the user commanding I-3P0 to ride a Segway had initially been considered. If this consideration had been pursued, tasks such as finding Segway vendors, purchasing the product, and incorporating a leaning mechanism would have been inserted into the timeline.

This further solidifies the importance of determining use cases – processes that initially weren’t considered may prove to be integral to the realization of the overall system and help with the overall planning of the project, being sure to fulfill every functional requirement of the system. In addition, these use cases are an overall insight to what the system will be able to offer. This is especially important on this team, which is split into three main sub-teams – Mechanical, Electrical, and Computer, and split even further which each sub-team.

4.1.3 Performance Criteria Determinations

After determining the use cases, the next set of decisions that need to be made is the quantifiable specification of the qualitative use cases. For example, if we want I-3P0 to be able to move forward, how quickly do we want him to perform this task? This step quantifies the goals and provides an initial rubric with which to judge each of the concepts which will be brainstormed.

Performance Metric	Target Value
Walking Speed	1 to 3 ft/s
Vertical terrain traversal ability	6 inches
Stride Length	1 ft
Life of Motors/Batteries specific to walking mechanism	TBD
Power consumption of motors/batteries	TBD
Maximum allowable laod on legs	150 lbs
Machinability	Limited to 3 axis CNC
Noise Level	60 dB
Height (total)	5’9”
Leg Length	34.5”

Weight of Legs	50 lbs
Ability to maintain traction (ability to walk on different surfaces)	Slips less than 0.5 inches/stride
Incline Traversal	Able to traverse and incline of 15 degrees
Ease of assembly (including ability of ECEs to get inside to wire) and disassembly	Max time of 3 hours
Ease of interfacing with torso	Max time of 1 hour
Ease of modifying/switching out parts if a component breaks	No permanent fastening mechanisms

Table 4: Performance Criteria Determinations

A qualitative performance metric was also added – aesthetic value, which was given the least weight among all the metrics.

After this, an ideal set of DOFs and requirements were determined which would allow the above performance criteria.

Joint	DOF	Range of Motion at Each Joint (max)
Hip	3	Roll: (+/-) 45 degrees
		Pitch: (+)60 degrees (-)30 degrees
		Yaw: (+) 30 degrees
Knee	1	(+) 30 degrees
Ankle	2	Pitch: (+/-) 20 degrees
		Yaw (+/-) 15 degrees

Table 5: Degree of Freedom Determination

4.2 Brainstorming Process

Walking humanoids is a research field that has been highly explored. Much of the initial brainstorming process for this system's walking mechanism comes from researching these pre-existing models, while also keeping in mind that the relatively restricted budget and time that was available.

4.3 Inspiration from Existing Humanoid Robots

4.3.1 Introduction:

Robotic walking mechanisms can be divided into two main categories: static and dynamic. They can be thought of as walking while standing and walking while falling respectively.

A robot that implements static walking is always balanced; that is, the projection of its center of gravity onto the ground is always within its ground contact area. Due to this fact, such a robot is much easier to control compared to its dynamic walking counterpart. This walking technique has been successfully used in many robots today. However, the movement of static walking is not true humanoid walking. It is not as adept at traversing uneven terrain as dynamic walking. In

addition, it is not very power-efficient, since active power is required to actuate every joint movement.

A robot that implements dynamic walking is not always in balance. Such a robot is continually falling and bracing itself as it walks. As a result, it draws power from gravity to actuate its forward movement, and is therefore more power-efficient than robots that use static walking. In addition, the gait of a dynamic walking robot is similar to that of an actual human, which grants it better capabilities in traversing uneven terrain. The main drawback to dynamic walking is that since the robot is not always in balance, it requires a complicated and robust feedback control system. Such a control system is extremely difficult to implement by university level students.

Cornell professor Andy Ruina, an expert in the field of humanoid walking robotics, has been consulted regarding this project. Professor Ruina's research in the past three decades has been focused on dynamic walking. His lab has made significant progress. However, after consulting Professor Ruina and performing some basic research (explained in the two paragraphs above), it was concluded that due to the time and budget constraints of Cornell Cup, it is too ambitious to purse dynamic walking. Instead, static walking was determined to be more feasible.

4.3.2 Research on Existing Robots with 6 DOF Legs:

Research conducted by team members had shown that most existing humanoid walking robots implement six degrees of freedom (DOF) in each leg: three at the hip, one at the knee, and two at the ankle. These degrees of freedom are required for walking, turning, and keeping the torso upright. Thus the initial design goal for I-3P0 was to create a 12 DOF (6 DOF per leg) walking mechanism. Four existing 12 DOF robots were studied for design inspiration. These robots include: Honda E1, Honda ASIMO, Aldebaran NAO, and RoboCup adult size humanoid league robots.

The E1 (Figure 75) was developed by Honda in 1987. It was among a series of experimental robots (E-series) created by Honda in order to research and develop humanoid walking mechanisms. In addition to being the first robot in the E-series to implement 12 DOF, E1 used static walking (robots after E1 used dynamic walking), which fit the initial design goals for I-3P0. E1 took each step by putting one leg in front of the other. It remained balanced by constantly keeping its center of gravity on top of the foot planted on the ground. E1 stood at 4 feet 2.7 inches tall (the legs were just over 2.5 feet long) and weighed 159 pounds. It was similar in size to the design goal for I-3P0. However, E1 could only walk at 0.25 km/h or 2.7 in/sec; this was quite slow compared to normal human walking. Overall, because the Honda E1 had many similarities to the design goals of I-3P0, it was a useful example to study.

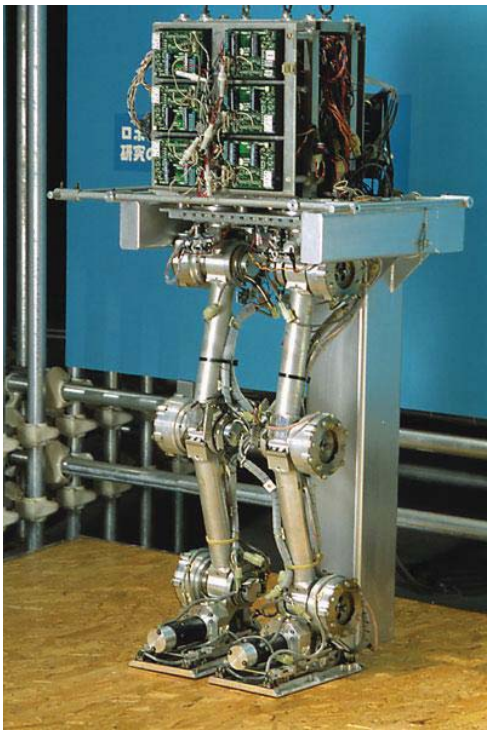

Figure 75: Honda E1

Developed in the 2000s, the Honda ASIMO (Figure 76) was a distant successor to the E-series. It stood 4 feet 3 inches tall and weighed 106 pounds. Like the E1, ASIMO also used 12 DOF for its legs, but it was able to achieve a human-like walking motion (dynamic). In addition, it was even able run at 6 km/h or 5.5 ft/sec. However, since ASIMO used dynamic walking, it was too advanced for the I-3P0 design, so it was used only for reference in the design process.

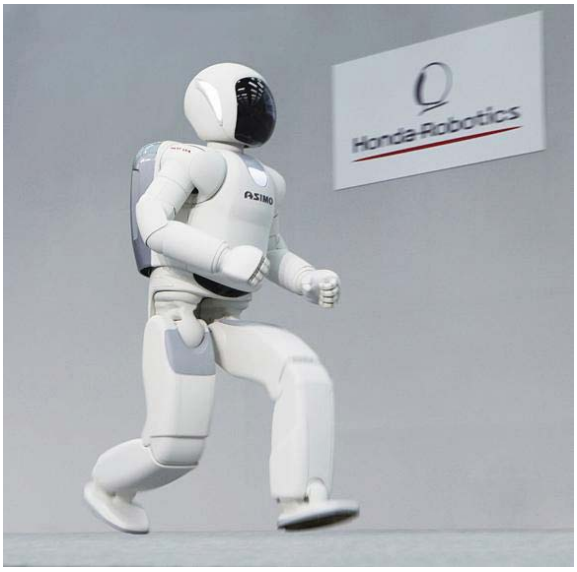

Figure 76: Honda ASIMO

The Aldebaran NAO (Figure 77) was first released in 2008 and is currently used in the RoboCup standard platform league. Developed by Aldebaran Robotics, NAO was a small, programmable, autonomous, humanoid robot meant for research and education. In fact, the Autonomous Systems Lab at Cornell used them for research. NAO was 22.5 inches tall and weighed 11.4 pounds, small and light enough to be hand-held. Despite its small size compared to I-3P0, it was studied due to its ability to walk and balance in a pseudo-static manner, which was the ultimate goal for I-3P0. NAO walked in a similar fashion to Honda E1, but it was much faster and more fluid. In addition, it was quite useful that NAO could pick itself up when it fell over, which was a potentially desired functionality for I-3P0.

Figure 77: Aldebaran NAO

The RoboCup adult size humanoid league robots had walking mechanisms that were the most similar to what was desired for I-3P0. These robots were designed and built by other college students, and so they were of a similar technical level to what I-3P0 could achieve. In general, these robots were around 5 feet tall, similar to I-3P0. However, they were light enough to be picked up by a single human while I-3P0 was planned to be much heavier. These robots walked in a motion similar to the NAO. In addition, some of them were able to sidestep. The initial 6 DOF concept design for the I-3P0 leg was based heavily on these RoboCup robots. A particularly good example was the 2013 runner-up: Team Taiwan (Figure 78), which exhibited very fluid and stable motion. The leg joints of these robots were studied in an attempt to identify ways that they can be implemented on I-3P0.

Figure 78: 2013 RoboCup Adult Size Humanoid League Runner-up: Team Taiwan

Ideally, Cornell Cup's I-3P0 design would exhibit the aforementioned 6 DOF per leg: hip yaw, hip roll, hip pitch, knee pitch, ankle pitch, and ankle roll. However, it was important to evaluate in more detail the need and mechanical feasibility for these degrees of freedom with a decision matrix.

4.3.1 Initial Concepts

In order to meet the turning requirement, several turning methods and mechanisms were brainstormed. Primarily, if the walking mechanism had at least five degrees of freedom, the joints would be able to be controlled in such a way that would facilitate turning. The additional turning mechanisms that would work regardless of degrees of freedom are contained in Figures 79-83.

4.3.1.1 Pivot and Locking Turning Mechanism

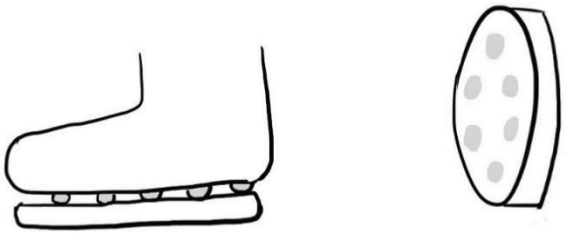

Figure 79: Pivot and Locking Turning Mechanism

The pivot and locking mechanism contained a flat circular plate, ball bearings, and a break to lock the plate in place. It was hypothesized that it could work by rotating the torso, which would in turn cause the lower half of the robot to turn the opposite direction by principle of momentum conservation. Then, the break would lock the plate in place, and the torso would rotate such that it faced the same direction as the feet.

4.3.1.2 Wheel Turning Mechanism

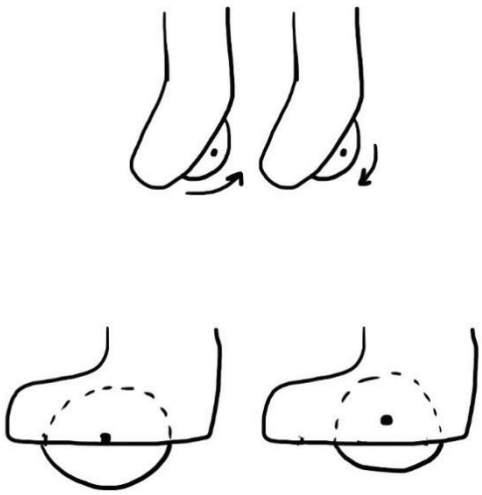

Figure 80: Wheel Turning Mechanism

Having wheels in the feet rotate in opposite would allow the robot to turn. Issues that arose were that the wheels would have to have enough power and traction to move 150 lbs or more. In addition, if the foot no longer touched the ground, the leg could pivot the drive axle.

4.3.1.3 Heely Turning Mechanism

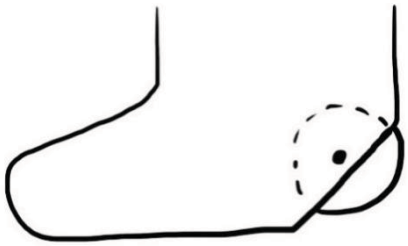

Figure 81: Heely Turning Mechanism

The Heely turning mechanism worked much like the wheel turning mechanism except the foot would be on the ground during the majority of the time, then weight would be shifted back on to the Heely wheel for turning. However, the weight shifting and motion required to have the mechanism rest on the wheel would have been just as difficult as having enough degrees of freedom to be able to turn without the mechanism.

4.3.1.4 Tank Tread Turning Mechanism

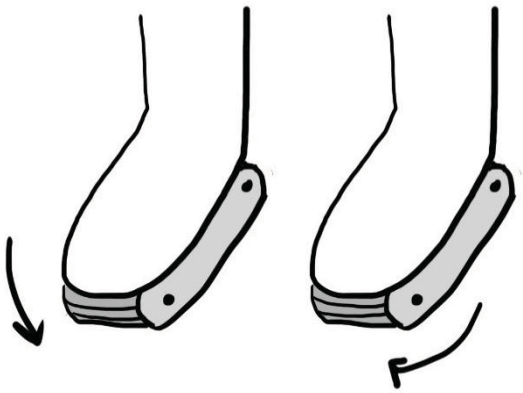

Figure 82: Tank Tread Turning Mechanism

Similar to the wheel mechanism, the tank tread mechanism would work by having the tread on each foot rotate in opposite directions. The motors would have to be powerful enough to move the entire weight of I-3P0.

4.3.1.5 Cam Shaft/Baby Doll Turning Mechanism

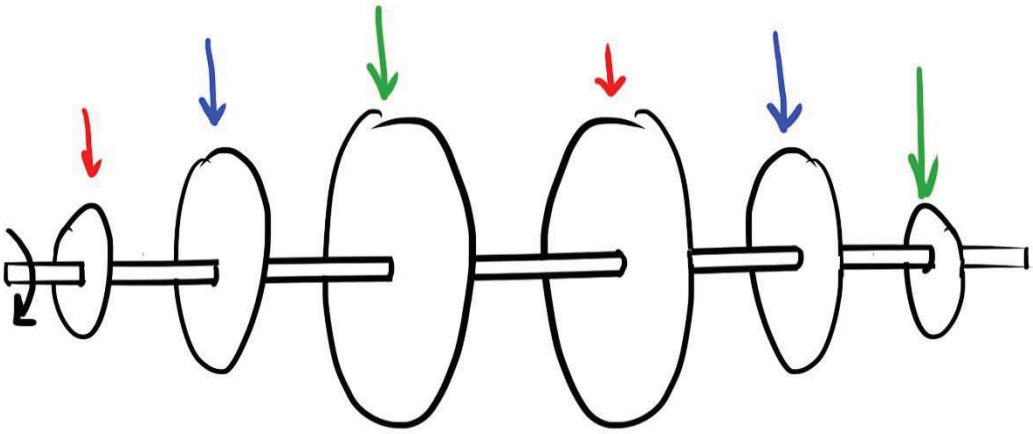

Figure 83: Cam Shaft/Baby Doll Turning Mechanism

The cam shaft mechanism was inspired by a children's walking doll found in the lab. The idea behind it was that if each hip were to move along differently sized paths, making the steps different sizes, the robot would slowly be able to change direction. In Figure 85, the blue circular path for each hip joint would ensure both legs took the same step length, and therefore the robot would move straight forward. The red circular paths would mean the left leg would have a smaller step than the right, making the robot turn left and vice versa with the green path. Though the concept was clear, the design needed to accomplish this turning mechanism was unclear.

4.4 Decision Matrices

4.4.1 Walking Degrees of Freedom

The first design decision that had to be made for I-3P0's walking mechanism was the number of degrees of freedom each leg would have. The degrees of freedom dictate the motion of the leg, but also its complexity in terms of both design and control. A decision matrix was created to be able to decide between the number of degrees of freedom and which joint and type the degree of freedom was. Criteria were chosen to help differentiate each mechanisms strengths and weaknesses, along with a defined rating system and weights. The Static 6 DOF mechanism received the highest total, and it was the idea presented at the team meeting.

Walking DOF			3 DOF Static (no turning) (hip: pitch, knee: pitch, ankle: pitch)		4 DOF Static (no turning) (hip: pitch, knee: pitch, ankle: pitch and yaw)		5 DOF Static (hip: pitch and roll, knee: pitch, ankle: pitch and yaw) TURN		6 DOF Static (hip: pitch, roll and yaw, knee: pitch, ankle: pitch and yaw)	
Criteria	Rating Explanations	Weight	**Rating**	**Weighted Rating**	**Rating**	**Weighted Rating**	**Rating**	**Weighted Rating**	**Rating**	**Weighted Rating**
Mechanism design difficulty	5: 1 week 3: 2 weeks 1: 4+ weeks	5	2	10	2	10	2	10	2	10
Ease of Machinability	5: 1 week 3: 2 weeks 1: 5+ weeks	5	3	15	2	10	2	10	2	10
Manufacturability (premade components ?)	5: >50% premade 3: 25% premade 1: <10% premade	5	3	15	2	10	2	10	2	10
Ease of Assembly	5: 1 hour 3: 2 hours 1: >3 hours	5	3	15	2	10	2	10	2	10
Weight Shifting	5: yes 1: no	5	1	5	1	5	1	5	5	25
Modularity	5: 100% modular 3: 50% modular 1: <25% modular	2	4	8	3	6	2	4	1	2
Ease of Interfacing with Rest of Body	5: <2 hours 3: 4 hours 1: >8 hours	4	5	20	5	20	2	8	2	8
Speed	5: 2 ft/s 3: 6 in./s 1: 2 in./s	2	1	2	1	2	2	4	2	4
Ability to turn	5: Yes 1: No	5	1	5	1	5	5	25	5	25
Stability	5: Falls over once every 15 minutes 3: Falls once every 5 minutes 1: Falls over once every minute	4	1	4	2	8	3	12	4	16
Controls difficulty	5: easish 3: okish 1: hardish	4	4	16	4	16	3	12	2	8
ECE difficulty	5: few wires 3: a decent amount 1: shit ton of wires tangled in chaos	2	4	8	4	8	3	6	2	4
Weight	5: kindergartener can carry 3: Lijia can	1	2	2	2	2	3	3	4	4

	carry 1: Arnold Schwartzenig ger									
Number of Actuated Components	5: <=1 3: 3 1: >5	3	3	9	3	9	2	6	1	3
Level of Dave Happiness	5: gives us an air mattress and unlimited pizza 3: smiles 1: storms off in a rage	1	1	1	2	2	3	3	4	4
Adaptability for fallback	5: yes 1: no	0.5	1	0.5	1	0.5	5	2.5	5	2.5
Stride Length	5: 1.5 ft 3: 6-10 in 1: 1 in	1	3	3	3	3	3	3	4	4
Noise Level	1:>80dB 3 = 50-70dB 5 = <50dB	0.5	3	1.5	3	1.5	3	1.5	2	1
Cost	5: <$500 3: $1000-$2000 1: >$4000	1	5	5	4	4	3	3	2	2
Total				145		132		138		152.5

Table 6: Partial Walking Mechanism Degree of Freedom Decision Matrix

4.4.2 Turning Mechanisms

Because a leg with 3 DOF or less cannot turn due to mechanical constraints, a separate turning mechanism had to be designed in order to meet the performance requirement. Using the same methodologies as in the previous decision matrix, a turning mechanism decision matrix was created. The mechanisms are described in Figures 79-83. The tank tread mechanism scored the highest and would most likely be pursued next semester or if time permits.

Turning Mechanism			Pivoting and Locking Plate		Heelys		Wheels		Tank Tread		Baby Doll (CAM)	
Criteria	Rating Explanations	Weight	Rating	Weighted Rating	Rating	Weighted Rating	Rating	Weighted Rating	Rating	Weighted Rating	Rating	Weighted Rating
Mechanism design difficulty	5: 1 week 3: 2 weeks 1: 4+ weeks	5	5	25	4	20	4	20	3	15	1	5
Ease of Machinability	5: 1 week 3: 2 weeks 1: 5+ weeks	5	3	15	4	20	4	20	5	25	1	5
Manufacturability (amt. premade components)	5: >50% premade 3: 25% premade 1: <10% premade	5	3	15	4	20	3.5	17.5	4	20	1	5
Ease of Assembly	5: 1 hour 3: 2 hours 1: >3 horus	5	3	15	2	10	2	10	2	10	1	5
Modularity	5: 100% modular 3: 50% modular 1: <25% modular	2	2	4	4	8	4	8	4	8	2	4
Speed	5: 20deg/s 3: 10deg/s 1: <5deg/s	2	1	2	4	8	4	8	5	10	3	6
Stability	5: Falls over <2% of time 3: Falls over 10% of time 1: Falls over >30% of time	4	4	16	2	8	2	8	5	20	2	8
Controls difficulty	5: easish 3: okish 1: hardish	3	2	6	3	9	3	9	4	12	2	6
ECE difficulty	5: few wires 3: a decent amount 1: shit ton of wires tangled in chaos	2	3	6	2	4	2	4	2	4	3	6
Weight	5: kindergartener can carry 3: Lijia can carry 1: Arnold Schwarzenegger	1	4	4	5	5	4	4	4	4	3	3
Number of	5: 1	1	2	2	3	3	3	3	1	1	1	1

Components	3: 3 1: >5											
Number of Actuated Components	5: <=1 3: 3 1: >5	3	2	6	2	6	2	6	5	15	1	3
Level of Dave Happiness	5: gives us an air mattress and unlimited pizza 3: smiles 1: storms off in a rage	1	2	2	3	3	3	3	4	4	3	3
Adaptability for fallback	5: yes 1: no	0.5	1	0.5	1	0.5	1	0.5	5	2.5	1	0.5
Height foot will be picked up	5: 6 in 3: 2-4 in 1: <0.25 in	1	1	1	1	1	1	1	1	1	2	2
Noise Level	1: 70-90dB 3 = 50-70dB 5 = <50dB	0.5	4	2	4	2	4	2	3	1.5	3	1.5
Ability to maintain traction	5: Slips less than .5 in 3: Slips between 1-3 in 1: Slips more than 5 in	3	5	15	5	15	5	15	5	15	5	15
Cost	5: <$500 3: $1000-$2000 1: >$4000	1	4	4	4	4	4	4	4	4	3	3
Total				140.5		146.5		143		172		82

Table 7: Turning Mechanism Decision Matrix

4.4.3 Joint Speed Requirements

4.4.3.1 Motivation

Joint speed requirements were needed to help drive a decision on the main drive motor's specifications along with a mass estimate. In order to get a better estimate of the plausible walking speeds, several videos of people walking were taken, the angular speed of the hip joint was analyzed, and MATLAB was used to calculate the required torque. This information was used to get a better of idea of motor availability for our desired walking speeds.

4.4.3.2 Measuring Hip Angular Speed

Once several videos were taken of people walking, a free software called PhysMo was utilized as shown in Figure 84. This software allows the user to measure angles and distances in each frame of the video while providing the time for each frame.

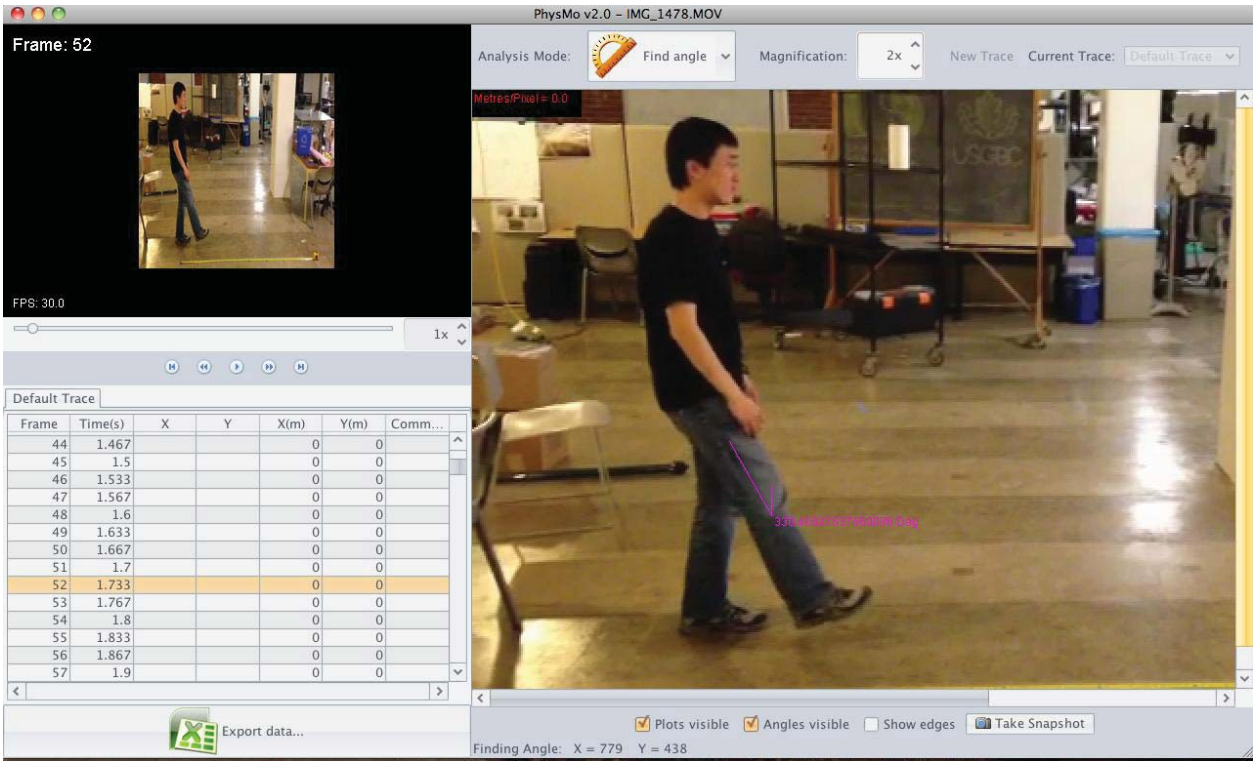

Figure 84: Example of PhysMo Workspace

The angle measured is dependent on human input, so the measurements are not perfectly reproducible. However, this estimate is much more accurate that an intuitive estimation.

4.4.3.3 Calculations

Joint speed was calculated by carefully using geometry and the time for each frame, as shown in Figure 85 and the following Equation 1.

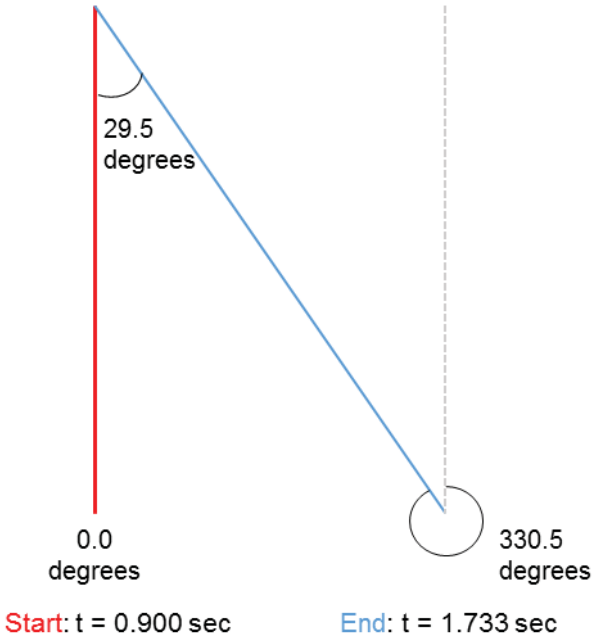

Figure 85: Leg Position Diagram

Equation 1:

$$\frac{d\theta}{dt} = \frac{\Delta\theta}{\Delta t} = \frac{29.5\ degrees}{(1.733\ \text{sec} - 0.900\ \text{sec})} = 34.5\ deg/sec$$

A MATLAB code, seen in Appendix A.1, was developed to calculate the appropriate motor torque by utilizing a numerical guess and check. The user can input motor torque at the operating point, mass, and length of the leg and generate plots of angular velocity versus time and angle from the vertical versus time, shown in Figure 86 and Figure 87. This helped determine whether or not a motor chosen would give the hip motion desired. For the example shown in Fig. 48 and 49 a torque of 100 in/lbs, a mass of 10 kg and a leg length of 0.82 meters (or 2.7 feet) was inputted.

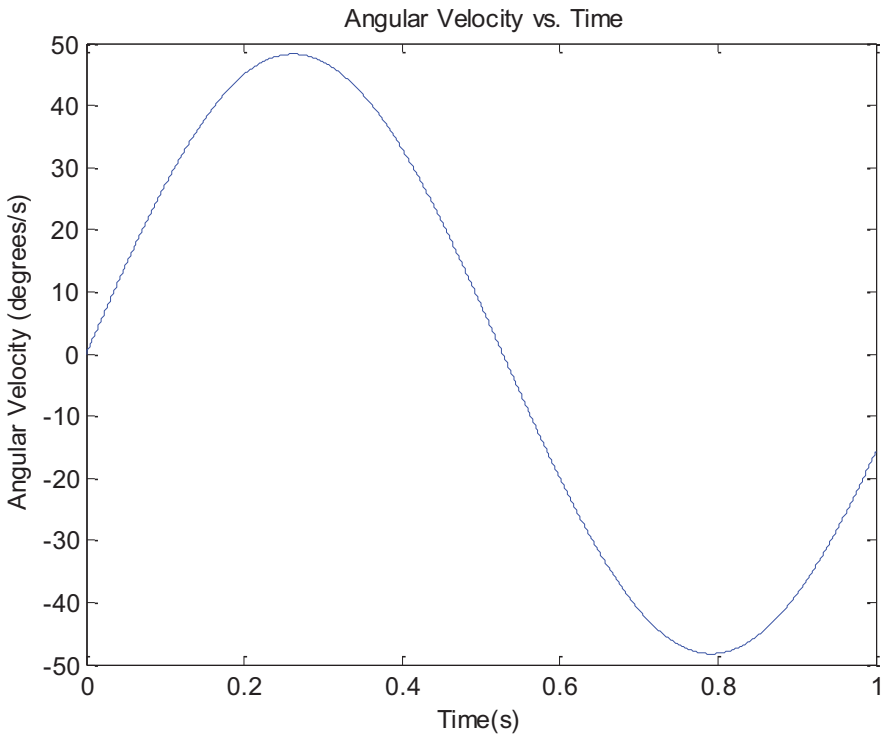

Figure 86: Angular Velocity of the Hip Joint versus Time

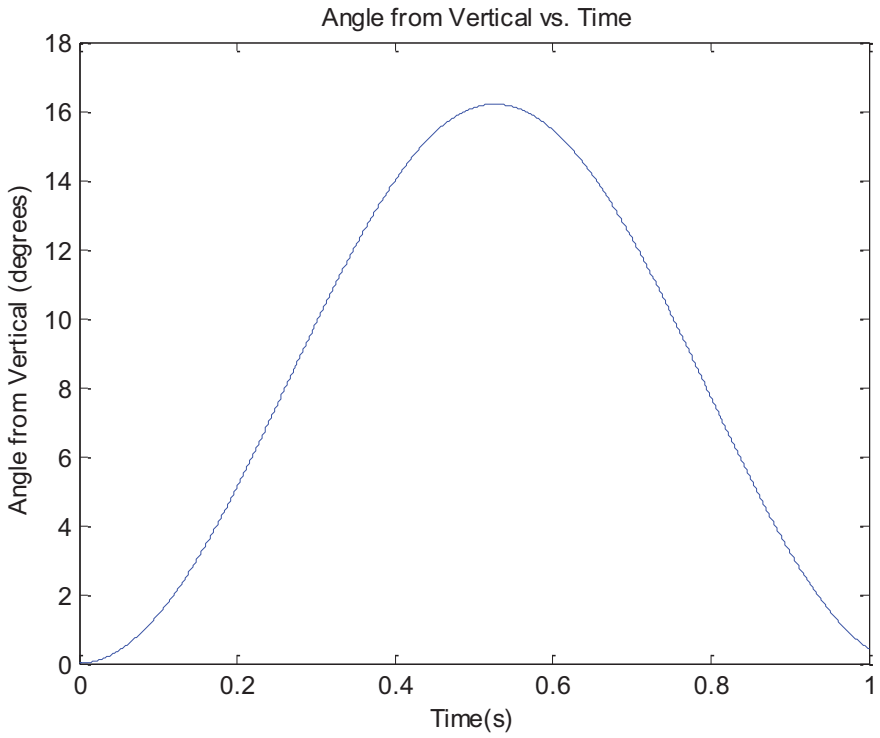

Figure 87: Angle of Leg from Vertical versus Time

4.4.3.4 Conclusions

After several attempts of recording walking speeds and performing the associated analysis, a hip joint speed of approximately 34.5 degrees/second was chosen. This decision was driven by the desire to minimize torque required while maintaining human-like motion.

4.5 Design Shift: 12DOF to 1DOF

After completing the joint speed requirements, it was apparent how simplified the calculations for developing the walking mechanism were becoming. In order to develop a 12DOF walking mechanism (6DOF per leg) as planned, estimates for the speed of each degree of freedom for each joint would need to be developed, subsequent motors would need to be selected, and all the components would need to be modified and iterated upon once all of the components were put together. The problem of walking would then reduce a series of recalibrations of the different electrical components and code until the solution was functional, and even then its success would not be guaranteed. There would be very few intermediate milestones that could be tested along the way to ensure that the system as a whole would function as planned by the given date. With these considerations in mind, the team chose to simply the problem into as few degrees of freedom as possible that would achieve the original goal of the system translating forward with a walking-like motion. This would reduce the number of components for troubleshooting (thus reducing time spent), reduce the number of motors to be purchased (thus reducing cost), reduce the weight of the system, and provide insight to developing a more complex and realistic solution in the future. After much consideration, the team developed two solutions that utilized only 1DOF for both legs.

4.6 Final Design: Four-Bar Linkage Mechanism, 1 DOF

4.6.1 Design Overview

After it was decided that the 12 DOF walking mechanism would be simplified to a 1 DOF system, the four-bar linkage design was created. The inspiration of this design came from wind-up walking toys. In such a toy, a single wind-up clockwork motor powers the entire walking motion. The motor is mechanically linked to a series on gears such that the entire system only has 1 DOF. The upper end of each leg is constrained to move in a circle with a fixed radius about the hip joint. At the same time, the two upper ends are constrained to be always on the exact opposite side of the circle (i.e. 180 degrees apart). In addition, both legs are constrained to be permanently vertical.

This mechanism creates a kinematically constrained walking motion with a sinusoidal variance in speed given a constant motor RPM. The motion of this mechanism is perfectly symmetrical forwards and backwards, so such a design allows for the ability to walk in both directions. However, due to the fact that there is only 1 DOF, the system can only walk in a straight line and lacks the ability to make turns. Despite this drawback, this mechanism was

chosen due to its simplicity and robustness. It was decided that having just the ability to walk in a straight line is sufficient for the first iteration of I-3P0.

The overall mechanical motion of the wind-up toy mechanism was implemented on the four-bar linkage design. However, one undesirable trait of the wind-up toy mechanism is its gearing system. Due to the lack of experience on using gears, it was decided that the gearing system would be replaced with a different mechanism that performs the same function. This mechanism was the four-bar linkage. The four bars in this system are: the top crank, the bottom crank, the leg, and the base plate. The top crank fixes the radius of the circle about which the top of the leg moves. The presence of the bottom crank in conjunction with the top crank keeps the leg always parallel to the base plate. The base plate is the "ground link" of the four-bar linkage; it does not move and is rigidly attached to the torso, resulting in the leg being always parallel to the torso, and hence perpendicular to the ground when I-3P0 is upright. Figure 88 shows the CAD model of the four-bar linkage mechanism.

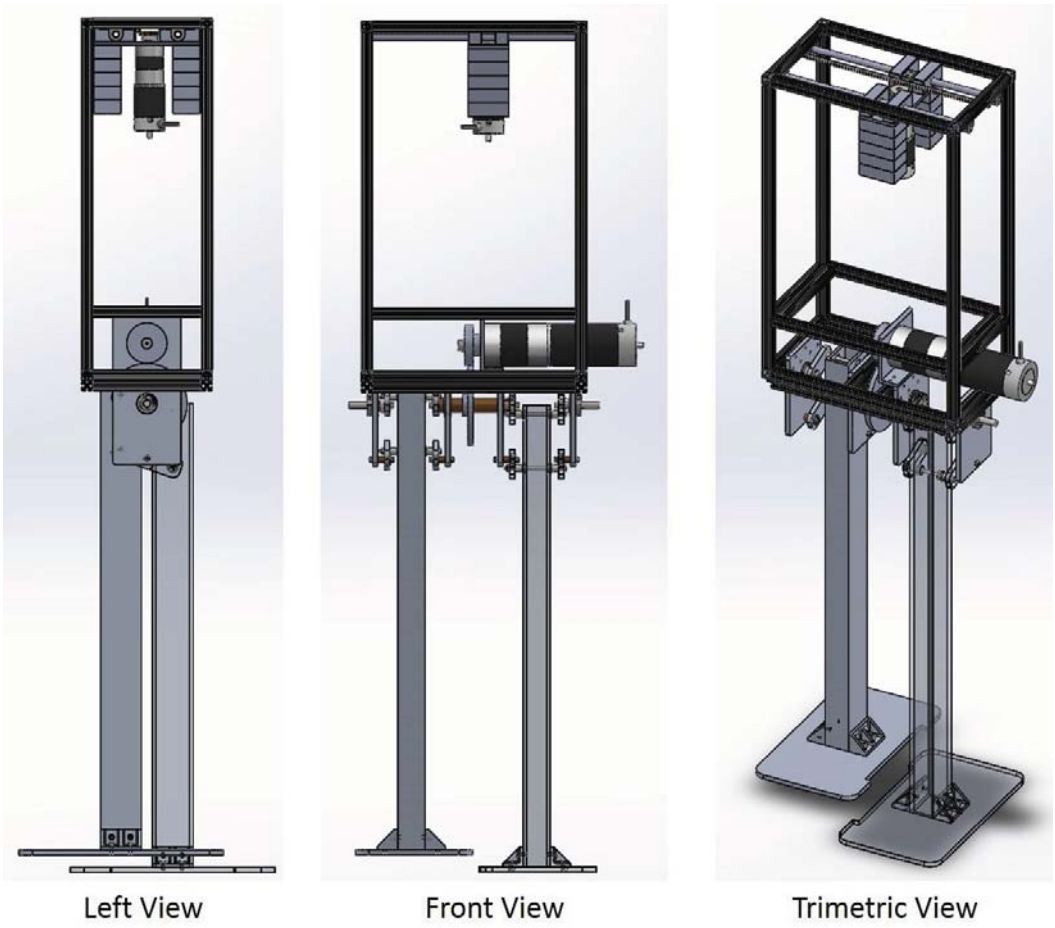

Figure 88: Design 1: Four-Bar Linkage Mechanism

The actuation system for this mechanism is fairly simple. The motor is mounted on the torso and is geared to the central driveshaft, which sits in two steel ball bearings. The motor actuates the driveshaft via a 2:1 gear ratio. The driveshaft turns the inner top crank of both legs, resulting in the circular motion of the legs' top joints. The lower and outer cranks and the outer driveshafts (all sitting in ball bearings) guide the four-bar linkage in a prescribed, 1 DOF motion. The result is the kinematically constrained walking motion described above.

4.6.2 Weight-Shifting Mechanism

The wind-up toy has wide, forked feet that cross over each other, so its center of gravity never moves outside of the contact area of either foot. As such, it can lift a foot at any time and still remain balanced on its other foot. On the other hand, for aesthetic reasons, it is undesirable for I-3P0 to have such crossed-over feet. So a weight shifting mechanism in the torso was devised in order to apply a counter-force that would balance I-3P0 as it walks.

This mechanism must move at the same frequency as the four-bar linkage. In addition, it must start in the correct position corresponding to the angular position of the four-bar linkage. As a result, an encoder is needed for the motor actuating the four-bar linkage (the walking motor). This way, the velocity and position of the walking motor can be reported to the controller of the weight-shifting motor, ensuring that the weight-shifting mechanism runs at the correct speed.

The weight-shifting mechanism contains an actuating motor attached to ten 1.7-pound deadweights, resulting in a total of 22 pounds of shifting weight. Each time I-3P0 takes a step, the motor accelerates the weight in the direction of the foot that is lifted off of the ground. This results in an equal and opposite reaction force that keeps I-3P0 upright. Figure 89 shows an annotated CAD model of the walking mechanism with the weight-shifting mechanism.

Figure 89: Annotated Four-Bar Linkage Walking Mechanism

4.6.3 Finite Element Analysis of the Ankles

Using ANSYS, finite element analysis (FEA) was performed in order to validate the structural integrity of the system. There are two locations of concern in regards to structural integrity: the bearing joints on the four-bar linkages and the bolted jolts at the ankles. The joints on the four-bar linkages are not easily analyzable via FEA, therefore they were overdesigned to ensure that they can withstand the loads that they are required to. The ankle, on the other hand, is fairly straight forward to analyze via FEA. Therefore, they were analyzed in order to potentially reduce mass.

FEA Setup:

To set up the FEA, a leg, a foot, and two ankle brackets were imported into ANSYS as an assembly. Internally, each ankle bracket was connected to the leg and foot by revolute joints at the screw holes. Two external conditions were applied: a fixed support on the bottom surface of the foot and a lateral force applied near the top of the leg. The fixed support simulated the fact that the ground would be in solid contact with the bottom of the foot when I-3P0 takes a step. The lateral force was a simple way to simulate the bending moment that the center of mass of I-3P0 applies on the leg when it takes a step. The force was 50 pounds applied equally on both bearing holes and was in line with their axes. Figure 90 shows the support and the force.

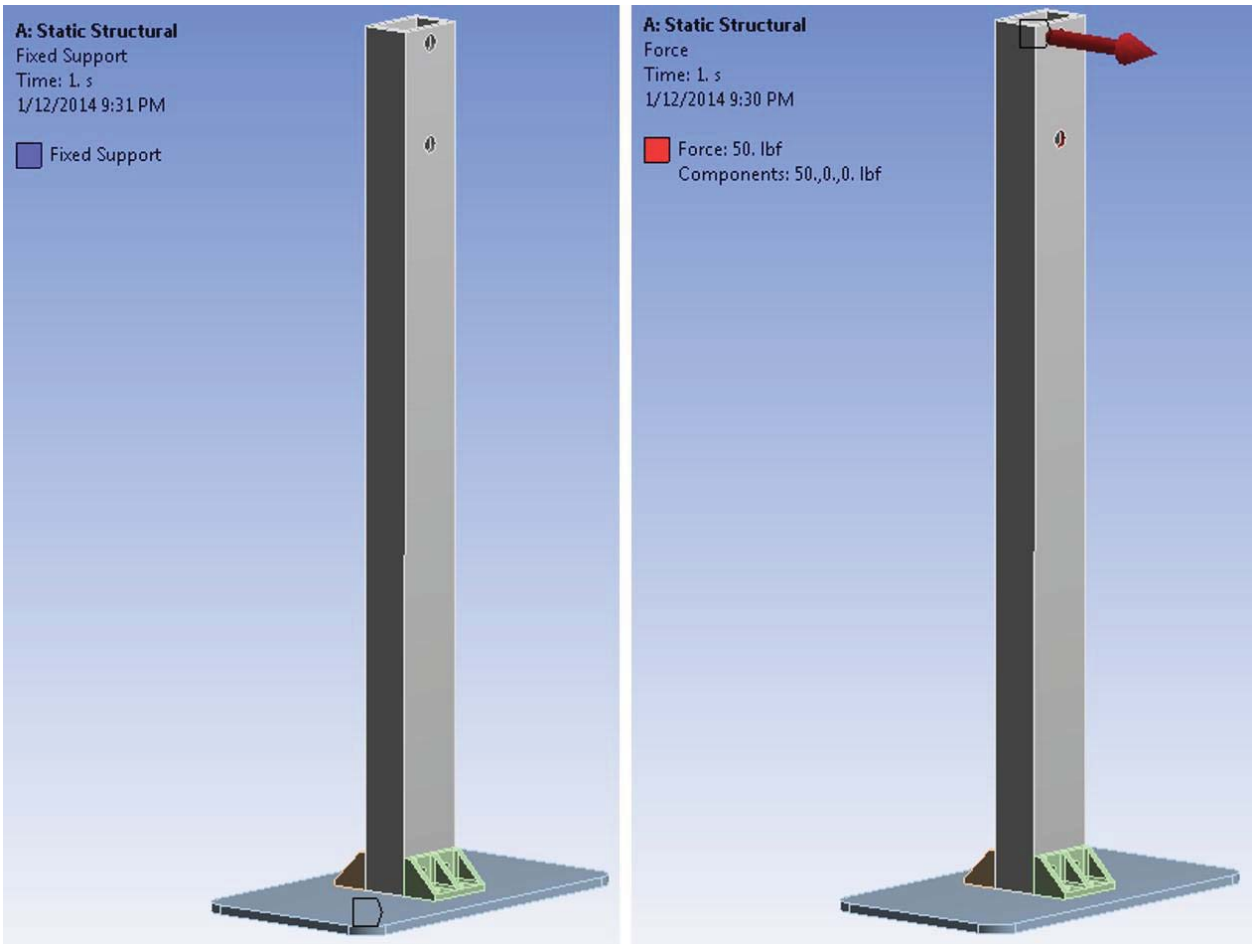

Figure 90: FEA Setup: External Support and Load

FEA Results:

As shown in Figure 91, the FEA results indicated that the maximum von-Mises equivalent stress occurred at the ankle bracket. It had a value of 1,915 psi. This was 20 times less than the yield strength of aluminum 6061-T6 (40,000 psi), which the ankle bracket was made of. As a result, the safety factor against yielding was 20. This was quite adequate for the purposes of I-3P0, meaning that the ankle joint was structurally sound. In addition, the maximum deformation that occurred at the top of the leg was 0.044 inches, which is quite insignificant, meaning that the leg should stay rigid during operation. Overall, the FEA results indicated that the leg-ankle-foot assembly had good structural integrity.

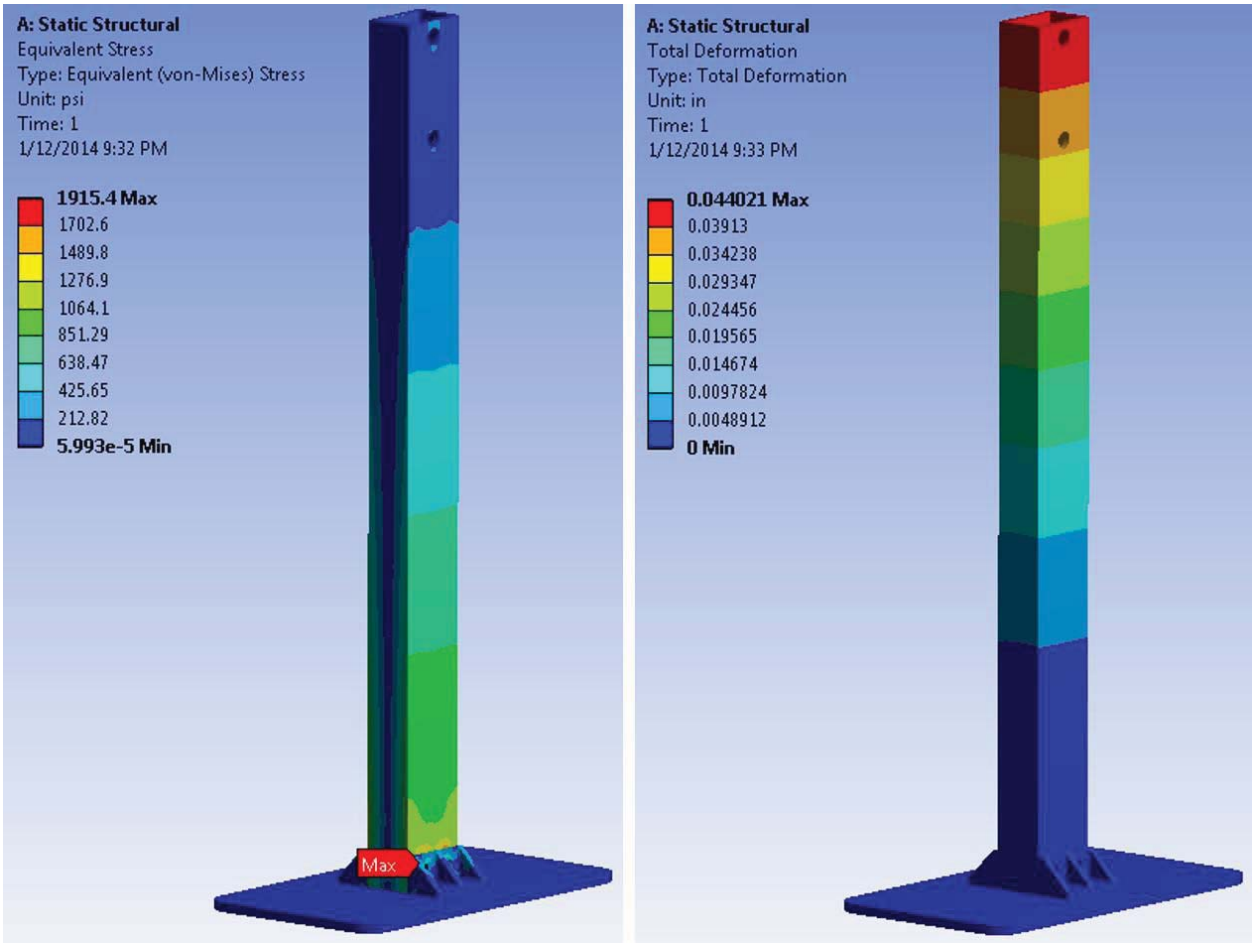

Figure 91: FEA Results: von-Mises Equivalent Stress and Total Deformation

4.6.4 Leg to Torso Integration

In order to integrate the legs with the torso, several design considerations had to be taken into account. The t-slotted bar has a cross section cannot be drilled into for large bolts, such as ¼-20. Instead, several 10-24 clearance holes were drilled in an alternating offset pattern, as seen in Figure 92. This pattern allows the interface to withstand forcing and torqueing well.

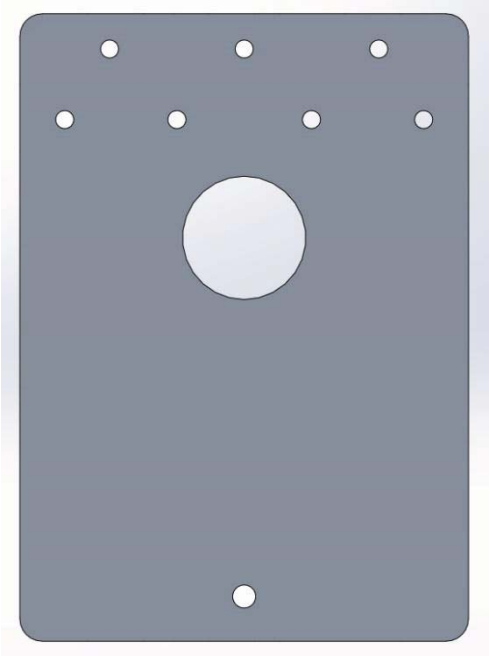

Figure 92: Offset Bolt Hole Array

Additionally, the leg motor protrudes into the torso, so spacing was critical. The face plate mount in Figure 93 constrains the motor horizontally and the steel two-hole clamp holds the motor in the correct vertical position. Both of these connection methods ensure the motor gear meshes with the driveshaft gear at all points during the cycle without slipping. Adhesive-backed rubber was added to the inner surface of the clamp to dampen vibration caused during the walking motion to prevent damage to the motor.

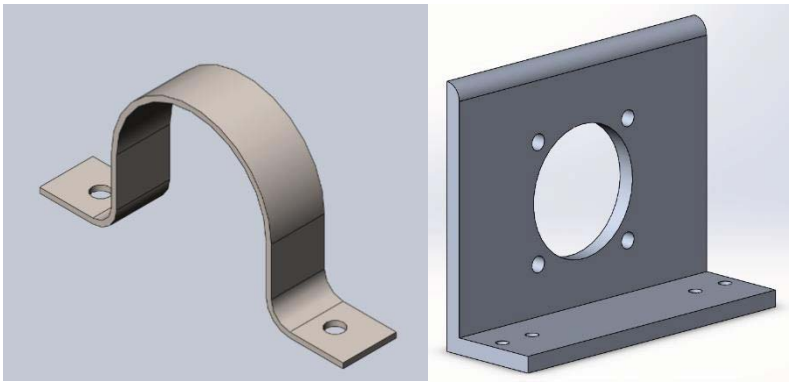

Figure 93: Motor Mounting Fixtures

A difficult component of creating I-3P0's walking mechanism was the upper leg assembly and integration with the torso. As seen in Figure 92, there were seven holes drilled in each vertical link base plate, but not all were utilized for the torso-leg integration. This was because some of screws would interfere with the crank motion. In addition, a few of the screws for the inner plates were un-installable due to tight spacing. Regardless, each plate had at least four of the seven holes utilized. Due to this, the integration was still robust enough to handle the forces placed on the system. Fortunately, it is very easy to adjust the position of t-slotted bar; positioning the cross beams (oriented front to back) in order to bolt the legs to the torso did not require precise tolerancing. This was also the case when clamping the leg motor to the t-slotted bar above it. Figure 94 shows the hip area of the fully assembled and integrated system.

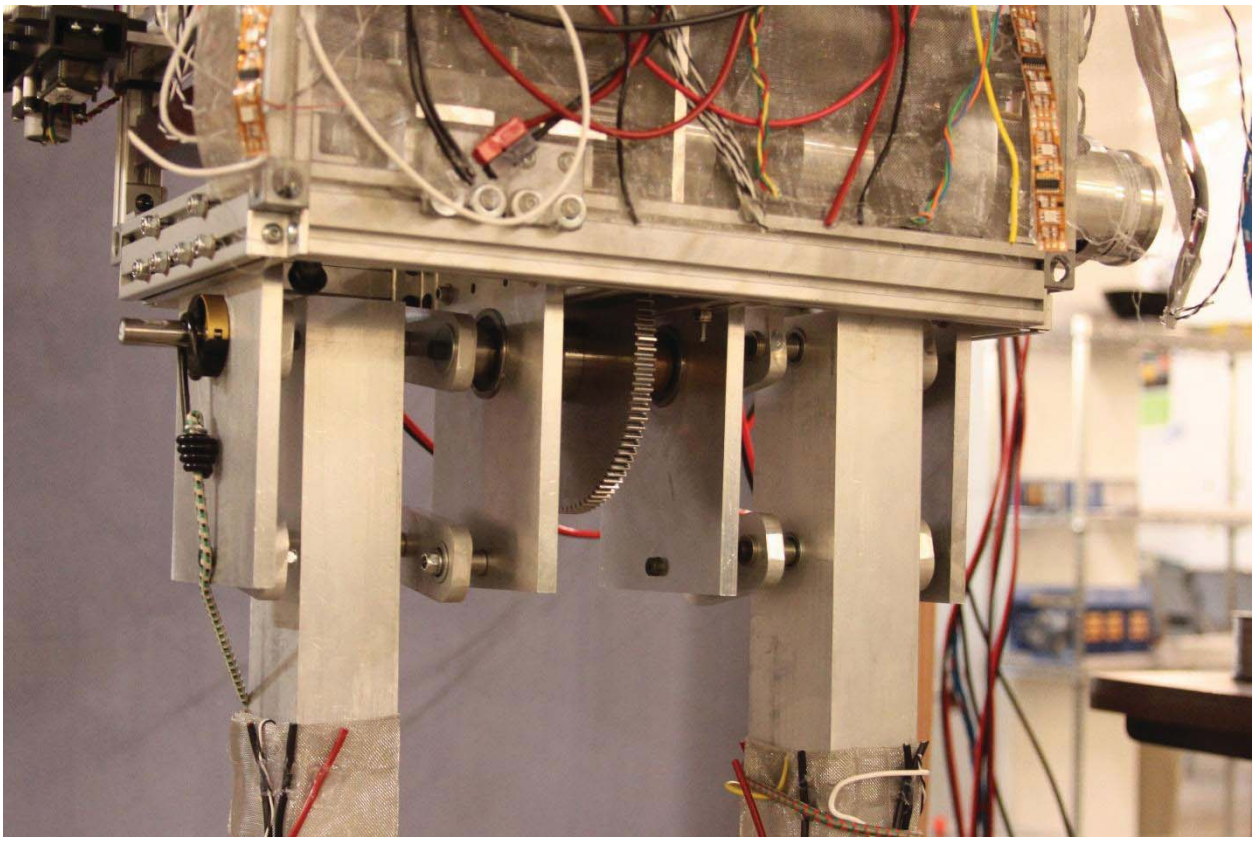

Figure 94: Fully Assembled and Integrated Four-Bar Linkage Mechanism

4.6.5 Manufacturing: Major Components

Most of the major components of the system were made from aluminum 6061-T6 stock. This was due to the fact that aluminum 6061-T6 is a relatively strong, lightweight, and low-price material.

Cranks:

All the crank pieces were machined from two 12” x 12” x 3/8” aluminum plates. A good rule of thumb is to carefully mark where you will be cutting the pieces from and to allow ample space between pieces. This allows for some error when using a drop saw or scroll saw. When machining the upper and lower crank pieces as shown in Figure 95, the distance between the two holes is the most critical dimension, as it ensures each leg has the same motion radius. In order to get the correct fillet radii on the corners, it is useful to print a to-scale drawing of the part. That way, more consistent results can be achieved with a grinder by directly placing the part on the drawing.

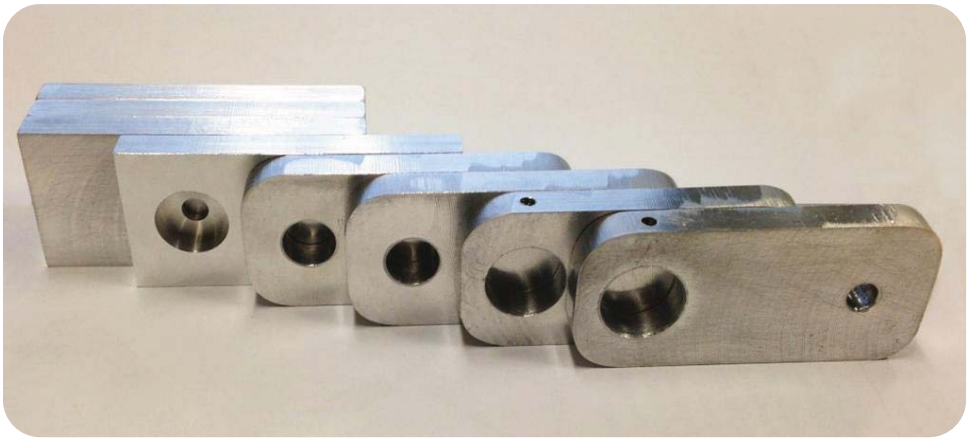

Figure 95: Cranks in Various Machining Stages

Legs:

The legs were relatively straightforward to machine. There were only three operations needed: cut the leg to length from the stock, drill and ream the bearing holes, and drill and tap the holes for bolting on the ankle bracket. The one operation that needed to be precise was the drilling and reaming of the bearing holes. Otherwise, the bearings would not be able to be press-fitted snuggly into the leg.

Ankle bracket:

There were a total of four ankle brackets, two on each ankle. Each bracket was made from a 3” x 1.5” x 1.5” aluminum blocks. One difficult part about machining the bracket was the 45° cut that needed to be made on one edge. On the milling machine, this cut can be accomplished by placing a 45° angle block below the stock inside the vise. This will hold the stock block at a 45° angle with one edge directly facing upwards. A regular end mill can then be used to cut away the edge, resulting in the desired 45° cut. Another difficult part about machining the bracket was the rounded fillets on its cutouts. A regular end mill would only be able to make square corner

cuts, with no fillets to alleviate stress concentration. Hence, a ball-end end mill was purchased from McMaster-Carr for the purpose of machining the cutouts on the ankle brackets.

Feet:

Another difficult component to machine was the foot. Due to its large size, the long edges (15”) could not be milled down while held in the vise in a horizontal manner. So it must be held vertically in the vise. When holding it in such a manner, care must be taken to minimize vibrations during machining.

Motor Gear Spacer:

Finally, the process of machining the motor gear spacer (0.25”-thick, 18-8 stainless steel washer) to fit over the motor shaft key required broaching. The machine shop at Cornell University had a broaching set for this purpose, so a 6mm wide by 3 mm deep keyway was made. The downside is that if a set is not available, it runs at a fairly high price ($40+), so an alternate solution is to choose a thick washer with an inner diameter that would fit over both the shaft and the key. Since the washer is used for a spacing purpose only, there is no harm in using this method, though the aesthetics may suffer slightly.

4.7 Motor Selection

The four-bar linkage walking mechanism has a single degree of freedom, so a single DC motor is used to actuate it. In addition, due to the kinematically constrained walking motion, no motor speed control is needed. Therefore, it was decided that a brushed motor would be used, since it does not require a controller for fixed speeds and costs less. In addition, due to the fact that the torque required is very high while the RPM required is very low, the motor needs to have a planetary gearhead to dramatically increase the gear ratio in order to trade RPM for torque. One other requirement is that the voltage of the motor must not exceed 24 volts, as dictated by the electrical power board used in I-3P0. Lastly, since the phase of the leg motion needs to match the position of the shifting mass in the torso, an optical encoder is needed for the motor.

4.7.1 The physical setup

- C-3PO total weight ≈ 150 lbs
- Weight of each leg ≈ 15 lbs

- Desired walking speed ≈ 1 ft/s
- Motor to driveshaft gear ratio = 2:1

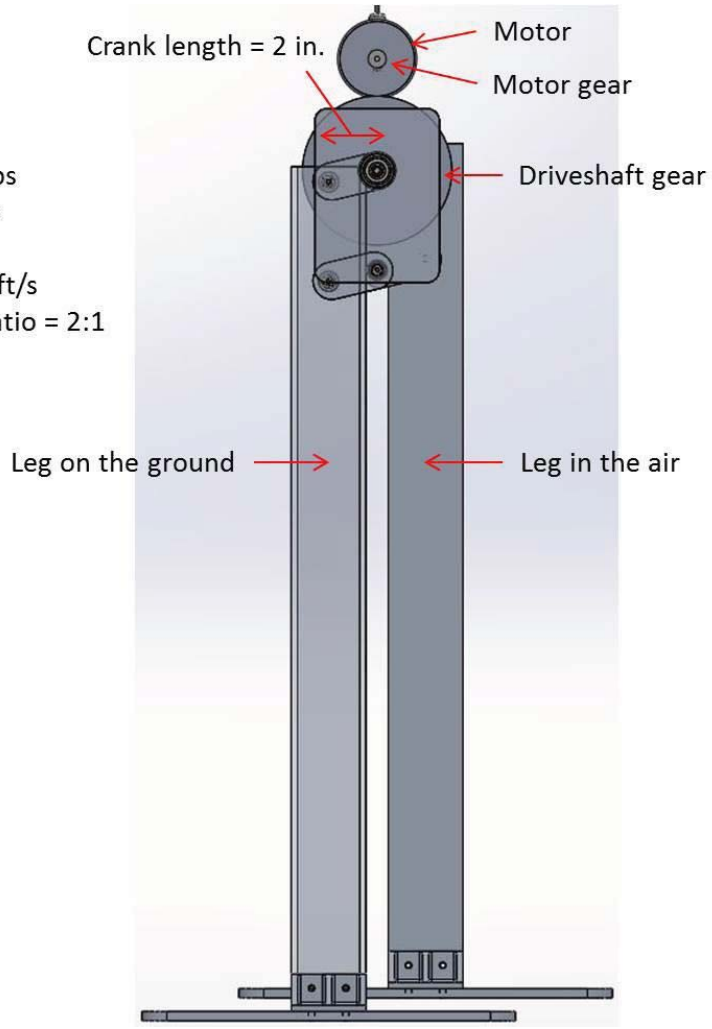

Figure 96: Design 1 Physical Set-up

4.7.2 Free body diagram:

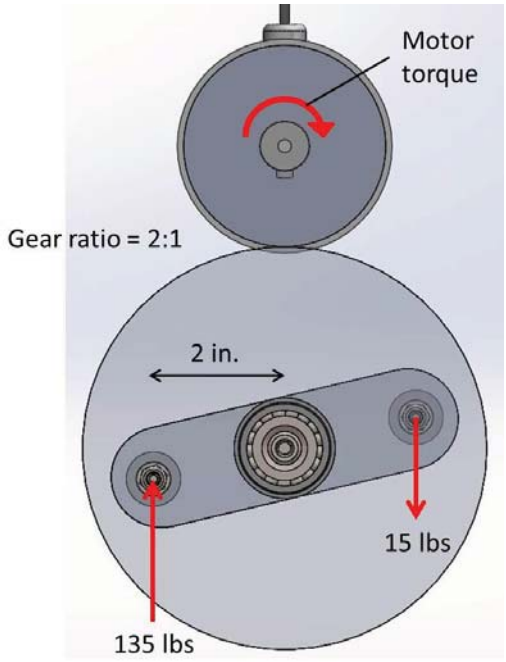

Figure 97: Free Body Diagram of Gear Ratio

4.7.3 Motor torque requirement calculations:

Variables:

F_1 = force from leg 1 (leg on the ground) on crank = 135 lbs

F_2 = force from leg 2 (leg in the air) on crank = 15 lbs

L = crank length = 2 in.

GR = gear ratio of motor to driveshaft = 2:1

T = motor torque

Based on the laws of mechanics, the following equation applies:

$F_1*L + F_2*L = GR*T$

➔ $T = (F_1*L + F_2*L) / GR$

$T = (135 \text{ lbs} * 2 \text{ in.} + 15 \text{ lbs} * 2 \text{ in.}) / 2$

$T = 150$ in-lbs

Now, since the weight of I-3P0 is a rough estimate, and in addition we have not taken into account any power losses due to friction, we chose to err on the side of caution and over-spec the motor torque by about 30%.

So: $T_{spec} = 1.3* T$

➔ **$T_{spec} \approx 200$ in-lbs**

4.7.4 RPM requirement calculations:

Variables:
v = desired I-3P0 walking speed ≈ 12 in./s
GR = gear ratio of motor to driveshaft = 2:1
L = crank length = 2 in.
f_m = motor revolutions per second

Based on kinematic constraints of the walking mechanism, the following equation applies:
$v = f_m / GR * 4L$
➔ $f_m = v/4L*GR$
$f_m = (12 \text{ in./s}) / (4 * 2 \text{ in.}) * 2$
$f_m = 3 \text{ rev/s}$

$RPM_{motor} = 60 \text{ s/min} * f_m$
RPM_{motor} = 180 RPM

4.7.5 Basic Spec Summary:

Motor shaft output torque ≈ **200 in-lbs**
Motor shaft output speed ≈ **180 RPM**

4.7.6 Final Decision:

The final motor choice is a DC brushed planetary gearmotor sold by Midwest Motion Products.
Motor part number: MMP D33-655B-24V GP81-025
Motor specifications (spec sheet):
Motor gearhead shaft output torque: 202 in-lbs
Motor gearhead shaft output speed (at full torque): 160 RPM
Rated DC voltage: 24 volts
Rated continuous current: 23.9 amperes
(Note: the EU series optical encoder on the spec sheet is needed)

4.8 Bill of Materials

Motor Mount Parts				
Used For	**Item**	**Part Number**	**Vendor**	**Quantity Used**
Motor mount	Steel Two-Hole Clamp	9439T16	McMaster	1
Motor Face Mount	Multipurpose 6061 Aluminum, 90 Degree Angle, 1/4" Thick, 2" x 4"	8982K58	McMaster	5" long, 4" x 1.6383" legs, 1/4" thick

	Legs, length: 1ft			
Adhesive-backed Rubber	Ultra-Strength Neoprene Rubber, Adhesive-Back, 1/4" Thick, 2" Width, 36" Long, Hardness: 50A (medium)	8463K63	McMaster	8" x 1.25" x 1/8" (approx. thickness)
Machining/Tools				
Used For	**Item**	**Part Number**	**Vendor**	
Cutting ankle bracket	Ball-end end mill	8887A341	McMaster	1
Ankle&Foot&Leg Parts				
Used For	**Item**	**Part Number**	**Vendor**	
Ankle Bracket	Multipurpose 6061 Aluminum (1.5" x 1.5" x 3 feet)	9008K47	McMaster	3" x 1.5" x 1.5", machined 4
Ankle Screws	Thread-Locking Socket Head Cap Screw (1/4"-20, 1/2" long)	91205A537	McMaster	16
Foot	Oversized Multipurpose 6061 Aluminum (3/8" Thick, 18" x 18")	89155K28	McMaster	15" x 8.625", machined 2
Leg	Multipurpose 6061 Aluminum Rectangular Tube (1/4" Wall Thickness, 2" x 3", 3' Length)	6546K283	McMaster	34" long, 2" x 3", machined 2
Motor&Gears				
Used For	**Item**	**Part Number**	**Vendor**	
Motor	Reversible DC Gearmotor with EU Series Encoder	MMP D33-655B-24V GP81-025	Midwest Motion Products	1
Motor Gear	Spur Gear (ISO Class 8, 20 deg. pressure angle, 78mm OD)	A 1C22MYKW15050A	SDP/SI	1
Driveshaft Gear	Spur Gear with Hub (ISO Class 8, 20 deg. pressure angle, 153 mm OD)	A 1C22MYK15100A	SDP/SI	1
Crank Pieces				
Used For	**Item**	**Part Number**	**Vendor**	
Long Crank Shaft	Fully Keyed Precision Drive Shaft with Certificate (3/4" OD, 3/16" Keyway Width, 6" Length)	8488T620	McMaster	1
Short Crank Shaft	Hardened Precision Steel Shaft (1/2" Diameter, 6" L Overall, 1/4"-20 x 1/2" D Tap Both Ends)	6649K100	McMaster	3" long, machined 2
Crank Crank lower Crank vertical link	Oversized Multipurpose 6061 Aluminum (3/8" Thick, 12" x 12")	89155K34	McMaster	2 aluminum plates to machine all

Crank drive Crank vertical link middle				pieces
Screws for Cranks onto Shafts	Black-Oxide Alloy Steel Socket Head Cap Screw (1/4"-20, 1/2" long)	91251A537	McMaster	4
Shaft Key	Zinc-Plated Steel Oversized Key Stock (3/16" x 3/16", 12" Length)	98491A117	McMaster	0.75" long
Spacers/ Screws/ Nuts/ Washers				
Used For	**Item**	**Part Number**	**Vendor**	
Small Spacer	18-8 Stainless Steel Unthreaded Spacer (1/2" OD, 1/2" Length)	92320A242	McMaster	8
Large Spacer	18-8 Stainless Steel Unthreaded Spacer (1" OD, 3/8" Length)	92320A403	McMaster	2
Sleeve Bearing (new)	SAE 863 Bronze Sleeve Bearing (for 3/4" Shaft Diameter, 1" OD, 3/8" Length)	2868T178	McMaster	2
Set Screw (for gears)	Thread-Locking Flat Point Set Screw (Nonmarring, Alloy Steel, 8-32 Thread, 1/2" Long)	94495A225	McMaster	2
Small Ball Bearing	Steel Ball Bearing (Flanged Open for 1/4" Shaft Diameter, 11/16" OD, 5/16" W)	6383K213	McMaster	12
New Large Ball Bearing	Steel Ball Bearing (Flanged Double Sealed for 3/4" Shaft Diameter, 1-5/8" OD)	6384K367	McMaster	2
Large Ball Bearing	Steel Ball Bearing (Flanged Open for 1/2" Shaft Diameter, 1-3/8" OD, 1/2" W)	6383K241	McMaster	2
Locknut	Zinc-Plated Grade 2 Steel Nylon-Insert Hex Locknut (10-24 Thread Size, 3/8" Width, 15/64" Height)	90631A011	McMaster	8
Shoulder Screw - 1.25	Alloy Steel Shoulder Screw (1/4" Diameter x 1-1/4" Long Shoulder, 10-24 Thread)	91259A544	McMaster	4
Driveshaft Washer	Zinc-Plated Steel Large-Diameter Flat Washer (1/4" Screw Size, 1" OD, .04"-.06" Thick)	91090A108	McMaster	2
Shaft Washer	Grade 2 Titanium Flat Washer (1/4" Screw Size, 3/4" OD, .03"-.05" Thick)	94051A220	McMaster	2
Motor Gear Spacer	18-8 Stainless Steel Thick Flat Washer, 3/4" Screw	98125A036	McMaster	1

	Size, 1-5/8" OD, .23"-.26" Thick			
Shoulder Screw - 4.0	Alloy Steel Shoulder Screw (1/4" Diameter x 4" Long Shoulder, 10-24 Thread)	91259A115	McMaster	4
Driveshaft gear spacer bearing	SAE 841 Bronze Sleeve Bearing, 3/4" Shaft Diameter, 1" OD, 7/8" Length	6391K264	McMaster	1
Driveshaft gear spacer bearing	SAE 841 Bronze Sleeve Bearing, 3/4" Shaft Diameter, 1" OD, 1-3/4" Length	6391K448	McMaster	1
Spacer/bearing between lower cranks and vertical linkage plates	SAE 863 Bronze Sleeve Bearing, 1/4" Shaft Diameter, 1/2" OD, 1/2" Length	2868T48	McMaster	4
I-3P0 leg to torso integration	Zinc-Plated Alloy Steel Socket Head Cap Screw, 10-24 Thread, 1-1/2" Length	90128A226	McMaster	40
I-3P0 leg to torso integration	18-8 Stainless Steel Nylon-Insert Hex Locknut, 10-24 Thread Size, 3/8" Width, 15/64" Height	91831A011	McMaster	40
I-3P0 leg to torso integration	Mil. Spec. Cadmium-Plated Steel Flat Washer, Number 10 Screw Size, .02"-.04" Thick, NAS1149-F0332P	95229A370	McMaster	80
Washers for 1/4"-20 socket head screws	18-8 Stainless Steel General Purpose Flat Washer, 1/4" Screw Size, 5/8" OD, .04"-.06" Thick (100 per pack)	92141A029	McMaster	2
I-3P0 leg 1/2" shaft collar	Quick-Release One-Piece Clamp-on Shaft Collar for 1/2" Diameter	1511K12	McMaster	2
OTHER				
Used For	**Item**	**Part Number**	**Vendor**	
Driveshaft and gear interface	1" wide Polyurethane adhesive-backed film	1867T21	McMaster	
Motor shaft and gear interface	2" wide Polyurethane adhesive-backed film	1867T22	McMaster	
Loctite	Loctite® Instant-Bonding Adhesive #430, 1 oz Bottle	66635A32	McMaster	
Foot pad foam (to reduce force of impact)	Natural Gum Foam, 5/16" Thick, 36" Width, Soft	8601K44	McMaster	3" x 5", 4 pads for each foot

4.9 Testing

Test	Purpose	Outcome	Action
Gear Meshing	Ensure motor placement is correct (when manually rotating legs)	1. Shaft rotation yields leg motion for whole cycle 2. Shaft rotation does not yield motion for whole cycle	1. None required 2. Adjust t-bar and motor mount locations accordingly, document final position
Suspended Walking	Ensure powered motor rotates legs as expected	1. Legs rotate at specified rate 2. Leg rotate, but not at specified rate 3. Legs do not rotate	1. None required 2/3. Determine if cause was mechanical/electrical/coding issue
Suspended Balancing	Ensure balancing mechanism coincides with steps	1. Balancing mechanism coincides with step 2. Balancing mechanism does not coincide with step	1. None required 2. Determine if cause was mechanical/electrical/coding issue.
Grounded Walking	Ensure balancing and walking mechanism keep 3PO balanced on ground	1. I3P0 walks without deviating from an upright position (+/-) for X steps. 2. I3P0 loses its balance (to be defined) 3. I3P0 cannot balance	1. None required 2. Document time and probable cause 3. Determine if cause was mechanical/electrical/coding issue.

Table 8 : Leg Testing Outline

Four major testing milestones were developed to gauge the success of the design and the actions to be taken if the milestones were not reached, as outlined in Table 8 : Leg Testing Outline. Since it was difficult to simulate how the system would behave as a whole, precise criteria for success could not be

determined before the tests were run in some cases. Before any major testing occurred, the leg assembly was rotated manually to ensure the legs could rotate a full cycle. It was noted that at top/bottom dead center (cranks perfectly vertical), would sometimes allow the cranks to rotate in an undesirable direction. This is caused by a singularity at that location. Simulations were run to visualize the issue. The black and blue bars are 4 inches long and represent the distance between the connection points on the vertical link base plates, while the red and green bars are 2 inches long and represent the center to center distance of the crank's holes.

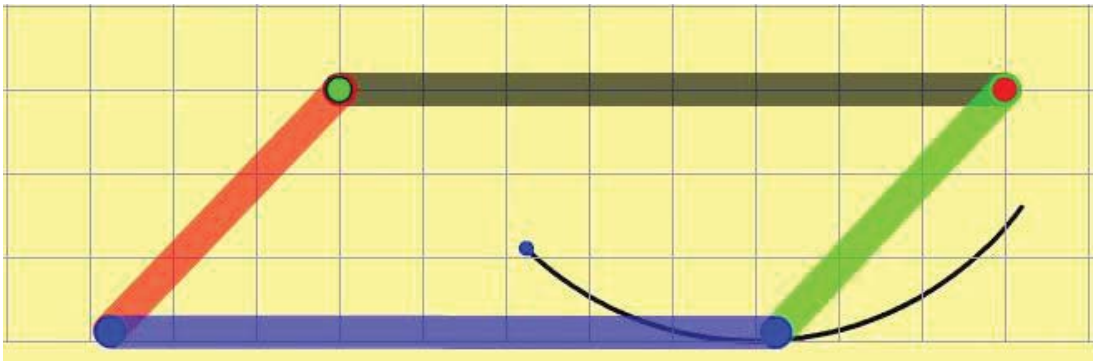

Figure 98: Four-bar Linkage Simulation, Part 1:

In one can see in Figure 98,the four-bar linkage traveling in the fixed-radius path intended, with all cranks parallel.

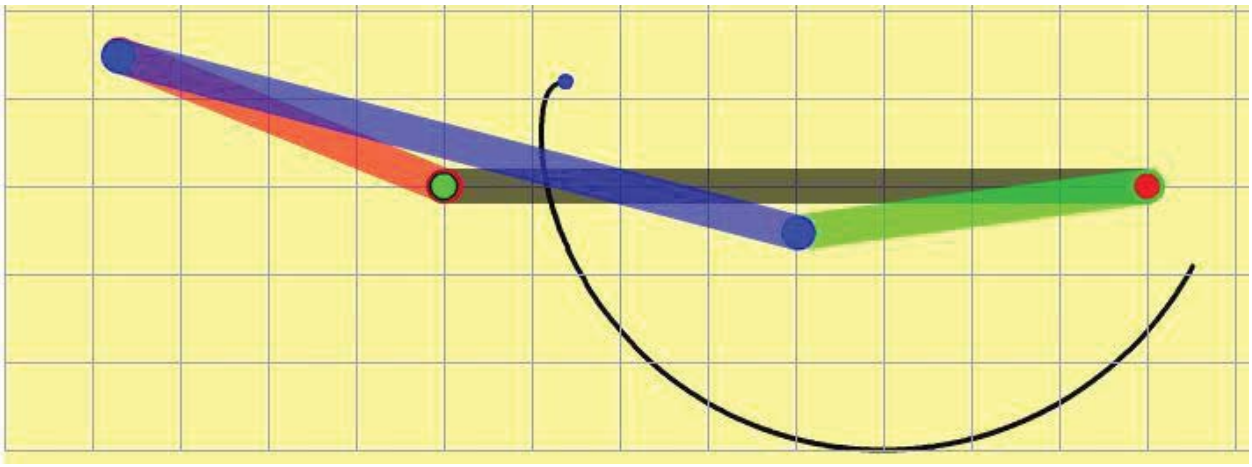

Figure 99: Four-bar Linkage Simulation, Part 2

However, once the point where all cranked are aligned has been passed, parallel orientation was sometimes lost. The cranks usually corrected at the start of the next cycle, but this operation was not ideal for walking.

The gears did mesh throughout the entirety of the cycle, so suspended walking was the next test performed. I-3P0 was suspended by climbing ropes from a wooden structure, similar to the set-up in Figure 100. The undesirable crank orientation was observed to occur at speeds under 0.25 revolutions

per second, well below the desired walking rate of 0.75 revolutions per second. At or above this speed, the legs were able to rotate without issue. The desired speed was the maximum speed at which the motor could move a 150-lb I-3P0 (predicted weight), which is a power-limited operating condition.

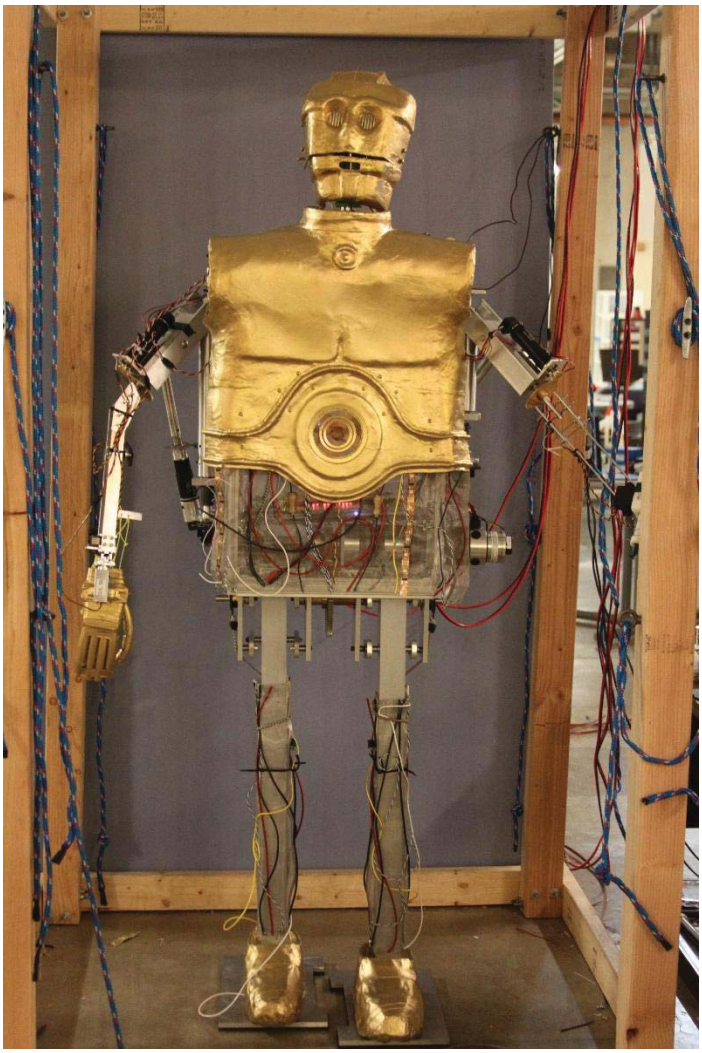

Figure 100: I-3P0 Positioned in Testing Rig

During the suspended walking test, many iterations were done to get the shifting weight to coincide with counteract the walking motion to keep I-3P0 upright. When moved to the ground, I-3P0 was able to walk up to four steps while inside the testing rig without falling over. As testing went on, the cup-end set screws dug into the driveshaft and caused the cranks to become slightly misaligned. As a result, the cranks were no longer 180° out of phase. The cup-end set screws were chosen for their ability to grip onto shafts, but ultimately dug in too far. At that point in testing, it was impossible to remove the set screws. Flat set screws could have been an alternate solution to prevent them from digging into the driveshaft.

One issue that was encountered during walk testing was the fact that the feet would move inwards each time I-3P0 took a step. This would cause I-3P0 to step on its own foot and would increase the risk of it

falling over. To resolve this problem, two modifications were implemented. The first modification was to cut out (via the milling machine) sections of the two feet that can potentially overlap. This increased the spacing between the feet without decreasing their effective sizes in terms of weight support. As a result, the feet ended up looking a bit like the wind-up walking toys' feet. The second modification was to attach stiff bungee cords from each hip shaft to the outside of each leg. The tension in the bungee cords helped to keep the legs apart when I-3P0 walks. With a combination of these two modifications, the issue of I-3P0 stepping on itself was completely resolved.

4.10 Future Alternative Design: Cam Mechanism, 1DOF

After it was decided that the first designs of the walking mechanism should be simplified to a 1 DOF mechanism, an alternate version of the Cam concept from earlier in the brainstorming process was revisited. This design, depicted in Figure 101 below, draws inspiration from Baby Alive's walking baby doll. Since the intention of the doll is unstable walking, mimicking the walking pattern of a human baby, the doll's mechanism had to be scaled up and modified for more stable humanoid-size walking.

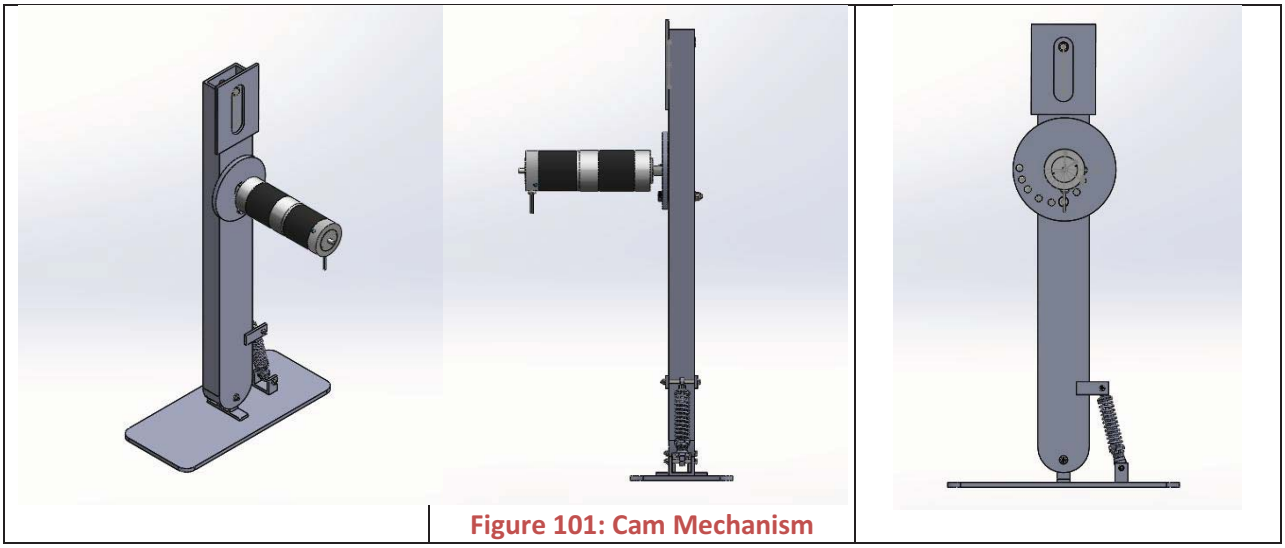

Figure 101: Cam Mechanism

Pictured above, the second walking mechanism design consists of similar foot, ankle, and leg components as are present in the first. However, this second design makes use of a cam and slot mechanism. A circular disk, or cam, is mounted to a driveshaft through a hole in the center of the disk. This driveshaft is geared to a motor, which is the same motor as the previous design. The disk is mounted to the leg via an off-center hole on the disk. In the figure above, multiple iterations of this hole are drilled at varying distances away from the center. This contributes to the modularity of the system design. Simple geometry and mechanics can be applied in order to decide which holes will manifest in different types of gait, allowing for the potential of the robot to possess different walking patterns, similar to the way in which a human is able to walk in an infinite number of manners.

The slot in the design allows for the vertical movement of the leg. This, in combination with the cam, allows the system to achieve a more human-like, circular motion in its gait as opposed to that of the first design.

Similar to the four-bar linkage design, this design only involves one motor, and therefore possesses the advantages of eliminating the cost of a second motor, and removing the inherent difficulties which come hand in hand with having multiple motors. For example, with two motors, the electrical and computer teams would have to spend some more time tweaking the system and setting the motors to be exactly 180° out of phase. Generally, there are less variables of error involved, and this design will hopefully be much easier to troubleshoot.

Even with all the benefits of this design, it also has several disadvantages. One of the system's biggest advantages is a double-edged sword – since the design is relatively simple in that it is essentially a few main components, it makes the system very cohesive and all-encompassing. However, this also makes it difficult because if the one mechanism doesn't work, the entire system doesn't work and has to be reworked, and in the worst case scenario, completely redesigned. Despite the large weight of this disadvantage, it was still decided that this mechanism might be one worthwhile to pursue due to its innovation and potential benefits.

4.10.1 Future Plans for Cam Mechanism

There is much room for improvement and iteration to be made with this cam mechanism. The next steps for this design are to create a more accurate mechanics and dynamics model for the purpose of perfecting the geometry of the design and to conduct finite element analyses on several of the components of interest in order to optimize the design for weight budgets. This will save much time in the manufacturing process next semester.

After this initial design is manufactured, there is even more room for design possibilities. Once the initial system is up and running, and if time permits, there is the possibility of adding on a knee joint to create more sophisticated humanoid walking. Additional features such as a mechanical brake may also be necessary to add onto the design at this point in order to prevent the entire system from toppling over in case of an electrical failure in the system. Even more sophistication can be added to the design in areas such as differing gait as the system is in action. For example, the pin going through the off-center hole in the cam might somehow be electrically controlled in order to facilitate an automatic movement from one hole to the next, allowing the system to change its mid-motion, as opposed to having to stop the system and mechanically change the hole which the pin is going through.

5 Aesthetics

5.1 Process

The team decided to use Worbla thermoplastic to make I-3P0's shell because it was lightweight, strong and slightly flexible, and also was easy to paint. Worbla is often used to make Cosplay costumes, so there are numerous online video tutorials the team watched in order to learn how to use it. The material was recommended to the team as an easy option to create I-3P0's shell by a costume maker. To reshape Worbla, it must be heated to at least 250-300 degrees Fahrenheit over an armature and then cooled to room temperature.

To create an armature for the head and torso, a block of styrofoam was carved using a serrated knife to form a head and chest (see Figure 102 below). The styrofoam block was created by layering four 2" pieces of styrofoam home insulation board and gluing them together using insulation caulk.

Figure 102: Styrofoam head and chest armatures

After carving the armature, it was covered in a layer of insulation caulk in order to smooth out the irregular surface of cut styrofoam. It was then coated with layers of acrylic gesso which were then sanded for a smoother finish. Sanding caulk releases toxic particles, so the layers of paint were sanded instead.

Once the layers of paint were finished, the whole armature was covered in release wax. An online tutorial detailed that this was necessary in order to get the Worbla to release cleanly. A sheet of Worbla was then melted over the armature using a heat gun.

Figure 103: Cooled, formed Worbla sheet

Once the Worbla was cooled, it was covered with layers of gesso and sanded to create a smooth finish for painting. Gesso is the priming medium used for canvases and maintains some flexibility when dry. This meant the paint wouldn't crack if the Worbla bent at all.

To determine the medium to paint I-3P0 gold, Rustoleum Metallic Gold spray paint was first tested. It ended up producing a good, metallic finish, and was the appropriate shade of gold, so this was used to paint the pieces of Worbla. The paint was not covered in shellac or any kind of varnish because any type of clear coat destroys the metallic finish of the spray paint and makes the paint appear flat yellow. All spray painting was done either outside or in the Upson Paint Booth.

Shoes were also made out of Worbla, however they were made using a slightly different process. Armatures were made by bending and taping plastic sheeting over a size 13 sneaker. Worbla was then melted over these armatures (see figure below). The priming and painting process used was the same as detailed above. Holes for the aluminum leg beams were cut out using the dremel.

Figure 104: Primed Worbla shoes

5.2 Torso and Face

The design of the torso and face was created freehand without the use of molds or professional recreation. All design references were based off of Star Wars films, images from web searches, and hobbyist web pages. After these parts were primed and sanded, two coats of gold spray paint were applied and allowed to dry.

Figure 105: Face parts spray painted outdoors to allow for proper ventilation

Figure 106: Finished torso portion

5.3 Head

While there no initial structural need for a physical head, it was decided that it would enhance the overall aesthetics of the face. Stainless steel Structural wire 0.102” was first bent into dividing outlines of the styrofoam head (transverse, frontal, and sagital) to give a general physical appearance. The 3 wire outlines were bound by 0.025” stainless steel wire wrapped around the junctions. Additional outlines were formed and added to show dimensions in the eyes, mouth, and chin. The resulting unit resembled a wire skull and was fixed at the junctions with hot glue.

To provide a fuller look and hide imperfections of the wire frame, it was decided to either cover the head or fill it with a wire mesh material. A paper pattern was created by covering the styrofoam head with paper and form fitting it with masking tape. The paper form was released and cut into even portions and used as a pattern to cut out wire mesh. The wire mesh parts were attached using the 0.025” stainless steel wire in a staple fashion with ends folded over to reduce injury due to frayed ends. The mesh form was pushed and fitted into the wire skull and attached with more 0.025” wire. The entire unit was spray painted gold and let to dry for 3 hours.

Figure 107: Side, front, and rear view of the face and head

Since the wire head frame was form fitted to the styrofoam mold, the Worbla face mask was well fitted directly on top. Several methods were discussed to attach the two parts together such as screws, hot glue, and wire. A thermoplastic Polymorph was chosen to affix the face, by simply using a heat gun to warm the plastic in a malleable form, placing it on the face mask and pressing the frame into the plastic.

5.4 Legs and Abdomen

To provide balance and authenticity to the aesthetics of I-3P0, the classic electrical wire abdominal portion was created. Scrap electrical wire from previous Cornell Cup projects was donated and hot glued to the wire mesh used for the head. The wires were arranged with inspiration from original film I-3P0. The wire mesh was attached to the Worbla cast using perfboard and bolts spray painted gold.

Figure 108: Electrical wire mesh cover on the abdomen and leg

Several methods to cover the legs were discussed such as using air duct attachments and plastic sheets however neither provided easy removal or easy fabrication. The mesh wire portion was extended onto the legs and was made removable with the use of velcro.

5.5 Bill of Materials

Part	Material	Part number	#	Price	Total	Retailer	Website	Purpose
1	Bright Metallic Spray Paint		1	9.98	9.98	Amazon	http://www.amazon.com/Rust-Oleum-7710830-Bright-Metallic-11-Ounce/dp/B000Z8FGE2/ref=sr_1_14?ie=UTF8&qid=1391989646&sr=8-14&keywords=metallic+gold+paint	I-3P0 Shell Testing
2	Generic Insulation Caulk-		3	4	12	Lowes		

	Liquid Nails							
3	Celluclay 1-lb. bag		1	10.52	10.52	Amazon	http://www.amazon.com/Activa-Celluclay-Instant-Papier-1-Pound/dp/B001144SDE/ref=sr_1_1?ie=UTF8&qid=1391988854&sr=8-1&keywords=celluclay	I-3P0 Shell Testing
4	Corrosion-Resistant Type 304 Stainless Steel Wire Cloth	85385T82	2	36.03	72.06	mcmaster	http://www.mcmaster.com/#standard-wire-mesh/=r5jasr	I3P0 Shell
5	Creative Paperclay - 16 oz.		1	12.39	12.39	Amazon	http://www.amazon.com/Creative-Paperclay-Modeling-Compound-16-Ounce/dp/B0013J0HI2/ref=sr_1_6?ie=UTF8&qid=1391988854&sr=8-6&keywords=celluclay	I-3P0 Shell Testing
6	Honey Wax (14 oz container)	2386K78	2	19.28	38.56	McMaster	http://www.mcmaster.com/#mold-release-wax/=qzudcy	Lots of release wax for I-3P0's moulds (~10 coats required)
7	Liquitex Professional Gesso (32 oz)		1	$23.9	$23.9	Amazon	http://www.amazon.com/Liquitex-Professional-White-Surface-Medium/dp/B000KNJF6W/ref=sr_1_sc_1?ie=UTF8&qid=1393715386&sr=8-1-spell&keywords=liquitex+profession+gesso	Paint Primer
8	Multipurpose Spray Shellac	7655T1	1	$11	$11	McMaster	http://www.mcmaster.com/#shellac-coatings/=qxokwb	Paint testing
9	Plastic Styrene Sheet - .020" thick	43330	1	$6.46	$6.46	US Plastic Corp	http://www.usplastic.com/catalog/item.aspx?itemid=22883	I-3P0 Shell Testing
10	Plastic Styrene Sheet - .030" thick	43331	1	$9.49	$9.49	US Plastic Corp	http://www.usplastic.com/catalog/item.aspx?itemid=22883	I-3P0 Shell Testing
11	Rustoleum Bright Coat Metallic Finish		3	7.61	22.83	Amazon	http://www.amazon.com/Rust-Oleum-7710830-Bright-Metallic-11-Ounce/dp/B000Z8FGE2/ref=sr_1_14?	I-3P0 paint

	Gold Spray Paint						ie=UTF8&qid=1391989646&sr=8-14&keywords=metallic+gold+paint	
12	Sandpaper - 150 Grit	4649A311	2	18.48	18.48	McMaster	http://www.mcmaster.com/#sanding-sheets/=qwrnwe	Polish torso
13	Sandpaper - 320 Grit	4692A71	1	$10.09	$10.09	McMaster	http://www.mcmaster.com/#sanding-sheets/=qxolqo	More paint testing
14	Stainless Steel Wire - 1lb spool, 0.064"	8860K19	2	12.94	25.88	McMaster	http://www.mcmaster.com/#metal-wire/=r5fvge	I-3P0 shell
15	Stainless Steel Wire - 1lb spool, 0.102"	8860K22	1	11.91	11.91	McMaster	http://www.mcmaster.com/#metal-wire/=r5fvge	I-3P0 shell
16	Stainless Steel Wire .025" Diameter, 1/4-lb SpooL	8860K13	1	8.15	8.15	McMaster	http://www.mcmaster.com/#stainless-steel-wire/=riq3vc	I3P0 shell last wire order
17	Styrofoam board		1	30	30	Lowes		
18	Worbla Thermoplastic - Jumbo sheet		1	$80	$80	Cosplay Supplies	http://www.cosplaysupplies.com/store.php?p=WORB1	I-3P0 shell
19	Worbla Thermoplastic - Sample sheet		1	$18	$18	Cosplay Supplies	http://www.cosplaysupplies.com/store.php?p=WORB-Sample	I-3P0 Shell Testing
	Total				**$431.7**			

6 Appendix

6.1 Lift Motor – Maxon Drive Spec

Your maxon drive

maxon motor
driven by precision

consists of:

Spindle Drive GP 32 S Ø32 mm, Ball Srew, Ø10 x 2
Part number 363973

RE 35 Ø35 mm, Graphite Brushes, 90 Watt
Part number 323890

Encoder HEDL 5540, 500 CPT, 3 Channels, with Line Driver RS 422
Part number 110512

Brake AB 28, 24 VDC, 0.4 Nm
Part number 228387

Your Contact

maxon motor worldwide
http://www.maxonmotorusa.com:80/maxon/view/content/contact_page
E-Mail: info@maxonmotor.com
Internet: http://www.maxonmotorusa.com:80

retail price:

1-4 Pieces	**USD 2,052.51**
5-19 Pieces	**USD 1,738.88**
20-49 Pieces	**USD 1,494.00**
from 50 Pieces	**On Request**

Terms and conditions

Spindle Drive GP 32 S Ø32 mm, Ball Srew, Ø10 x 2
Part number 363973

General Information	
Gear Art	GP
Outer diameter	32 mm
Gear variant	KS

Gearhead Data	
Number of stages	1
Reduction	5.8 : 1
Reduction absolute	23/4
Max. motor shaft diameter	6 mm
Max. feed velocity	72 mm/s
Max. feed force (continuous)	474 N
Max. feed force (intermittent)	1255 N
Sense of rotation drive to output	=
Max. efficiency	75 %
Weight	300 g
Average backlash no load	0.7 °
Mechanical positioning accuracy	0.037 mm
Mass inertia	4.2 gcm²
Gearhead length (L1)	51 mm
Max. transferable continuous performance	140 W
Max. transferable short-time performance	180 W

Technical Data	
Spindle length	200 mm
Radial play	max. 0.05 mm, 5 mm from flange
Axial play of the nut	max. 0.01 mm
Max. radial load	200 N, 15 mm from flange
Max. axial load (dynamic)	2700 N
Max. permissible force for press fits	2700 N
Recommended input speed	8000 rpm
Max. short-time input speed	8000 rpm
Recommended temperature range	-15...+80 °C
Number of autoclave cycles	0

RE 35 Ø35 mm, Graphite Brushes, 90 Watt

Part number 323890

Values at nominal voltage	
Nominal voltage	24 V
No load speed	7740 rpm
No load current	169 mA
Nominal speed	7000 rpm
Nominal torque (max. continuous torque)	101 mNm
Nominal current (max. continuous current)	3.62 A
Stall torque	1200 mNm
Starting current	41.1 A
Max. efficiency	86 %

Characteristics	
Terminal resistance	0.583 Ω
Terminal inductance	0.191 mH
Torque constant	29.2 mNm/A
Speed constant	328 rpm/V
Speed / torque gradient	6.55 rpm/mNm
Mechanical time constant	5.44 ms
Rotor inertia	79.2 gcm²

Thermal data	
Thermal resistance housing-ambient	6.2 K/W
Thermal resistance winding-housing	2 K/W
Thermal time constant winding	33.1 s
Thermal time constant motor	844 s
Ambient temperature	-30...+100 °C
Max. permissible winding temperature	+155 °C

Mechanical data	
Bearing Type	ball bearings
Max. permissible speed	12000 rpm
Axial play	0.05 - 0.15 mm
Radial play	0.025 mm
Max. axial load (dynamic)	5.6 N
Max. force for press fits (static)	110 N
(static, shaft supported)	1200 N
Max. radial loading	28 N, 5 mm from flange

Other specifications	
Number of pole pairs	1
Number of commutator segments	13
Direction of rotation	Clockwise (CW)
Number of autoclave cycles	0

Product	
Weight	340 g

Encoder HEDL 5540, 500 CPT, 3 Channels, with Line Driver RS 422

Part number 110512

General Information

Counts per turn	500
Number of channels	3
Line Driver	DS26LS31
Max. speed	12000 rpm
Shaft diameter	3 mm

Technical Data

Supply voltage Vcc	5.0V ± 10.0%
Driver used logic	EIA RS 422
Min. angular acceleration	250000 rad / s²
Output current per channel	-20...20 mA
Signal rise time	180 ns
Measurement condition for signal rise time	CL=25pF, RL=2.7kOhm,
Signal fall time	40 ns
Measurement condition for signal fall time	CL=25pF, RL=2.7kOhm,
Phase shift	90 °e
Phase shift, inaccuracy	45 °e
Index synchronized to AB	Yes
Max. moment of interia of code wheel	0.6 gcm²
Operating temperature	-40...+100 °C
Orientation encoder to motor defined	-1.0 °

6.2 Turn Motor – Maxon Drive Spec

Your maxon drive

maxon motor
driven by precision

Consists of:

Planetary Gearhead GP 42 C Ø42 mm, 3 - 15 Nm, Ceramic Version
Part number 203129

RE 40 Ø40 mm, Graphite Brushes, 150 Watt
Part number 218009

Encoder MR, Type L, 256 CPT, 3 Channels, with Line Driver
Part number 225783

Your contact

maxon motor worldwide
http://www.maxonmotor.com/maxon/view/content/company_contact_form
E-Mail: e-shop@maxonmotor.com
Internet: www.maxonmotor.com

Non-binding price info excl. shipping and packing cost, excl. VAT.

1-4 Pieces	**USD 983.63**
5-19 Pieces	**USD 832.63**
20-49 Pieces	**USD 674.25**

General Terms and Conditions: http://www.maxonmotor.com/maxon/view/content/terms_and_conditions_page

Summary of the selected drive

Consists of:

Planetary Gearhead GP 42 C Ø42 mm, 3 - 15 Nm, Ceramic Version
Part number 203129

RE 40 Ø40 mm, Graphite Brushes, 150 Watt
Part number 218009

Encoder MR, Type L, 256 CPT, 3 Channels, with Line Driver
Part number 225783

Operating range

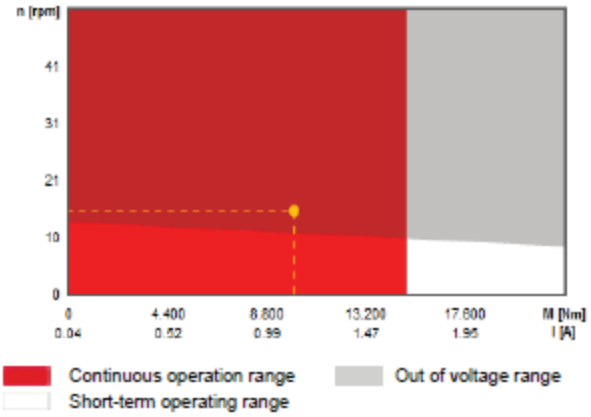

Data for combination	
Max. motor voltage	24 V
No load speed	623 rpm
Max. continuous torque	15000 mNm
Nominal current (max. continuous current)	2.2 A
Permissible intermittent torque	22000 mNm
Total length	141.1 mm
Max. diameter	42 mm

Planetary Gearhead GP 42 C Ø42 mm, 3 - 15 Nm, Ceramic Version
Part number 203129

General Information		
Gear Art	GP	
Outer diameter	42	mm
Gear variant	C	
Gearhead Data		
Reduction	156 : 1	
Reduction absolute	156/1	
Max. motor shaft diameter	8	mm
Number of stages	3	
Max. continuous torque	15	Nm
Intermittently permissible torque at gear output	22	Nm
Sense of rotation drive to output	=	
Max. efficiency	72	%
Weight	460	g
Average backlash no load	1	°
Mass inertia	9.1	gcm²
Gearhead length (L1)	70	mm
Max. transferable continuous performance	81	W
Max. transferable short-time performance	120	W
Technical Data		
Radial play	max. 0.06 mm, 12 mm from flange	
Axial play	max. 0.3	mm
Max. radial load	150 N, 12 mm from flange	
Max. axial load (dynamic)	150	N
Max. permissible force for press fits	300	N
Recommended input speed	8000	rpm
Max. short-time input speed	8000	rpm
Recommended temperature range	-40...+100	°C
Number of autoclave cycles	0	

Information about gearhead data http://www.maxonmotor.com/medias/CMS_Downloads/DIVERSES/12_203_EN.pdf

RE 40 Ø40 mm, Graphite Brushes, 150 Watt
Part number 218009

Values at nominal voltage		
Nominal voltage	48	V
No load speed	4050	rpm
No load current	38.8	mA
Nominal speed	4920	rpm
Nominal torque (max. continuous torque)	177	mNm
Nominal current (max. continuous current)	2.2	A
Stall torque	1580	mNm
Starting current	19.2	A
Max. efficiency	91	%
Characteristics		
Terminal resistance	2.24	Ω
Terminal inductance	0.612	mH
Torque constant	82.2	mNm/A
Speed constant	116	rpm/V
Speed / torque gradient	3.53	rpm/mNm
Mechanical time constant	4.19	ms
Rotor inertia	118	gcm²
Thermal data		
Thermal resistance housing-ambient	4.65	KW-1
Thermal resistance winding-housing	1.93	KW-1
Thermal time constant winding	35.7	s
Thermal time constant motor	736	s
Ambient temperature	-30...+100	°C
Max. permissible winding temperature	+155	°C
Mechanical data		
Bearing Type	ball bearings	
Max. permissible speed	12000	rpm
Axial play	0.05 - 0.15	mm
Radial play	0.025	mm
Max. axial load (dynamic)	5.6	N
Max. force for press fits (static)	110	N
(static, shaft supported)	1200	N
Max. radial loading	28 N, 5 mm from flange	
Other specifications		
Number of pole pairs	1	
Number of commutator segments	13	
Direction of rotation	Clockwise (CW)	
Number of autoclave cycles	0	
Product		
Weight	480	g

Information about motor data http://www.maxonmotor.com/medias/CMS_Downloads/DIVERSES/12_049_EN.pdf

Encoder MR, Type L, 256 CPT, 3 Channels, with Line Driver
Part number 225783

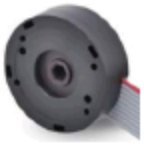

General Information		
Counts per turn	256	
Number of channels	3	
Line Driver	Yes	
Max. speed	18750	rpm
Technical Data		
Supply voltage Vcc	4.7...5.2	V
Driver used logic	TTL	
Output current per channel	0...5	mA
Phase shift	90	°e
Phase shift, inaccuracy	45	°e
Index synchronized to AB	Yes	
Max. moment of interia of code wheel	1.7	gcm²
Operating temperature	-25...+85	°C

6.3 Twist Motor – Maxon Drive Spec

Your maxon drive

maxon motor
driven by precision

Consists of:

Planetary Gearhead GP 32 A Ø32 mm, 0.75 - 4.5 Nm, Metal Version
Part number 166167

RE 30 Ø30 mm, Graphite Brushes, 60 Watt
Part number 310008

Encoder HEDS 5540, 500 Counts per turn, 3 Channels
Part number 110511

Your contact

maxon motor worldwide
http://www.maxonmotor.com/maxon/view/content/company_contact_form
E-Mail: e-shop@maxonmotor.com
Internet: www.maxonmotor.com

Non-binding price info excl. shipping and packing cost, excl. VAT.

1-4 Pieces	**USD 695.00**
5-19 Pieces	**USD 542.00**
20-49 Pieces	**USD 458.63**

General Terms and Conditions: http://www.maxonmotor.com/maxon/view/content/terms_and_conditions_page

Summary of the selected drive

Consists of:

Planetary Gearhead GP 32 A Ø32 mm, 0.75 - 4.5 Nm, Metal Version
Part number 166167

RE 30 Ø30 mm, Graphite Brushes, 60 Watt
Part number 310008

Encoder HEDS 5540, 500 Counts per turn, 3 Channels
Part number 110511

Operating range

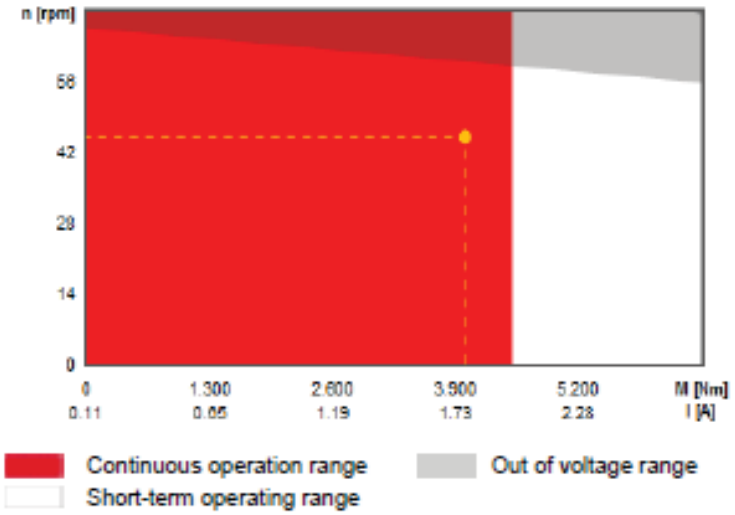

Data for combination	
Max. motor voltage	24 V
No load speed	2397 rpm
Max. continuous torque	4500 mNm
Nominal current (max. continuous current)	2.28 A
Permissible intermittent torque	6500 mNm
Total length	111.2 mm
Max. diameter	32 mm

Planetary Gearhead GP 32 A Ø32 mm, 0.75 - 4.5 Nm, Metal Version
Part number 166167

General Information		
Gear Art	GP	
Outer diameter	32	mm
Gear variant	A	
Gearhead Data		
Reduction	85 : 1	
Reduction absolute	14976/175	
Max. motor shaft diameter	4	mm
Number of stages	3	
Max. continuous torque	4.5	Nm
Intermittently permissible torque at gear output	6.5	Nm
Sense of rotation drive to output	=	
Max. efficiency	70	%
Weight	190	g
Average backlash no load	1	°
Mass inertia	0.7	gcm²
Gearhead length (L1)	43.1	mm
Max. transferable continuous performance	33	W
Max. transferable short-time performance	47	W
Technical Data		
Radial play	max. 0.14 mm, 5 mm from flange	
Axial play	max. 0.4	mm
Max. radial load	140 N, 10 mm from flange	
Max. axial load (dynamic)	120	N
Max. permissible force for press fits	120	N
Recommended input speed	6000	rpm
Max. short-time input speed	6000	rpm
Recommended temperature range	-40...+100	°C
Number of autoclave cycles	0	

Information about gearhead data http://www.maxonmotor.com/medias/CMS_Downloads/DIVERSES/12_203_EN.pdf

RE 30 Ø30 mm, Graphite Brushes, 60 Watt
Part number 310008

Values at nominal voltage		
Nominal voltage	36	V
No load speed	8590	rpm
No load current	106	mA
Nominal speed	7840	rpm
Nominal torque (max. continuous torque)	86.6	mNm
Nominal current (max. continuous current)	2.28	A
Stall torque	1000	mNm
Starting current	25.2	A
Max. efficiency	87	%
Characteristics		
Terminal resistance	1.43	Ω
Terminal inductance	0.281	mH
Torque constant	39.8	mNm/A
Speed constant	240	rpm/V
Speed / torque gradient	8.61	rpm/mNm
Mechanical time constant	2.98	ms
Rotor inertia	33.1	gcm²
Thermal data		
Thermal resistance housing-ambient	6	KW-1
Thermal resistance winding-housing	1.7	KW-1
Thermal time constant winding	16.1	s
Thermal time constant motor	593	s
Ambient temperature	-30...+100	°C
Max. permissible winding temperature	+125	°C
Mechanical data		
Bearing Type	ball bearings	
Max. permissible speed	12000	rpm
Axial play	0.05 - 0.15	mm
Radial play	0.025	mm
Max. axial load (dynamic)	5.6	N
Max. force for press fits (static)	110	N
(static, shaft supported)	1200	N
Max. radial loading	28 N, 5 mm from flange	
Other specifications		
Number of pole pairs	1	
Number of commutator segments	13	
Direction of rotation	Clockwise (CW)	
Number of autoclave cycles	0	
Product		
Weight	260	g

Information about motor data http://www.maxonmotor.com/medias/CMS_Downloads/DIVERSES/12_049_EN.pdf

Encoder HEDS 5540, 500 Counts per turn, 3 Channels
Part number 110511

General Information		
Counts per turn	500	
Number of channels	3	
Line Driver	No	
Max. speed	12000	rpm
Shaft diameter	3	mm
Technical Data		
Supply voltage Vcc	5.0V ± 10.0%	
Driver used logic	TTL	
Min. angular acceleration	250000	rad / s²
Output current per channel	-1...5	mA
Signal rise time	180	ns
Measurement condition for signal rise time	CL=25pF, RL=2.7kOhm,	
Signal fall time	40	ns
Measurement condition for signal fall time	CL=25pF, RL=2.7kOhm,	
Phase shift	90	°e
Phase shift, inaccuracy	45	°e
Index synchronized to AB	Yes	
Max. moment of interia of code wheel	0.6	gcm²
Operating temperature	-40...+100	°C
Orientation encoder to motor defined	-1.0	°

6.4 Balancing Motor Info OBSOLETE

Your maxon drive

maxon motor
driven by precision

consists of:

Planetary Gearhead GP 52 C Ø52 mm, 4 - 30 Nm, Ceramic Version
Part number 223081

EC 90 flat Ø90 mm, brushless, 90 Watt, with Hall sensors
Part number 323772

Encoder MILE, 800 CPT, 2 Channels, with Line Driver RS 422
Part number 409996

Your Contact

maxon motor worldwide
http://www.maxonmotorusa.com:80/maxon/view/content/contact_page
E-Mail: info@maxonmotor.com
Internet: http://www.maxonmotorusa.com:80

retail price:

1-4 Pieces	**USD 856.88**
5-19 Pieces	**USD 747.13**
20-49 Pieces	**USD 623.26**
from 50 Pieces	**On Request**

Terms and conditions

Planetary Gearhead GP 52 C Ø52 mm, 4 - 30 Nm, Ceramic Version

Part number 223081

General information

Gear Art	GP
Outer diameter	52 mm
Gear variant	C

Gearhead Data

Reduction	4.3 : 1
Reduction absolute	13/3
Max. motor shaft diameter	8 mm
Number of stages	1
Max. continuous torque	4 Nm
Intermittently permissible torque at gear output	6 Nm
Sense of rotation drive to output	=
Max. efficiency	91 %
Weight	460 g
Average backlash no load	0.6 °
Mass inertia	12 gcm²
Gearhead length (L1)	49 mm
Max. transferable continuous performance	580 W
Max. transferable short-time performance	880 W

Technical Data

Radial play	max. 0.06 mm, 12 mm from flange
Axial play	0 - 0.3 mm
Max. radial load	500 N, 12 mm from flange
Max. axial load (dynamic)	200 N
Max. permissible force for press fits	500 N
Recommended input speed	6000 rpm
Max. short-time input speed	6000 rpm
Recommended temperature range	-15...+80 °C
Extended temperature range	-40...+100 °C
Number of autoclave cycles	0

EC 90 flat Ø90 mm, brushless, 90 Watt, with Hall sensors

Part number 323772

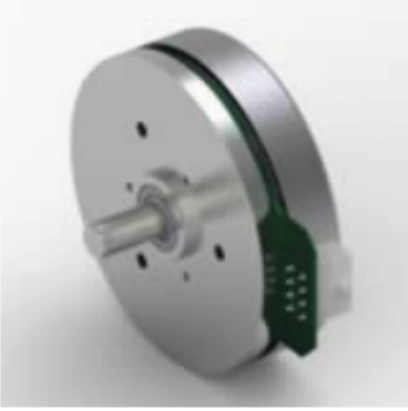

Values at nominal voltage

Nominal voltage	24 V
No load speed	3190 rpm
No load current	538 mA
Nominal speed	2590 rpm
Nominal torque (max. continuous torque)	444 mNm
Nominal current (max. continuous current)	6.06 A
Stall torque	4690 mNm
Starting current	70 A
Max. efficiency	84 %

Characteristics

Terminal resistance	0.343 Ω
Terminal inductance	0.264 mH
Torque constant	70.5 mNm/A
Speed constant	135 rpm/V
Speed / torque gradient	0.659 rpm/mNm
Mechanical time constant	21.1 ms
Rotor inertia	3060 gcm²

Thermal data

Thermal resistance housing-ambient	1.57 K/W
Thermal resistance winding-housing	2.7 K/W
Thermal time constant winding	34.1 s
Thermal time constant motor	234 s
Ambient temperature	-40...+100 °C
Max. permissible winding temperature	+125 °C

Mechanical data

Bearing Type	ball bearings
Max. permissible speed	5000 rpm
Axial play	0.14 mm
Max. axial load (dynamic)	12 N
Max. force for press fits (static)	180 N
(static, shaft supported)	8000 N
Max. radial loading	60 N, 8 mm from flange

Other specifications

Number of pole pairs	12
Number of phases	3
Direction of rotation	Clockwise (CW)
Number of autoclave cycles	0

Product

Weight	600 g

Encoder MILE, 800 CPT, 2 Channels, with Line Driver RS 422

Part number 409996

General information

Counts per turn	800
Number of channels	2
Line Driver	AM26C31QD
Max. electrical speed	5000 rpm
Max. speed	5000 rpm

Technical Data

Supply voltage Vcc	5.0V ± 10.0%
Output Signal	INC
Driver used logic	Differential, EIA RS 422
Output current per channel	-20...20 mA
Signal rise time	30 ns
Measurement condition for signal rise time	CL=25pF, RL=1kOhm, T
Signal fall time	30 ns
Measurement condition for signal fall time	Cl=25pF,RL=1kOhm, T=
Min. state length	500 ns
Sense of rotation	A vor B CW
Max. Current consumption at standstill	15 mA
Max. moment of interia of code wheel	65 gcm²
Operating temperature	-40...+100 °C

Product

Weight	10 g

6.5 Balancing Motor FINAL

MIDWEST MOTION PRODUCTS

MMP

REVERSIBLE DC GEARMOTOR

Model Number:

MMP S22-346H-24V GP52-03.7

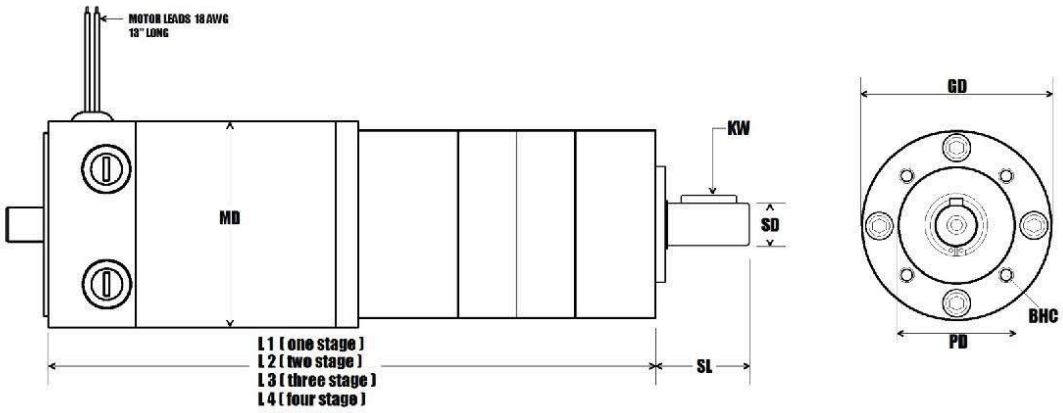

DIMENSIONS:	NOTE: OPTICAL ENCODER & INTEGRAL BRAKE OPTIONS AVAILABLE - SEE ADDITIONAL PAGES FOR DETAILS	
MD = 2.25" (57mm)	SL = 25mm (21mm usable)	Note: Center of output shaft contains an M-4 threaded hole
GD = 2.05" (52mm)	SD = 0.472" (12mm)	BHC (dia) = 40mmØ (4 ea) M5 x 10mm deep
L1 = 6.31" (160mm)	KW = 2mm(H) x 4mm(W) x 16mm(L)	PD = 32mm, pilot length = 3mm

PLANETARY GEARMOTOR OUTPUT PARAMETERS:	VALUE	UNITS	TOLERANCE
Gearhead Ratio (exact)	3.70 : 1		
Gearhead Shaft Output Speed (at full-load)	784	RPM	MAX
Gearmotor Rated Continuous Torque	9	In-Lbs	MAX
Gearmotor Rated Peak Torque	70++	In-Lbs	-----
Gearhead Standard Backlash	42	Arc Minutes	MAX
Gearhead Efficiency	80%	-----	-----
Output Shaft Radial Load Capacity	45	Lbs	MAX
Output Shaft Axial Load Capacity	13	Lbs	MAX
Gearmotor Total Weight	3.2	Lbs	MAX

++ All Peak Torque values are dependent upon duty. Contact our sales office for details.

DC MOTOR PERFORMANCE PARAMETERS:	VALUE	UNITS	TOLERANCE
Rated DC Voltage	24	DC VOLTS	-----
Rated Continuous Current	5.15	AMPERES	-----
No-Load Speed	3300	RPM	MAX
Rated Speed	2900	RPM	+/- 15%
Rated Continuous Power Out	107	WATTS	+/- 15%
Rated Continuous Torque	50	OZ-IN	-----
Peak Torque (motor only)	500	OZ-IN	-----
No-Load Current	0.61	AMPERES	MAX
Back EMF Constant (Ke)	7.2	V/KRPM	+/- 10%
Torque Constant (Kt)	9.7	OZ-IN/AMP	+/- 10%
DC Armature Resistance	0.84	OHMS	+/- 15%
Armature Inductance	0.44	mH	+/- 15%
Armature temperature	155	DEG. C	MAX

MIDWEST MOTION PRODUCTS
DESIGN, MANUFACTURING & DISTRIBUTION - MOTION CONTROL EQUIPMENT
10761 Ahern Avenue SE Watertown, MN 55388
Phone: 952-955-2626 Fax: 480-247-4096
www.midwestmotion.com email: sales@midwestmotion.com

Option1: Optical Encoder Option

Contact sales for pricing

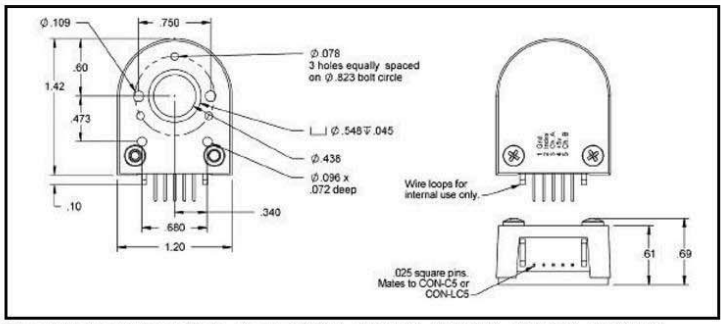

EU Series Interconnects/Functions		
Pin #:	Function:	Color:
1	Ground	Brown
2	Index	Violet
3	Channel A	Blue
4	+5 Volts	Orange
5	Channel B	Yellow

*Resolutions available from stock: 32 PPR, 100 PPR, 250 PPR, 500 PPR, 1024 PPR
(Use suffix "EU-xxx" after model # to designate resolution)
Encoder is mounted integrally to the back of the motor or brake.
Includes an index pulse, and 12" long flying leads.

Option2: "IP-65" Optical Encoder 512 / 1000 PPR

Contact sales for pricing

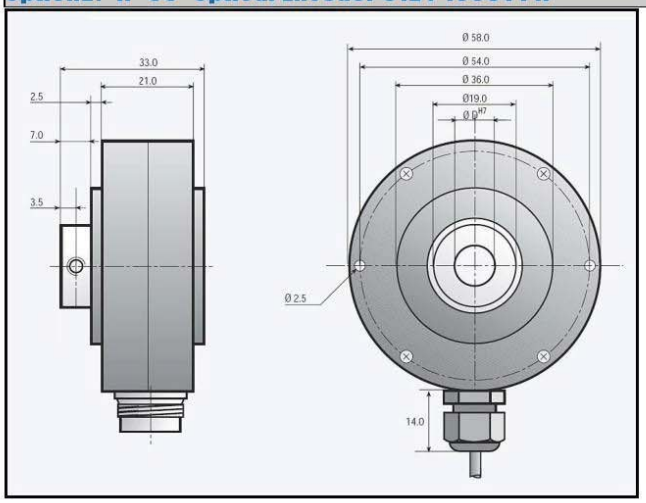

Ei Series Interconnects/Functions	
Function:	Color:
0 Volts	White
+ Volts	Brown
A	Green
B	Yellow
0	Grey
A-	Pink
B-	Blue
0-	Red

Features:

- IP-65 rated protection for harsh environments
- Index pulse
- Complementary output signals
- 6 ft long cable
- 512 or 1000 PPR Resolutions available from stock, others available.

Use Suffix "Ei-xxx" after model number to designate resolution.
Consult our sales office for additional information.

MIDWEST MOTION PRODUCTS
DESIGN, MANUFACTURING & DISTRIBUTION - MOTION CONTROL EQUIPMENT
10761 Ahern Avenue SE Watertown, MN 55388
Phone: 952-955-2626 Fax: 480-247-4096
www.midwestmotion.com email: sales@midwestmotion.com

Option 3: Integral Brake Option — Contact sales for pricing

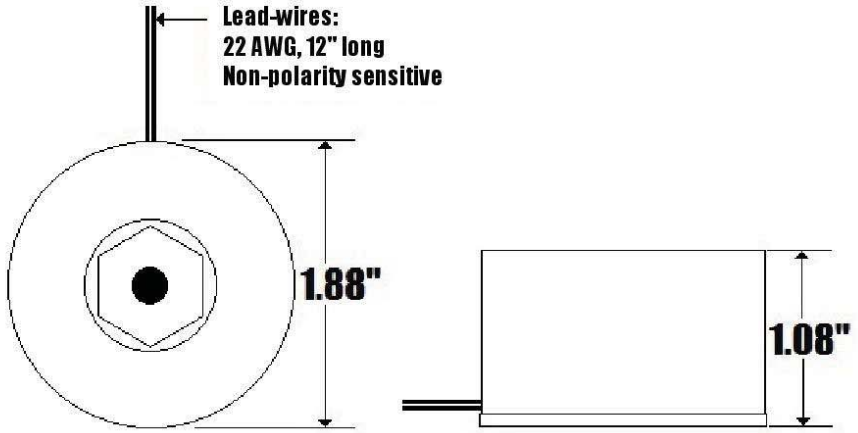

The MMP small frame gearmotors and motors are sufficiently served by a 5 in-lb brake, when used correctly.
Typical (24v) brake current = 375 mA;
All brakes (12v, 24v, 36v, 48v, 90v & 115vac) are 9 Watt devices

Use suffix "BR-005" after model number to designate the brake and holding torque.

IMPORTANT NOTE: IF THE BRAKE IS TO BE ENERGIZED BY A VOLTAGE LEVEL OTHER THAN THE SPECIFIED OPERATING VOLTAGE OF THE MOTOR, PLEASE SPECIFY THE BRAKE OPERATING VOLTAGE SEPARATELY. IF NOT OTHERWISE NOTED, IT IS ASSUMED THE BRAKE'S COIL VOLTAGE WILL MATCH THE MOTOR VOLTAGE.

This part number suffix also identifies a "Failsafe" type brake. (engages in the ABSENCE of input power)

For a "Power ON" brake, or a brake that is engaged with POWER APPLIED, please specify suffix "**BR-005n**".

All brakes are integrally mounted to the back of the motor and equipped with mounting holes and a shaft extension for an encoder.

The rear surface of the standard brake can be made to serve as an encoder mounting surface.
Please specify if both brake and encoder options are required.

*For additional details or assistance configuring the model number for brake and encoder options, please feel free to contact our sales offices.

MIDWEST MOTION PRODUCTS
DESIGN, MANUFACTURING & DISTRIBUTION - MOTION CONTROL EQUIPMENT
10761 Ahern Avenue SE Watertown, MN 55388
Phone: 952-955-2626 Fax: 480-247-4096
www.midwestmotion.com email: sales@midwestmotion.com

6.6 Walking Motor Info

Model Number:

MMP D33-655B-24V GP81-025

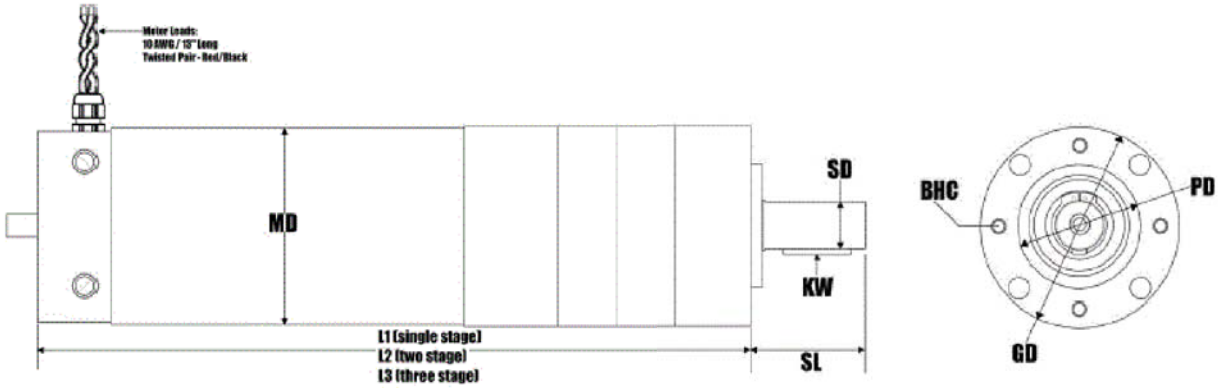

DIMENSIONS:	NOTE: OPTICAL ENCODER & INTEGRAL BRAKE OPTIONS AVAILABLE - SEE ADDITIONAL PAGES FOR DETAILS	
MD = 3.13" (80mm)	SL = 49mm (40mm usable)	Note: Center of output shaft contains an M-6 threaded hole
GD = 3.20" (81mm)	SD = 0.748" (19mm); +0, -21µm	BHC (dia) = 65mmØ (4 ea) M6x12mm deep
L2 = 11.25" (286mm)	KW = 3mm(H) x 6mm(W) x 28mm(L)	PD = 50mm, pilot length = 5mm

PLANETARY GEARMOTOR OUTPUT PARAMETERS:	VALUE	UNITS	TOLERANCE
Gearhead Ratio (exact)	25.01 : 1		
Gearhead Shaft Output Speed (at full-load)	160	RPM	MAX
Gearmotor Rated Continuous Torque	202	In-Lbs	MAX
Gearmotor Rated Peak Torque	1062++	In-Lbs	-----
Gearhead Standard Backlash	33	Arc Minutes	MAX
Gearhead Efficiency	75%	-----	-----
Output Shaft Radial Load Capacity	135	Lbs	MAX
Output Shaft Axial Load Capacity	27	Lbs	MAX
Gearmotor Total Weight	14.3	Lbs	MAX

++ All Peak Torque values are dependent upon duty. Contact our sales office for details.

DC MOTOR PERFORMANCE PARAMETERS:	VALUE	UNITS	TOLERANCE
Rated DC Voltage	24	DC VOLTS	-----
Rated Continuous Current	23.9	AMPERES	-----
No-Load Speed	4530	RPM	MAX
Rated Speed	4000	RPM	+/- 15%
Rated Continuous Power Out	509	WATTS	+/- 15%
Rated Continuous Torque	172	OZ-IN	-----
Peak Torque (motor only)	1250	OZ-IN	-----
No-Load Current	1.11	AMPERES	MAX
Back EMF Constant (Ke)	5.3	V/KRPM	+/- 10%
Torque Constant (Kt)	7.2	OZ-IN/AMP	+/- 10%
DC Armature Resistance	0.14	OHMS	+/- 15%
Armature Inductance	0.09	mH	+/- 15%
Armature temperature	155	DEG. C	MAX

Option1: Optical Encoder Option — Contact sales for pricing

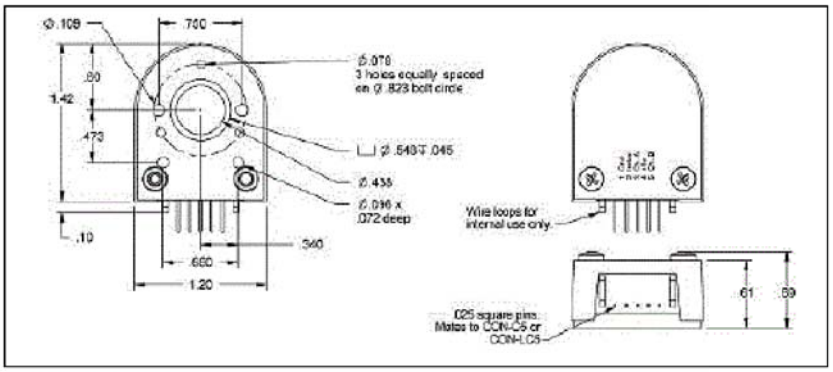

EU Series Interconnects/Functions		
Pin #:	Function:	Color:
1	Ground	Brown
2	Index	Violet
3	Channel A	Blue
4	+5 Volts	Orange
5	Channel B	Yellow

*Resolutions available from stock: 32 PPR, 100 PPR, 250 PPR, 500 PPR, 1024 PPR
(Use suffix "EU-xxx" after model # to designate resolution)
Encoder is mounted integrally to the back of the motor or brake.
Includes an index pulse, and 12" long flying leads.

Option 3: Integral Brake Option — Contact sales for pricing

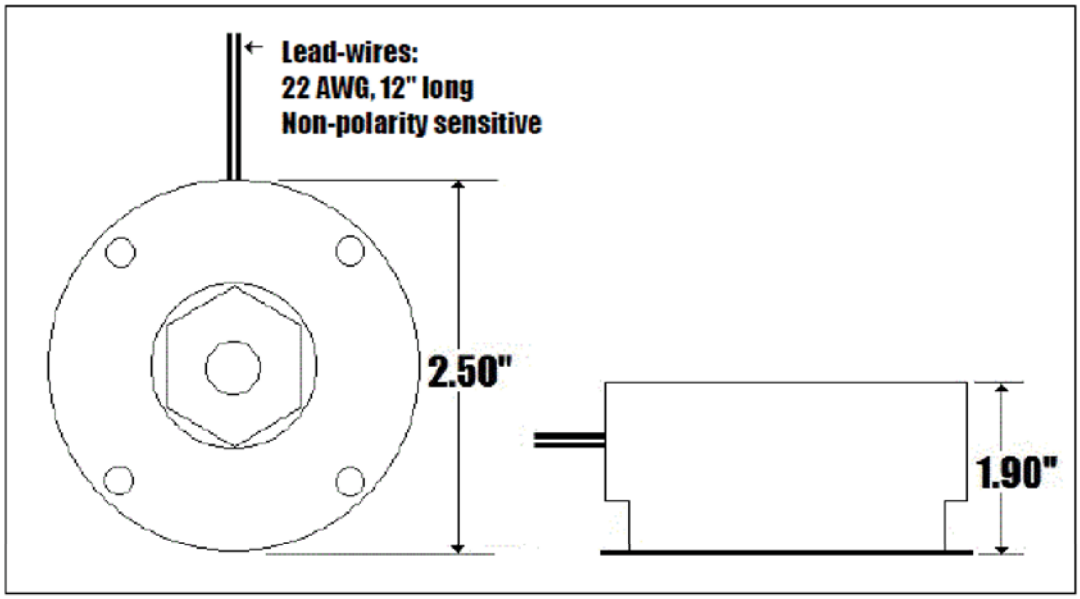

The MMP mid frame gearmotors and motors are sufficiently served by a 15 in-lb brake, when used correctly.
Typical (24v) brake current = 400 mA;
All brakes (12v, 24v, 36v, 48v &90v) are 9.6 Watt devices

7 Citations:

"Robotics/Types of Robots/Walkers." *Wikibooks*. N.p., 31 Aug. 2012. Web. 7 Dec. 2013. <http://en.wikibooks.org/wiki/Robotics/Types_of_Robots/Walkers>.

"History of Honda's Robot Development." *Honda Worldwide Site*. N.p., 2013. Web. 16 Oct. 2013. <http://world.honda.com/ASIMO/history/e1_e2_e3/index.html>.

Honda Belgian Branch. "Honda ASIMO Demonstration." *YouTube*. YouTube, 20 Feb. 2013. Web. 16 Oct. 2013. <http://www.youtube.com/watch?v=xt090WrKU3w>.

Ackerman, Evan. "Honda Robotics Unveils Next-Generation ASIMO Robot." *IEEE Spectrum*. N.p., 8 Nov. 2011. Web. 20 Oct. 2013. <http://spectrum.ieee.org/automaton/robotics/humanoids/honda-robotics-unveils-next-generation-asimo-robot>.

"Nao (robot)." *Wikipedia*. Wikimedia Foundation, 12 Dec. 2013. Web. 15 Dec. 2013. <http://en.wikipedia.org/wiki/Nao_(robot)>.

"Aldebaran Robotics NAO Specifications." *Aldebaran Community Website*. N.p., 2013. Web. 15 Dec. 2013. <https://community.aldebaran-robotics.com/nao>.

BotSportTV. "RoboCup 2013 Adult Size FINAL: TAIWAN / JAPAN." *YouTube*. YouTube, 01 July 2013. Web. 20 Oct. 2013. <http://www.youtube.com/watch?v=xqWELifR2P0>.

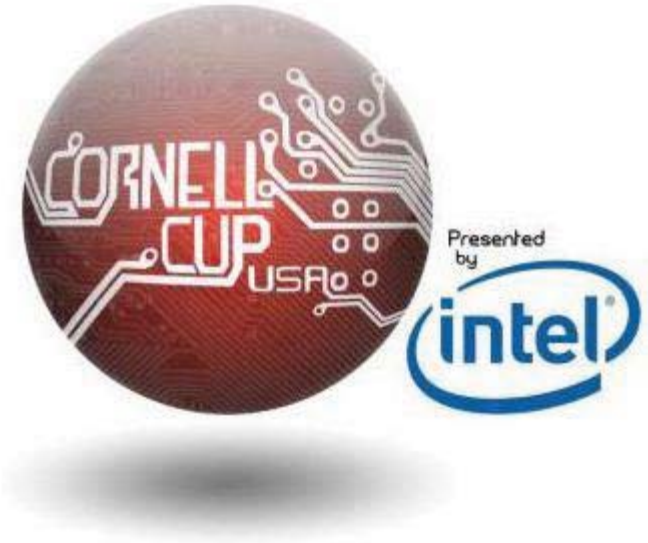

R2-I2

Made for students,
by students

Table of Contents

1 R2-I2 Head

1.1 Requirements

The list of requirements for R2-I2's head is a list of criterion on which the head can be judged after construction is completed. When completing decision matrices and making design decisions, the following list should be the primary focus.

Performance Specification	Weight
Rotational speed	2
Range of Motion	4
Space Inside the Head (for ECE team)	4
Torque	3
rotational acceleration	2
Rotational inertia	3
weight of the head	2
Feasibility of Manufacturing	5
Cost	1
Aesthetics (Shape, etc)	2
Repariability	3
Noise Level	1
Abiliity to Mount Sensors	4
Power Usage	4
Likelihood to Fail	4

Table 1: Performance Specifications for R2-I2 Head

Many of these requirements are for the purpose of choosing a motor. For instance, rotational speed, range of motion, torque, rotational acceleration and inertia, weight of head, and power usage are all factors that go into the motor spec'ing process. The electrical engineers need to mount various sensors in the head, such as a Kinect. For that reason, space inside the head and ability to mount sensors are important aspects of the head design. Then the next concern is construction and maintenance. The head needs to be relatively simple to make, and simple to repair in the case of a, hopefully rare, failure. Finally, the head needs to carry aesthetic value.

1.2 Astromech Forums

Building R2-I2 replicas is a very popular hobby among Star Wars enthusiasts. One builder decided to create a Yahoo group called *astromech builders* where all builders of star wars droids can discuss their plans, ask questions, and post pictures. This group has since expanded into a much larger community present on *astromech.net*. As will be discussed later, the solutions posted on the astromech forums were very important to us.

1.3 Design Areas

There are three main areas we concentrated on for coming up with design ideas. Firstly, there was the actual structure of the dome. R2's dome has an 18.25" base diameter and a maximum height of 11". Finding such a dome is a difficult ordeal. Our first option was a squirrel baffle, which bird enthusiasts use over their birdfeeders to prevent squirrels from falling onto the feeders from above and eating the seeds. Other options were to use a large mirrored dome traditionally placed around security cameras and a custom manufactured plastic dome (Figure 1).

Figure 1: Potential options for R2-I2 Dome

While all three of these options provided us with the proper 18.25 inch outer diameter, only a custom-made dome would have the proper height. In addition, the previous three solutions would be difficult to machine – cutting the proper slots and acquiring the right brushed aluminum effect would take us much longer than having it custom-made. Luckily, many of the members of the astromech forums are experienced machinists who provide specific, detailed parts. If a part is high in demand, the machinists will manufacture and ship them, a process referred to on the forum as a "part run". Cornell Cup USA decided to enter the part run for a lasercut fiberglass dome that is used on a vast majority of astromech builder's droids. With this product, although more expensive than the other options, we are able to capture the likeness or R2-D2's head almost exactly. This dome is also machined such that it interfaces well with specific bearings often used on other R2-D2 droids.[1] These were features that we believed paid off over attempting to make the dome ourselves.

Figure 2: Astromech Dome

[1] Photo credit: http://astromech.net/forums/attachment.php?attachmentid=5897&d=1316146915

The dome from the astromech community is designed to work with the Rockler bearing[2]. This bearing has a flat section on the inner diameter that is traditionally used for the drive system, has a radius close to that of R2, and has mounting holes that interface directly with the dome that we bought.

The third and final area of research was the drive system. For our drive system research we focused on manufacturability and noise. One of our performance criteria for the head is that it is able to rotate 360° to either side and be able to allow various electrical cords to run from the head to the powerboard in the chassis without tangling. Three main methods of driving R2's head were found during research. The first involved a large gear around the diameter of R2 that would be driven by a vertically mounted motor in the chassis with a small gear on its axle. While this option would provide us with precise positioning, the large gear was made through a difficult CNC process and was not feasible.

The second drive option involved a motor mounted in the center of R2 and a center supporting shaft that is used to rotate the head. This method eliminates the need for a supporting bearing because the head is supported by the center shaft. However, the person who used this method did so because he had a spare toy motor with axle from his child that he wanted to use, and not really because it was a good method. Cords wrapping around the center shaft would be an issue, and the purchased dome may have stress issues when being supported by a single center point.

Another possible method of turning the head involved a rubber wheel directly in contact with the Rockler Bearing. While similar to the gear method, the wheel method is much simpler to implement. However it does have tradeoffs – since the drive of the head is controlled by the friction between the bearing and the rubber wheel, there is possibility of slipping, and so accurate positioning of the head may be difficult. To alleviate this, a method of sensing the position of the head would need to be implemented.

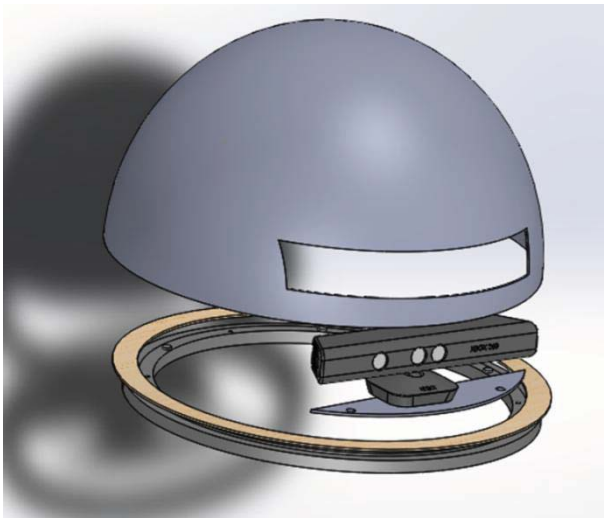

Figure 1: R2-D2 head concept

[2] http://www.rockler.com/lazy-susan-heavy-duty-swivel

1.4 Motor Drive and Mount Selection

As previously outlined, the critical component of the head is the ability to quickly and accurately position the sensors contained within the dome. The dome is also required to have continuous rotational freedom of movement to allow for responsive sensor positioning and tracking. There cannot be a limitation on the range of motion which would prevent the head from rotating further in one direction causing it to "unwind" in the opposite direction of rotation to meet the positioning needs. From research of previously attempted design methods and independent assessment of design possibilities, the sub team concluded that three main motor drive systems would reasonably meet the requirements: Center Drive Shaft, Gear Drive and Rubber Wheel Drive. With speed, accuracy and sensor mounting as the main factors, the sub team assessed the suitability of each of these three options.

The rubber wheel drive was selected as the design which gave the best combination of these attributes. However, the design still held a possibility of slipping, so the next step in the design process was researching ways to mitigate the slipping problem. The two main methods which emerged were the use of a belt tensioner, such as the ones used in automobiles, and a spring tension assembly. The spring tensioner design was utilized in lieu of the belt tensioner primarily on the basis of space available between the chassis and outer casing of the R2 torso. Thus, further design efforts were spent mitigating the slippage concerns from the rubber wheel selection.

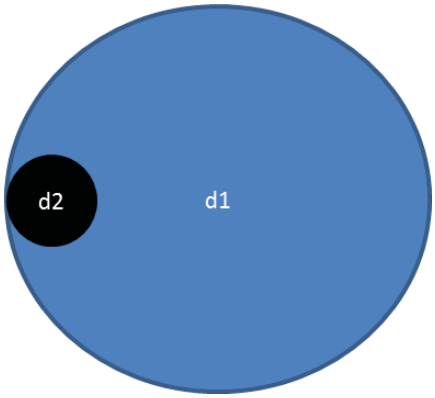

D1 = Inner diameter of Head
D2 = diameter of wheel turning inner diameter of head
Ratio of D1/D2 = 8.5

1.5 Motor Mount Design Calculations

The motor drive mount design was based on the following criteria, minimizing wheel to dome slippage and meeting rotational kinematics requirements. One of the primary weaknesses that had to be overcome with the rubber wheel method was the development of a mechanism to ensure that there

was sufficient force applied to keep the wheel firmly in contact with the dome to ensure that there is no slippage as the motor drives the dome around the Rockler bearing. Based on the torque estimates derived for the motor selection process, it is possible to approximate the applied force required to ensure positive contact between the rim and the 2-inch rubber wheel. (Note: the coefficient of friction is a low estimate derived from the coefficient of friction of rubber in contact with other similar materials)

Torque	Due to Accel (Nm)	Sub-total (Nm)	Total (Nm)
Head	0.68	0.7	**0.9**
Sensor	0.19	0.2	
Power (W)	**2.7**		
	Power (W)	Torque (Nm)	Speed (rpm)
Operating Point	2.7	0.9	30
Operating Point w/ Ratio	2.7	0.1	255

Table 2: R2-D2 Head operating point calculation

Torque	0.1	Nm
Contact Force	2.0	N
Coefficient of Friction	0.4	
Tension Required	5.0	N
Tension Required	1.1	Lbf

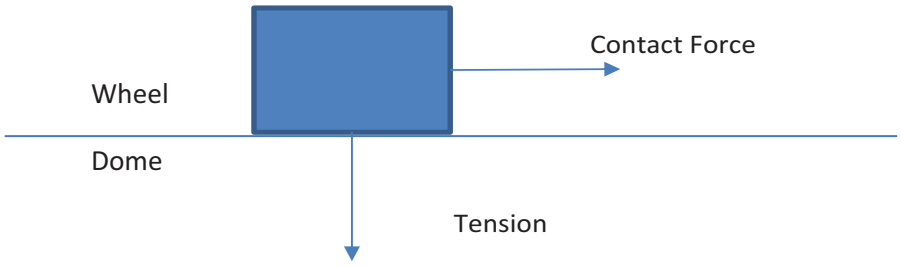

Figure 2: Wheel/Dome contact area FBD

Thus, when the motor is mounted, approximately 5.0 N or 1.1 lbf are required to prevent slipping. A safety margin of 1.5 was applied to mitigate the effects of the coefficient of friction approximation as well as any rotational resistance resulting from friction in the Rockler bearing assembly. Thus, the required force necessary to mitigate slipping between the wheel and the dome is 7.5N or 1.7 lbf.

1.6 Assembly Design

Original design iterations looked directly attaching the motor mount to the outer shell of the R2-I2 torso casing. However, since our design had a much stronger aluminum frame, it proved to be a more stable and robust mounting location. This also relieved any possible concerns of mounting to a curved inner surface. However, this causes a slightly greater displacement between the mounting bracket and the edge of the R2 dome. In order to make contact but without making the mount assembly too long, a less efficient third order lever system is used with the spring acting on the bracket between the motor and the hinge. This will require a slightly larger spring force of 1.4x greater to generate the required force to mitigate friction. The assembly, pictured in Figure 4, requires a spring force of approximately 11.5N or 2.6 lbf.

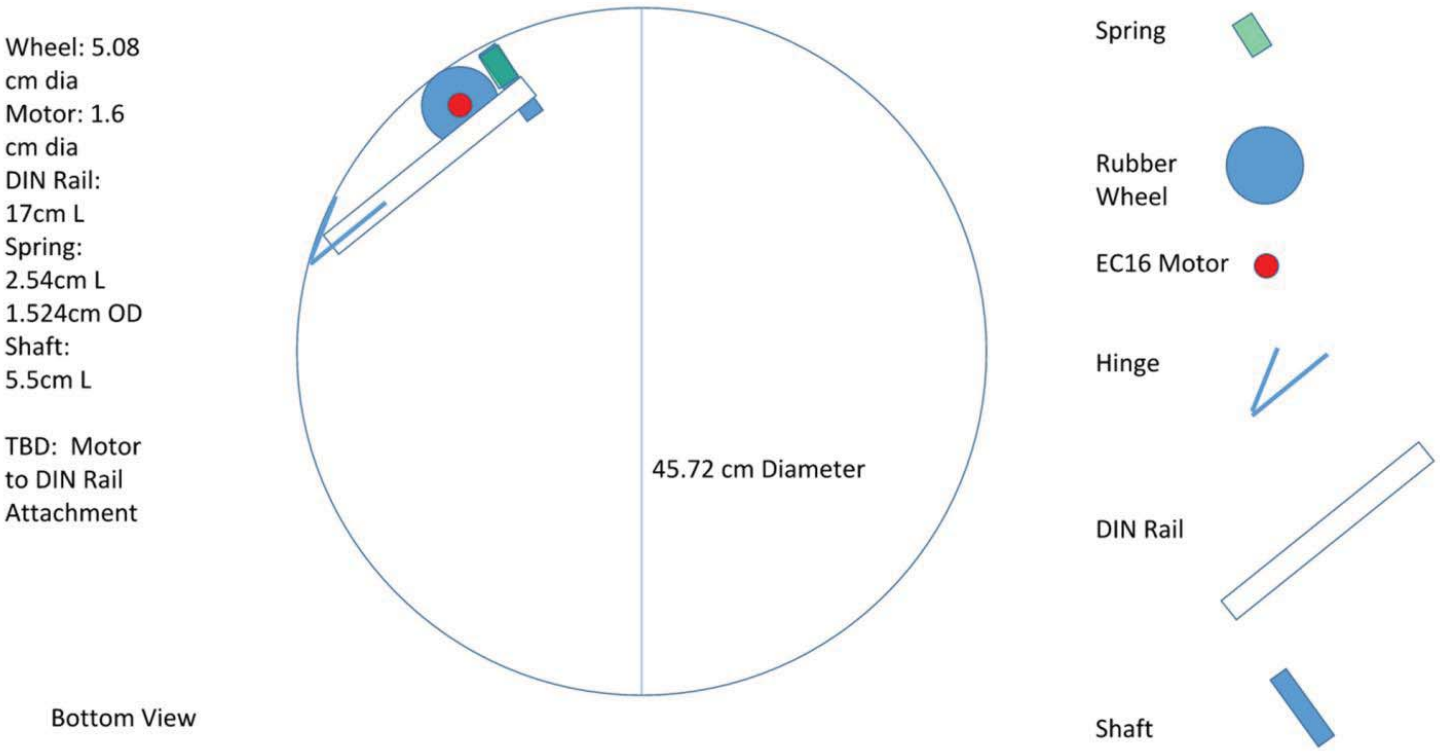

Figure 3: Motor mounting schematic

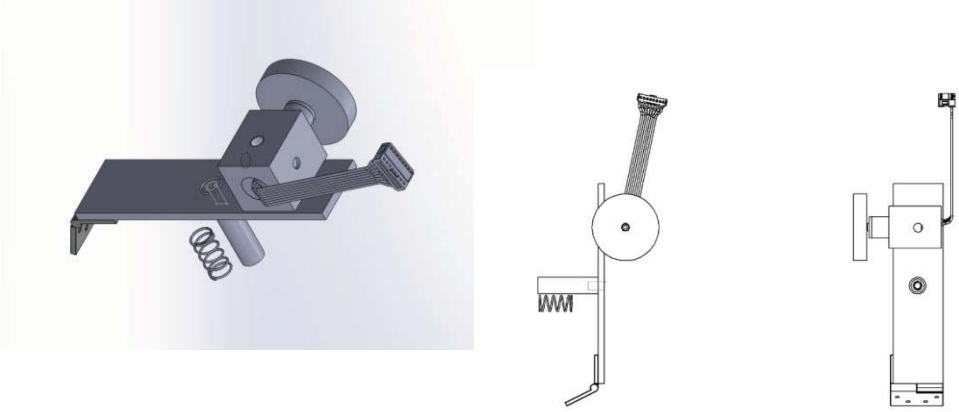

Figure 4: Head Motor Mount detailed CAD and detailed schematic

The motor is a Maxon EC16 motor type which is mounted within an aluminum block. The motor is fixed into place utilizing set screws. There is some concern about motor slippage with this arrangement. Initial designs however will retain the set screws to ensure reparability and ease of motor replacement as required. If the set screws do not provide enough force to retain the motor in place under load, then adhesives will be used and the whole block assembly will require replacement in order to replace the EC16.

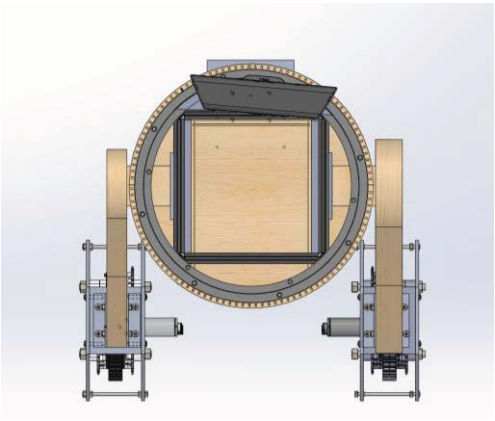

Figure 5: Location of motor mount

The motor mount assembly will be seated in the rear portion of the R2 chassis in order to stay clear of any wiring harnesses that will be rotating in the center of the chassis assembly to ensure that the head assembly has full continuous rotational capability.

1.7 Changes in Head Design

1.7.1 R2's head turning

The final proposed design used a hinge with a spring to keep constant pressure between the turn wheel and the bearing. This caused some problems, the biggest of which was the play in the hinge. This caused the wheel to not be straight but rather angled on the bearing so that when the wheel turned it had a tendency to drive up or down on the surface of the bearing depending on the direction of the spin as shown in Figure 6. This caused the wheel to slip completely off of the bearing after a few revolutions and also produced unnecessary stress on the whole assembly.

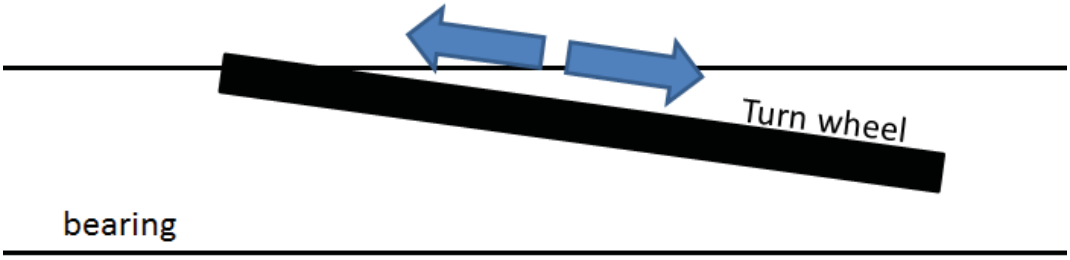

Figure 6: Turn Wheel Misalignment

The solution to this problem was the removal of the hinge and spring. Instead we machined a simple bracket for the motor. This removed the effects of the play in the hinge and kept the turn wheel aligned with the bearing. The benefits of the spring were also removed but the effects were minimal. The wheel would slip during high speed rotations but was not an issue for normal use. Figure 7 shows the actual turn wheel with no misalignment.

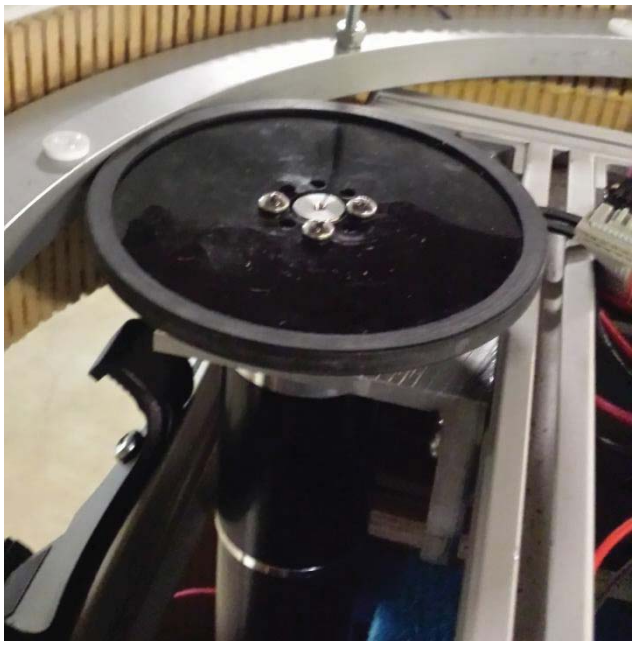

Figure 7: Actual Head Motor Mount

The overall head design was also expanded to include mounting platforms for both the bearing itself and for the Kinect. The thickness of R2's chassis was reduced so the original mounting method needed to be changed. The implemented design bolted the bearing onto 3 short sections of T-bar coming off of the top of the structural frame. This is shown in Figure 8. A section of acrylic plastic was cut to provide a stiff platform for the Kinect.

Figure 8: Bearing Mount

1.7.2 Head Flap

In order for the Kinect to be used, we cut a section of R2's head out to act as a window. To preserve the aesthetics of R2, the section was saved and mounted to the head as a flap that can open and close. Figure 9 shows the full flap assembly. As shown, a curved section of aluminum was glued to the cut out section of the dome. The curved arm was then attached to the servo powering the assembly. The whole assembly rotates around the servo's rotation point causing the flap to seem to move both out from the rest of the dome surface and up to clear the opening.

Figure 9: Head Flap Assembly

1.8 Future Considerations

1.8.1 Vibration/Stability Concerns

As the assembly undergoes construction and testing, there are some potential concerns with the current design selection. First, the center mounted shaft and spring assembly was chosen to make the overall design more compact. However, there may be some potential for vibration due to the

motor rotation at the end of a relatively long lever arm. If that is the case, a secondary guide rail can be affixed near the motor mounting block to minimize movement of the assembly. The second area of concern will remain slippage due to the fact that the friction and torque calculations are all based upon estimates with a conservative safety margin applied. This can be overcome by upgrading to stronger springs or adding a second spring to the guide rail portion.

1.8.2 Positional Accuracy

In addition to being responsive to inputs, the R2 head also needs to be accurate in its alignment to ensure proper positioning of head mounted sensors. The proposed plan to track the rotation for feedback to the motor controller is to use a simple optical sensor and a strip of black and white markings across the inner portion of the dome. This encoder measures the number of blocks that pass through over a given time and can convert that to precise angular control. As the dome spins, angular movement can be tracked by the optical sensor and be used in a feedback control loop. With proper calibration and minimal slippage between the dome and the wheel, this should provide precise control for sensor positioning.

2 R2-D2 Locomotion

2.1 Goals and Use Cases

The first step in designing R2-I2 was developing preliminary goals and design objectives. These are broad design objectives that outline the major goals of the robot. During a group brainstorm, we came up with the following goals for R2:

- R2 comes when called
- R2 moves around
- R2 has active obstacle avoidance
- R2 can act as a tool storage system
- R2 can move his head around
- R2 utilizes a tablet

Using these goals, we established an overall challenge definition: Design and develop a wheeled robot which implements tool storage, voice commands, and localization and involve the use of a tablet. Narrowing this down to a mechanical engineering specific challenge, we re-defined the challenge: Design and develop a wheeled robot which has localization capability and can store tools.

2.1.1 Use Cases

Use cases are potential ways a user can interact with the robot in either a normal function or a misuse of the robot. The following is a list of potential use cases we developed for R2.

Use Cases	Misuses
User picks up and moves R2	User blocks R2's way

User takes tools out of R2	User jams drawer
User puts tools in R2	User puts too much weight in drawar
User tries to turn off R2	User jams finger in R2 drawer
User charges R2	User spills water on R2
User interacts with tablet interface	User manually turns the head
User assembles/disassembles R2	User pushes R2 over
User addresses R2	Operator drives R2 into obstacle
User calls R2 (general)	
User calls R2 from behind	
User asks R2 to dance	
User tracks what's in tool storage	
User wants to find R2	
Operator drives R2: • **Straight line** • **Turn** • **Backwards**	

Table 3: R2-D2 Use Cases

2.2 Performance Criteria

Performance criteria are measures such as weight and cost which are defined for the project, and are the criteria that the design is judged on. They are given corresponding weights which are used in decision matrices to determine the optimal design. The locomotion subteam brainstormed and developed the performance criteria and weights, and then consulted the rest of the MechE team for review of the criteria and confirmation of weight values. The performance criteria and corresponding weights for the locomotion system are as follows.

Criteria	Weight
Speed	3
Turn Radius	4
Stability	2
Acceleration	2
Ability to change direction	4
Braking	3
Cost	1
Feasibility of Manufacturing	5
Reparability	3
Noise Level	1
Power Usage	4
Likelihood to fail	4

Table 4: Locomotion performance criteria

2.3 Preliminary Size and Speed Estimates

The entire MechE subteam held a group wide brainstorming session to develop preliminary estimates for R2-I2's size, including dimensions and weight, as well as speed and acceleration estimates. Some

quick internet research provided the actual height and diameter of R2-D2 from the movies. We want to be as close to real scale as possible, so we specified these dimensions as the size to base our designs around. Similar research provided the weights of other R2-D2 replica bots that hobbyists have created. Depending on materials used, the robot can weigh anywhere from 50-150 pounds. Our robot will also be utilized as a mobile toolbox, so we conservatively estimated an extra 50 pounds for tools.

R2-I2's max speed is estimated to be about 4.4 ft/s or 1.34 m/s, approximately human walking speed. In determining acceleration, a good rule of thumb for estimating the acceleration of an agile robot is to use two times the velocity. Thus, the acceleration was estimated at about 9 ft/s^2. An initial sketch with the developed dimensions is included below.

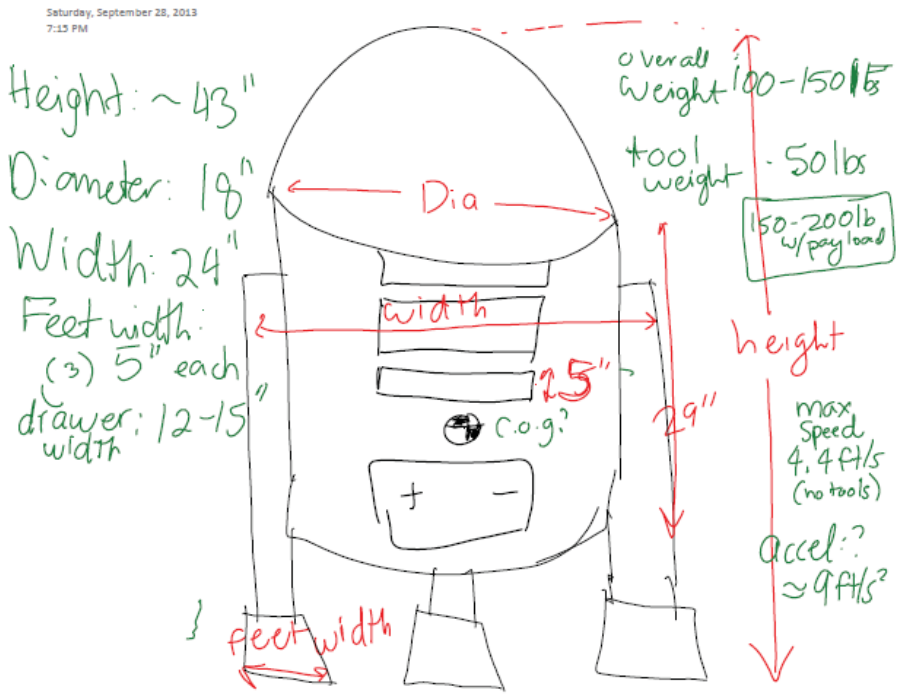

Figure 10: Initial size and speed estimates

2.4 Research

2.4.1 Three-wheeled ModBot

Previous work was completed on developing a possible three-wheeled ModBot. Due to the similarity in locomotion design, the documentation was consulted to check for notes and information that could be useful in designing R2's locomotion system. The following info was noted as being of possible use:

- Ball transfer worth looking into. "Traditional casters, when worn, often get stuck when a transverse load is applied and do not perform well under all conditions. The ball transfer allows the front end of the ModBot to change direction quickly and accurately without providing a great deal of resistance."

- A rubber treaded wheel will be most able to provide the traction required for a two wheel drive system
- The recommended wheel was the Dubro Treaded Lite Airplane Wheel with 5 inch diameter and 5mm axle diameter
- Keeping the robot level is very important for the vision system.

2.4.2 Previous Solutions

Many Star Wars enthusiasts have created their own R2-D2 replicas, so there are many previous design solutions to research. Specifically, the locomotion systems of hobbyist robots were observed. We learned that there were many methods and almost every hobbyist designed their locomotion system differently. The solutions range from single wheel, to two wheels, to chain driven systems, to direct drive systems. A few of the designs that inspired our drivetrain design are shown below in Figure 9 and 10.

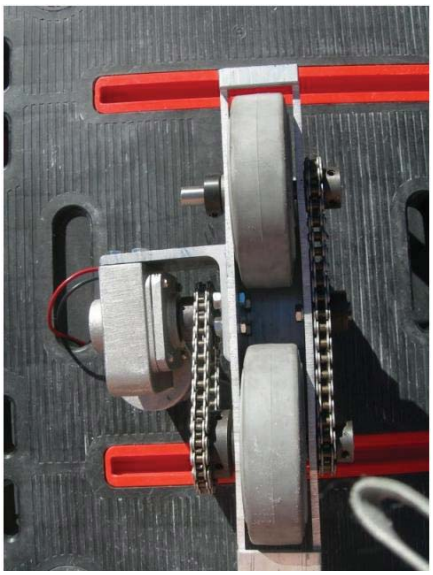

Figure 11: Researched locomotion design #1

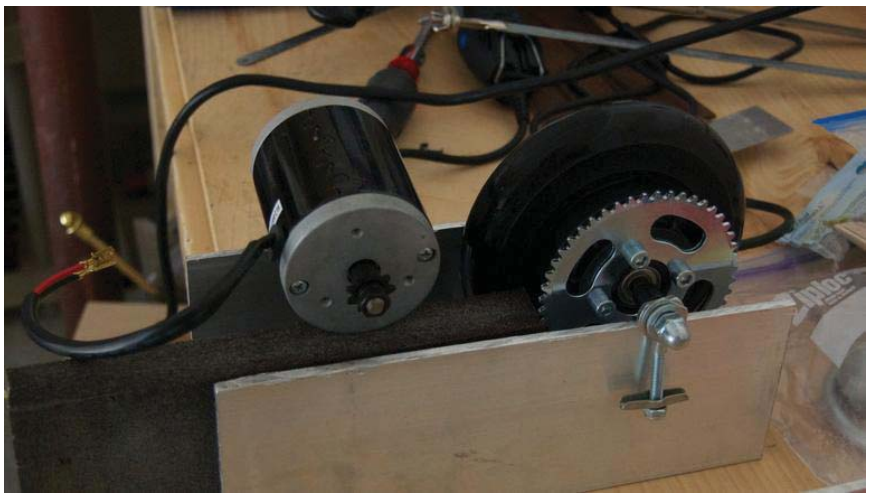

Figure 12: researched locomotion design #2

2.5 Preliminary designs

2.5.1 Sketches

Every sub-team member created sketches of possible designs for the locomotion system, exploring every possible option. No idea is a bad idea and just because other solutions already exist does not mean they are the most efficient or effective solutions. Some of the sketched designs are imaged below.

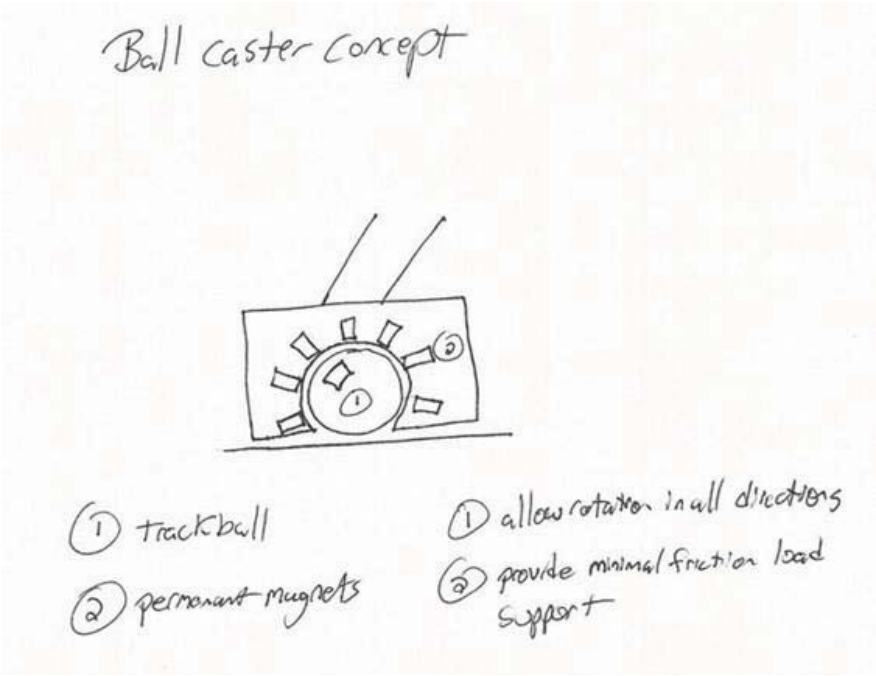

Figure 13: Locomotion Brainstorm Concept - Ball Caster

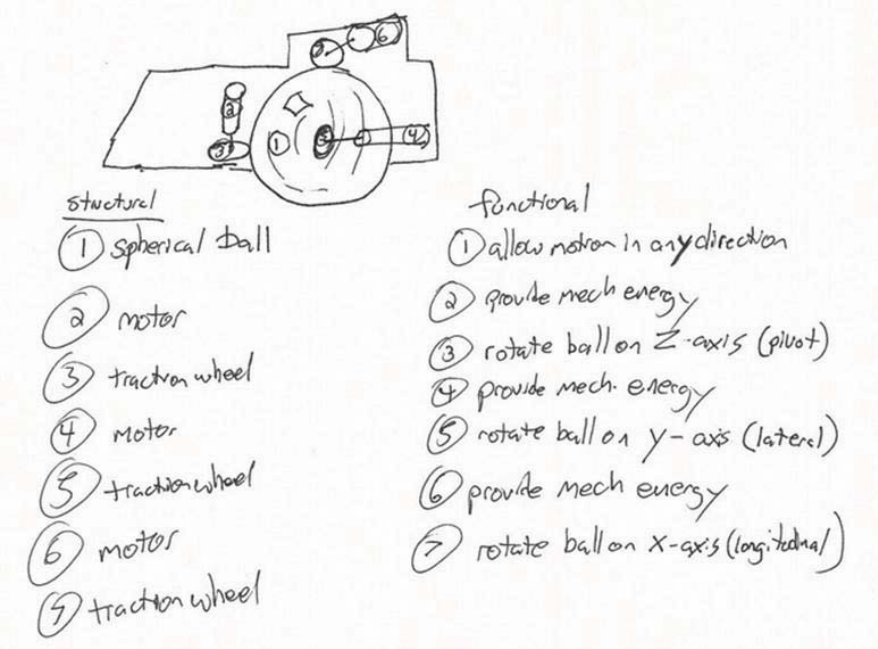

Figure 14: Locomotion Brainstorm Concept - Ball Caster (ctd.)

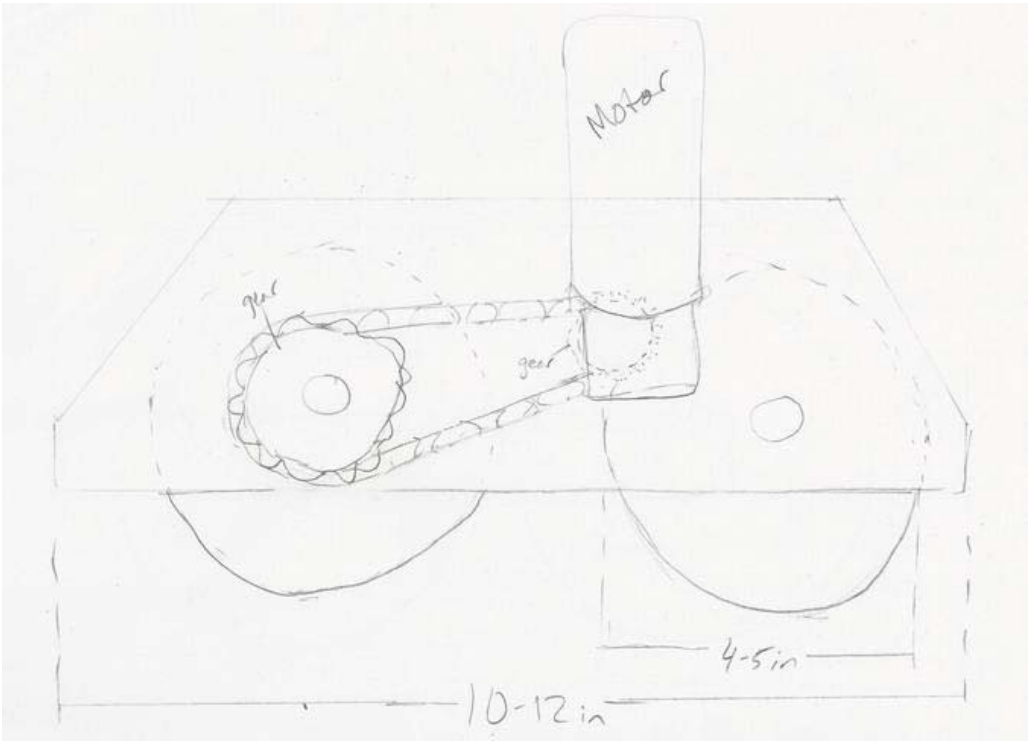

Figure 15: Locomotion Brainstorm Concept – Belt System

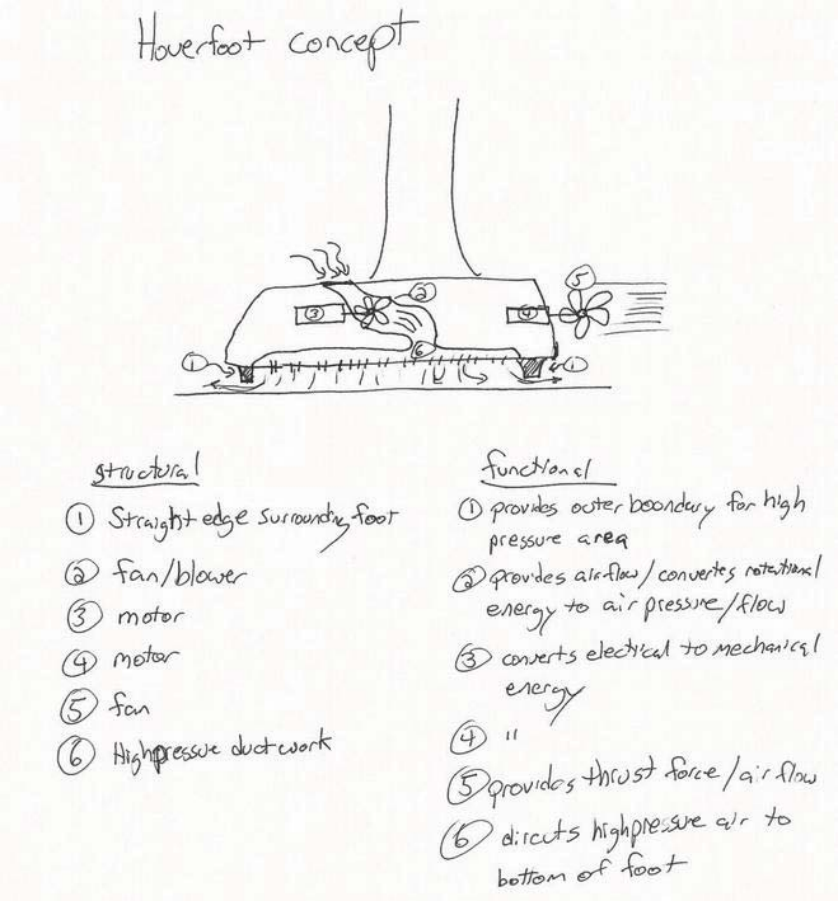

Figure 16: Locomotion Brainstorm Concept - Hoverfoot

2.5.2 Choosing a design

When choosing a design, a decision matrix is generally the best method for narrowing down concepts based on performance criteria. As a group, each design should be evaluated against each specific performance criteria; where each comparison is given a numerical value on a scale consistent with every other comparison. The weights are then multiplied by the numerical value for each comparison, and then summed to get a numerical rating for each design. This method is not extremely definitive in determining the optimal design, depending on the judgment on weights and the ratings of each design to the criteria. It is, however, a good method for narrowing down the designs to a few options which likely best meet the performance criteria. Below is the decision matrix completed for the locomotion designs proposed by the group. The three options that were decided to be worthwhile to pursue were: a motor with one wheel, a motor with two wheels, or the use of mecanum wheels. After a group discussion, it was decided that mecanum wheels were unnecessary for the needs of the robot and likely unfeasible due to the required orientation of mecanum wheels. It was then decided that 2 wheels would provide better traction and stability than a single wheel per foot and that following designs would use two wheels as the underlying basic concept. The center foot would, like the 3 wheeled ModBot, have a ball transfer, or grid of ball transfers.

All design options involved the concept that R2-I2's legs would be tilted as opposed to vertical as he sometimes appears in the movies. This was a unanimous decision by the group, with the idea that a slanted design will greatly improve stability, an important performance criteria. Slanted legs lower the center of mass and also increase the tilting moment that the robot can resist.

Criteria	Weights	Motor, one normal wheel, chain reduction	Hoverfoot	Mouse/ Trackball	Tank track	Magnetic ball caster	Motor with 2 normal wheels, chain reduction	Mecanum wheels	Motor with belt/chain through legs	Motor at feet
Speed	**3**	5	2	3	3	4	5	5	x	x
Turn Radius	**4**	4	2	5	3	5	3	5	x	x
Stability	**2**	4	1	3	5	3	5	4	x	x
Acceleration (multiple directions)	**2**	4	2	3	3	5	4	3	x	x
Ability to change direction	**4**	5	2	5	3	5	4	5	x	x
Braking	**3**	4	1	2	3	5	4	2	1	2
Cost (High # = low cost)	**1**	4	1	2	2	1	4	2	x	x
Feasibility of Manufacturing	**5**	5	2	2	3	1	5	5	1	2
Reparability	**3**	4	4	2	3	2	4	5	x	x
Noise Level	**1**	2	2	2	2	5	2	2	x	x
Power Usage (higher is better)	**4**	3	2	3	2	2	3	3	x	x
Likelihood to fail (low is likely to fail)	**4**	5	1	2	4	2	5	4	1	2
Total		154	68	107	110	116	148	147	12	24

Table 5: Decision Matrix for Locomotion Mechanism

2.6 Modeling

2.6.1 Basic CAD design

A very preliminary CAD model was created to convey the proposed design to the entire team for feedback. It resembles the final design, but varies extensively and lacks many details.

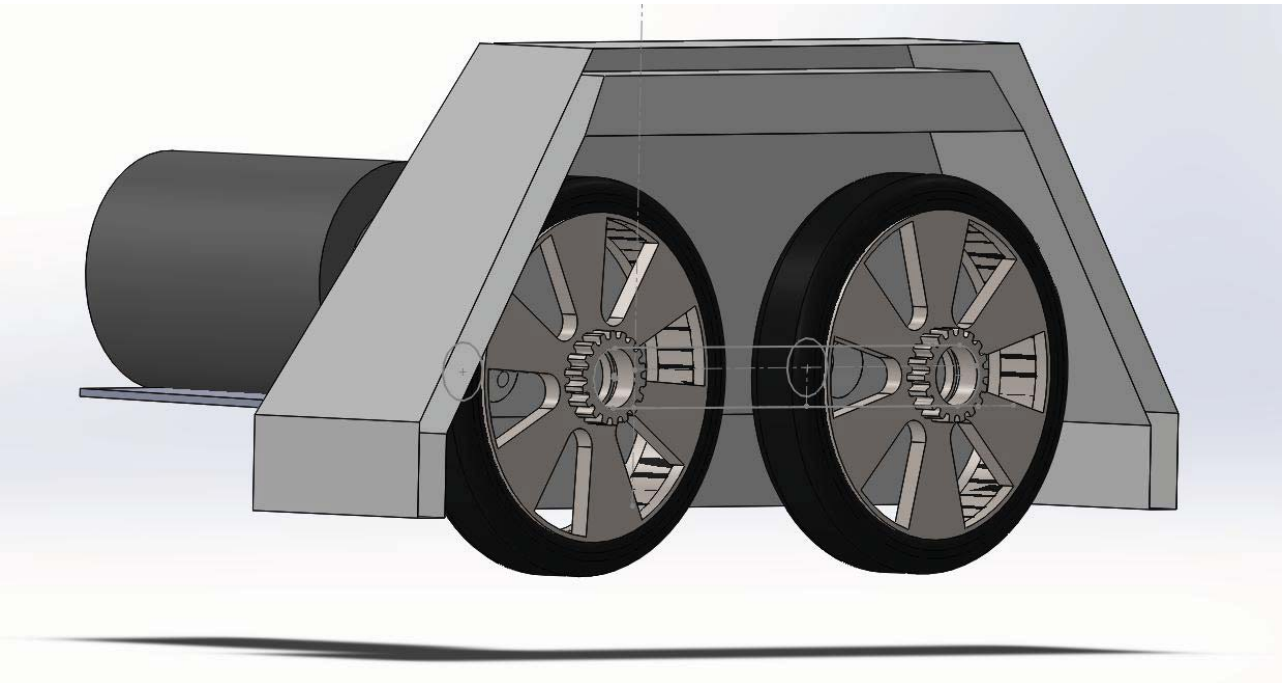

Figure 17: Basic CAD Design

2.6.2 Design Iteration

Iteration is a very important part of design. SolidWorks allows for easy design iteration, because simple changes can be quickly drawn up and displayed to the group to successfully convey proposed ideas and solutions to problems with previous models. The CAD model for R2-I2 was edited many times as new problems with the design were realized and better solutions become apparent. The final design was the result of over 20 iterations.

2.7 Wheel Selection

2.7.1 Goals

Wheel selection was performed through the design of the locomotion mechanisms. Because wheels are an integral portion of the overall stability and function of R2-I2 it was important that all aspects of the wheels were considered before choosing the right one. Our goal was to select a wheel that was inexpensive, easily installed, easily integrated in the system, and durable. While the design of

R2-I2's legs has been calculated to provide maximum stability for the structure, the wheel selection plays a large role in the efficiency of the system.

While the wheels of R2-I2 are an important part the system, a lot of resources and tools are available to guide a user in determining the needs of their project and suggesting options. In our case, we simply needed a standard wheel used for large loads and could be dependent on stability and traction. Our intention was to not spend a significant amount of time on selecting wheels, as there were not many technical difficulties associated with it.

2.7.2 Performance Criteria and Mechanism Requirement

Wheel selection began with no preexisting idea on what to look for. The goal was simply to find a solution for a wheel. While researching wheels multiple Performance Criteria became apparent for this system.

- **Feasibility** was our top priority when considering each option of wheel. Feasibility pertained to the mounting and drive needed for each of the wheels. All the wheels considered were relatively similar in fact. All wheels were made of either rubber or polyurethane as these two materials are most widely used for high traction high load wheels. Feasibility of a wheel was dependent on much extra attention and experience was required to implement the wheel. Some of the wheels required machining on our part which was understood as something to avoid,
- **Cost** was another criteria that was important to the decision. While it was absolutely not a determining factor, it played a role in choosing between two wheels of similar characteristics. Because wheels are very standard parts, it was not difficult to find two exact wheels for very different prices.
- **High traction** was another important factor in deciding wheels. Most of the wheels we decided on had a round or flat edge, which is standard for the average caster wheel. Conventionally, higher surface area is indicative of higher traction so wheels with treads were looked into as well.
- **Size** was somewhat a variable criterion for the system, as any range between 3-6 inch diameter wheels would not change the stability or power provided to the system. Simple changes in how the mounting would be implemented and size of foot would change but no catastrophic event would occur if the wheel were not exactly 5'.
- **Ease of integration** became an important topic. Methods of mounting the wheels became an issue, as a final decision about how the wheels would be powered would change the needs of the mounting. There were 2 choices, to provide a direct drive to the axis of the wheel or to the wheel through belt drive. It was decided finally to have the wheels be chain driven with the motor above the two wheels. In the event that a mount or wheel broke, it was important that these parts could be easily replaced so development would not be dependent on a standard part.

2.7.3 Preliminary Design

2.7.3.1 Decision Matrix- Wheel Selection

There were two options to have the wheels be belt driven. First, was the option of buying wheels and sprockets separately, and then attaching them in the lab. The problem arose when mounting came into question, as it was difficult to ensure that the wheels would stay in the same place. This issue pertained to the other option of buying wheels that were manufactured with sprockets already attached. It was assumed that these wheels would be more expensive as they are used for more specific uses. However, a search of wheels with sprockets was relatively easy to find through hobbyist and BattleBot forums.

Table 6 is the decision matrix for the top 5 choices for wheels.

Criteria	Weights	 Grey Hub GD500CT600-1-112	 BattleKits robot Wheels-High traction	 BattleKits robot Wheels- Hard plastic	 Vex robotics-Versa Wheel	 Global Industrial
Feasibility	5	2	4	4	5	2
Cost	1	2	2	3	5	2
Traction	4	2	3	3	5	3
Size	2	3	4	4	4	3
Manufacturability	3	1	5	5	4	2
Mounting	3	1	4	4	5	3
Totals		32	69	70	106	57

Table 6: Decision Matrix for top 5 Wheel Choices

It was the intention to buy the most inexpensive and most feasible parts. It was initially believed that purchasing separate wheel and sprockets would provide us with these parts. However, after perusing many robotics forums and hobbyists sites, the Vex Versa wheels stood out as the top contender. It featured the highest traction ability, with a custom "W" tread to maximize tread (coefficient of friction is 1.2), rating of 200 pounds, and best of all the implementation was the most simple out of all the options. Vex robotics makes custom wheels with built in mountings for sprockets. On top of that, Vex robotics sells mounts especially for the wheels. The two major issues outlined earlier were solved using just one part. No extra machining will be required, and implementation will be relatively easily. Another major factor in choosing this wheel was price, as it was nearly ¼ of the price as any other option.

The size of the wheel was determined from prior research of durable wheels that could support a large amount of weight. Last year, the Cornell Cup project team worked towards two robots, one of which is the DuneBot. The robot required very complex however, first gen and second gen version of the robots went through many forms of wheels as the development process proceeded. From old documentation it was determined that a 5' diameter wheel size was a standard for mid-size robots and could support the weight associated with robots of a large weight (up to 800 pounds).

2.7.4 ANSI Chain

The use of the VexPro system restricted us to use ANSI standard chain. The system we are using supports either #25 or #35 ANSI chain, depending on the selected sprockets. The calculated tension in the chain is about 60 N or 14 lbs. The max load for #25 and #35 chains are 114 lbs and 269 lbs respectively, so either provides a very large factor of safety. Ultimately, the #35 chain was chosen. It is cheaper than the #25, likely because it is more common. Bike chain is usually #40 and is something we are familiar with. A size and strength close to this should be suitable for the needs of R2-I2.

Figure 18: VEXpro VersaWheel

2.8 Legs and shoulders

2.8.1 Cutting

Each leg was cut from 2x6 wood boards. The necessary tools needed to correctly size and cut the legs were: a miter saw, table saw, band saw, and router. The process is outlined below.

1. First, on the miter saw, the boards were cut to size and the angled cuts were made at the bottom of the leg. The miter saw is the best tool for these cuts rather than a jigsaw or band saw, as it allows for straight edge cuts at precise angles.
2. Next, the narrow section of the leg was split on the table saw, and cut using the ¾" angle on the band saw. The wider, upper section of the leg is already at 5.5", the stock dimension for 2"x6" boards. Using a compass, a 2.25" radius semicircle was marked at the top of the leg to obtain a circular edge, ensuring the top of the circle corresponded to the length of the leg. This cut was then made on the band saw, leaving about a 1/16" of material which would be sanded down later.
3. The ¾"x3"x3" square indent in the leg, meant for strengthening the interface between the leg and shoulder, is the trickiest cut on the leg.
    a. First, a template was cut on the miter saw out of scrap plywood. This template was a square with a square cut out of the center (see Figure 20). The square cutout was the length of the desired square (3") plus the distance from the edge of the router bit to the edge of the router, a value which will change depending on the router and router bit used. This distance is visually defined in Figure 19.
    b. The template was then centered at the center of the 2.25" radius circle cut earlier.
    c. The edges of the jig were set parallel to the bottom edge of the leg, and the jig was clamped to ensure the shoulder would be parallel to the ground, and thus R2 would be perfectly vertical.
    d. After setting the depth of router to ¾", the groove was bored out.
4. The entire leg was then sanded using an orbital hand sander, making sure to sand the circular top to size and round all edges.
5. Finally, the holes for mounting the leg to the L-brackets on the feet can be drilled using a ¼" drill bit on the drill press.

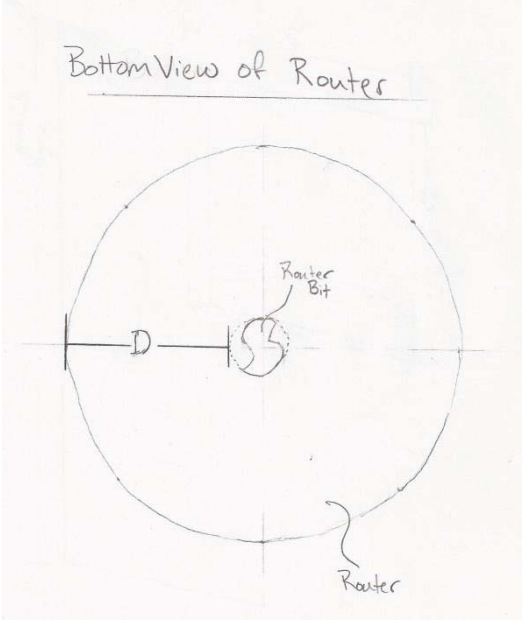

Figure 19: Bottom view of router defining distance D

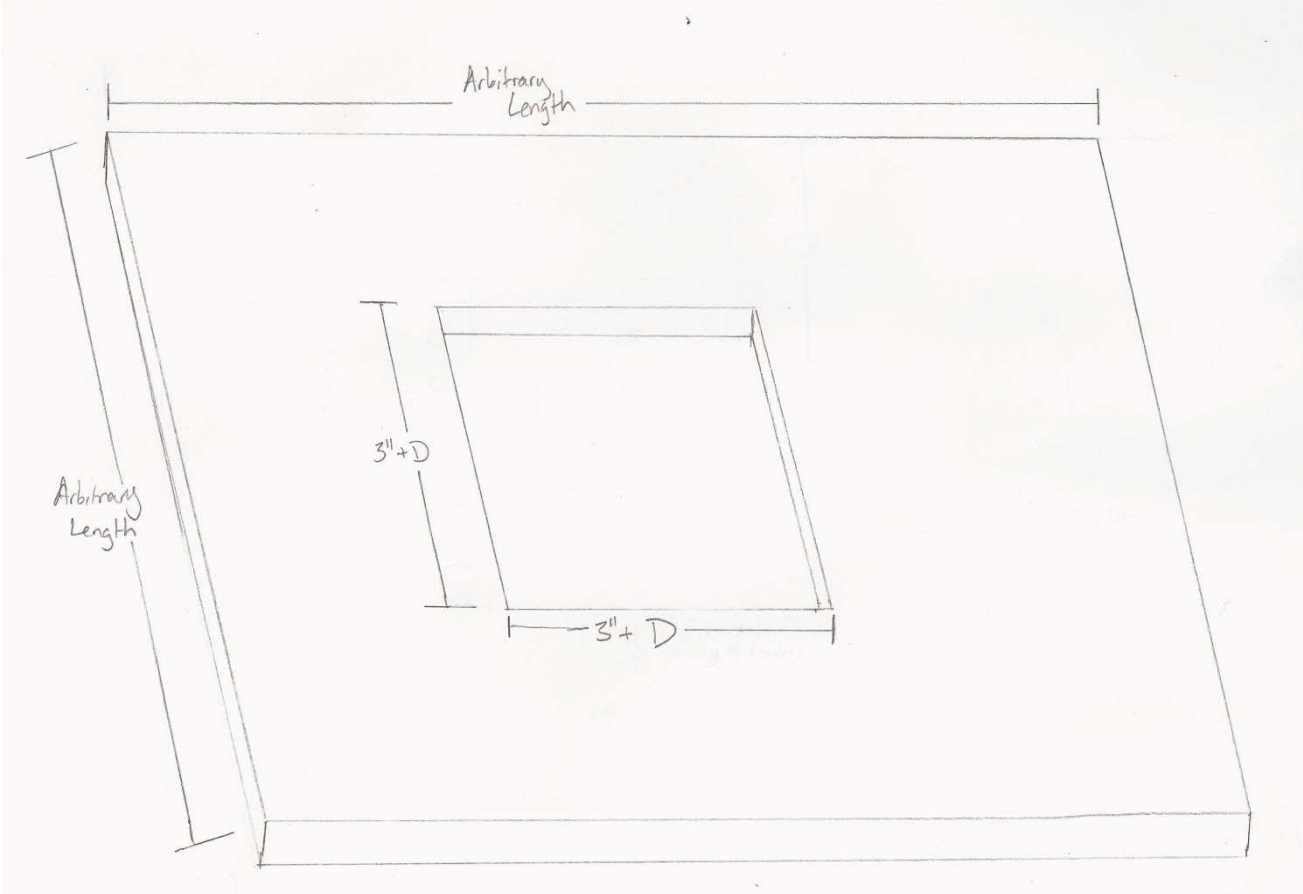

Figure 20: Sketch of recess router jig

6. The center leg was cut from a 2”x6” board.
    a. It was split to 4” wide on the table saw.
    b. It was then cut to length and the angles were cut on the miter saw.
    c. The holes for mounting the leg to the L-brackets on the center foot was drilled using a ¼” drill bit on the drill press in the same fashion as the side legs.
7. The shoulders themselves were cut in two pieces identical pieces. A 2”x4” was split to 3” and cut to 4” length. Four of these were cut to have two for each leg.

2.8.2 Assembly

The two shoulder pieces were first glued together and screwed together with wood glue and 2” wood screws. The holes for the screws were countersunk about ½” and then the holes were filled with wood plugs to conceal the screws. The result is a 3”x3”x4” shoulder piece (see Figure 21).

Next the shoulders were installed into the ¾” groove in the main leg. It was fastened with wood glue and 2” wood glue. The holes were countersunk and plugged in the same fashion as the shoulders. The plugs were then sanded down to be flush with the surface of the leg.

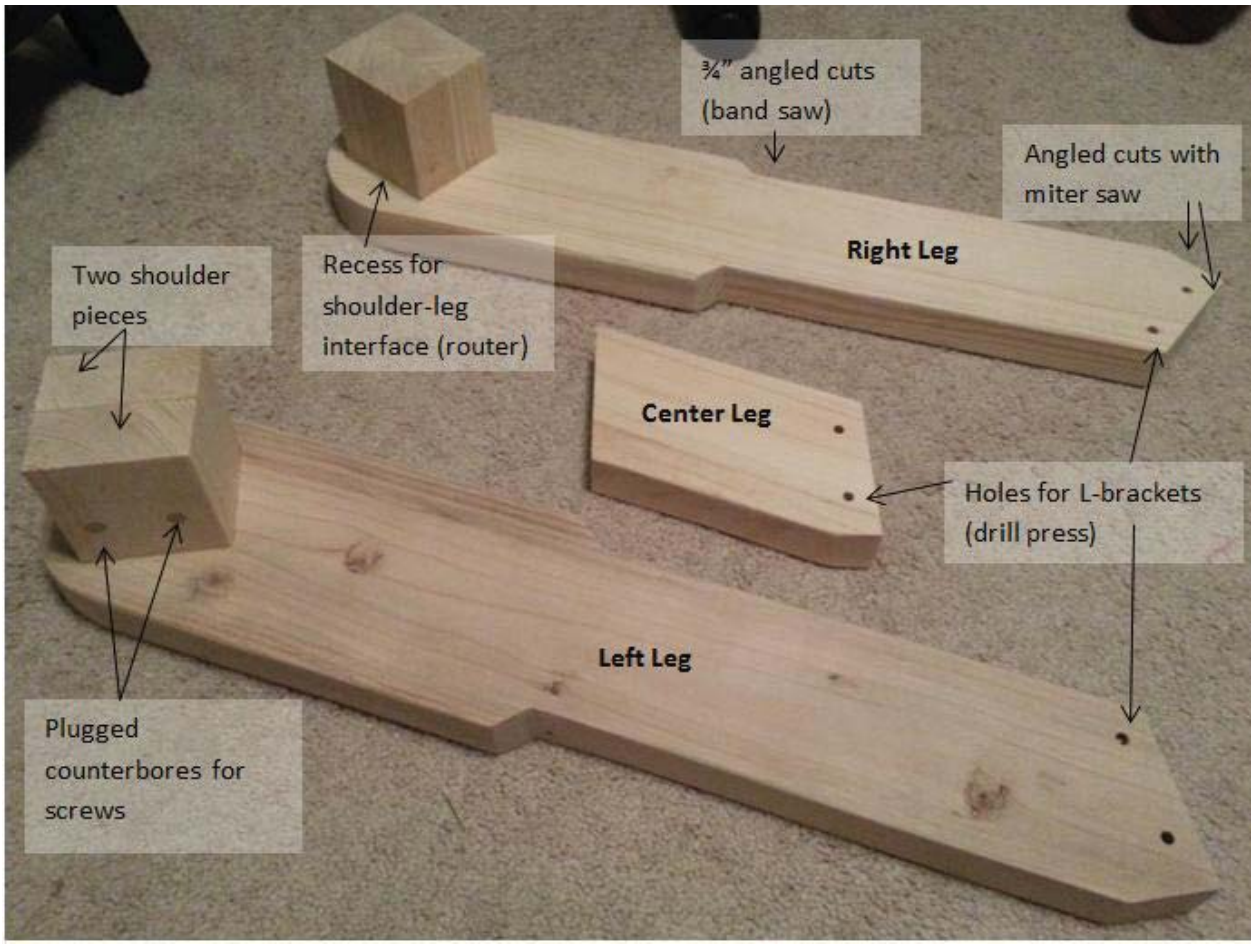

Figure 21: Center and side leg assemblies

2.9 Machining

2.9.1 Side Plates

Originally, each side plate had one slot and one hole for the axles. After initial assembly, it was discovered that the chain would not fit correctly unless both axles were adjustable, thus a second slot was added to each side plate. These slots were machined on the mill using a ½" end mill bit. After boring out the hole with a ½" drill bit, the end mill is used to slowly create the slot.

We planned on using the band saw to cut the angled edges of the side plates, however, we were instructed to not use the band saw for large pieces of aluminum as it can damage the blade. Instead, we purchased an inexpensive jigsaw with an aluminum blade to make the cuts. The plates were clamped down with a straight edge clamped over the plate to use as a guide for the jigsaw. A long piece of T-bar worked well for this. The clamp must be positioned away from the mark of the cut by the distance from the jigsaw blade to the edge of the jigsaw. The mark was then lubed with WD-40. Beeswax is the recommended lube for cutting aluminum, but WD-40 worked sufficiently if it is all that is available. It is important to cut slowly when cutting aluminum with a jigsaw. After the cuts are made, the edges can be smoothed with a powered random-orbital sander.

2.9.2 Shoulder Brackets

The holes for the shoulder brackets were countersunk using the chamfer bit so the heads of our #14 wood screws would be flush with the surface of the plates when attached to the wood shoulders. These screw heads are ½" at their widest, so the countersink was made just over ½".

2.10 Assembly

2.10.1 VexPro system

The front wheel and rear wheel of each foot are slightly different. The front wheel is attached to both the chain to the motor and the chain to the rear wheel, while the rear wheel is only connected to the front wheel, thus the front wheel needs two sprockets and the rear only needs one. The front wheels get a VersaHub on each side, then a bearing, then the sprocket (see Figure 22). The system is held together by 8-32 threaded rod through the sprockets and nuts on each side. The rear wheel has a hub, bearing, and sprocket only on one side and a bearing on the other side.

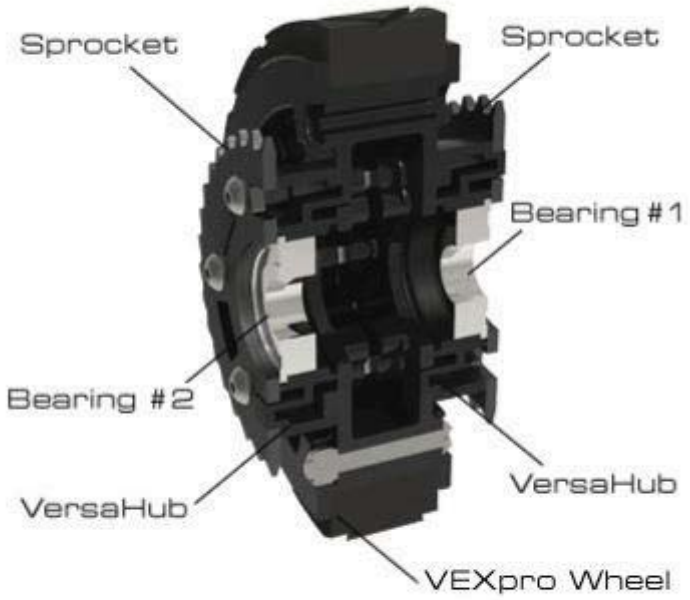

Figure 22: Vex Pro system

2.10.2 Foot Assembly

We found the most effective sequence of assembling the foot to be as follows, starting with the ½" top piece of the foot (see Figure 23):

1. Attach the L-brackets to the top with ¼"-20 x 1" screws and nuts.
2. Attach the motor bracket underneath with ¼"-20 x ¾" screws.
3. Attach the Maxon DCX motor to the motor bracket with M4 screws.
4. Attach the 11 tooth, 3/8" pitch, sprocket to the motor and secure with an M4 set screw.
5. Attach the side plates to the top plate with ¼"-20 x 1" screws.
6. Slide axle through one side plate, through one nylon spacer, through the wheel assembly, through one nylon spacer and then through the other side plate, fasten with ½"-20 nuts
   i. Note: the wheel with only one sprocket has a second, shorter nylon spacer on the side of the wheel that does not have a sprocket
7. Slide ¼"-20 threaded rod through side plates and nut on each side

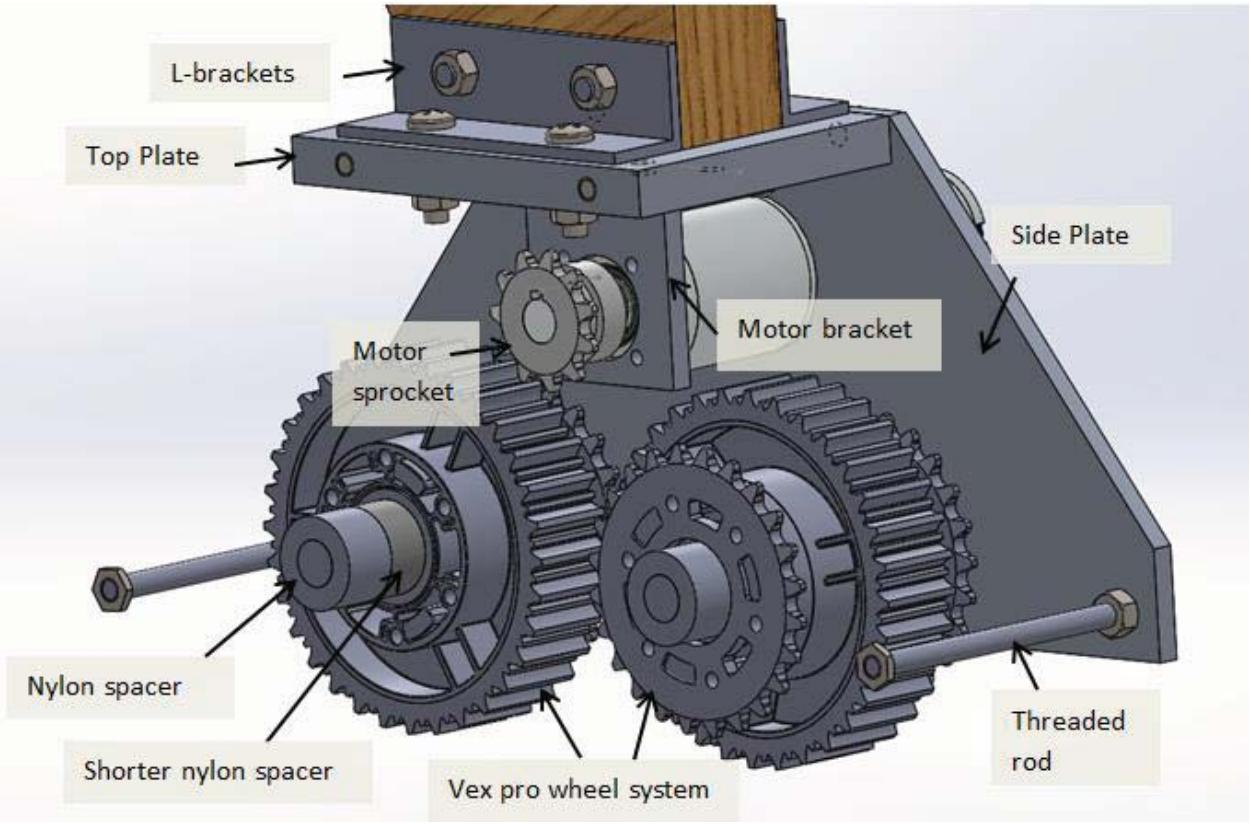

Figure 23: Cut-away view of left foot

2.10.3 Chain tensioning

Once the foot and wheel assemblies are in place, the chains can be sized and installed. The axles were removed to install the sized chain and then the axles were reinstalled. At this point, the chains were pulled tight in order to mark the location for the counter bores to hold the ½"-20 nuts in place. The side plates had to be removed to machine the counter bore. Unfortunately, the counter bores did not tension the chains perfectly, and one of the chains was slightly dragging on the ground. In order to fix this, we used ThermoMorph plastic to create plugs to hold the rear axle back. A modest amount of the heated plastic was plugged into the rear slots on each side of leg. This is done most effectively with two people so one person can pull the chains tight while the second applies the ThermoMorph plastic.

2.11 Motor Selection

Using the specified performance goals, one can begin the process of motor selection. It may be important to get the motor selection done quickly, in case the lead times for the desired motors are a bottleneck in later stages of the process. However, it is important to keep in mind that the iterative nature of the design process may result in significant changes in performance goals or motor requirements.

For R2-I2 locomotion, significant changes to the locomotion design resulted in the need to reselect motors. In each case, the Cornell Cup Motor Selection Guide was used to select motors; the final selection process will be detailed below.

2.11.1 Torque/Speed Requirement

The most important criteria for choosing motors are the desired maximum speed and torque requirement. In the case of R2-I2, the acceleration requirement was set at an equivalent acceleration of .5m/s^2 up a 5 degree ramp (standard maximum grade of a handicap ramp).

On flat ground, this corresponds to an equivalent acceleration of about 1.4 m/s^2:

$$F = ma + mgsin(5\ degrees) = m\big(a + gsin(5)\big) = m(.5 + .85) = 1.35 * m$$

$$a_{equivalent} \approx 1.4\frac{m}{s^2}$$

Also important will be the weight of R2-I2; preliminary weight estimates suggested that R2-I2 would be around 150 lbs., or 68 kg.

Using these values, we can approximate the required force output for all wheels:

$$a = 1.4\frac{m}{s^2}$$

$$F = ma = 68\ kg * 1.4\frac{m}{s^2} = 95.2\ N$$

Since we have four wheels, we can divide this force output by four to get the required force output per wheel:

$$F = \frac{95.2\ N}{4\ wheels} = 23.8\frac{N}{wheel}$$

Next, we must convert this force requirement to a torque requirement per wheel. Using the diameter of the preliminary wheel selection (4 in = .1016 m), we can make this conversion:

$$M = F * r_{wheel}$$

$$M = 23.8\frac{N}{wheel} * \frac{.1016}{2}m = 1.21\frac{Nm}{wheel}$$

Each motor controls two wheels, so we must output twice the torque:

$$M = 1.21\frac{Nm}{wheel} * 2\frac{wheels}{motor} = 2.42\frac{Nm}{motor}$$

However, our drive system also implements a chain reduction between motor sprocket (with 11 teeth) and wheel sprocket (with 24 teeth). This reduction ratio of 2.18:1 can be used to calculate the desired motor torque output:

$$2.42\frac{Nm}{motor} * \frac{1}{2.18} = 1.11\frac{Nm}{motor}$$

Next, one can calculate the motor speed requirement, usually in RPM. The performance goal for R2-I2 was to achieve a speed of 1 m/s. With the given wheel diameter, this corresponds to an RPM of:

$$1\frac{m}{s} * \frac{1\,revolution}{\pi * .1016\,m} = 3.13\frac{revolutions}{s} = 188\,RPM$$

Finally, we must account for the chain reduction, and calculate the necessary motor RPM:

$$188\,RPM * 2.18 = 410\,RPM$$

Using the torque and RPM requirements, we can start looking at potential motor solutions.

2.11.2 Motor Options

We wanted only brushed motors, because the motor control would be easier and cheaper.

The three options we decided to explore further were the RE35, RE40, and DCX35L. We compared these motors on a number of criteria; most importantly, we needed all necessary requirements (such as desired torque, speed) to be met. In addition, the CS team needed encoders to measure the position/speed of the robot. Maxon encoders for the chosen motors ranged from four counts per revolution to over a thousand counts per revolution. With the chain reduction, gearbox reduction and small wheel size, it was determined that even 4 counts per revolution would provide a decent level of feedback for the CS team—therefore, the most inexpensive encoder was chosen in each combination:

$$4\,counts\,per\,revolution$$

$$Assume\,gearbox\,reduction\,of\,12{:}\,1, chain\,reduction\,of\,2{:}\,1$$

$$4\,counts * 12 * 2 = 96\,counts\,per\,wheel\,revolution$$

$$wheel\,diameter = 4\,in$$

$$wheel\,circumference = 12.5\,in$$

$$resolution = \frac{12.5}{96}\frac{inches}{count} = .13\,in/count$$

	RE 40 Ø40 mm, Graphite Brushes, 150 Watt	RE 35 Ø35 mm, Graphite Brushes, 90 Watt	DCX 35 L Ø35 mm, Graphite Brushes, ball bearings, CONFIGURABLE
Motor PN	148867	323890	
Gear Name	GP42 12:1	GP32 14:1	GPX42 15:1
Gear PN	203115	166158	
Sensor Name	Encoder HEDS 5540	Encoder HEDS 5540	ENX16 EASY
Sensor PN	110511	110511	
Base Cost	932.01	680.51	665.7
Lead-time	Standard Stock	Standard Stock	11 days
Operating Current	5.77 A	3.62 A	4.26 A
Max Cont. Torque	170 mNm	101 mNm	121 mNm
Scaled Cont. Torque (with gearbox)	1.65 Nm	1.06 Nm	1.47 Nm
Nominal Speed	6930 rpm	7000 rpm	7160 rpm
Scaled Nominal Speed (with gearbox)	578 rpm	500 rpm	477 rpm
Weight	480 g	340 g	380 g
Total Length	105 mm	106 mm	89 mm
Max diameter	40 mm	35 mm	42 mm
Efficiency	91 %	85 %	89 %
Max Radial Load (motor)	28 N (5 mm from flange)	28 N, 5mm from flange	65 N, 5 mm from flange
Wattage	150	90	80

Table 7: Specifications for Three Motors

The gearboxes chosen were the ones closest to the desired reduction ratio. An example calculation is found below:

Motor operating pointt at 24V: 121 mNm, RPM = 7160

Desired RPM = 410

$$reduction = \frac{operating\ rpm}{desired\ rpm} = \frac{7280}{410} = 17{:}1$$

The RE40 appeared to be too much power for our requirements, while the RE35 had too little torque with the chosen gearbox, and too little speed with the next highest gearbox available. This left the DCX35L as the most feasible solution—in addition, the DCX was the cheapest combination explored.

To confirm that the DCX would meet our requirements, we needed to make sure that factors such as the max radial load, electrical requirements, and thermal limits were all met.

2.11.3 Radial Load

To calculate the max radial load (also called an overhung load in some cases) on our motor, we need to analyze the loads on the motor sprocket. We can use the formula:

$$OHL(n) = \frac{9550 * kw * F}{N * R} = \frac{M * F}{R}$$ [3]

Where,

N =	Force (N)
Kw =	Transmitted Power (kw)
F =	Load connection factor
N =	RPM of shaft
R =	Radius in meters (m)
M =	Torque (Nm)

The load connection factor for a single chain drive is 1.0. The radius of our drive sprocket is .75 in = .019 m. Therefore, the radial load exerted on our motor shaft will be:

$$Load\ (N) = \frac{torque}{radius} = 1.11\frac{Nm}{.019m} = 58.4\ N$$

Although the max radial load of our motor is only 65N, the max radial load of the GPX42 gearbox (which is where the load will be applied) is 150 N at 12 mm from the flange. Since the sprocket will be around 18 mm from the flange, the max radial load at 18 mm is:

$$150N * \frac{12mm}{18\ mm} = 100N$$

Therefore, we are running the motor at conditions well under the max radial load of the motor.

2.11.4 Thermal Limits

It is also important to make sure that the motor is operating below thermal limits. First, one must calculate the power losses in the motor using the equation:

$$P_J = P_{el} - P_{mech}$$

(where P_J = power loss, P_{el} = electrical power, P_{mech} = mechanical power)

The electrical power can be approximated using the efficiency losses in motor and gearbox. The maximum gearbox efficiency is 81%, while the motor efficiency is 88%.

[3] Source: DieQua Corporation

Our requirement for torque after the gearbox is 1.11 Nm. Therefore, the required torque output of the motor (taking into account gearbox reduction) is:

$$M_{motor} = \frac{1.11}{15 * .81} = .091\ Nm = 91\ mNm$$

$$RPM_{motor} = 410\ RPM * 15 = 6150\ RPM$$

Using our operating point, we can calculate our mechanical power:

$$.091\ Nm * 6150\ rpm * \frac{2\pi}{60} = 59\ watts$$

Therefore, our electrical power is:

$$P_{el} = \frac{59\ watts}{motor\ efficiency} = \frac{59}{.88} = 67\ watts$$

Our power loss can then be calculated:

$$P_J = P_{el} - P_{mech} = 67 - 59\ watts = 8\ watts$$

In addition, we now have information on the current draw for our motors:

$$I = \frac{67\ watts}{24\ V} = 2.79\ A$$

With a power loss (heat dissipation) of 8 watts and values for the thermal resistances for the given motor, we can calculate the increase in motor temperature:

$$\Delta T_W = \left(6.98\ {}^{K}/_{W} + 2.1\ {}^{K}/_{W}\right) * 8\ W = 73\ K$$

This is a fairly large temperature increase. Using an ambient air temperature of 25°C, the motor will heat up to 98°C. While this is still below the thermal limit of 155°C, it is closer than we like. If a housing system is used to cover the motor, overheating may be a problem. Therefore, it may be useful to explore cooling options to help accelerate motor heat dissipation.

2.11.5 Motor Selection Guide

If using Maxon Motors, the online motor selection guide can be a valuable resource for finding motors or confirming that the motor you have chosen will work in the given application. The basic motor selection guide allows one to input required torque and RPM, and will display a list of potential motor/gearbox combinations that will work for those given parameters. Additional requirements such as drive mechanism, motor length, etc. can be added to narrow results to fit the necessary criteria.

2.12 Material Selection

2.12.1 Finite Element Analysis

The design for R2-I2's foot utilizes a fixed axle with chain driven wheels. Since most of the load will be placed on this half inch axle, we want to test the design in ANSYS to see if steel or aluminum will be needed for the axle. Al 6061-T6, with a yield strength of 276 MPa is used for the first modeling.

The foot geometry was simplified slightly by removing non necessary components, such as nuts and bolts which slow down the analysis and shouldn't greatly vary the stresses in the axle. The two wheels were modeled as fixed supports and a load of 222 N was placed on the top surface of the foot. This corresponds to a weight of about 50 lbs. This estimates the weight of the robot to be 150 lbs with even weight distribution to each foot. This is a conservative estimate because there will be more weight on the front foot than the two back feet.

The max deformation and max equivalent stress are .0125 mm and 8.4 MPa, respectively, when modeled as aluminum alloy Al 6061-T6. The material only effects the deformation, as stress is dependent only on geometry. The material choice, however, does determine the safety factor in stress, which is about 32.8, allowing us to say with relative certainty that aluminum is a satisfactory material choice for this part.

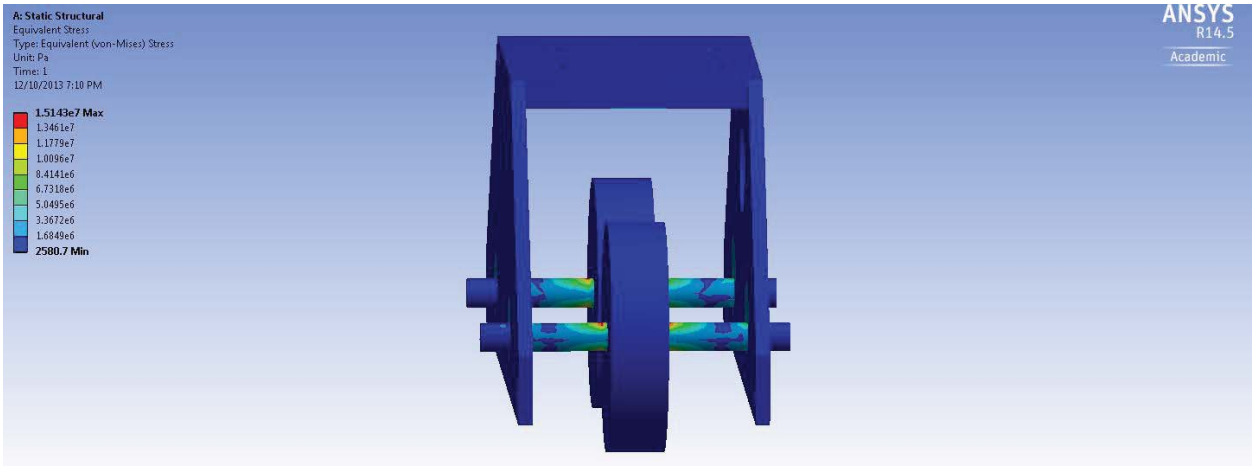

Figure 24: Screenshot of ANSYS Stress analysis on locomotion

2.12.2 R2-I2 Legs

We determined that we wanted to use wood for the "legs" of R2-I2. This was determined because one of the main functional requirements was that the general system be relatively light and sturdy. Although we considered using aluminum, we determined that the "legs" had little functional value. If we determined we wanted to use the legs for some type of non-negligible function, we would have to redesign the legs. Further, we determined that wood was very easy to machine, and stylize meaning that it would not be too difficult to meet the aesthetic requirements that we had. It was very important that R2-I2 actually look somewhat like his inspiration, R2-D2, including stylization.

Wood was the obvious choice. For our first design, we determined the simplest solution was to use a 2x6 piece of stock wood.

2.13 Final design

The final design makes use of the Versa Wheel and Versa hubs from Vex Pro Robotics, as well as the Maxon DCX35L motor with planetary gear head and encoder. The sprocket attached to the motor is an ANSI standard sprocket which will be bored to size and have a manually machined keyway to fit to the motor. All chain in the assembly is ANSI standard #35. The housing and L-brackets are aluminum and will be machined to size. The leg and shoulder are cut from standard 2x6 spruce lumber.

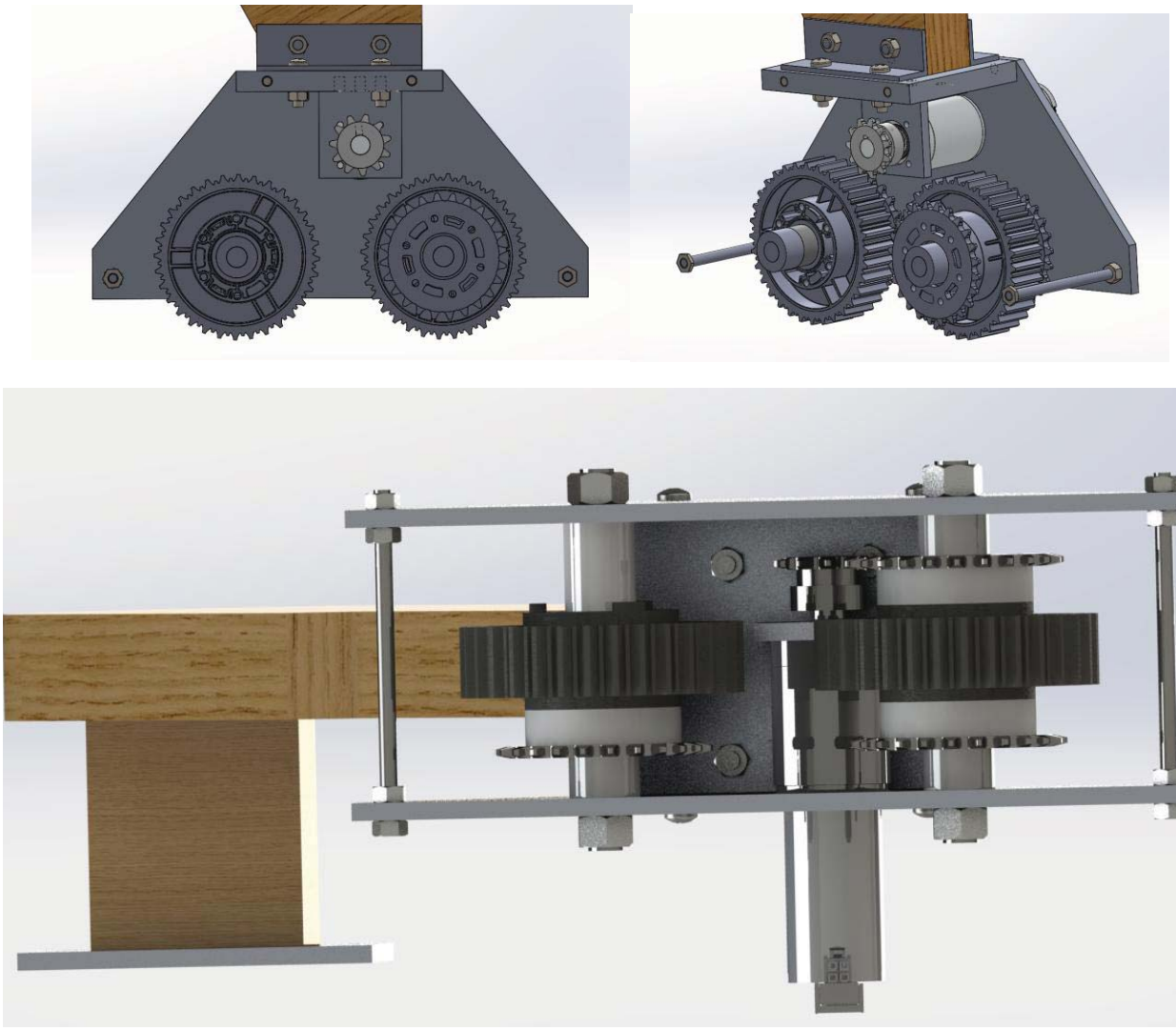

Figure 25: Detailed CAD of locomotion system

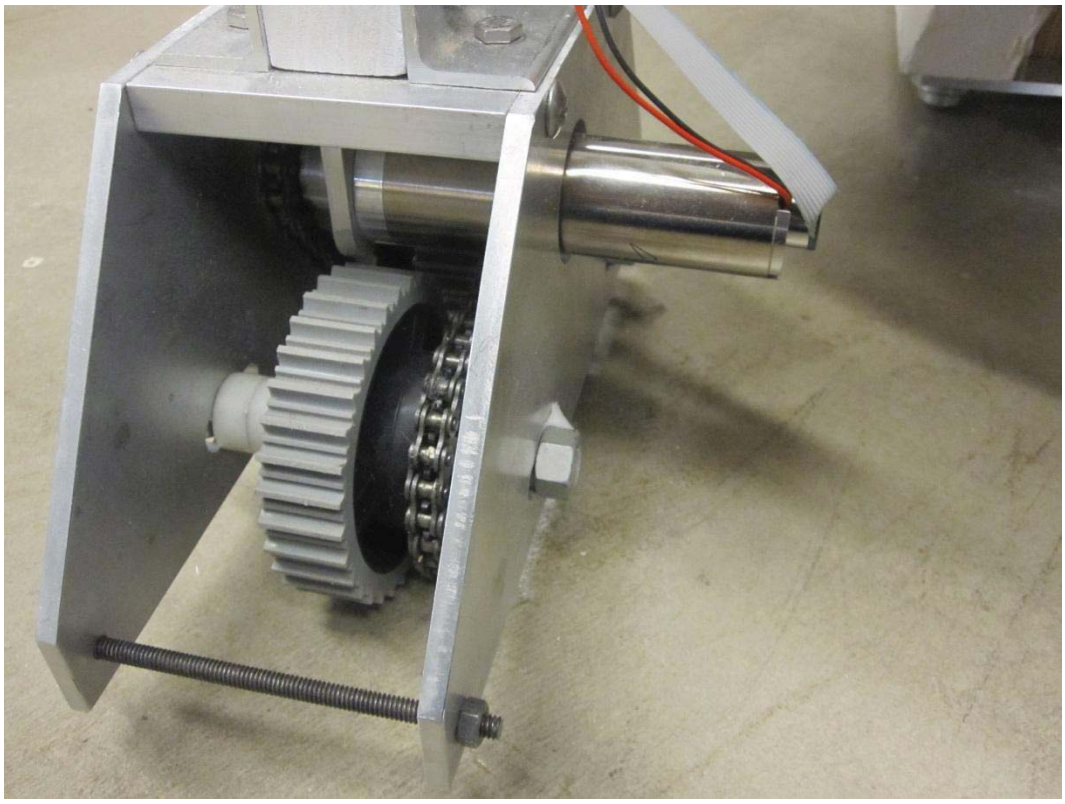

Figure 26: Final fabricated locomotion system

2.14 Additional Challenges

2.14.1 ANSI/Metric Interfacing

Maxon motors is a company based in Switzerland. Therefore, all of their motors have metric dimensioning—including the provided motor shaft. In our case, the DCX motor chosen had a shaft diameter of 12 mm. In addition, the shaft had a 4mm keyway along its length.

Our wheels/hubs/sprockets, however, were all based on non-metric standards. Most importantly, the sprockets were designed to work with ANSI standard chain, an American system.

Therefore, we needed to find a sprocket with metric inner diameter and keyway that fit ANSI standard chain. This proved a complicated find; therefore, we needed to try other solutions.

One option we looked at was using keyway couplings, such as the one shown below:

Figure 27: McMaster keyway coupling

This would allow us to transition from a metric standard shaft to a shaft of a size we wanted. However, it proved difficult to find a keyway coupling that met our criteria.

Another option was to use a bracket to attach the sprocket. If we could find (or machine) a bracket for a metric keyway, we could machine mounting points for the sprocket we had chosen. The advantage to this design is that we could machine the part to the exact specifications that we needed. Unfortunately, we couldn't find an existing solution that met our needs, so we decided to explore other options before designing our own sprocket mount.

One final option was to buy a machinable-bore sprocket (for ANSI chain), and bore out the correct shaft diameter and keyway ourselves. This would require specialized tools, such as a keyway broach with specifications identical to that of the standard Maxon motor shafts.

It was decided that buying a machinable sprocket and boring out the keyway was the most feasible solution. A keyway broach set was purchased off of McMaster in order to machine the keyway in the sprockets.

A sprocket was chosen with a number of criteria. The motor selection happened concurrently, so it was important that the number of teeth of this sprocket resulted in a reduction that was appropriate for the motor/gearbox combination that would eventually be chosen. In addition, the required bore size was taken into account-- including the additional depth needed for the keyway. We made sure that the shaft diameter including the raised keyway was within the recommended bore size range for the sprocket we ended up choosing:

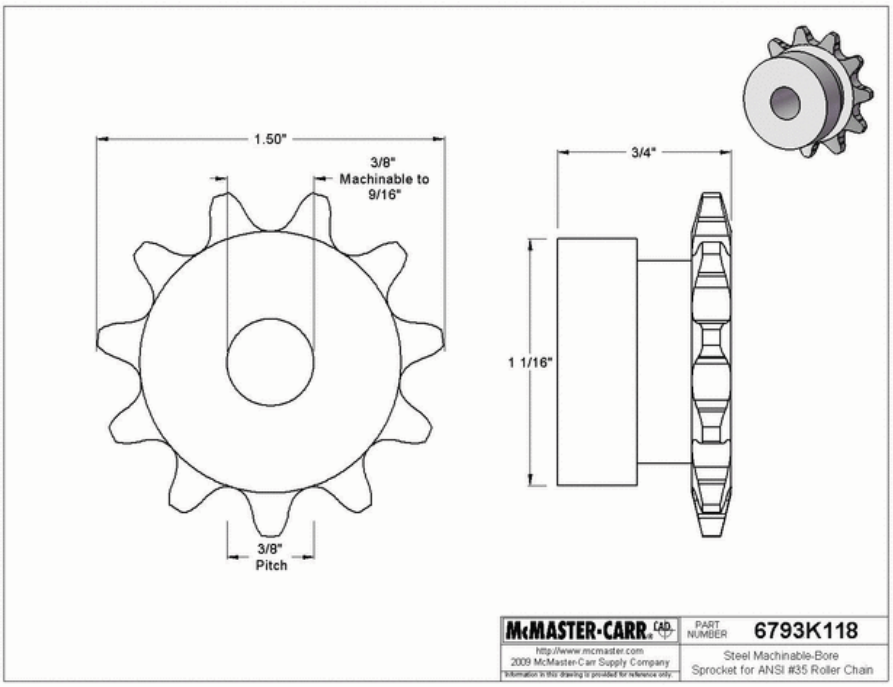

Figure 28: Sprocket Drawing

3 R2-I2 Chassis

3.1 Introduction

The R2-I2 chassis is one of three sub-groups within the R2 droid and houses the toolbox framework, drawers, and outer shell.

3.2 Use Case Determination

The primary purpose of the R2-I2 droid is to serve as a toolbox in the Cornell Cup lab. Below are the intentional and unintentional cases where the user interacts with the R2-I2 toolbox. These use cases consider the primary use of the R2-I2 droid (serving as a mobile tool box) as well as interactions with operators and maintenance personnel (i.e. packaging and assembling). The use cases and misuses influence the requirements and timeline generation because it helps frame the objectives for the R2-I2 droid.

3.2.1 Use Cases

- User vocally calls R2
- User turns on tablet
- User searches for tool on tablet that is in a drawer
- User searches for tool on tablet that is missing from the drawers
- User opens drawer

- User retrieves tool from drawer
- User closes drawer
- User turns off tablet
- User searches for where tool should be returned
- User returns tool to drawer
- User replaces damaged parts
- User disassembles R2 for packaging
- User assembles R2

3.2.2 Misuses

- User searches for tool not in inventory database
- User incorrectly types name of tool in tablet search
- User returns tool to incorrect location in drawers
- User pulls drawers all the way out of the chassis
- User bumps into R2 causing drawers to pop open
- User knocks R2 over
- User opens all drawers at the same time

3.3 Requirements

At the beginning of this project, the list of originating requirements in Table 8 was developed. As the project progressed through various planning stages, the requirements were refined and extended into the derived requirements in Table 9. These requirements were used as a reference as the project progressed into the design phases.

Index	Originating Requirement
OR.1	The R2 toolbox shall hold tools of various sizes.
OR.2	The toolbox shall securely close when not in use.
OR.3	The toolbox shall notify the user what drawer the desired tool is located in.
OR.4	The toolbox shall alert the user which tools are missing.
OR.5	The toolbox shall fit within the R2 chassis.
OR.6	The toolbox shall have the same colors and design features as the R2 character from Star Wars.
OR.7	The toolbox shall have a user interface to search for tools.
OR.8	The toolbox shall be the same size as the R2 character from Star Wars.
OR.9	The toolbox shall move across the lab.
OR.10	The toolbox shall recognize voice commands.

Table 8: Originating Requirements of R2D2

Index	Derived Functional Requirement	Source OR
DR.1	R2 shall recognize the location of voice commands.	OR.10
DR.2	R2 shall move to operator's location.	OR.9

DR.3	R2 shall recognize obstacles in its path.	OR.9
DR.4	R2 shall avoid obstacles in its path.	OR.9
DR.5	R2 shall stop moving when it reaches the source of the voice command.	OR.9
DR.6	A search algorithm shall be executed to determine location of tool in toolbox.	OR.7
DR.7	Search results shall be displayed on the tablet screen.	OR.7
DR.8	Search results shall notify operator which drawer the desired tool is in.	OR.3
DR.9	Search results shall inform operator if desired tool is not in toolbox.	OR.4
DR.10	The drawer holding the desired tool shall light up.	OR.3
DR.11	The drawer shall electronically un-latch.	OR.3
DR.12	The R2 chassis shall remain stable and upright when drawer(s) are opened.	OR.5
DR.13	Tools shall be displayed in an organized layout within each drawer.	OR.1
DR.14	Removal of the tool triggers a missing tool indicator.	OR.4
DR.15	Software algorithm shall record which tool is removed.	OR.4
DR.16	The R2 chassis shall be 30" tall.	OR.8
DR.17	The diameter of the R2D2 chassis shall be 18.25".	OR.8
DR.18	The drawer depths shall be 3", 4", and 5".	OR.1
DR.19	The chassis shall have an access panel for electronics maintenance.	OR.9
DR.20	The chassis design shall allow for the addition of extra sensors.	OR.9
DR.21	The tablet screen shall be on the surface of the chassis at all times.	OR.7
DR.22	A tablet shall be used for the user search interface.	OR.7

Table 9: Derived Requirements

3.3.1 Tools List

Before entering the design phase, the electrical, computer science, and mechanical sub-teams were all consulted to determine the list of tools in Table 10 that the R2-I2 toolbox should be able to hold. This list resulted in an estimate weight that the system would need to handle which affects the locomotion motor specifications, and it affects the size of the drawers required to fit the desired tools, affecting the size of drawers selected

Tool	Estimated Weight [lbs]
Allen Wrenches (all sizes)	1.6
Phillips and Flat head screwdrivers (various sizes)	2.6
Frequently used nuts and screws (labeled and organized)	1.5
Calipers	0.6
Wrenches	4
wire cutters	1.9
solder	0.5
flux pen	0.1
solder sucker	0.25
electrical tape	0.5
wire spools	2.2
Empty, sealable container (are removable)	1.5

Table 10: Tool List for R2-I2

3.4 Chassis Design Considerations

When designing the toolbox drawers, the initial decisions were made based on our design criteria of accessibility, modularity, and practicality.

Because there was such flexibility in the mechanical design of the toolbox, we chose to design the chassis to accommodate the electrical engineering components. With wires coming from the sensors on the shell of the chassis, the drawers, the legs, and the battery, a lot of open space would be needed to be able to trouble shoot the components effectively. As such, we chose to have both sides of the shell be completely removable in order to maximize accessibility.

While we wanted the drawers to be as modular as possible so that a wide variety of tools could be accommodated, we chose to fix the drawer depths and instead add dividers and foam cutout tool organizers within the drawers to promote modularity. This would simplify any required machining and provides a reasonable constraint during the design process.

We also decided to stray slightly from our Star Wars inspiration and chose to have the R2 chassis completely perpendicular to the floor instead of leaning back at an angle. This design constraint maximizes the space available for drawers and tool storage and eliminates the concerns of tools sliding when R2 is in motion while overall increasing the practicality of the system. In addition, the constraint simplifies (and improves) the frame design.

A final design consideration was the mounting of the Dell tablet. Since it'd been planned to use the tablet to display the inventory system, it needed to be placed on the front of R2, but also needed to be removable in case it needed to be charged or worked on.

3.4.1 Limiting Factors in Shell Design

The creation of the shell of the chassis proved an interesting design challenge. We wanted the shell to accommodate the set size of the head and also be safe and easy to modify for sensors placement, the plan for which wasn't finalized until the tail end of the overall project. This was a result of many factors, including:

- Lack of performance certainty: If it so happened that the sensors didn't return good data, or just didn't work for whatever reason, the sensors would have to be switched out
- Uncertainty in mounting: we didn't know what the final sensor and accompanying wires and circuit boards (if existent) would look like, and therefore could only plan so much for them.

This was mostly a matter of cross-team communication and concurrent timelines (they weren't going to have a final sensor design until much after our deadline for purchasing shell material) which wasn't possible to avoid at the time.

3.4.2 Material Selection

Prefabricated Plastic, Prefabricated Cardboard, Sheet Metal, and Wood were all considered. Prefabricated plastic posed the problem of being expensive (as shown in Table 11), not being the

correct diameter, and being difficult to machine. The R2 head we'd decided to order is 18.25" in diameter, and the only standard size of prefabricated plastic sold was 18". In order to ensure a smooth transition from head to chassis, we decided not to use the 18" prefabricated materials. In addition, using prefabricated plastic required the inconvenient and potentially dangerous process of cutting out holes for the drawers with just the tools and machines available to us. These were also reasons for not choosing prefabricated cardboard.

Sheet metal was a better material consideration in terms of machining. It would be much easier to cut out drawer holes while flat and then bend to the desired radius. However, it would be difficult to modify after bending the material. Here, the limiting factor was once again the uncertainty of sensor placement. Additionally sharp edges were a safety hazard.

Thus, wood seemed to be the most viable option for material selection. It'd be relatively simple to machine and also modify post-bending. Web research brought us to a material called medium density fiberboard (MDF). MDF is a wood product with material properties such as high flexibility and high density which fit our needs. In order to most effectively bend the MDF to the desired radius, we decided to implement a common carpentry technique called kerfing. This process entails scoring the wood at regular increments with kerfs, which are then filled with glue and bent.

The final purchase made was pre-kerfed MDF from Rockler Woodworking and Hardware.

Material	Size	Vendor	Unit Price	Total Price
PVC (plastic)	18" diameter	US Plastic	$71.34/foot	$142.68
Acrylic (plastic)	18" diameter	ePlastics	$315.98/foot	$631.96
Sonotube (cardboard)	18" diameter	Sonoco	$75.85/12feet + transportation costs	$75.85 + transportation costs
Sheet Metal	2' x 4'	McMaster Carr	$43.51	$87.02
MDF (wood)	2' x 4'	Rockler	$21.99	$43.98

Table 11: Material Selection Comparison

3.4.3 Manufacturing

In order to fabricate the shell, the following procedure was implemented. This involves two main manufacturing processes – one for pre-machining the shaping mount (pictured in Figure 29), and one for the shell itself.

3.4.3.1 Mount Pre-Machining

Described below is the process of manufacturing the shaping mount to be used to shape the shell later on.

1. Using a jigsaw (or table router if available), cut four semi-circles out of plywood of 17.75" diameter. This represents the inner radius of the MDF: head radius – thickness of MDF.

2. Cut a plank of lumber about 2’ tall and at least 6 inches wide.
3. Measure and mark two lines of mounting points along the lumber. There should be eight rows of markings – two for each of the semi-circles.
4. Using a power drill and wood screws with L-brackets, screw into these holes, making sure to stop after each set of two holes and match the appropriate semi-circle with the newly mounted L-brackets, adjusting if necessary.
5. Putting the semi-circles into place, mark the locations of the L-bracket holes you will be drilling into the semi-circles. These holes will be used to insert bolts and fully secure the semi-circle shapers onto the plank.
6. Drill these holes, making one on each of the shapers slightly larger than the other to allow for tolerances.
7. Using bolts and nuts (we used ¼-20), secure the shapers onto the plank.

* **Note:** Try to be as accurate as possible in keeping the mounted semi-circles parallel with each other. Even the slightest deviation from complete parallelism will alter the look of the shell and throw off the mounting process later on.

Figure 29: Kerfed wood on shaper

3.4.3.2 Shell Manufacturing

1. Using a jigsaw or similar tool, cut the pre-kerfed sheet of MDF to the proper height specified in the appropriate drawings. Cut the material to a longer width (about an inch longer on each side) than specified in the drawings – this extra material will be used in mounting the wood to its shaper later on and will be cut off.
2. Measure and draw necessary holes.

3. Cut out any necessary holes if finalized. This includes the rectangle for the tablet, and the rectangles for the drawers.
    a. Use a ¼" drill to make holes at diagonal corners in each of the rectangles.
    b. Using a jigsaw, cut the shape out as cleanly and evenly as possible.
    c. Sand the edges down for a nice finish.

    *** Note:** Though it was originally planned to have slots of wood in between each of the drawers, as pictured below, these ended up being very small and weak, and breaking off when the shell was brought off its mount, as pictured in Figure 31, so we decided to make one large rectangular hole for all the drawers.

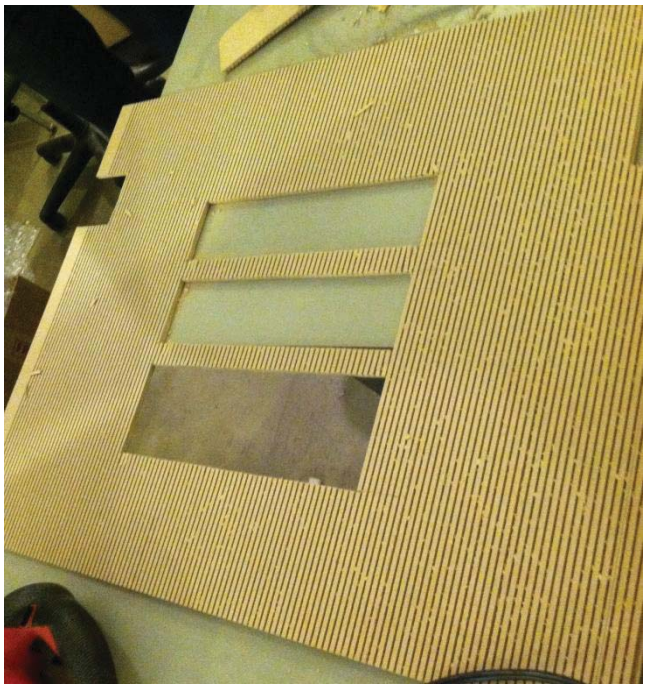

Figure 30: Kerfed wood with rectangular cut-outs

4. Prepare the wood for mounting and gluing by cleaning out any woodchips that may be lodged in the kerfs. These will get in the way of your glue later on if left.
5. Cover each of the semi-circle mounts with a thick plastic sheet to prevent the MDF from sticking to them.
6. Using wood screws, a power drill, and the aid of multiple people, line the sheet of MDF up with the mount, making sure to hold it parallel to the edge of the shapers. Screw the MDF down to each of the semi-circle shapers on either side.
7. Turn the mount over and carefully fill all the kerfs with white glue. White glue is less self-cohesive and viscous and is therefore better for the first round of gluing – it fills in the kerfs more fully. In addition, when dried, it expands less than yellow or wood glue. While gluing this first layer, be sure to go slowly and get the white glue as deep into the slots as possible.
8. If necessary, bungee cords can be utilized in order to pull in any less secure segments of wood and to get a better curve.

9. Let the shell sit for 24 hours.
10. Refill each of the kerfs with yellow glue.
11. Let the shell sit for another 24 hours.
12. When the glue has hardened properly and the shell seems secure enough, take it off the wood mount.
13. Cut the appropriate amount of material off the ends that were screwed onto the shaper.
14. Tweak if necessary – trim, sand, etc. In our experience, even in post-bending the shell has been able to withstand jigsawing, dremmeling, and a good deal of vibration in general. This step involved a lot of trial-and-error and taking the shell back on and off the robot in order to get the dimensions perfect. Due to the accumulation of slight deviations in the physical fabricated robot from nominal design, our original nominal design for the kerfed wood didn't work out as well so we just persisted with tweaking the curved MDF until it fit properly – which it did in the end.

Figure 31: Curved shell on drawer-side of R2

3.4.4 Sensor Implementation

R2 possesses a mass of sensors in order to facilitate his autonomous capabilities and obstacle avoidance. The ultrasonic rangefinders were mounted onto various places on R2 – three on each leg, two in the LIDAR foot, one on the shell. Because the rangefinders on R2's legs had to face specific angles and directions and there was still some chance of them having to be moved around, moldable plastic was sculpted around the rangefinders and given the proper surface shape to mount to the particular positions on R2. Velcro, favored for its easy removal and replacement, was then used to attach these molded plastic mounts to the body.

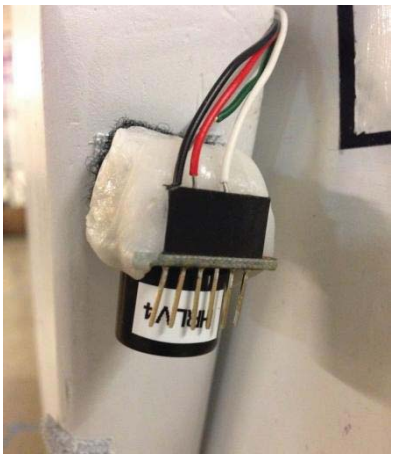

Figure 32: Ultrasonic rangefinder encased in moldable plastic and mounted onto R2's leg

The two rangefinders in R2's LIDAR foot were easier to implement. We cut two holes into the foot and secured the rangefinders in these holes with the moldable plastic. All wiring was done prior to mounting.

Figure 33: Ultrasonic rangefinder s encased the LIDAR foot

3.4.5 Tablet Mounting

Figure 34: Purchased LotFancy Tablet Mount

The original plan for securing the tablet to R2 had been to use a mount with the ability to tilt and swivel. The tablet mount would then be attached to a set of drawer slides, in between the top and middle drawers, and have the extra feature of being slid in and out of R2's chassis. Though this was a great idea in theory, the spacing between the drawers was too small to allow for the entire mechanism. Therefore, we decided to purchase the tablet mount depicted in Figure 34, remove the extra O-clamp attachment and drill two holes into the top portion of the plastic. We put M5 bolts through the drilled holes and fixed the mount to a piece of T-bar which was then attached to the chassis.

Figure 35: Tablet Mount on Chassis

3.4.6 Button Placement

For the purpose of making R2 a more user-friendly robot, several buttons were mounted to his shell. This included the power button, the motherboard power, a charging port, and a reset button. The

locations of these buttons were finalized after curving the board so the holes for them were made using appropriately-sized drills. These buttons are pictured in Figure 36 below.

Figure 36: Power and other buttons on R2

3.4.7 Mounting

Keeping with the plan to have a removable shell, more permanent attachment plans such as gluing or nailing weren't feasible. Therefore, we machined eight small (about 1.5" tall and wide) wooden blocks, four for each side of the shell, which were mounted to the wooden circular base of R2 using long 8-32 bolts and screws. L-brackets were also fixed to these wooden blocks such that once the shell was mounted, their faces were flush against the wood. The L-bracket holes matched up with accompanying holes on the wooden shell, and a set of smaller M5 screws bolted from the outside were used to hold the shell in place.

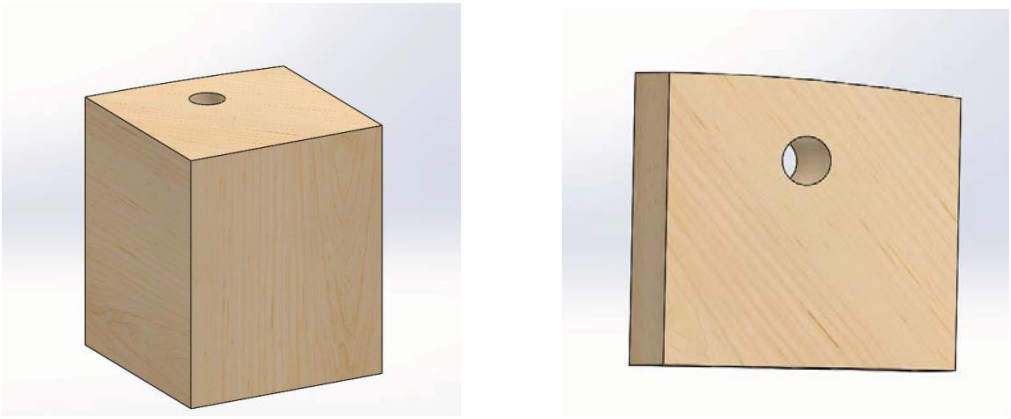

Figure 37: Isometric and top views of wooden blocks

Note from the top view of the wooden block in Figure 37 that the outer edge follows a curve which possesses the same radius as R2's base. This makes it such that the curved edge sits flush with the inside of the shell. Both sides of the shell were mounted in this fashion. The drawer-side half of the shell was cut a little bit longer than the drawer-side so we were able to fasten it at the top to threaded T-bar for extra security. As the number of attachment points increased on R2's shell, the better it was able to hold its shape, long after being taken off the shaping mount.

3.5 Drawer Mechanism Design

3.5.1 Decision Matrices

Table 12 and Table 13 are the decision matrices for the drawer style and drawer latch mechanism. For the drawer style, the three options considered were standard pull-out drawers (like a standard filing cabinet), a modified lazy Susan design (seen in Figure 38), and a rotating conveyer belt design (inspired by the design seen in Figure 39). The pull-out drawers and Lazy Susan designs were the top two, with scores of 35 and 33, respectively. Both the pull-out drawers and Lazy Susan designs would allow for adjustable partitions within each drawer/shelf, increasing modularity. The rotating shelves conveyor belt design is an inefficient use of space and not easily manufacturable. Ultimately the pull-out drawers were selected due to high accessibility to the tools and high manufacturability.

Figure 38: Rotating Lazy Susan Drawer Design

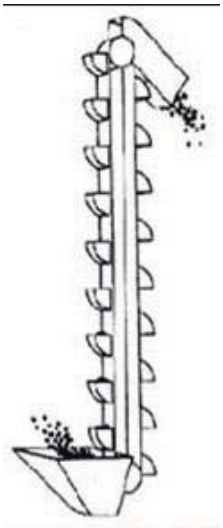

Figure 39: Conveyor Belt Design

Once the pull-out drawers were selected for the drawer style, the next step was to select drawer slides and a drawer latch mechanism. The drawer slides could attach to the bottom of the drawers, the two outside left and right faces of the drawers, or suspend to the top of each drawer. The side slides were selected because they maximize the space available for drawer depth. After researching a variety of common drawer latch mechanisms, the options outlined in Table 14 were measured against a series of performance criteria. A value was assigned to each performance criteria, and these values were then normalized to allow all weighted scores to be compared on the same scale. Final scores for each option were calculated, and the push-open mechanism had the highest score of 15.35 with the magnetic latch with slide close behind at 14.79. Ultimately the push-open mechanism was selected because it provided a smooth finish to the front of the R2D2 chassis and was a fully pre-manufactured part, two performance criteria that were weighted very highly.

Drawer Style								
Attribute	**How to Measure**	**Min. Limits**	**Max. Limits**	**Scale Definition**	**Weight**	**Designs (1-5 scale)**		
						Drawer Slides (standard)	***Modified Lazy Susan Shelves***	***Rotating Shelves on Conveyor Belt***
Feasibility of Manufacturing	Amount of time to machine (weeks)	0	2 weeks	1=>2weeks 3=1week machining 5=premade interface	5	4.5	4	3
Accessibility of tool	Time required to remove tool	0	2 seconds	3 = 2, 5 = <1	5	3	1	1
Organization	Time required to locate tools (sec.)	0	30	1 = 10+, 3= 5, 5=<2	5	3	2	2
Reparability	How easy is it to fix identified high risk components	just replace part	Repair time of single component is less than assembly time	1 = complete disassembly, 3 = some disassembly, 5 = just replace part	4	3	4	2
Ease of Assembly	Assembly time (min.)	0	60 minutes	1 =60+, 3 = 30, 5 = <10	4	3	3	1
Weight Budget of the Drawers	lbs	5lbs minimum	100	1= 0-5lbs 3=15lbs 5=30+lbs	3	4	5	3
Cost	$	0	$500	1 = 200+, 3 = 100-120, 5 = <70	2	5	4	1
Noise Level	dB	0	75 dB	1 = 70-90, 3 = 50-70, 5 = <50	2	5	5	3
Force to open/close	N	0	15	1 = 10+, 3 = 5, 5 = <3	2	5	5	5
				Total Score:		**35.5**	33	21

Table 12: Drawer Style Decision Matrix

R2D2 Drawer Latch Mechanisms											
	Value			**Normalized Value**					**Final Score**		
	Option A	Option B	Option C	Option A	Option B	Option C	Weight	Normalized Weight	Option A	Option B	Option C
Cost (per one drawer/shelf configuration)	$15	$10	$50	0.7	0.8	0	4	0.1818182	2.8	3.2	0
Time of Installation	15 minutes	7 minutes	25 minutes	0.4	0.72	0	2	0.0909091	0.8	1.44	0
Number of Pre-manufactured component/ Number of parts to machine	1.25	1	0.333333	1	0.8	0.266667	3	0.1363636	3	2.4	0.8
Aesthetic Finish	5	3	4	1	0.5	0.75	4	0.1818182	4	2	3
Compatibility with circular R2D2 frame	3	3	4	0.5	0.5	0.75	4	0.1818182	2	2	3
Easy to open (Human Centric Design spirit metric)	5	4	4	1	0.75	0.75	2	0.0909091	2	1.5	1.5
Likelihood of accidental opening	2	4	1	0.25	0.75	0	3	0.1363636	0.75	2.25	0
						Total Score:	22	1	**15.35**	14.79	8.3

Table 13: Drawer Latch Mechanism Decision Matrix

Option	Description
Option A	Push-Open Mechanism
Option B	Magnetic Latch with Slide
Option C	Rotary shelves with sliding door

Table 14: Latch Mechanism Choices

Easy to open		Aesthetic Finish	
5	Can be opened with one hand, individual finger dexterity not required	5	Smooth finish, no visible external components
4	Straightforward mechanism requiring one hand	4	Any external mechanisms are blended into R2D2 aesthetics
3	Requires manipulation with one hand	3	Minimal external mechanisms, not immediately noticeable
2	Straightforward mechanism requiring two hands	2	Noticeable external mechanisms,
1	Requires manipulation with two hands	1	External mechanisms draw undesirable attention
Compatibility with circular R2D2 frame		**Likelihood of accidental opening**	
5	Circular design, can match frame exactly	5	Can only be opened by intentional manipulation of latch
4	Design can be easily modified to match frame	4	Can be opened with simple motion that could be unintentional
3	Design requires moderate amount of effort to match frame	3	Can be opened by small child
2	Design requires extensive amount of effort to match frame	2	Can easily be opened when bumped or jarred
1	Design is not compatible with frame	1	Could open by rolling motion of R2D2 across room

Table 15: Decision Matrix Explanations

The series of CAD models below (Figure 40, Figure 41, Figure 42, and Figure 43) shows the design of the R2 chassis that we had at the end of our first semester on this project. Several key changes were made when we set out to manufacture the design. These changes are discussed in the next section of this documentation.

In addition to the initial assumptions described at the beginning of this section, additional decisions to finalize the design were made after the decision matrix process. Originally the tablet was going to be mounted within the chassis and pull out in the same plane as the drawers, but after considering the requirement that the tablet face must be visible at all times, we decided to mount the tablet on the opposite side of the chassis that the drawers open from. This solution allows maximum user access to the drawers within the chassis while still meeting the visibility requirement for the tablet. We considered mounting the tablet in the R2 head, but size and electronics restrictions did not allow this to be a feasible option. In addition, we finalized the depths of each drawer to be 1.63, 2.63, and 3.63 inches. The range of depths provides the optimal set-up for housing a variety of different size tools. After consulting with the electrical and computer sub-team, we also added hidden sections beneath each drawer to house electronic components.

Figure 40: Concealed Electronics Panel beneath each drawer

Figure 41: Tablet Mount opposite drawer openings

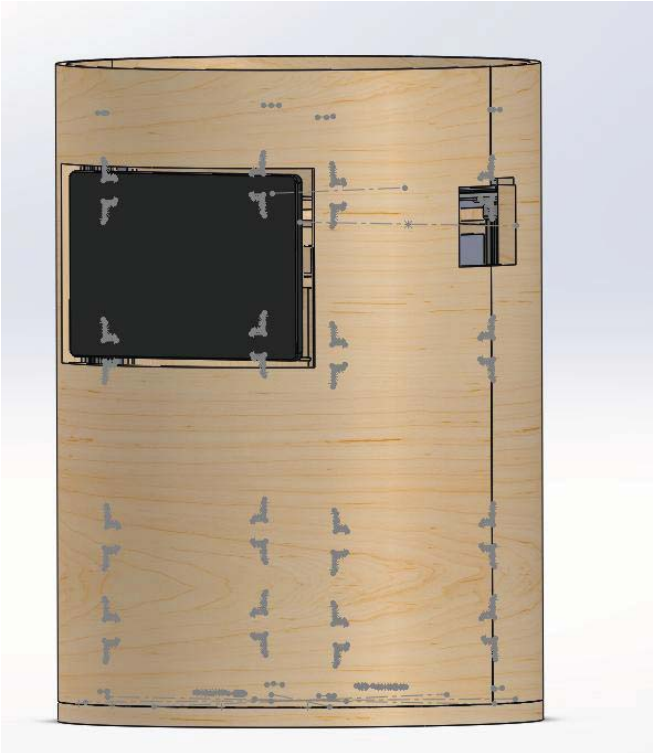

Figure 42: Visible Tablet mounted flush with chassis shell

Figure 43: Pull Out Drawer Design and drawer slides within chassis

3.6 Drawer Design Changes and Finalization

When it came to fabricating the drawer system, due to our collective inexperience in carpentry and related fields, many unforeseen concerns came up. The drawer design ended up going through a great deal of design decisions and changes.

3.6.1 Material Section

3.6.1.1 Sensor Foam

The main factors considered for this process were price, quantity, thickness. There would have to be enough foam to cover each of the three drawers and it would have to be thick enough to cover all of the sensor below the metal lever.

Originally we bought one foot of 5/16" Natural Gum Foam for $11.65 on McMaster (Product #8601K44), but when we did tests to test the integrated sensors in the foam the foam proved to be too dense and would not compress enough to trigger the sensor. Even the heavier tools used such as a tape measure would not trigger the sensors so this added factors to consider: firmness and density. The Natural Gum Foam had a firmness of 5-10 psi and density of 26 lbs/ft^3. We moved this foam aside and decided it was necessary to buy new sensor foam.

At first we only needed a 1/4" thick foam which then led us to buy 3 pieces of the firm Quick-Recovery Super-Resilient Foam (Part #86375K151) from McMaster for $12.13 each with a firmness of 8-14 psi and density of 16 lbs/ft^3 , but the electrical team changed the switch used for a larger one so we then needed foam that was 3/16" thick. Instead of buying completely new foam for this, we decided to buy the same quantity of the same foam, but with a smaller thickness so we could layer the two. However instead of firm, we got the soft version (Part

#86375K151) because the firm product only comes in 1/4" thickness for the firm version. Each of the foams had one sticky side so we used this to attach the thinner piece on top to the thicker piece on bottom.

3.6.1.2 Tool Foam

In picking this foam the same factors were considered except density because it was irrelevant to this aspect. In the original plans we wanted each drawer to have different foam thicknesses based on the tools they would hold, however due to space constraints this idea was scrapped and instead we decided to make all three of them 1/2" inch thick. The most cost effective foam we found for this job was Walmart's Blue Ozark Trial Camping Pad for $7.97. One pad was enough to cut out three pieces as well as extras.

3.6.1.3 Finalized Tool List

Tools Held
Top drawer: needle-nose pliers, calipers, hex key set, wire strippers
Middle Drawer: (6 boxes) fasteners, M5 screws, 1/4" locknuts, 1/4" bolts, #8 locknuts, and #8 bolts
Bottom Drawer: Philip's head screwdriver, flathead screwdriver, roll of electrical tape, and tape measure

Tools Removed
Top Drawer: wrench
Middle Drawer: L brackets, washers
Bottom Drawer: multimeter, spool of wire

3.6.2 Cutting Methods

3.6.2.1 Foam Cutting Methods

The most important factors that were considered when choosing a method for cutting foam were cost, complexity, and precision. Our two options were a hot wire cutter and a precise X-ACTO knife, both of which we picked out primarily due to their low cost compared to the other options available such as a hot knife. However, shapes needed to be cut out of the foam for the tools and the sensors, and it would not be feasible to use hot wire to accomplish this task. In addition, constructing a hot wire cutter, although inexpensive, would have taken a substantial amount of time. This remained our backup option until we bought and tested a precision knife. The knife worked very well for our purposes, which included cutting through both the denser sensor foam and the lighter tool foam. Although the smaller cuts made for the sensors in the denser foam using the knife were not ideally clean, it was largely unnoticeable. If the foam was cut slightly smaller than the size of the sensors, the foam would wrap around them so that both the sensors were held securely in place and the rough edges of the foam cuts were inconspicuous. Regarding the lighter foam to be used to encase the tools, the knife cut

extremely well. We ultimately chose the Heavy Duty Precision Knife (4-7/8" Long Handle) from McMaster as our tool for cutting the foam, since it performed more than adequately for our precision testing, and was very cheap with a unit price of $4.41.

Figure 44: Heavy duty precision knife

Figure 45: Drawer 1 (3”)

Figure 46: Drawer 2 (3")

Figure 47: Drawer 3 (4")

Important note: it was very easy to make thin slices in the foam so it's always better to leave the overall size slightly big rather than small because it could be easily cut down. Similarly, it's better to leave the holes for the sensors slightly small to keep them snug because more foam could be cut later. However, it is better to leave the cuts for the tools slightly large this way they can sit in their spots more easily instead of having to be pushed into slightly too small space.

3.6.2.2 Cutting Wood Drawer Pieces

Due to an underestimate of the space the electrical components of R2 would take up inside the chassis, the initial plan for each drawer to have differing heights of 3", 4" and 5" was scrapped. Instead two drawers were made to a height of 3" and one to a height of 4".

The first step to making the drawer was to use a pencil and tape measures to mark the dimensions from the CAD of the drawer on the pieces of wood to be cut. For the curved part of the drawer we got 2 pencils and tied a string to the center of each pencil. Then we put one pencil at the center of the curve, and the string was measured to match the radius of it. Then we drew it in a fashion similar to using a giant compass.

Next we clamped down the pieces and jig sawed them. Due to human error and slight warp of wood, the cuts were not perfect but they were accurate enough for our purposes that they did not need to be redone. Then the sensor foam was laid out over the thin board and each of the sensor locations were marked. The foam was then removed and the pin locations were marked in pencil and drilled using a 3/16" inch drill bit.

Important Note: Unlike the foam, it is not easy to make small extra cuts with a jig saw afterward to fix mistakes for assembly. For any slightly too large edges, we sanded them down to size using a random-orbital sander.

3.6.3 Assembly of the Drawer

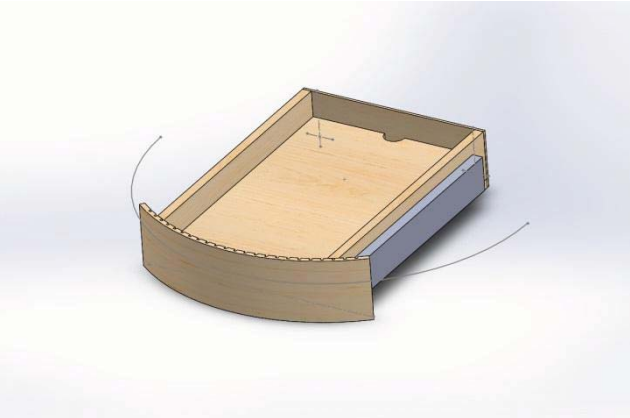

Figure 48: 3” Drawer CAD

After all the parts were prepared, the drawer was assembled using 3/4" stainless steel wood screws. They were assembled in the following order: each connecting block was screwed to each side plate, which was then screwed to the drawer base. After this was completed, the curved shell for the drawers was attached using wood screws.

The assembly was slightly complicated by the fact that edges of some pieces were not 100% precise due to some human error with the jig saw and due to the wood warping. This also made it harder to attach the outer shell to the drawer because their curves did not align perfectly. Another small issue was some of the pieces of foam were not cut down to their proper size and were a little too tight a fit to place in the drawers, but this was an easy fix that only required cutting down some more of the foam.

Figure 49: Two 3" drawers and one 4" drawer

Next we used a tape measure to precisely place the slider at the center height on the side of the drawers. We used a pencil to mark this position and then we used No. 6 zinc plated steel 3/8" wood screws to attach them to the wood. These screws did not hold as well as anticipated since they were too short so we then had to switch to longer screws with the same diameter.

An unanticipated issue that arose was that the back of each drawer was not as accessible as expected. This was due to the curvature of the outer shell. Thus, we had to remove the unreachable tools listed previously in the "Tools Foam" section of "Material Selection."

3.6.4 Integrating the Drawers

The drawers were integrated into R2's T-bar frame using Standard Side-Mount Drawer Slides (Stainless Steel, 10", Full Extension) from McMaster. The inner sliding components of the sliders were attached to both sides of the drawers itself with wood screws. The outer stationary components were mounted onto the T-Bar with regular M5 screws and drop-in fasteners. The T-bar to which the slides were mounted were also adjusted to account for the height of each drawer. It was particularly important to keep the pairs of slides at the same position in both the vertical and horizontal directions to ensure smooth sliding of the drawers.

3.6.5 Drawer Mechanisms

Although the push-open mechanism was originally selected for the drawers, we encountered many problems during the process of implementing them. We eventually decided on a basic pull-out

drawer mechanism, and instead of using push pins, we made small semi-circular cuts in the top of each drawer shell for finger holds.

One major roadblock with the push pins was figuring out a way to mount them, since the holes in the attachable mount were too small to fit most screws, including the ones that we had. Our solution to this problem was using thermoplastic beads, which when heated could be molded like clay around the pin. Two holes were drilled through the thermoplastic on either side of the pin to allow for bolts that could mount the pin to the T-bar.

Figure 50: Push pin embedded in moldable plastic with holes drilled for screws

However, an important factor that we did not account for when deciding on the push-open mechanism was the mass of R2-I2 versus the force that setting off the pin would require. Once the pins were mounted using the thermoplastic, we tested them by pushing on the drawers. The force on the drawers intended to set off the push pins instead caused R2-I2 himself to slide backwards. This would not be a problem when R2 was powered but this led to concern of applying too much force and torque on the locomotion motors instead. Due to this problem, the push-open mechanism was no longer feasible considering our time limitations and the type of push pin we had. In the future, this situation could perhaps be resolved with push pins that are easier to set off.

3.7 Integration with Other Components

The system was designed for easy assembly and disassembly. As such, the head and legs fit onto the chassis via one simple attachment point each onto the internal aluminum frame. Figure 51 shows how the system will be assembled and disassembled.

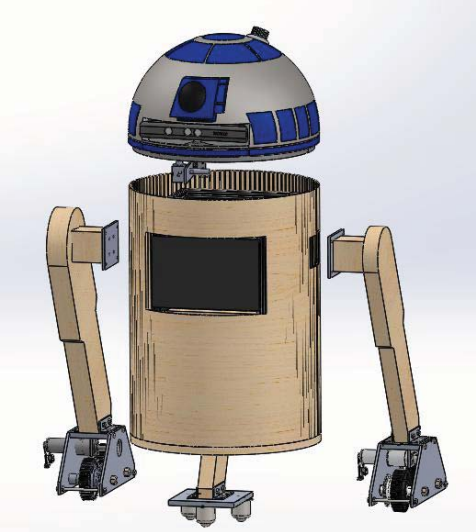

Figure 51: Chassis Integration with head and legs

3.7.1 Chassis to Head

The attachment point between the head and the chassis is a set of three shorter pieces of t-bar which were depicted in Figure 8. The Rockler Bearing is bolted down to these pieces, which are in turn bolted to the chassis frame. The original plan of coutersinking the bearing onto the rim around the kerfed MDF was scrapped due to the change in thickness of the MDF. Originally, the MDF was to be ¾" thick, but it was decided that ¼" thickness would be easier to bend. There was a brief concern of the thin MDF breaking, but since the shell carries close to no load, this was soon dismissed.

3.7.2 Chassis to Locomotion Elements

R2-I2 was designed such that all of the load would be supported by the internal frame, in order to eliminate the possibility of failure due to wood material inconsistencies. As such, to attach the legs to the frame, there are cutouts in the shell to allow the legs themselves be bracketed to the internal aluminum t-extrusion bars. The shell is divided in half where the outer legs join the metal frame to facilitate easy assembly.

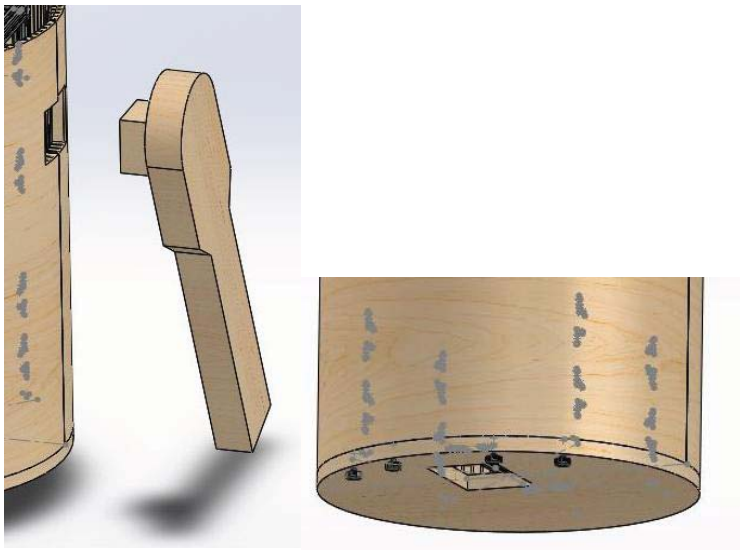

Figure 52: Chassis-Leg Attachment

3.8 Test Plans

Some preliminary test plans were outlined in Table 16 and Table 17 to ensure that each requirement is met in the final design.

Test Number	Test Method	Test Facilities	Entry Condition	Exit Condition
TP.1	Test Procedure: User searches for tool not in toolbox inventory	Tablet	Completion of tool search algorithm	Algorithm displays accurate search results
TP.2	Test Procedure: User calls R2D2 across the lab	User 30 ft away from R2D2 in the same room	Integration of locomotion and voice recognition subsystems	R2D2 navigates lab and moves to the location of user
TP.3	Test Procedure: User puts heavy tool in drawer	2 automatic drills	Complete assembly of drawer frame and drawers	Drawer doesn't break when tools are put in drawer
TP.4	Test Procedure: User retrieves tool from drawer	Phillips head screwdriver	Integration of tool search algorithm and complete assembly of drawers	Correct drawer location is displayed on tablet and user successfully opens drawer and pulls out tool
TP.5	Measure dimensions of outer chassis.	Measuring tape.	Fully assembled chassis	Measured dimensions satisfy requirement.

TP.6	Compare aesthetics of chassis to character in Star Wars movies	Star War movies.	Fully assembled chassis and finalized aesthetics.	Colors and features match movie character depiction.
TP.7	Pull out all drawers	Flat floor.	Fully assembled chassis and drawers	Chassis remains upright and stable when all drawers are opened.
TP.8	Measure drawer depths	Measuring tape.	Fully assembled drawers.	Measured dimensions satisfy requirement.

Table 16: Test procedures for R2-I2

	OR.1	OR.2	OR.3	OR.4	OR.5	OR.6	OR.7	OR.8	OR. 9	OR.10
TP.1			X	X			X			
TP.2									X	X
TP.3	X				X					
TP.4	X	X								
TP.5								X		
TP.6						X				
TP.7										
TP.8										

	DR.1	DR.2	DR.3	DR.4	DR.5	DR.6	DR.7	DR.8	DR.9	DR.10	DR.11	DR.12	DR.13	DR.14	DR.15	DR.16	DR.17	DR.18	DR.19	DR.20	DR.21	DR.22
TP.1						X	X	X	X												X	X
TP.2	X	X	X	X	X																	
TP.3												X						X				
TP.4										X	X		X	X	X							
TP.5																X	X					
TP.6																						
TP.7												X										
TP.8																		X				

Table 17: Test plan tables for R2-I2

3.9 Future Plans

3.9.1 Design Refinements

A major design flaw in our project was the shell. We designed the shell to our best abilities but after actually using the robot and seeing just how much the shell needed to be taken on and off, it

would be a good idea to change the design in future iterations. This may involve completely changing materials or just changing the location of the attachment points to the chassis.

Since the push-pin latch mechanism was not implemented in our final design, a possible alternate design may be an electrically-automated switch which would let the desired drawer pop out an inch or two. This would easily indicate which drawer housed the user's desired tool.

4 R2-I2 Aesthetics

4.1 Head

R2-D2's iconic head was custom made by an R2-D2 enthusiast and is made out of fiberglass. The creator of the head is a professional car painter, and he provided recommendations on how best to paint R2-D2's head. However, due to time and budget limitations, his recommendations were modified, and the following steps were followed to paint the head:

1. Tape off all areas to be painted blue with painters tape
2. Sand the areas to be painted with sandpaper (220-400 grit)
3. Spray blue areas with Rustoleum Metallic Finish Blue Spray paint
    a. Multiple (2-3 coats) were required to achieve a smooth finish
    b. Note that marine fiberglass and wood primer is dissolved by acetone based spray paint so the two should not be used together
4. Let dry 1 day
5. Remove tape around blue areas and reapply tape to cover recently painted blue areas
6. Apply Silver Rub-n-Buff according to package instructions. Apply using finger, buff using terry washcloth
7. Let dry fully
8. Remove tape around blue areas
9. Use acrylic paint to touch up any areas that need it
    a. Do not tape any of the Rub-n-Buffed areas, the adhesive will pull of the Rub-n-Buff. Acrylics and artist paint brushes were used because spray paint couldn't be used without tape
10. Let dry again

Figure 53: Finished R2 Dome

Once the head was painted, three holoprojectors and his radar eye were added. The projectors and eye were 3D printed on Makerbots from CAD models downloaded from http://www.thingiverse.com/. The pieces were hot glued together and then spray painted with the blue metallic spray paint. The lenses were cut from plastic balls (like the ones found in ball pits). The lenses were spray painted using Rustoleum Satin black spray paint, and were then hot glued into the 3D printed parts.

The parts were then applied to R2-D2 using Velcro. This was also useful for transporting the droid because the pieces were fragile and could be removed during transportation.

4.2 Body

R2-D2's shell was made of painted plastic styrene sheeting that was then bolted to the kerfed MDF. This allowed the ECE team to continue working on the droid while the aesthetics were made in parallel.

Once the holes for shelving and the tablet were cut in the kerf board, the board was measured and a matching piece was cut out of plastic sheeting. Squares and other designs were then taped off on the plastic sheeting so that the sheet could be spray painted. The plastic sheet was then spray painted using Metallic Blue, Satin Black, and Gray Primer spray paint. After pulling off the tape, the lines were

touched up using acrylic paint and artist paint brushes. This process was repeated for the second piece of kerf board.

Before settling on this process, the team tried printing the designs on poster paper and attaching it to the plastic sheeting with rubber cement. However, the rubber cement did not provide strong adhesion and it caused wrinkles in the paper, which is why the team did not also try attaching the paper directly to the kerf board.

4.3 Legs and Feet

R2-D2's wooden legs were spray painted white using Rustoleum Matte White spray paint.

Figure 54: R2's legs

In order to mount the LIDAR in R2-D2's front foot, a trapezoid was cut out of styrofoam and a slot to fit the LIDAR was cut in the front of the trapezoid. The foot was then covered with plastic styrene sheeting and spray painted matte white. The foot was then velcroed down to the metal plate of the front foot.

Figure 55: R2's LIDAR foot

4.4 Parts List

Item	Quantity		Total Cost	Vendor	Website
Rust-oleum Painter's Touch Ultra Cover Matte Spray - White	1		8.92	Amazon	http://www.amazon.com/Rust-Oleum-249126-Painters-Multi-Purpose-12-Ounce/dp/B002BWOS7G/ref=sr_1_1?ie=UTF8&qid=1394753608&sr=8-1&keywords=rustoleum+painters+touch+2x+matte+white
Silver Leaf Rub n Buff	3	8.78	26.34	Amazon	http://www.amazon.com/AMACO-Metallic-Finish-Silver-0-5-Fluid/dp/B00081G2HG/ref=sr_1_1?s=arts-crafts&ie=UTF8&qid=1394753800&sr=1-1&keywords=silver+leaf+rub+n+buff
Rust-oleum Metallic Spray Paint - Cobalt Blue	1		10.74	Amazon	http://www.amazon.com/Rust-Oleum-7251830-Metallic-Cobalt-11-Ounce/dp/B000LNWCKM/ref=sr_1_1?ie=UTF8&qid=1394753187&sr=8-1&keywords=rustoleum+metallic+spray+cobalt+blue
Plastic Styrene Sheet - .020" thick	1		$6.46	US Plastic Corp	http://www.usplastic.com/catalog/item.aspx?itemid=22883
Rustoleum Satin Black Spray	1		$4	Walmart	

Paint					

5 Appendix

5.1 R2-D2 Head Motor Selection

Your maxon drive

maxon motor
driven by precision

Consists of:

Planetary Gearhead GP 16 A Ø16 mm, 0.1 - 0.3 Nm, Metal Version, Sleeve Bearing
Part number 110322

EC 16 Ø16 mm, brushless, 30 Watt, with Hall sensors
Part number 400162

Encoder MR, Typ M, 128 CPT, 3 Channels, with Line Driver
Part number 228177

Your contact

maxon motor worldwide
http://www.maxonmotor.com/maxon/view/content/company_contact_form
E-Mail: e-shop@maxonmotor.com
Internet: www.maxonmotor.com

Non-binding price info excl. shipping and packing cost, excl. VAT.

1-4 Pieces	**USD 450.88**
5-19 Pieces	**USD 387.25**
20-49 Pieces	**USD 321.75**

General Terms and Conditions: http://www.maxonmotor.com/maxon/view/content/terms_and_conditions_page

Summary of the selected drive

Consists of:

Planetary Gearhead GP 16 A Ø16 mm, 0.1 - 0.3 Nm, Metal Version, Sleeve Bearing
Part number 110322

EC 16 Ø16 mm, brushless, 30 Watt, with Hall sensors
Part number 400162

Encoder MR, Typ M, 128 CPT, 3 Channels, with Line Driver
Part number 228177

Operating range

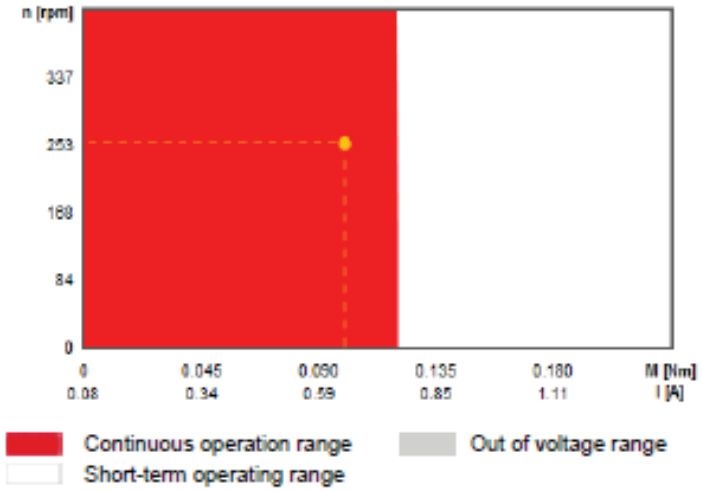

Data for combination	
Max. motor voltage	24 V
No load speed	50021 rpm
Max. continuous torque	121.12 mNm
Nominal current (max. continuous current)	0.754 A
Permissible intermittent torque	225 mNm
Total length	75.4 mm
Max. diameter	16 mm

Planetary Gearhead GP 16 A Ø16 mm, 0.1 - 0.3 Nm, Metal Version, Sleeve Bearing
Part number 110322

General Information		
Gear Art	GP	
Outer diameter	16	mm
Gear variant	A	

Gearhead Data		
Reduction	19 : 1	
Reduction absolute	3249/169	
Max. motor shaft diameter	2	mm
Number of stages	2	
Max. continuous torque	0.15	Nm
Intermittently permissible torque at gear output	0.225	Nm
Sense of rotation drive to output	=	
Max. efficiency	81	%
Weight	23	g
Average backlash no load	1.6	°
Mass inertia	0.05	gcm²
Gearhead length (L1)	19.1	mm
Max. transferable continuous performance	6.6	W
Max. transferable short-time performance	9.9	W

Technical Data		
Radial play	max. 0.06 mm, 6 mm from flange	
Axial play	0.02 - 0.1	mm
Max. radial load	12 N, 6 mm from flange	
Max. axial load (dynamic)	8	N
Max. permissible force for press fits	100	N
Recommended input speed	8000	rpm
Max. short-time input speed	8000	rpm
Recommended temperature range	-15...+100	°C
Extended temperature range	-40...+100	°C
Number of autoclave cycles	0	

Information about gearhead data http://www.maxonmotor.com/medias/CMS_Downloads/DIVERSES/12_203_EN.pdf

Encoder MR, Typ M, 128 CPT, 3 Channels, with Line Driver
Part number 228177

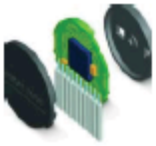

General Information		
Counts per turn	128	
Number of channels	3	
Line Driver	Yes	
Max. speed	37500	rpm

Technical Data		
Supply voltage Vcc	4.7...5.2	V
Driver used logic	TTL	
Output current per channel	0...5	mA
Phase shift	90	°e
Phase shift, inaccuracy	45	°e
Index synchronized to AB	Yes	
Max. moment of interia of code wheel	0.1	gcm²
Operating temperature	-25...+85	°C

EC 16 Ø16 mm, brushless, 30 Watt, with Hall sensors
Part number 400162

Values at nominal voltage		
Nominal voltage	48	V
No load speed	39600	rpm
No load current	80.7	mA
Nominal speed	34800	rpm
Nominal torque (max. continuous torque)	7.87	mNm
Nominal current (max. continuous current)	0.754	A
Stall torque	72.5	mNm
Starting current	6.35	A
Max. efficiency	79	%
Characteristics		
Terminal resistance	7.56	Ω
Terminal inductance	0.477	mH
Torque constant	11.4	mNm/A
Speed constant	836	rpm/V
Speed / torque gradient	554	rpm/mNm
Mechanical time constant	4.21	ms
Rotor inertia	0.725	gcm²
Thermal data		
Thermal resistance housing-ambient	16.3	KW-1
Thermal resistance winding-housing	1.68	KW-1
Thermal time constant winding	1.91	s
Thermal time constant motor	240	s
Ambient temperature	-20...+100	°C
Max. permissible winding temperature	+155	°C
Mechanical data		
Bearing Type	ball bearings	
Max. permissible speed	70000	rpm
Axial play	0 - 0.14	mm
Max. axial load (dynamic)	3	N
Max. force for press fits (static)	35	N
(static, shaft supported)	250	N
Max. radial loading	10 N, 5 mm from flange	
Other specifications		
Number of pole pairs	1	
Number of phases	3	
Direction of rotation	Clockwise (CW)	
Number of autoclave cycles	0	
Product		
Weight	34	g

5.2 R2-D2 Locomotion Motor Information

Your configuration

maxon motor
driven by precision

Part number*: B71761144644

Consists of:

Motor - DCX35L GB KL 24V
Planetary gearhead - GPX42 15:1
Sensor - ENX16 EASY 256IMP

maxon motor worldwide
http://www.maxonmotor.com/maxon/view/content/contact_page

E-Mail: e-shop@maxonmotor.com
Internet: www.maxonmotor.com

Total price	CHF 686.90	1-4 Pieces
	CHF 578.20	5-19 Pieces
	CHF 492.00	20-49 Pieces

Delivery ex works in max. 11 working days after receipt of order via E-Shop

General Terms and Conditions: http://www.maxonmotor.com/maxon/view/content/terms_and_conditions_page

Interactive 3D model
Click on the icon to activate your 3D model

Your configuration can be viewed here:
http://www.maxonmotor.com/maxon/view/configurator/?ConfigID=B71761144644

Motor - DCX35L GB KL 24V
Planetary gearhead - GPX42 15:1
Sensor - ENX16 EASY 256IMP

Drawings are not to scale!

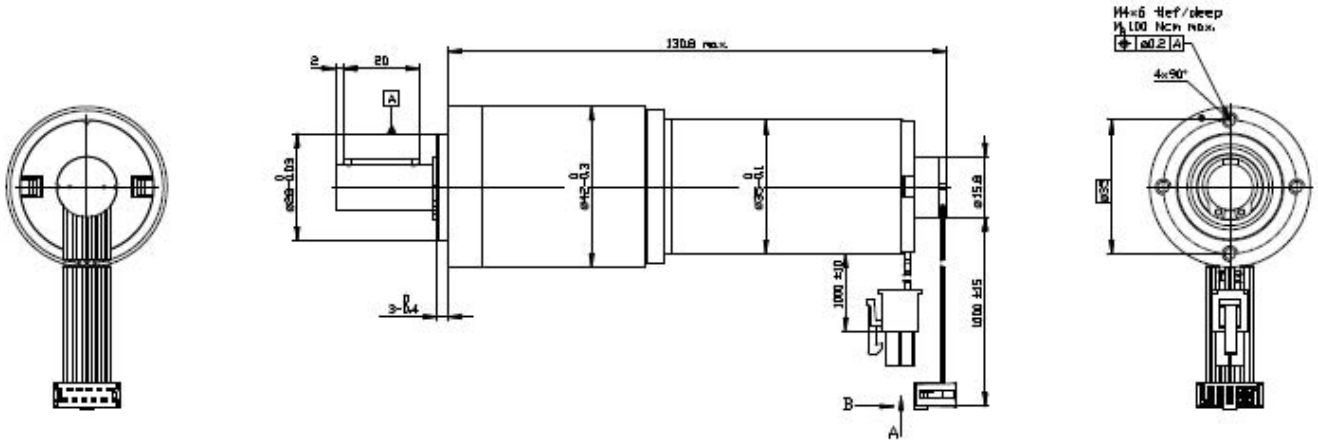

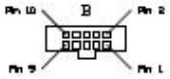

Stecker Typ Sensor sensor connector type	
JST ZHR-10	
Steckerbelegung pin allocation	
Pin 1	Nicht verbinden do not connect
Pin 2	VCC
Pin 3	GND
Pin 4	Nicht verbinden do not connect
Pin 5	Kanal A \ channel A \
Pin 6	Kanal A channel A
Pin 7	Kanal B \ channel B \
Pin 8	Kanal B channel B
Pin 9	Kanal I \ channel I \
Pin 10	Kanal I channel I

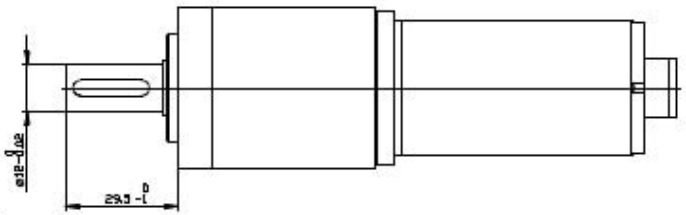

Stecker Typ Motor motor connector type	
Molex 39-01-2048	
Steckerbelegung pin allocation	
Pin 1	rot / red (+)
Pin 2	schwarz / black (-)

Kabel nicht dargestellt
no cable visualisation

Summary of your selected configuration

Motor - DCX35L GB KL 24V
Planetary gearhead - GPX42 15:1
Sensor - ENX16 EASY 256IMP

Total weight of the drive: 790 g

Functions		
Reduction	15 : 1	
Number of stages	2	
Commutation	Graphite brushes	
Supply voltage	Nominal voltage 24 V	
Motor bearings	Preloaded ball bearing	
Counts per turn	256	
Form and Fit		
Gear shaft	with key	
Shaft length L1	29.5	mm
Key length L2	20	mm
Amount of threads	4	
Thread diameter	M4	
Pitch circle diameter TK	35	mm
Electrical connection, motor	Cable	
Connector type, motor	Molex 39-01-2040	
Cable length L1 for motor	1000	mm
Cable type	AWG18	
Electrical connection, encoder	configured	
Cable length L1 for encoder	1000	mm
Connection orientation (motor)	0	degree
Connection orientation (encoder)	0	degree
Add-ons		
Labeling	Standard labeling	

Drive disposition

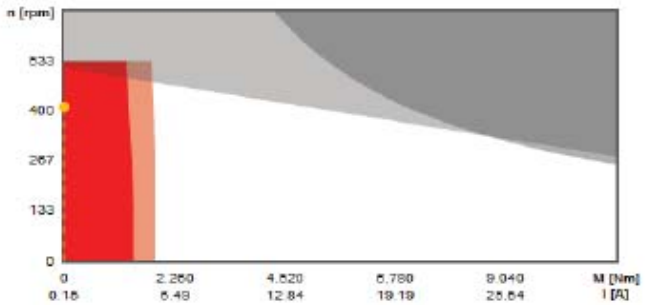

Continuous operation range
Short-term operating range
Continuous operation range at reduced thermal resistance Rth2 50%
Out of voltage range
Selected operating point

Values of the drive at max. available voltage		
Max. motor voltage	24	V
No load speed	515	min-1
Continuous torque	1470.15	mNm
Nominal current (max. continuous current)	4.26	A

Your operating point - The required data for the load		
Required voltage	19	V
Max. load speed	410	min-1
Effective load torque (rms)	1110	rms
Effective load current (rms)	3.26	A

Motor - DCX35L GB KL 24V

Values at nominal voltage		
Nominal voltage	24	V
No load speed	7720	rpm
No load current	146	mA
Nominal speed	7160	rpm
Nominal torque (max. continuous torque)	121	mNm
Nominal current (max. continuous current)	4.26	A
Stall torque	2030	mNm
Starting current	69.3	A
Max. efficiency	88.7	%
Characteristics		
Max. output power	117	W
Terminal resistance	0.346	Ohm
Terminal inductance	0.121	mH
Torque constant	29.3	mNm/A
Speed constant	326	rpm/V
Speed/torque gradient	3.86	rpm/mNm
Mechanical time constant	3.91	ms
Rotor inertia	96.6	gcm^2
Thermal data		
Thermal resistance housing to ambient	6.98	K / W
Thermal resistance winding to housing	2.1	K / W
Thermal time constant of the winding	43	s
Thermal time constant of the motor	1030	s
Ambient temperature	-40..100	°C
Max. permissible winding temperature	155	°C
Mechanical data		
Max. permissible speed	12300	rpm
Min. axial play	0	mm
Max. axial play	0.1	mm
Radial backlash	0.02	mm
Max. axial load (dynamic)	7	N
Max. force for press fits (static)	22.6	N
Max. radial load	65.3	N
Further specifications		
Number of pole pairs	1	
Number of collector segments	11	
Weight	410	g
Number of sterilization cycles	0	
Typical noise level	48	dBA

Information about motor data: http://www.maxonmotor.com/medias/CMS_Downloads/DIVERSES/12_049_EN.pdf

Sensor - ENX16 EASY 256IMP

Type		
Counts per turn	256	
Number of channels	3	
Line Driver	RS422	
Max. external diameter	15.8	mm
Max. housing length	8.5	mm
Max. electrical speed	120000	rpm
Max. speed	30000	rpm
Technical data		
Supply voltage	4.5..5.5	V
Output signal driver	Differential, EIA RS 422	
Output current per cable	-20...20	mA
Min. state length	30	°el
Max. state length	175	°el
Signal rise time/Signal fall time	20/20	ns
Min. edge separation	500	ns
Direction of rotation	A for B, CW	
Index position	A low & B low	
Index synchronously to AB	yes	
Index pulse width	90	°e
Typical current at standstill	17	mA
Moment of inertia, pulse wheel	0.05	gcm^2
Weight (Standard cable length)	20	g
Operating temperature range	-40..100	°C
Number of sterilization cycles	0	

Datasheet: http://www.maxonmotor.com/medias/CMS_Downloads/DIVERSES/ENXEASY_en.pdf